GENETIC ANALYSES OF DISEASE RESISTANCE AND ORNAMENTAL TRAITS IN DIPLOID *ROSA* SPP.

A Dissertation

by

ELLEN LOUISE YOUNG

Submitted to the Office of Graduate and Professional Studies of
Texas A&M University
in partial fulfillment of the requirements for the degree of

DOCTOR OF PHILOSOPHY

Chair of Committee,	David H. Byrne
Co-Chair of Committee,	Patricia E. Klein
Committee Members,	Brent H. Pemberton
	Kevin Ong
	David M. Stelly
Head of Department,	R. Daniel Lineberger

August 2020

Major Subject: Horticulture

ABSTRACT

Roses (genus *Rosa*) are among the most popular ornamental plants. Traditional rose breeding is a slow and tedious process, but breeding efficiency can be improved by marker-assisted selection. Marker-assisted selection, however, requires a thorough understanding of the genetic control of the traits of interest. To characterize the genetic control of certain traits of interest, eight segregating diploid rose families were developed. Families were phenotyped for black spot and cercospora resistance, defoliation, flower intensity, and plant architecture (number of primary shoots, height, length, width, longest dimension, volume, apical dominance, and growth habit). Families were genotyped for single nucleotide polymorphisms (SNPs) using genotyping by sequencing. Seventy-three rose cultivars were genotyped and phenotyped in the same manner.

Heritability was estimated for both datasets. Broad-sense heritability was high for black spot, defoliation, and flower intensity, but low for cercospora. All four traits also had low narrow-sense heritability, indicating a high degree of non-additive effects. Architecture traits generally had low to moderate broad-sense heritability and low narrow-sense heritability, again indicating non-additive effects. Genotype by environment interactions were generally high within a year, reflecting the growth of the plants over the course of the year, but relatively low over years. Narrow-sense heritability estimates for length, width, longest dimension, and apical dominance were

slightly higher in once-flowering genotypes than continuous flowering genotypes, suggesting that some germplasm has stronger additive effects for these traits.

Association mapping was performed for both datasets. Three clusters of associations were identified for black spot and cercospora on chromosomes 2, 3, and 6. When flowering type was controlled for, five clusters associated with flower intensity were identified on chromosomes 2, 4, and 5. Ten clusters associated with plant vigor (height, length, width, longest dimension, and volume) were identified. Vigor clusters on chromosomes 1, 2, 4, and 7 may coincide with previously identified quantitative trait loci (QTLs), but the six other clusters appear to be novel.

In conclusion, disease resistance, defoliation, flower intensity, and architecture traits had a range of heritability estimates with mostly non-additive heritability. Potential genomic regions controlling these traits were identified but require validation. To facilitate this, a high-density integrated consensus linkage map was developed from the three largest families in preparation for a QTL analysis. Future work will use this map in QTL analyses, enabling marker-assisted selection for these traits of interest.

DEDICATION

To my loving grandparents, Lorenz and Jeanette Degner and William and Dolores Roundey, who have always encouraged my educational pursuits.

ACKNOWLEDGEMENTS

I would like to thank my graduate advisor, Dr. David Byrne, for his guidance and support during my time at Texas A&M University. Being a part of your lab has been a wonderful opportunity and I've learned so much from you. I would also like to thank my co-chair, Dr. Patricia Klein, who has been a huge part of my graduate education; my research would not have been possible without your help. Thanks also to my committee members, Drs. Brent Pemberton, Kevin Ong, and David Stelly, for their guidance and support.

Many thanks to Natalie Anderson and Pamela Hornby, for all the time and energy spent on keeping plant materials alive and well. I am deeply grateful for all your help. Thank you to Natalie Patterson, who helped me with various lab techniques and performed much of the genotyping work. Also thank you to the many student workers, past and present, who have assisted with field work over the years.

Thank you to my labmates, past and present, whose support has been invaluable. Special thanks to Drs. Muqing Yan, Xuan Wu, and Zena Rawandoozi, who shared their knowledge with me. I also owe much to my fellow students Jeekin Lau and Nolan Bentley, whose script-writing skills far surpass mine. Thank you for your helpfulness and patience.

Thank you to my family and friends, especially my parents, sisters, and friend Kiralyn Brakel. Your encouragement and support have been vital. Thank you, also, for tolerating many unsolicited plant facts. Finally, thank you to my husband, Dr. Pierce

Young, without whose love, support, and editing skills this dissertation would have been truly impossible; and to Peter Young, who provided extra motivation.

CONTRIBUTORS AND FUNDING SOURCES

Contributors

This work was supervised by a dissertation committee consisting of Drs. David Byrne (chair), Patricia Klein (co-chair), and Brent Pemberton of the Department of Horticultural Sciences; Dr. Kevin Ong of the Department of Plant Pathology and Microbiology; and Dr. David Stelly of the Department of Soil and Crop Sciences.

The data in Chapter II was partially provided by Christian Bedard (Weeks Roses, Wasco, CA) and Natalie Anderson of the Department of Horticultural Sciences. The data in Chapter III was partially provided by Dr. Brent Pemberton. The data analyzed for Chapters IV and V was partially provided by Dr. Patricia Klein. The analyses in Chapters IV and V were conducted in part by Nolan Bentley of the Department of Horticultural Sciences and with assistance from Jeekin Lau of the Department of Horticultural Sciences.

All other work conducted for the dissertation was completed by the student independently.

Funding Sources

This work was made possible in part by the USDA Specialty Crop Research Initiative project “Combating Rose Rosette Disease: Short Term and Long Term Approaches”; a fellowship from the Texas A&M University College of Agriculture and Life Sciences; a research assistantship from the Department of Horticultural Sciences;

and scholarships from the Belsterling Foundation, Sugar Creek Garden Club, and the Houston Rose Society.

TABLE OF CONTENTS

Page

LIST OF FIGURES

Page

LIST OF TABLES

Page

CHAPTER I

INTRODUCTION

I.1 The genus *Rosa*

Roses (*Rosa* spp., family Rosaceae) rank among the most important ornamental plants both culturally and economically. They have been cultivated for over 4000 years, most likely beginning in China around 2700 B.C. Roses have been of mythological, medicinal, culinary, and/or festive significance for various cultures, including the Greeks, Romans, and medieval Persians (Krüssman, 1981). Today, roses retain their significance as a symbol of love in Western culture and remain immensely popular both as cut flowers and as garden plants. In 2014, garden roses alone accounted for over $200 million in sales in the United States (USDA, 2015). Furthermore, when 18 categories of ornamental plants such as flowering annuals, flowering trees, etc. were considered, roses by themselves made up 3% of United States ornamental plant sales in 2013 (Hodges et al., 2015).

Roses, however, are a broad category themselves: the genus *Rosa* encompasses between 100 and 200 species (Wissemann, 2003) whose ploidy levels range from diploid to decaploid with a base chromosome number of 7 (Jian et al., 2010). Members of the genus are found throughout the Northern Hemisphere (Wissemann, 2003). In the traditional taxonomy, the genus was split into four subgenera: *Hulthemia, Eurosa* (now called *Rosa*), *Platyrhodon,* and *Hesperhodos* (Rehder and Dudley, 1940; Wissemann, 2003). Most species were contained in subg. *Rosa*, which was divided into ten sections.

This classification, however, was based on morphological characters and is only partially supported by molecular data. Current evidence suggests that subg. *Rosa* is not monophyletic and that, instead of four subgenera, the genus forms two main clades (Bruneau et al., 2007; Fougère-Danezan et al., 2015), which have been termed *Synstylae* and allies and *Cinnamomeae* and allies (Fougère-Danezan et al., 2015). As a result, current recommendations include that the three small subgenera should be reclassified as sections (Fougère-Danezan et al., 2015; Ritz and Wissemann, 2005), current sections *Cinnamomeae* and *Carolinae* should be merged (Bruneau et al., 2007; Fougère-Danezan et al., 2015), and a new section *Americanae* should be formed to contain the North American species *Rosa setigera* Michx. (Lewis, 2016). These recommendations have not yet been formally accepted. Phylogenetic analyses in the genus are complicated by the existence of many natural interspecific hybrids (Fougère-Danezan et al., 2015), which may require more revisions to the taxonomy of roses.

While roses have been cultivated in Europe and Asia for millennia, intermixing between Asian and European roses did not begin until 1792 with the introduction to Europe of several Asian species and cultivars, including ‘Old Blush’, a *Rosa chinensis* Jacq. cultivar (Guoliang, 2003). These introductions bore novel (from the European perspective) traits such as repeat flowering and true red color, helping to lay the foundation for modern roses (Marriott, 2003). Modern rose cultivars trace primarily to seven rose species—*R. chinensis, Rosa foetida* Hermm., *Rosa gallica* L., *Rosa gigantea* Colett ex Crép., *Rosa moschata* Herrm., *Rosa multiflora* Thunb. ex Murr., and *Rosa wichurana* Crép. (Bruneau et al., 2007)—with minor contributions from other species

such as *Rosa rugosa* Thunb. and *Rosa phoenicea* Boiss. (Table 1) (Crespel and Mouchotte, 2003). With the exceptions of *R. foetida* and *R. rugosa*, these species have all been sorted into the *Synstylae* clade (Fougère-Danezan et al., 2015; Bruneau et al., 2007), indicating that the genetic potential of a large portion of the rose genus has not been extensively utilized in rose breeding.

Table 1 Seven key rose species contributing to the development of modern roses. 'Traditional section' reflects classification according to Rehder and Dudley (1940) and Wisseman (2003). 'Possible new classification' reflects phylogeny of Bruneau et al. (2007) and Fougère-Danezan et al. (2015).

Species	Ploidy	Traditional section	Possible new classification
R. chinensis	2x	*Indicae*	*Synstylae* & allies
R. foetida	4x	*Pimpinellifoliae*	*Cinnamomeae* & allies
R. gallica	4x	*Rosa*	*Synstylae* & allies
R. gigantea (syn. *R. odorata* var. *gigantea*)	2x	*Indicae*	*Synstylae* & allies
R. moschata	2x	*Synstylae*	*Synstylae* & allies
R. multiflora	2x	*Synstylae*	*Synstylae* & allies
R. wichurana	2x	*Synstylae*	*Synstylae* & allies

Modern rose breeding can be a challenge due to this complex history and other fertility issues. Considerable genetic distance between potential parents can result in reduced fertility (Spethmann and Feuerhahn, 2003) and crosses within the traditionally-defined sections are generally more successful (Smulders et al., 2011). As evidenced by the history of rose breeding, interspecific hybridization is certainly possible, but when hybrids are successfully produced between distant species, the hybrid may be sterile due to meiotic imbalances (Lewis and Basye, 1961). Likewise, interploidy crosses are frequently performed, as modern cultivars tend to be tetraploid, triploid, and diploid, but some evidence suggests that crosses within ploidy levels are more successful in terms of

seedling production (Zlesak, 2009; El Mokadem et al., 2002). Another study, however, found interploidy crosses to have good hip set, seed germination, and seedling production (Ueckert, 2014); thus, the success of interploidy crosses likely depends on the genotypes involved (Spethmann and Feuerhahn, 2003). Triploid hybrids resulting from crosses between diploid and tetraploid parents may be sterile or have reduced fertility (Smulders et al., 2011). B chromosomes are rarely observed in roses, but their occurrence has been linked to pollen sterility (Lata, 1982); generally, pollen fertility varies dramatically depending on the genotype (Spethmann and Feuerhahn, 2003). Finally, even in less distant crosses, seed germination is low (Gudin, 2003). Issues such as these make breeding for traits of interest potentially complex, especially when obscure germplasm is involved.

I.2 Traits of interest

While novel colors and flower shapes have historically been the focus of rose breeding efforts, in recent decades priorities have shifted to the development of low-maintenance roses. A survey of rose breeders and enthusiasts indicated that increased disease resistance was the single greatest improvement breeders could make to rose cultivars. Other priorities included fragrance, flower color, number of flowers, and plant size (Byrne et al., 2019; Waliczek et al., 2018). A willingness-to-pay study found heat and disease tolerance to be high priority for consumers in the southern United States (Chavez et al., 2019). Thus, while ornamental traits are still important, the development of disease resistant roses is a priority for rose breeding.

I.2.1 Disease resistance

One of the most common diseases of rose is black spot, which is caused by the fungus *Diplocarpon rosae* Wolf (Wolf, 1912). First recorded in 1815 in Sweden, the pathogen now has a worldwide distribution (Drewes-Alvarez, 2003) and is recognizable by its dark, circular foliar lesions which are followed by chlorosis and defoliation (Horst and Cloyd, 2007). The development and spread of the disease is dependent on environmental conditions: symptoms do not develop below 10°C or above 29°C and high humidity is required for conidia germination (Gachomo and Kotchoni, 2007). Moreover, the pathogen is likely spread by water splash (Münnekhoff et al., 2017). 13 unique races of black spot have been identified (Zurn et al., 2018) and major genes conferring resistance to specific races have been identified in roses. *Rdr1* and *Rdr2*, both on chromosome 1, confer resistance to race 5 (Von Malek et al., 2000; Spiller et al., 2011) and race 4 (Hattendorf et al., 2003; Zurn et al., 2018), respectively. *Rdr3* confers resistance to race 8 but has not been successfully mapped (Whitaker et al., 2010). *Rdr4* on chromosome 5 confers resistance to 12 of the 13 identified black spot races (Zurn et al., 2018). Quantitative trait loci (QTLs) conferring partial resistance have also been identified on chromosomes 3 and 5 (Yan et al., 2019; Soufflet-Freslon et al., 2019). As most of the major genes confer race-specific resistance, either pyramiding of major genes or breeding for partial resistance is needed to develop black spot-resistant roses. Most roses are at least somewhat susceptible (Horst and Cloyd, 2007), but wild rose species including *R. wichurana*, *R. multiflora*, and *R. rugosa* have been suggested as

possible sources of resistance (Debener, 2019; Smulders et al., 2011; Schulz et al., 2009).

Though not as damaging as black spot, cercospora leaf spot is another common foliar disease of roses with a global distribution (Mangandi and Peres, 2009; Davis, 1938). The disease is caused by the fungus *Rosisphaerella rosicola* Pass., formerly known as *Cercospora rosicola* Pass. (Videira et al., 2017) and was first described in 1874 (Davis, 1938). Similar to black spot, cercospora causes dark, circular lesions on leaves, but lesions may develop a lighter necrotic center (Mangandi and Peres, 2009). As with black spot, defoliation eventually follows (Davis, 1938). The fungal spores are dispersed by water splash to nearby plants (Dunwell et al., 2014). Unfortunately, considerably less work has been performed on cercospora than on other rose diseases; however, members of the same genus are known to cause foliar diseases in a variety of other crops. For many of these species, disease development is encouraged by warm temperatures and high humidity (Pham et al., 2015; Weiland and Koch, 2004; Mian et al., 2008; Cooperman and Jenkins, 1986). Optimal conditions have not yet been determined for *R. rosicola.* Pathogen races and host resistance have also been identified in other species. *Cercospora beticola* Sacc., for instance, which causes one of the worst foliar diseases of sugarbeet, does not appear to have unique races, and there appears to be quantitative resistance to the disease (Weiland and Koch, 2004). On the other hand, in *Cercospora sojina* K. Hara, which affects soybean, at least 11 races have been identified, a major race-specific resistance gene has been mapped (Mian et al., 2008), and other candidate resistance genes have been identified (Pham et al., 2015). Cowpea (affected by

Cercospora canescens Ellis & G. Martin) likewise appears to have monogenic resistance to the disease (Duangsong et al., 2018). In roses, no resistance genes have been identified and it is unknown if there are unique pathogen races as in black spot. A five-year cultivar trial revealed a range of cercospora susceptibility in cultivars; notably, several cultivars with lower black spot incidence had higher cercospora susceptibility (Hagan et al., 2005). Evaluations of 15 rose populations resulted in a broad-sense heritability (H^2) estimate of 0.83 and a narrow-sense heritability (h^2) estimate of 0.57, indicating that selection for cercospora resistance should be feasible. Moreover, the same study identified QTLs on chromosomes 1 and 3 over multiple environments that explained 8.5% and 7.7% of the phenotypic variance, respectively (Kang, 2020). Thus, while there is potential for resistance breeding, further work is needed to identify sources of resistance and the genes or QTLs involved.

Of relatively recent concern is rose rosette disease (RRD), which was described in the 1940s and in 2011 was determined to be caused by a virus, now named rose rosette virus (RRV) (Laney et al., 2011). The virus is spread by the eriophyid mite *Phyllocoptes fructiphilus* Keifer (Amrine et al., 1988) and the disease is currently widespread in the central and eastern United States, though it occurs elsewhere in the country as well (Windham et al., 2014). The primary symptom is witches' broom or rosette growth on the plant; death usually occurs within a few years (Windham et al., 2014). Development of roses resistant to the virus or to the mite vector is of great importance to the American rose industry but may prove challenging: approximately 95% of roses are likely susceptible to RRD, and many of the possibly resistant roses are

species, species hybrids, or cultivars not extensively used in breeding (Byrne et al., 2015).

I.2.2 Ornamental traits

As garden roses are grown primarily for their flowers, abundant and consistent flowering throughout the growing season is highly desirable. Prior to the introduction of *R. chinensis*, most European roses bloomed only in the spring (once-flowering, OF); *R. chinensis*, however, can bloom throughout the growing season (continuous flowering, CF) (Marriott, 2003). Flowering type (CF or OF) is controlled by a single gene, *RoKSN*, which is as a member of the *TERMINAL FLOWER 1* (*TFL1*) gene family. In OF roses, *RoKSN* codes for a floral repressor, but CF roses contain a retrotransposon in *RoKSN* that prevents the production of the repressor (Iwata et al., 2012). *RoKSN* is located in the 27-33 Mbp region of chromosome 3 but has not been precisely mapped (Hibrand Saint-Oyant et al., 2018). Within CF roses, however, there is still variation in the degree of flowering. Possible genetic explanations include MADS-box genes encoding transcription factors that are crucial for floral organogenesis (Liu et al., 2018) and gibberellic acid biosynthesis genes that have been shown to be upregulated during bud burst (Choubane et al., 2012). Flower productivity is also known to be affected by heat stress (Greyvenstein, 2013) and light intensity (Girault et al., 2008).

Plant architecture, or the shape of the plant as determined by environmental and genetic factors, has been shown to greatly affect the visual quality of roses (Boumaza et al., 2009; Garbez et al., 2018). Various environmental factors can impact architecture in roses: light (Khayat and Zieslin, 1982; Demotes-Mainard et al., 2013), temperature

(Djennane et al., 2014), water (Demotes-Mainard et al., 2013), mechanical stimulation (Morel et al. 2012), and nitrogen availability (Huché-Thélier et al., 2011). While these studies demonstrate that rose architecture can be manipulated, identifying the genetic control(s) of architecture characteristics remains of interest in rose breeding. This has resulted in two approaches to studying rose plant architecture. Broadly speaking, the first approach seeks to describe the architecture of the plant in full, though with as few parameters as possible; the second approach focuses on one or a few architectural traits and their genetic control, without attempting to describe the whole plant. Both approaches have yielded intriguing results.

Many of the studies in the plant descriptor approach have broken down the plant into its basic components of axis and metamers, a metamer being defined as an internode, a node, axillary bud(s), and a leaf. An early study found that the number and length of axes, the number of metamers per axis, and the number of branching orders was enough to distinguish between the rose varieties ‘Radrazz’ and ‘Meiratcan’ (Morel et al., 2009). To distinguish eight genotypes, Crespel et al. (2013) identified seven necessary and sufficient architectural characteristics (number of determined axes, number of long axes of branching order 3, branching order number, number of metamers on long axes, length of long axes, basal diameter of short axes, and branching angle short axes) from a panel of 35 potential characteristics that enabled the development of unique architectural profiles. Six of these characteristics (basal diameter being excluded) were subsequently found to have moderate to high broad-sense heritability in the same genotypes, though there were significant genotype x year interactions (Crespel et al.,

2014). Similar architecture traits (number of determined axes, branching angle of long axes of branching order 2, number of short axes of branching order 3, length of short axes of branching order 4, length of the long axes, and number of branches on long axes in the distal zone) were assessed in two diploid rose populations, and most had moderate to moderately high broad-sense heritability. QTLs explaining 7-20% of the phenotypic variation were identified for these traits (Li-Marchetti et al., 2017). Finally, a study focused specifically on describing compact growth types examined larger-scale characteristics: plant height, number of primary shoots (analogous to the number of determined axes), length of primary shoots, number of nodes on primary shoots, number of secondary shoots per primary shoot, and number of tertiary shoots per primary shoot. Compact growth types were frequently associated with a high number of primary shoots (Wu et al., 2019a), and number of primary shoots as well as plant height were also highly heritable (Wu et al., 2019b).

In contrast, the second approach to plant architecture in roses focuses on a limited number of traits that do not by themselves fully describe plant architecture, even though individual traits may be the same as traits in the first approach. For example, Yan et al. (2005b) investigated ten traits which included shoot length and stem thickness, which were examined in the studies mentioned previously, but for the specific purpose of assessing rose vigor, not describing whole-plant architecture. Yan et al. (2005b) also assessed number of internodes, chlorophyll content, shoot leaf area, leaf dry weight, stem dry weight, total dry weight, specific leaf area, and absolute growth rate, and found that these had high heritability. QTLs were identified for all of these traits with notable

clusters on chromosomes 2 and 6 (Yan et al., 2007). Plant height, vigor, stem length, and number of side shoots, among other traits, had moderate to high broad-sense heritability in a tetraploid population; however, number of side shoots was found to have a high degree of genotype x environment interaction (Gitonga et al., 2014). This is similar to the genotype x environment interaction found by Wu et al. (2019b) for the analogous trait number of secondary shoots per primary shoot. Branching was also examined by Djennane et al. (2014), though it was quantified as the ratio between the number of secondary shoots and the total number of buds on the primary shoot. A major QTL was identified that co-localized with a *MAX* gene homologue; in *Arabidopsis thaliana* (L.) Heynh, *MAX* genes have been implicated in strigolactone-related pathways. Finally, a diploid rose population was assessed for number of nodes, length of internodes, growth habit, height, elevation angle, stem diameter, and internode length. All of these traits had moderately high to high broad-sense heritability and QTLs explaining 7-59% of the phenotypic variation were identified (Kawamura et al., 2015; Kawamura et al., 2011).

In short, a wide array of architecture traits, from small-scale traits requiring digitization to large-scale traits such as plant height, have been studied to date in roses. Many of these traits have moderate to high heritability, indicating that breeding for improved architecture is a feasible goal. Moreover, the many QTLs identified so far are promising for future attempts at efficient breeding for these and other architecture traits.

I.3 Modern tools and methods for rose breeding

In recent years, the tools available for rose genetics and breeding have expanded considerably. One notable improvement has been in the area of genotyping technologies.

Genotyping by sequencing (GBS), which can produce tens or hundreds of thousands of single nucleotide polymorphisms (SNPs) in relatively little time and for a relatively low cost, has been successfully used in plants (He et al., 2014) including roses (Yan et al., 2018; Heo et al., 2017). The development of the WagRhSNP 68K Axiom array for rose has also enabled high-throughput SNP genotyping of roses of various ploidy levels (Koning-Boucoiran et al., 2015). The release of three rose genomes--a fragmented genome of *Rosa multiflora* Thunb. (Nakamura et al., 2018) and two genomes of *R. chinensis* 'Old Blush' (Hibrand Saint-Oyant et al., 2018; Raymond et al., 2018)--means that markers can be linked to candidate genes and the function of these genes can be more fully explored. These advancements should assist marker-assisted breeding efforts and potentially pave the way for genomic selection (Smulders et al., 2019).

To map the many phenotypic traits of interest in rose, a number of linkage maps have been created for both diploid and tetraploid rose. Most of these early maps were low-density due to the markers used and involved approximately 100 individuals each. The first integrated consensus map (ICM) for diploid roses represented a considerable step forward, using 597 markers over 530 cM to unify four populations, each of 80-170 individuals (Spiller et al., 2011). This map was then used to locate several major genes, including *Rdr1*, *Blfa* (controlling pink flower color), *RB* (the recurrent blooming gene now identified with *RoKSN*), and *RoSPINDLY* (a gibberellin signaling gene). Furthermore, QTLs for powdery mildew, petal number, and prickles were mapped, illustrating the usefulness of consensus linkage maps for further genetic analyses.

Thanks in part to advances in genotyping methods, recent linkage maps have involved considerably more markers. Yan et al. (2018) employed SNPs from GBS to develop an integrated consensus map for three diploid rose populations with almost six times as many markers as the first ICM. Similarly, Li et al. (2019) developed a map for a single diploid population with over 2,000 markers generated by restriction-site associated DNA sequencing (RAD-seq) technology. In tetraploid roses, use of the WagRhSNP array has resulted in a map of 10,835 SNPs over a total map length of 421.92 cM (Zurn et al., 2018) and one of 25,695 SNPs over 573.66 cM (Bourke et al., 2017). These high-density and ultra-high-density maps have also been enabled by the development of new algorithms and programs that can efficiently map such large numbers of markers, such as MDSmap (Preedy and Hackett, 2016), Lep-Map (Rastas et al., 2016), LPmerge (Endelman and Plomion, 2014), and polymapR (Bourke et al., 2018). While these maps likely have more markers than are needed for most population sizes, they illustrate that marker number is no longer a limiting factor in genetic analyses in roses.

QTL analyses have proven beneficial to rose genetics (see QTLs identified for traits of interest, above) and, given the genotyping advances and the availability of the rose genome, will likely continue to be so. The simplest studies use single-marker analysis in one or a few biparental families, which tests for the association of an individual marker and a phenotype with linear regression. This approach has the advantage of not requiring a linkage map but may result in the underestimation of the QTL effect. Interval mapping, which requires a linkage map, is more powerful (Collard

et al., 2005) and has been used extensively in roses. A more complex but more powerful approach employing identity-by-descent and pedigree information has also been used in roses (Yan et al., 2019) via the program FlexQTL™ (Bink et al., 2008). With any QTL method, having a large population size is imperative for QTL detection, especially for QTL with small effects. Moreover, QTLs need to be validated in independent populations to eliminate possible false positives (Würschum, 2012).

Association mapping provides an alternative way to explore the genetic control traits of interest in roses. As implemented in genome-wide association studies (GWAS), association mapping employs linkage disequilibrium in an unstructured population to identify marker-trait associations. By using a panel of unrelated genotypes, GWAS can exploit many generations of meiotic events rather than the single meiosis permitted by traditional QTL mapping in a biparental family. The resulting higher resolution means that a GWAS may identify a single nucleotide associated with the trait of interest while QTL mapping potentially will identify a large genomic region containing many genes. Moreover, since GWAS rely on diverse germplasm, the results may be more readily employed in a breeding program, whereas a QTL analysis in a single or few populations may be useful only in those or related populations (Oraguzie et al., 2007). The success of a GWAS will depend on a variety of factors, including the level of linkage disequilibrium, the degree of relatedness within the panel, and the panel size used (Myles et al., 2009). GWAS have been successfully performed in a mix of tetraploid, triploid, and diploid roses to determine the genetic basis of adventitious root formation (Nguyen et al., 2017; Nguyen et al., 2020) and petal color (Schulz et al., 2016).

I.4 Conclusion

This study has two chief objectives. The first objective is to characterize diploid rose populations and cultivars for black spot and cercospora resistance; flower productivity; and architectural traits. The second objective is to identify markers associated with desirable phenotypes via single-marker analysis and association mapping. The ultimate goal is to lay the foundation for marker-assisted selection for these important traits of roses.

CHAPTER II

DEVELOPMENT OF SEGREGATING DIPLOID ROSE POPULATIONS

II.1 Synopsis

In order to develop large diploid rose populations segregating for traits of interest and to explore the fertility of new germplasm, 95 diploid by diploid rose crosses were performed from 2015 to 2017. Parents were chosen primarily for their presumed resistance to rose rosette disease (RRD) or for their adaptation traits and included species (*Rosa setigera* Michx., *Rosa palustris* Marsh., and *Rosa rugosa* Thunb.), species hybrids, cultivars, and breeding lines from the Texas A&M breeding program. Cross success was assessed by five parameters: percent hip set, number of seedlings per pollination, percent seed germination, number of seedlings per pollination, and number of seedlings per hip. The pollen fertility of select parents was also assessed. Eight parental combinations resulted in populations of over 100 individuals: 'Snow Pavement' x 'Lena' (346), TAMU7-30 x 'Oso Happy Smoothie' (319), TAMU7-20 x 'Oso Happy Smoothie' (196), J06-20-14-3 x 'Papa Hemeray' (191), *R. setigera*-ARE x 'Ole' (122), J06-20-14-3 x *R. palustris* EB-MM (119), TAMU7-30 x 'Srdce Europy' (117), and 'Snow Pavement' x 'Ole' (103). Most parents chosen for their RRD resistance performed poorly in crosses. As pollen germination rates were not correlated with the parameters of cross success, pollen fertility alone cannot explain the cross failures. A more likely explanation is genetic distance between breeding parents. Parents of interest for future breeding include the species *R. palustris* EB-MM, *R. setigera*-ARE, and *R.*

rugosa f. *alba*-ARE; the cultivars ‘Oso Happy Smoothie’ and ‘Srdce Europy’; and Texas A&M breeding lines M4-4, TAMU7-20, and TAMU7-30.

II.2 Introduction

Roses (*Rosa spp.*) have been cultivated for over 4000 years for ornamental, medicinal, and culinary purposes (Krüssman, 1981). Found throughout the northern hemisphere, the genus includes 100-200 species, most of which belong to the subgenus *Rosa.* Traditional morphology-based taxonomy divides this subgenus into ten sections (Wissemann, 2003; Rehder and Dudley, 1940), but this is not fully supported by molecular evidence (Fougère-Danezan et al., 2015; Bruneau et al., 2007; Ritz and Wissemann, 2005). The deliberate breeding of roses began in China, likely over 1000 years ago (Guoliang, 2003), and breeding efforts expanded considerably with the introduction of Chinese roses to Europe in the eighteenth century (Joyaux, 2003). Modern roses are derived primarily from ten different species: *Rosa canina* L. (sect. *Caninae*), *Rosa chinensis* Jacq. (sect. *Indicae*), *Rosa foetida* Herrm. (sect. *Pimpinellifoliae*), *Rosa gallica* L. (also known as *Rosa rubra* Blackw., sect. *Rosa*), *Rosa gigantea* Colett ex Crép. (sect. *Indicae*), *Rosa moschata* Herrm. (sect. *Synstylae*), *Rosa multiflora* Thunb. ex Murr. (sect. *Synstylae*), *Rosa phoenicea* Boiss. (sect. *Synstylae*), *Rosa rugosa* Thunb. (sect. *Cinnamomeae*), and *Rosa wichurana* Crép. (sect. *Synstylae*) (Crespel and Mouchotte, 2003). While this has resulted in tens of thousands of cultivars (Cairns, 2000), it is only a fraction of the potential diversity of the rose genus.

Novel flower colors and shapes have always been a priority for rose breeding, including for garden rose breeding. In the 21st century, however, disease resistance and

hardiness have also become breeding priorities (Gudin, 2003; Hutton, 2012; Byrne et al., 2019; Waliczek et al., 2018), which can necessitate the use of new germplasm—namely, species and obscure species hybrids. Frequently, little is known about the fertility of these new potential breeding parents, necessitating a trial-and-error approach for each potential parent.

The breeding priorities at the Rose Breeding and Genetics Program at Texas A&M University, College Station, Texas, reflect the current emphasis on well-adapted roses. Breeding goals include adaptation to the subtropical Texas climate, resistance to the fungi black spot (*Diplocarpon rosae* Wolf) and cercospora (*Rosisphaerella rosicola* Pass.), consistent flowering, and attractive plant architecture (Byrne, 2015). Now of particular importance is combining these attributes with resistance to rose rosette disease (RRD), a fatal disease of roses caused by the Emaravirus *Rose rosette virus* (RRV). Currently, approximately 95% of roses are estimated to be susceptible to RRD, and many of the possibly resistant roses are species, species hybrids, or obscure cultivars not extensively used in breeding (Byrne et al., 2015).

Of the species thought resistant, three diploid species are of particular interest: *Rosa setigera* Michx., *Rosa palustris* Marsh. (Amrine, 1996), and *R. rugosa* (M. Windham, personal communication). *R. setigera* (sect. *Synstylae*), a climbing rose native to North America, is the only known dioecious member of the genus *Rosa*. The sex of individual plants cannot be reliably determined visually and instead the pollen must be tested for germination (Kevan et al., 1990). Approximately 20 first-generation hybrids of *R. setigera* are reported (Cairns, 2000). *R. palustris* (sect. *Carolinae*) is also native to

North America (Wissemann, 2003) but has been used in rose breeding even less than *R. setigera* with fewer than 10 first-generation hybrids of *R. palustris* reported. Interestingly, this includes hybrids between *R. palustris* and the third species of interest, *R. rugosa* (Cairns, 2000). *R. rugosa* has been used in breeding enough to be considered one of the founding species of modern roses (see list above) but is still notoriously difficult to breed with (Zlesak, 1998). Pre-existing hybrids of these three species may prove to be better parents for RRD resistance breeding. Regardless, breeding for RRD resistance will likely be difficult from a perspective of parent fertility alone, and experimentation is needed to identify fertile genotypes for breeding.

This study, therefore, had two main goals. The first was to investigate the fertility of new germplasm—*R. setigera, R. palustris, R. rugosa,* and their hybrids—to enable effective breeding with these genotypes in the future. The second was to develop, from these and other genotypes, diploid rose populations segregating for RRD resistance and other traits of interest (black spot resistance, plant architecture, etc.) large enough for future genetic studies.

II.3 Materials and methods

II.3.1 Parent selection

Parents were chosen based on their presumed RRD resistance, fertility, and adaptation to the central Texas climate (Tables 2, 3). In 2015, parents believed to be resistant to RRD were two accessions of *Rosa palustris* f. *plena* W.H. Lewis from the Antique Rose Emporium, Independence, TX, one once-flowering and one continuous-flowering (*R. palustris* f. *plena* OB-ARE and *R. palustris* f. *plena* EB-ARE,

respectively); ‘Basye’s Purple’, a hybrid between *Rosa foliolosa* Nutt. ex. Torr. & A. Gray and *R. rugosa*; and the shrub roses ‘Papa Hemeray’, ‘Oso Happy Smoothie’, and ‘Red Drift’. Two fertile shrub roses from the Texas A&M breeding program, J06-20-14-3 and M4-4, were also used. These roses were developed from *R. wichurana* and *Indicae*-derived parents and are known to be well-adapted to local conditions. ‘Old Blush’ was also used as a parent due to its historical importance to rose breeding.

In 2016, updated RRD resistance information and ploidy determination resulted in a slightly different selection of parents. New in 2016 were the climbing rose *R. setigera* hybrids ‘Baltimore Belle’ and ‘Srdce Europy’; 14 accessions of *R. setigera* from the Chambersville Tree Farm in McKinney, TX (denoted by CH) and the Antique Rose Emporium (denoted by ARE); the *R. rugosa* hybrid ‘Topaz Jewel’; ‘Champneys’ Pink Cluster’, a noisette rose significant to historical rose breeding; and a continuous-flowering *R. palustris* accession provided by Malcolm Manners, Lakeland, Florida (*R. palustris* EB-MM). The shrubs ‘Lena’ and ‘Ole’ were used for their fertility and horticultural traits. ‘Basye’s Purple’, ‘Papa Hemeray’, ‘Oso Happy Smoothie’, and the afore-mentioned *R. palustris* f. *plena* accessions were used again. TAMU7-20 and TAMU7-30, Texas A&M breeding lines, were added for their adaptation qualities. Again, ‘Old Blush’ was used as a parent.

Table 2 Female parents used in diploid rose crosses from 2015 to 2017. 'Section' indicates section of the rose genus to which the species belongs or primary section(s) from which the cultivar was derived based on available pedigree information. Sections are based on the traditional taxonomy of Rehder and Dudley (1940) and Wisseman (2003). Names in parentheses indicate patented name when needed to avoid confusion.

Genotype	Year	Section
Baltimore Belle	2016	*Synstylae, Rosa*
Basye's Purple	2015-2016	*Carolinae, Cinnamomeae*
Champney's Pink Cluster	2016	*Synstylae, Indicae*
J06-20-14-3	2015-2017	*Synstylae, Indicae*
Lena (Baiena)	2016-2017	*Synstylae, Indicae*
M4-4	2015-2017	*Synstylae, Indicae*
Moser House Shed Rose	2017	Unknown
Old Blush	2015-2017	*Indicae*
Ole (Baiole)	2016-2017	*Synstylae, Indicae, Pimpinellifoliae*
Oso Happy Smoothie (ZLEcharlie)	2015-2016	*Synstylae*
Papa Hemeray	2015-2017	*Indicae, Synstylae*
Purple Pavement	2017	*Cinnamomeae*
R. palustris f. *plena* EB-ARE	2015	*Carolinae*
R. palustris f. *plena* OB-ARE	2015	*Carolinae*
R. rugosa f. *alba*-ARE	2017	*Cinnamomeae*
R. setigera-ARE	2016	*Synstylae*
R. setigera-CH-33-17-50	2016	*Synstylae*
R. setigera-CH-33-18-42	2016	*Synstylae*
R. setigera-CH-33-18-52	2016	*Synstylae*
R. setigera-CH-HRG	2016	*Synstylae*
R. setigera-CH-NBW	2016	*Synstylae*
R. setigera-CH-NL	2016	*Synstylae*
R. setigera-CH-U1	2016	*Synstylae*
R. setigera-CH-U2	2016	*Synstylae*
R. setigera-CH-U3	2016	*Synstylae*
R. setigera-CH-U4	2016	*Synstylae*
Red Drift (Meigalpio)	2015	*Synstylae*
Sarah van Fleet	2017	*Cinnamomeae*
Snow Pavement	2017	*Cinnamomeae*
TAMU7-20	2016-2017	*Synstylae, Indicae*
TAMU7-30	2016-2017	*Synstylae, Indicae*
Topaz Jewel (MORyelrug)	2016-2017	*Cinnamomeae, Synstylae, Indicae*

Table 3 Male parents used in diploid rose crosses from 2015 to 2017. 'Section' indicates section of the rose genus to which the species belongs or primary section(s) from which the cultivar was derived based on available pedigree information. Sections are based on the traditional taxonomy of Rehder and Dudley (1940) and Wisseman (2003). Names in parentheses indicate patented name when needed to avoid confusion.

Genotype	Year	Section
Basye's Purple	2015-2016	*Carolinae, Cinnamomeae*
J06-20-14-3	2015-2017	*Synstylae, Indicae*
Lena (Baiena)	2016-2017	*Synstylae, Indicae*
M4-4	2015-2017	*Synstylae, Indicae*
Old Blush	2016	*Indicae*
Ole (Baiole)	2016-2017	*Synstylae, Indicae, Pimpinellifoliae*
Oso Happy Smoothie (ZLEcharlie)	2016-2017	*Synstylae*
Papa Hemeray	2015-2016	*Indicae, Synstylae*
R. palustris f. *plena* EB-ARE	2015-2017	*Carolinae*
R. palustris EB-MM	2016-2017	*Carolinae*
R. palustris f. *plena* OB-ARE	2015-2017	*Carolinae*
R. palustris OB-PrM	2017	*Carolinae*
Snow Pavement	2017	*Cinnamomeae*
Srdce Europy	2016	*Synstylae*
Sweet Vigorosa	2017	Unknown
Topaz Jewel (MORyelrug)	2017	*Cinnamomeae, Synstylae, Indicae*

In 2017, new parents were added once again. These included several *R. rugosa* hybrids ('Purple Pavement', 'Snow Pavement', and 'Sarah Van Fleet'), as well as an accession of *R. rugosa* f. *alba* Rehder from the Antique Rose Emporium. Another accession of *R. palustris* from Prairie Moon Nursery, Winona, MN (*R. palustris* OB-PrM) was added as a pollen parent. Finally, the floribunda 'Sweet Vigorosa' was used as a pollen parent, as at that time it had not contracted RRD. The breeding lines J06-20-14-3, M4-4, TAMU7-20, and TAMU7-30 were employed again, as were 'Lena', 'Ole', 'Papa Hemeray', 'Topaz Jewel', 'Old Blush', the two *R. palustris* f. *plena* accessions, *R. palustris* EB-MM, and 'Oso Happy Smoothie'.

In all years, use of a parent as male or female was determined by plant availability and past performance as either male or female. In all, over the three years, 95 unique crosses were made (Table 4).

Table 4 Diploid rose crosses made from 2015 to 2017 by the Texas A&M Rose Breeding and Genetics Program and Weeks Roses.

Female	Male	Year
Baltimore Belle	M4-4	2016
Baltimore Belle	Papa Hemeray	2016
Basye's Purple	J06-20-14-3	2015-2016
Basye's Purple	Old Blush	2016
Basye's Purple	*R. palustris* f. *plena* EB-ARE	2015
Basye's Purple	*R. palustris* f. *plena* OB-ARE	2015
Basye's Purple	Srdce Europy	2016
Champney's Pink Cluster	Old Blush	2016
Champney's Pink Cluster	*R. palustris* f. *plena* EB-ARE	2016
Champney's Pink Cluster	*R. palustris* EB-MM	2016
J06-20-14-3	Basye's Purple	2016
J06-20-14-3	Papa Hemeray	2015-2016
J06-20-14-3	*R. palustris* f. *plena* EB-ARE	2015-2016
J06-20-14-3	*R. palustris* EB-MM	2016
J06-20-14-3	*R. palustris* f. *plena* OB-ARE	2015-2016
J06-20-14-3	*R. palustris* OB-PrM	2017
J06-20-14-3	Srdce Europy	2016
Lena (Baiena)	*R. palustris* f. *plena* EB-ARE	2016-2017
Lena (Baiena)	*R. palustris* EB-MM	2017
Lena (Baiena)	*R. palustris* f. *plena* OB-ARE	2016-2017
Lena (Baiena)	*R. palustris* OB-PrM	2017
Lena (Baiena)	Snow Pavement	2017
Lena (Baiena)	Sweet Vigorosa	2017
Lena (Baiena)	Topaz Jewel (MORyelrug)	2017
M4-4	Basye's Purple	2015-2016
M4-4	*R. palustris* f. *plena* EB-ARE	2015-2017
M4-4	*R. palustris* EB-MM	2016-2017
M4-4	*R. palustris* f. *plena* OB-ARE	2015-2017
M4-4	*R. palustris* OB-PrM	2017

Table 4 Continued

Female	Male	Year
M4-4	Srdce Europy	2016
M4-4	Sweet Vigorosa	2017
Moser House Shed Rose	M4-4	2017
Old Blush	Basye's Purple	2015
Old Blush	*R. palustris* f. *plena* EB-ARE	2015-2017
Old Blush	*R. palustris* EB-MM	2016-2017
Old Blush	*R. palustris* f. *plena* OB-ARE	2015-2017
Old Blush	Srdce Europy	2016
Ole (Baiole)	*R. palustris* f. *plena* EB-ARE	2016-2017
Ole (Baiole)	*R. palustris* EB-MM	2017
Ole (Baiole)	*R. palustris* f. *plena* OB-ARE	2016
Ole (Baiole)	Snow Pavement	2017
Ole (Baiole)	Topaz Jewel (MORyelrug)	2017
Oso Happy Smoothie (ZLEcharlie)	J06-20-14-3	2015
Oso Happy Smoothie (ZLEcharlie)	M4-4	2015
Oso Happy Smoothie (ZLEcharlie)	Papa Hemeray	2015
Oso Happy Smoothie (ZLEcharlie)	*R. palustris* f. *plena* EB-ARE	2016
Oso Happy Smoothie (ZLEcharlie)	*R. palustris* EB-MM	2016
Oso Happy Smoothie (ZLEcharlie)	*R. palustris* f. *plena* OB-ARE	2016
Oso Happy Smoothie (ZLEcharlie)	Srdce Europy	2016
Papa Hemeray	Basye's Purple	2015
Papa Hemeray	*R. palustris* f. *plena* EB-ARE	2015-2017
Papa Hemeray	*R. palustris* EB-MM	2016-2017
Papa Hemeray	*R. palustris* f. *plena* OB-ARE	2015-2017
Purple Pavement	M4-4	2017
R. palustris f. *plena* EB-ARE	J06-20-14-3	2015
R. palustris f. *plena* EB-ARE	M4-4	2015
R. palustris f. *plena* EB-ARE	Papa Hemeray	2015
R. palustris f. *plena* OB-ARE	J06-20-14-3	2015
R. palustris f. *plena* OB-ARE	M4-4	2015

Table 4 Continued

Female	Male	Year
R. rugosa f. *alba*-ARE	M4-4	2017
R. rugosa f. *alba*-ARE	*R. palustris* EB-MM	2017
R. setigera-ARE	Lena (Baiena)	2016
R. setigera-ARE	Ole (Baiole)	2016
R. setigera-CH-33-17-50	M4-4	2016
R. setigera-CH-33-17-50	Papa Hemeray	2016
R. setigera-CH-33-18-42	M4-4	2016
R. setigera-CH-33-18-52	Papa Hemeray	2016
R. setigera-CH-HRG	M4-4	2016
R. setigera-CH-NBW	M4-4	2016
R. setigera-CH-NL	M4-4	2016
R. setigera-CH-U1	Old Blush	2016
R. setigera-CH-U2	Papa Hemeray	2016
R. setigera-CH-U2	Srdce Europy	2016
R. setigera-CH-U3	M4-4	2016
R. setigera-CH-U3	Oso Happy Smoothie (ZLEcharlie)	2016
R. setigera-CH-U4	Oso Happy Smoothie (ZLEcharlie)	2016
Red Drift (Meigalpio)	*R. palustris* f. *plena* EB-ARE	2015
Sarah van Fleet	J06-20-14-3	2017
Snow Pavement	Lena (Baiena)	2017
Snow Pavement	Ole (Baiole)	2017
Snow Pavement	*R. palustris* f. *plena* OB-ARE	2017
TAMU7-20	Oso Happy Smoothie (ZLEcharlie)	2016-2017
TAMU7-20	*R. palustris* f. *plena* EB-ARE	2016
TAMU7-20	*R. palustris* EB-MM	2016
TAMU7-20	*R. palustris* f. *plena* OB-ARE	2016
TAMU7-20	Srdce Europy	2016
TAMU7-30	Oso Happy Smoothie (ZLEcharlie)	2016-2017
TAMU7-30	*R. palustris* f. *plena* EB-ARE	2016
TAMU7-30	*R. palustris* EB-MM	2016
TAMU7-30	*R. palustris* f. *plena* OB-ARE	2016
TAMU7-30	Srdce Europy	2016
Topaz Jewel (MORyelrug)	Lena (Baiena)	2017
Topaz Jewel (MORyelrug)	Ole (Baiole)	2017

Table 4 Continued

Female	Male	Year
Topaz Jewel (MORyelrug)	*R. palustris* f. *plena* EB-ARE	2016
Topaz Jewel (MORyelrug)	*R. palustris* f. *plena* OB-ARE	2016

II.3.2 Crossing procedure

Crosses were made primarily at Texas A&M University, College Station, TX and by collaborators at Weeks Roses, Wasco, CA. Pollen was collected each year and stored in vials in a -20° freezer. Flowers were hand-emasculated and pollen applied with a soft brush. If flowers were pollinated in the greenhouse, flowers were left uncovered, but flowers pollinated outside were covered with tulle netting to prevent subsequent pollen contamination by insects. Hips were harvested as they ripened with most being harvested in October/November of the year of the cross. Seeds were extracted from hips, stratified in Metro-Mix® 900 (Sun Gro Horticulture, Agawam, MA) for at least two months at approximately 2°C, and removed in February from cold storage to the greenhouse for germination.

Number of pollinations, number of hips, number of seeds, and number of seedlings were recorded when possible. Five parameters were calculated when possible to gauge cross success: percent hip set (number of hips/number of pollinations), percent seed germination (number of seedlings/number of seeds), number of seeds per pollination, number of seedlings per pollination, and number of seedlings per hip. Statistics were performed in JMP Pro® 15 (SAS Institute Inc., Cary, NC).

II.3.3 Ploidy determination

Mitotic root squashes were performed on some parents to determine or confirm the ploidy, as entirely diploid populations were desired for subsequent genetic studies. Squashes were performed according to the protocol of Zlesak (2009). At least five cells with a clear number of chromosomes were required to verify the ploidy of an individual. Due to availability of root tissue, ploidy was frequently determined after a genotype was used in a cross; therefore, interploidy crosses were occasionally performed and these were excluded from the subsequent analyses.

II.3.4 Pollen fertility assessment

Pollen fertility for select parents (dependent on pollen availability and if the fertility was in doubt) were assessed by germinating pollen in a sucrose solution as in the hanging drop pollen assay of Zlesak (2004) with the modification that pollen was tested in solutions of 1.5%, 5%, 10%, and 15% sucrose (weight/volume). Pollen was tested the same year it was used in pollinations, and one test per sucrose concentration per genotype was performed. Pollen germination was estimated after 3-4 hours. Pollen tubes were only counted if they were at least the length of the pollen grain from which they emerged. This assay was also used to determine the sex of the various *R. setigera* accessions. Additionally, pollen from eight additional *R. palustris* accessions not used in pollinations were tested to determine potential usefulness for future pollinations. Statistics were performed in JMP Pro® 15. ANOVA was used to test for differences in germination rates between sucrose solutions. Pearson's product-moment correlation

coefficient was used to test for correlations between male pollen germination and the five parameters of cross success.

II.4 Results

II.4.1 Parent performance and populations produced

Over the three years, approximately 9,300 pollinations were performed. 13,663 seeds were produced, resulting in approximately 2,300 seedlings (Appendix A). Hip set ranged from 0 to 96% (Table 5). Seed germination varied from 0 to 77% with a mean of approximately 15%. On average, only one seed per pollination was obtained, though this varied dramatically. Seedlings per pollination and seeds per pollination were very strongly correlated, as were seedlings per hip with seeds per pollination and seedlings per hip with seedlings per pollination (Table 6, Fig. 1). Percent hip set was moderately strongly correlated with seeds per pollination and seedlings per pollination. These strong correlations, however, were mostly due to the effect of a single cross (*R. rugosa* f. *alba*-ARE x *R. palustris* EB-MM) and should be interpreted with caution.

Table 5 Mean, range (minimum-maximum), and standard error of the mean (SEM) of five parameters of cross success in diploid rose pollination results over three years (2015-2017). % hip set = number of hips/number of pollinations; seeds/poll. = seeds/number of pollinations; % seed germ. = number of seedlings/number of seeds; seedlings/poll. = number of seedlings/number of pollinations; seedlings/hip = number of seedlings/number of hips.

Parameter	Mean	Range	SEM
% Hip set	23.6	0-96.3	2.5
Seeds/poll.	1.2	0-35	0.4
% Seed germ.	14.8	0-76.9	1.7
Seedlings/poll.	0.3	0-8.8	0.1
Seedlings/hip	0.8	0-10	0.2

*Table 6 Pearson's product-moment correlation coefficients between cross success parameters and maximum pollen germination for all parents tested for pollen germination and used in diploid rose crosses between 2015 and 2017. % hip set = number of hips/number of pollinations; seeds/poll. = seeds/number of pollinations; % seed germ. = number of seedlings/number of seeds; seedlings/poll. = number of seedling/number of pollinations; seedlings/hip = number of seedlings/number of hips; max. pollen germ. = highest percent pollen germination from four sucrose concentrations. ns, $p > 0.05$; *, $0.01 \leq p \leq 0.05$; **, $0.001 \leq p \leq 0.01$; ***, $0.0001 \leq p \leq 0.001$; ****, $p < 0.0001$.*

	% Hip set	Seeds/poll.	% Seed germ.	Seedlings/ poll.	Seedlings/ hip	Max. pollen germ.
% Hip set	1					
Seeds/poll.	0.52****	1				
% Seed germ.	0.24*	0.15^{ns}	1			
Seedlings/poll.	0.49****	0.94****	0.31**	1		
Seedlings/hip	0.3**	0.71****	0.56****	0.78****	1	
Max. pollen germ.	0.06^{ns}	0.16^{ns}	0.05^{ns}	0.11^{ns}	0.19^{ns}	1

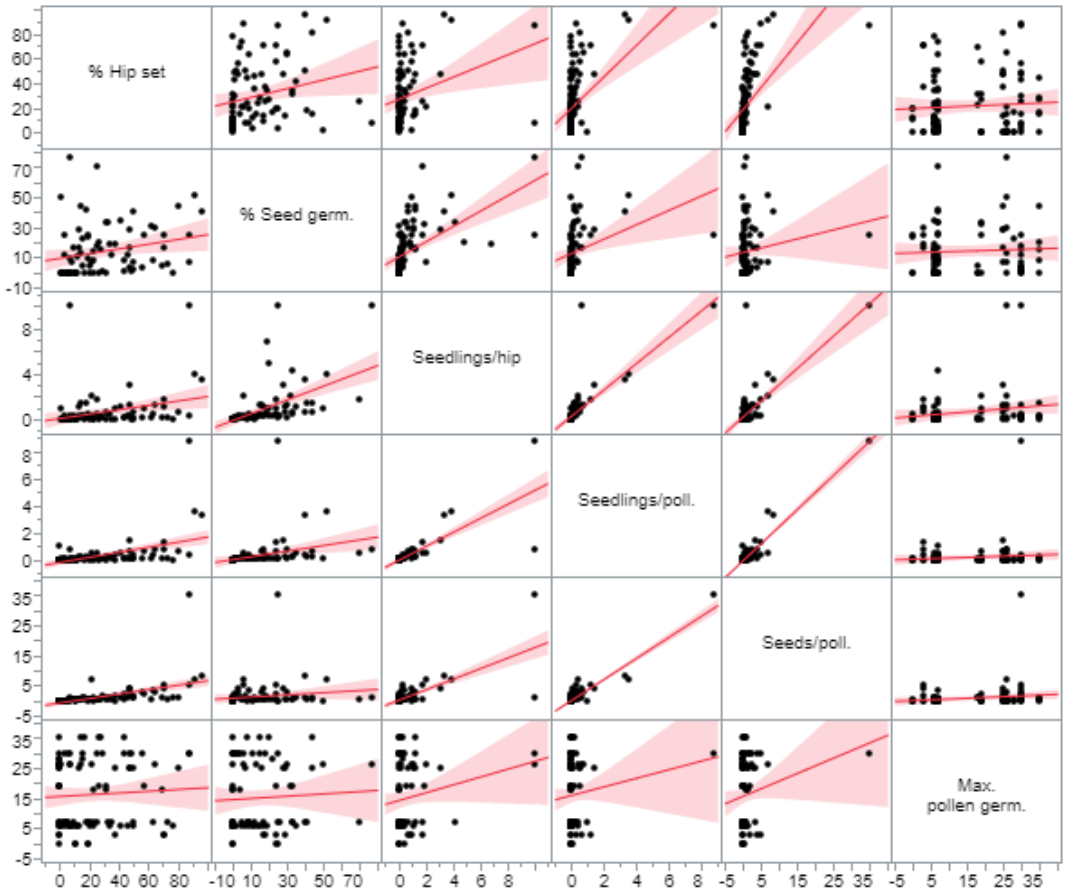

Figure 1 Scatterplot of correlations between parameters of cross success and pollen germination in diploid rose crosses made 2015-2017. Correlations were tested with Pearson's product-moment correlation. % hip set = number of hips/number of pollinations; seeds/poll. = seeds/number of pollinations; % seed germ. = number of seedlings/number of seeds; seedlings/poll. = number of seedlings/number of pollinations; seedlings/hip = number of seedlings/number of hips; max. pollen germ. = highest percent pollen germination from four sucrose concentrations.

Due to design issues and statistical constraints, interactions between male and female parents could not be tested; however, to compare the performance of specific parents, the average percent hip set, percent seed germination, number of seeds per pollination, number of seedlings per pollination, and number of seedlings per hip were examined per parent, including per male parent. *R. setigera*-ARE had the highest hip set

among female parents (Fig. 2a). Among male parents, ‘Lena’ and ‘Ole’ yielded higher hip set, but this is likely because data on number of pollinations were only available for these cultivars when they were crossed with *R. setigera*-ARE. Aside from these two cultivars, ‘Oso Happy Smoothie’ and *R. palustris* OB-PrM when used as male parents yielded the highest hip set (Fig. 2b).

Most female parents produced under five seeds per pollination (Fig. 3a). The only female parents that produced five or more seeds per pollination were *R. rugosa* f. *alba*-ARE, *R. setigera*-ARE, and the *R. rugosa* hybrid ‘Purple Pavement’. Again, crosses with ‘Lena’ and ‘Ole’ as male parents yielded a higher number of seeds per pollination than crosses with other males; however, the same caveat as above applies. Otherwise, *R. palustris* EB-MM as a male parent yielded the highest number of seeds per pollination (Fig. 3b).

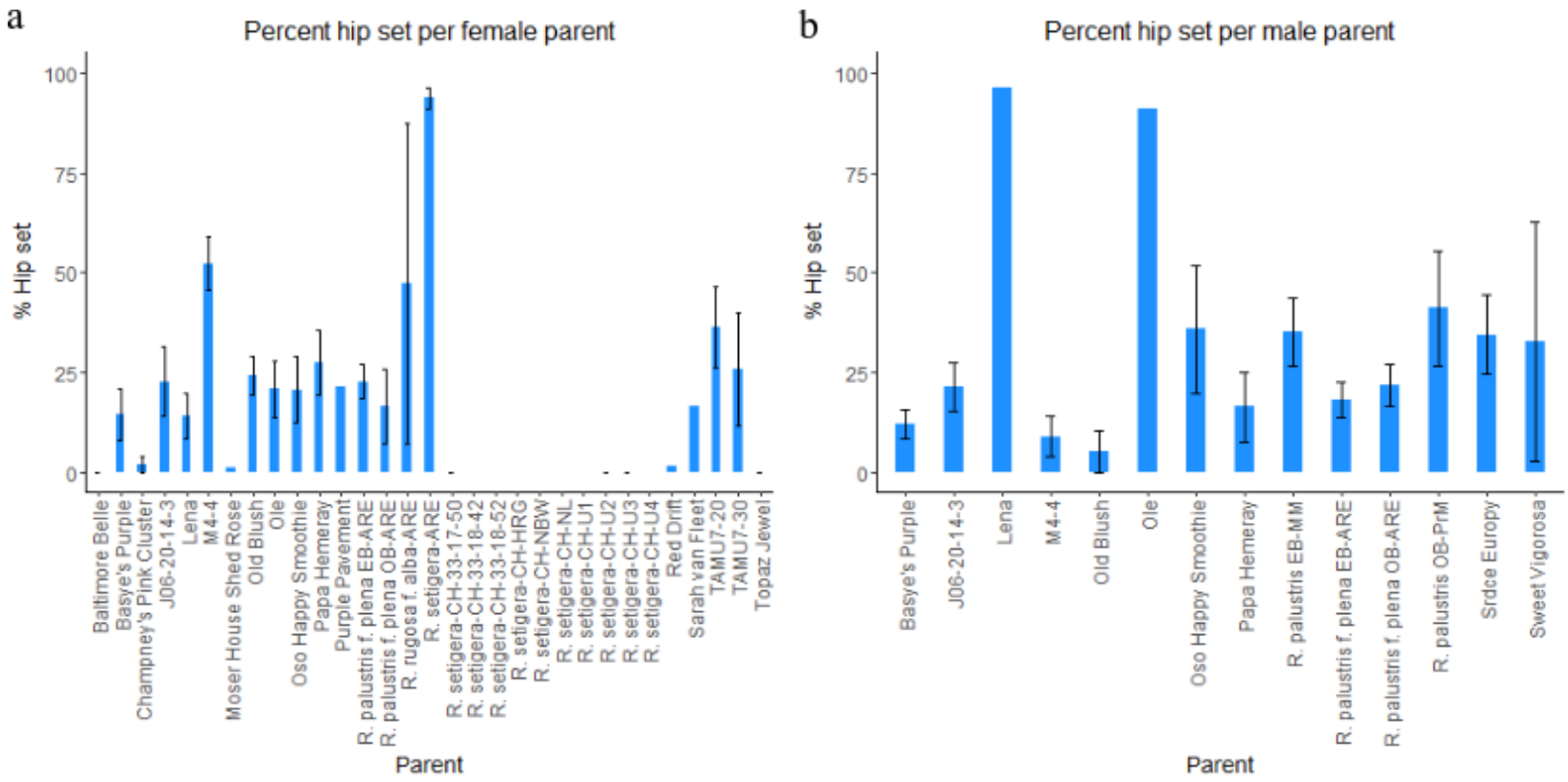

Figure 2 Average percent hip set (number of hips/number of pollinations) for female parents (a) and male parents (b) used in diploid rose crosses made 2015-2017. Error bars reflect standard error of the mean.

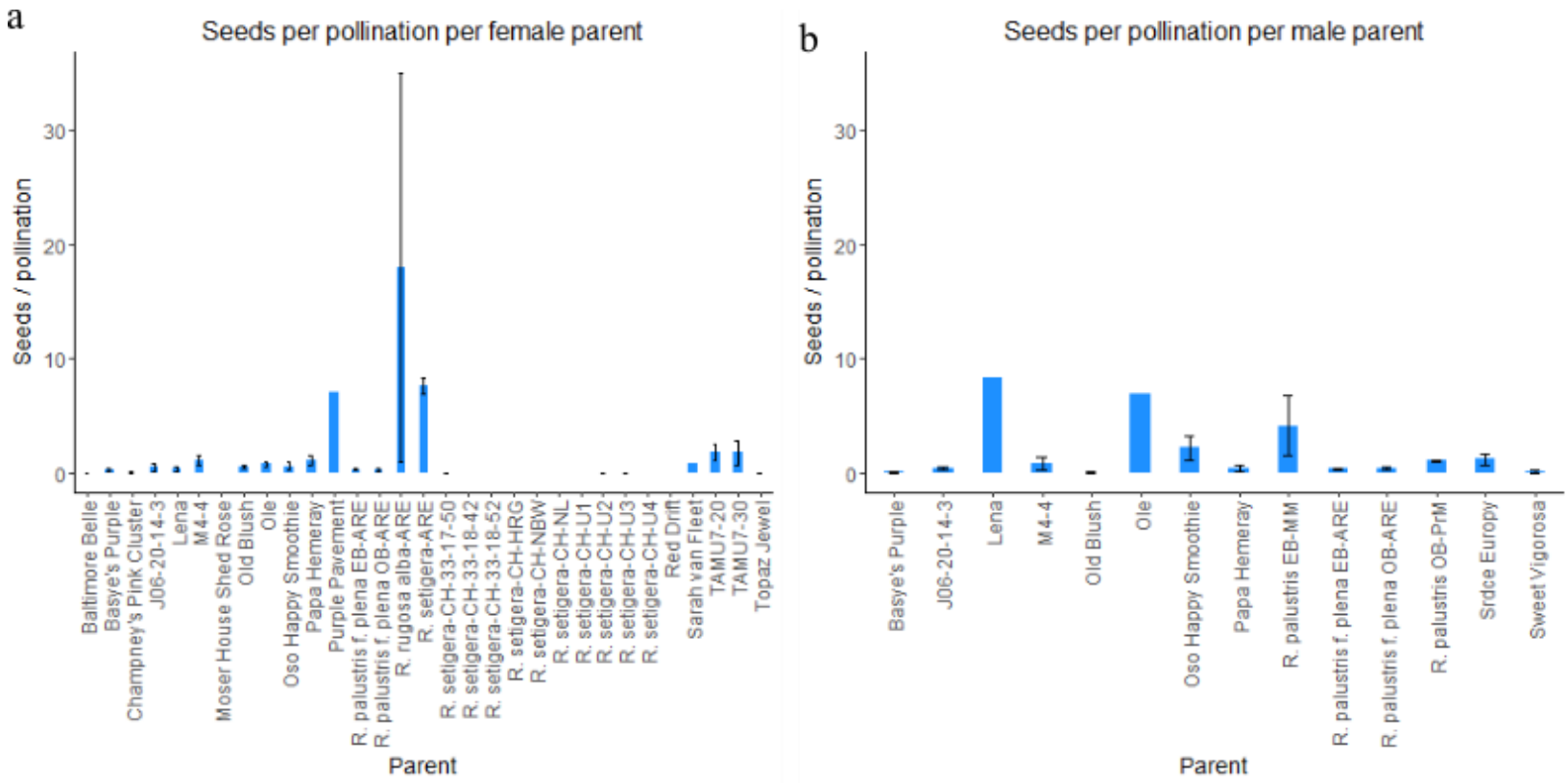

Figure 3 Average number of seeds per pollination for female parents (a) and male parents (b) used in diploid rose crosses made 2015-2017. Error bars reflect standard error of the mean.

The females *R. rugosa* f. *alba*-ARE, *R. setigera*-ARE, and ‘Moser House Shed Rose’ resulted in the highest percent of germinated seed (Fig. 4a); however, the ‘Moser House Shed Rose’ results must be interpreted with caution, as only two seeds were produced. Crosses with the Texas A&M breeding line M4-4 as a male parent yielded a higher percent of germinated seed than any other male parent, closely followed by ‘Srdce Europy’ and ‘Ole’ (Fig. 4b).

The females *R. rugosa* f. *alba*-ARE and *R. setigera*-ARE resulted in the highest number of seedlings per pollination (Fig. 5a), but *R. rugosa* f. *alba*-ARE and ‘Snow Pavement’ resulted in the highest number of seedlings per hip (Fig. 6a). Crosses with ‘Lena’, ‘Ole’, and *R. palustris* EB-MM as male parents resulted in the highest number of seedlings per pollination (Fig. 5b). Crosses with ‘Ole’, ‘Lena’, and M4-4 resulted in the highest number of seedlings per hip among the male parents (Fig. 6b).

The most successful parental combination in terms of number of seedlings produced over three years was ‘Snow Pavement’ x ‘Lena’ (346), followed by TAMU7-30 x ‘Oso Happy Smoothie’ (319) and TAMU7-20 x ‘Oso Happy Smoothie’ (196). Five other combinations resulted in populations over 100: J06-20-14-3 x ‘Papa Hemeray’ (191), *R. setigera*-ARE x ‘Ole’ (122), J06-20-14-3 x *R. palustris* EB-MM (119), TAMU7-30 x ‘Srdce Europy’ (117), and ‘Snow Pavement’ x ‘Ole’ (103). However, as seedlings were counted shortly after germination, this is not necessarily indicative of the final population size.

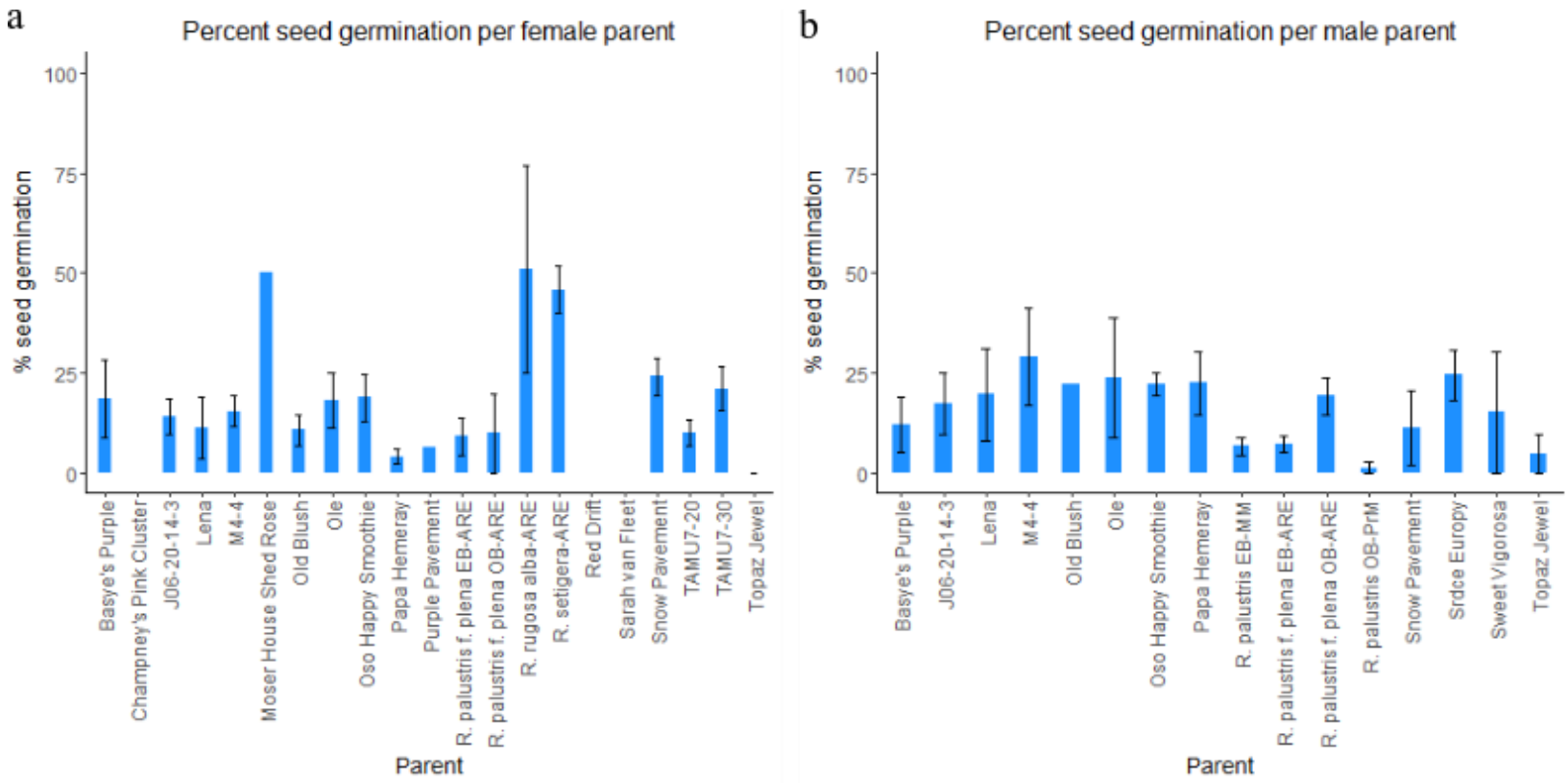

Figure 4 Average percent seed germination (number of seedlings/number of seeds) for female parents (a) and male parents (b) used in diploid rose crosses made 2015-2017. Error bars reflect standard error of the mean.

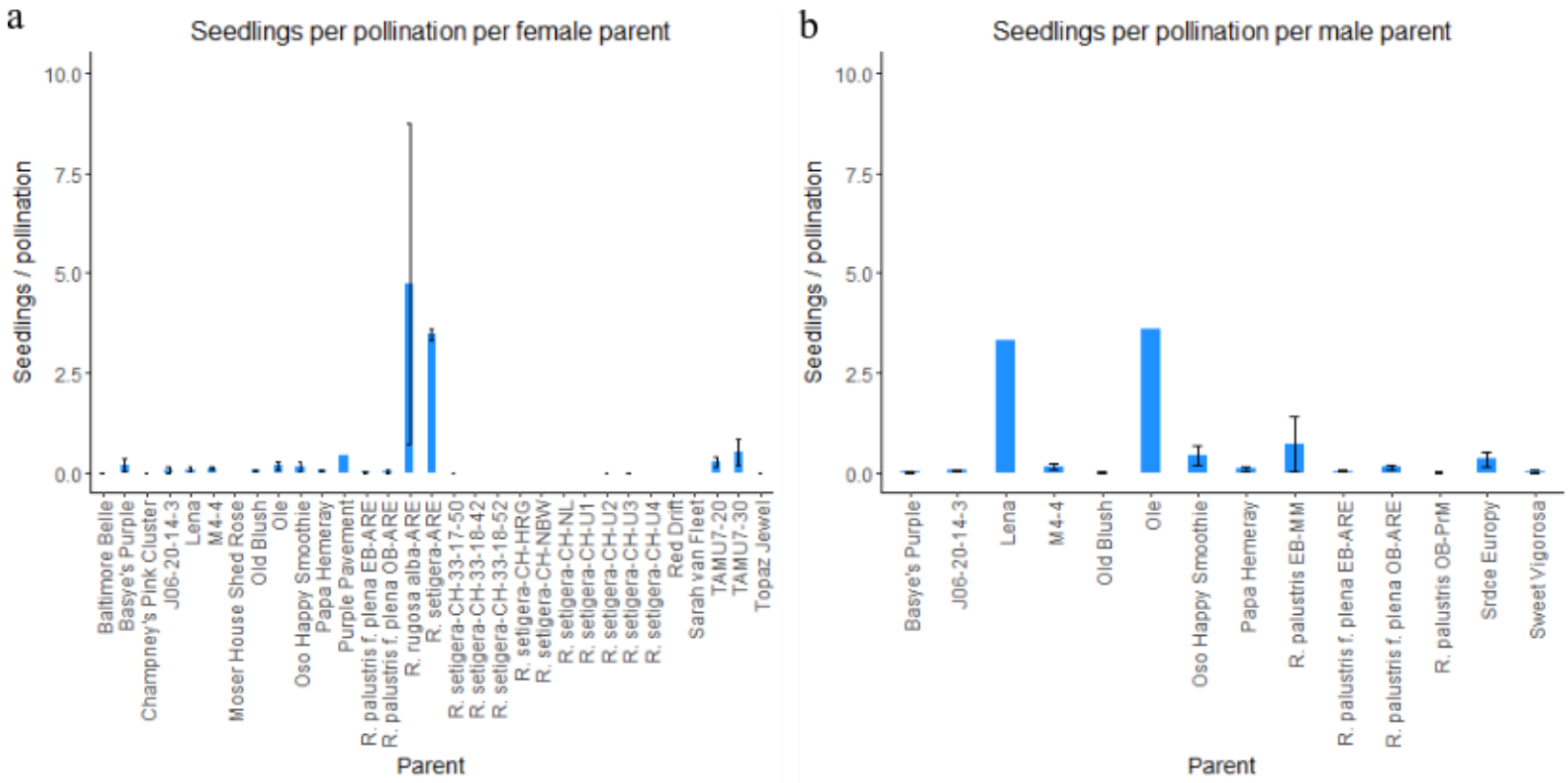

Figure 5 Average number of seedlings per pollination for female parents (a) and male parents (b) used in diploid rose crosses made 2015-2017. Error bars reflect standard error of the mean.

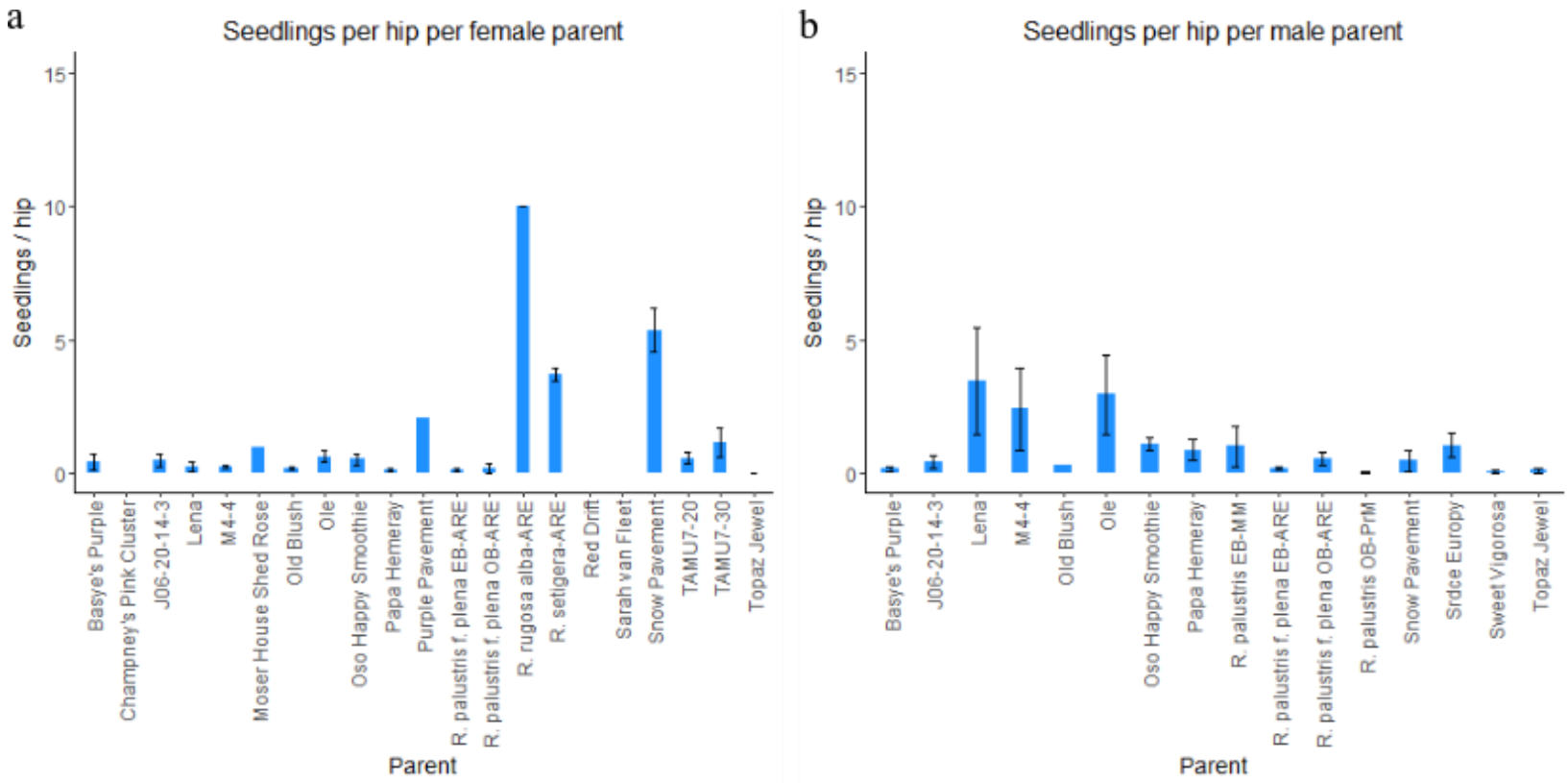

Figure 6 Average seedlings per hip for female parents (a) and male parents (b) used in diploid rose crosses made 2015-2017. Error bars reflect standard error of the mean

II.4.2 Ploidy determination

The ploidy level of ‘Champney’s Pink Cluster’, ‘Papa Hemeray’, ‘Oso Happy Smoothie’, *R. palustris* f. *plena* EB-ARE, and *R. palustris* f. *plena* OB-ARE was confirmed to be diploid via the root squash procedure (Table 7). ‘Srdce Europy’ was also found to be diploid. ‘Nearly Wild’ was confirmed to be triploid (Zlesak, 2009). ‘Little Buckaroo’ was found to be triploid despite previous evidence suggesting that it was diploid (Ueckert, 2014). ‘Geschwinds Nordlandrose’, however, was found to be tetraploid. Any seedlings that resulted from crosses with these higher ploidy levels were excluded from the subsequent genetic study.

Table 7 Ploidy determinations for select rose parents.

Genotype	Ploidy
Champney's Pink Cluster	2x
Oso Happy Smoothie	2x
Papa Hemeray	2x
R. palustris f. *plena* EB-ARE	2x
R. palustris f. *plena* OB-ARE	2x
Srdce Europy	2x
Little Buckaroo	3x
Nearly Wild	3x
Geschwinds Nordlandrose	4x

II.4.3 Pollen fertility assessment

Pollen germination ranged from 0% to 45%, depending on the genotype (Table 8). There was no significant difference in the maximum germination rates from the four sucrose solutions ($p<0.05$) (Fig. 7); however, for an individual genotype, the pollen germination rate could vary considerably across sucrose solutions. Pollen germination was not correlated with any of the parameters of cross success (Table 6, Fig. 1).

A considerable difference in pollen germination rates between the *R. palustris* f. *plena* accessions and the *R. palustris* EB-MM accession was observed, with the latter having a maximum pollen germination of 30% while the *R. palustris* f. *plena* accessions were consistently under 10%. The remaining eight *R. palustris* accessions had variable pollen germination rates as well. The three Texas A&M breeding lines tested had some of the highest pollen germination rates; the only one not tested, TAMU7-30, produced few anthers and consequently there was insufficient pollen for testing. Finally, most of the *R. setigera* accessions for which pollen was available were determined to be male; only *R. setigera*-CH-U2 and *R. setigera*-CH-U4 were identified as female.

Table 8 Percent pollen germination for 29 diploid rose genotypes tested in four sucrose solutions, arranged from greatest maximum germination to least. Blank cells indicate that a clear count could not be obtained from the test.

Genotype	1.5% sucrose (%)	5% sucrose (%)	10% sucrose (%)	15% sucrose (%)	Maximum germination (%)
Champney's Pink Cluster	14	45	30	14	45
TAMU7-20	38				38
J06-20-14-3	22	20	35	35	35
R. palustris EB-MM	9	14	30	19	30
Old Blush		10	11	28	28
R. palustris OB-FF-1	28	20	15	21	28
M4-4	5	12	15	26	26
R. rugosa f. alba-ARE	8	18	13	25	25
Srdce Europy	25				25
R. setigera-CH-HRG	5	22	8	20	22
Papa Hemeray		19	8	16	19
R. palustris OB-PrM	<1	17.5		9	18
R. palustris OB-FF	4	8	13	11	13
R. palustris f. *plena* OB-ARE	1	1	7	3	7
R. palustris f. *plena* EB-ARE	0	0	0	6	6
R. setigera-CH-NBW	0	<1	<1	6	6
R. setigera-CH-33-17-50	1	5	1.5	4.5	5
R. setigera-CH-33-18-52	0	<1	2	5	5
Oso Happy Smoothie	0	<1	<1	3	3
R. setigera-CH-U3	0	1	3	2	3
R. setigera-CH-NL	0	0	<1	1	1
Basye's Purple	0	0	0	0	0
R. palustris-AMP-1	0	0	0	0	0
R. palustris-AMP-2	0	0	0	0	0
R. palustris-AMP-3	<1	0	0	0	0
R. palustris-SPR	0	0	0	0	0
R. palustris-SR1	0	0	<1	0	0
R. setigera-CH-U2	0	0	0	0	0
R. setigera-CH-U4	0	0	0	0	0

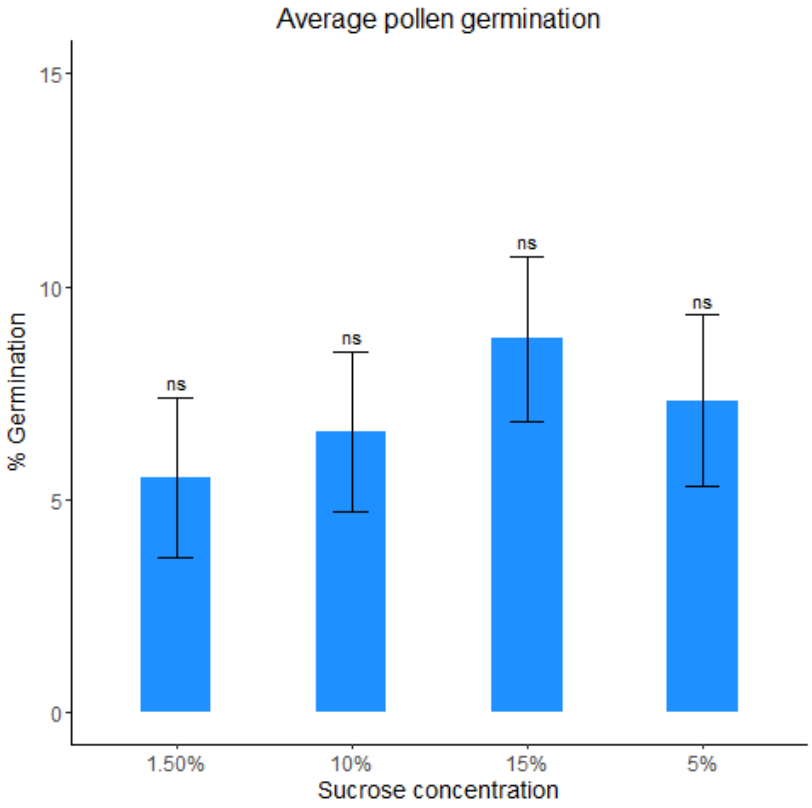

Figure 7 Comparison of average diploid rose pollen germination rates from germination solutions with different sucrose concentrations. Error bars reflect standard error of the mean. ns = means were not significantly different (ANOVA, $p<0.05$).

II.5 Discussion

II.5.1 Cross success and explanations

Most parents chosen for their presumed RRD resistance performed poorly by all or most of the parameters of cross success. Exceptions were *R. palustris* EB-MM, 'Oso Happy Smoothie', *R. setigera*-ARE, 'Srdce Europy', and *R. rugosa* f. *alba*. Thus, should these cultivars and accessions prove to be resistant, they may be useful parents for RRD resistance breeding.

Of parents chosen for traits besides RRD resistance, J06-20-14-3, M4-4, ‘Lena’, and ‘Ole’ performed well as male parents by all or most of the parameters of cross success. Interestingly, although M4-4 was chosen for traits other than RRD resistance, it has not yet succumbed to RRD, and is therefore of particular interest for future breeding. While TAMU7-20 and TAMU7-30 did not perform exceptionally well according to percent hip set, etc., they were used in crosses that produced high numbers of seedlings (when paired with ‘Oso Happy Smoothie’ and ‘Srdce Europy’). This emphasizes the importance of choosing good parental combinations rather than simply choosing a fertile parent.

Roses are known to have low rates of seed germination (Gudin, 2003; Anderson and Byrne, 2007), so some difficulties in producing large populations are to be expected. Specific explanations for the success or failure of particular crosses can be more complicated, however.

Pollen germination alone does not appear to explain the success or failure of crosses in this study. This is somewhat unexpected, as logic and previous reports both indicate that hip set should be strongly correlated with the pollen fertility of the male parent (Spethmann and Feuerhahn, 2003). Not all male parents used in this study were tested for pollen germination, and for those tested, usually only one test per sucrose solution was performed; thus, the pollen germination rates here may not be sufficient to illuminate this relationship. Moreover, there are multiple ways of testing pollen fertility; for instance, Ueda and Akimoto (2001) used an acetocarmine staining procedure to assess pollen fertility and found most species tested had much higher levels of pollen

fertility than seen in this study, while their percent hip set showed a range similar to this study. Therefore, there is much room for future exploration of the correlation between pollen germination and cross success.

Genetic distance between parents is also known to be a factor in rose crossing success (Spethmann and Feuerhahn, 2003), and this seems more explanatory of cross success than pollen fertility in this study. For instance, the crosses *R. setigera*-ARE x 'Lena' and *R. setigera*-ARE x 'Ole' were consistently among the top performing in terms of percent hip set, etc. *R. setigera* belongs to the section *Synstylae*, and both 'Lena' and 'Ole' trace in part to section *Synstylae*. Other high-performing crosses follow a similar pattern, including *R. rugosa* f. *alba* x *R. palustris* EB-MM. While officially *R. rugosa* f. *alba* belongs to section *Cinnamomeae* and *R. palustris* belongs to section *Carolinae* in the traditional taxonomy, there is molecular evidence that these two species may belong to the same clade (Fougère-Danezan et al., 2015). When crossed with a *Synstylae*- and *Indicae*-derived genotype (M4-4), *R. rugosa* f. *alba* did not perform as well, which is consistent with previous reports (Zlesak, 1998; Rieksta et al., 2003). Thus, while *R. rugosa* f. *alba* has breeding potential, more work is needed to identify parents that are sufficiently related to *R. rugosa* f. *alba* to be compatible in crosses but still have desirable ornamental qualities. Alternatively, the *R. rugosa* hybrid 'Snow Pavement' could be used instead of *R. rugosa* f. *alba*, as it crossed successfully with 'Lena' and 'Ole' (*Synstylae, Indicae*). It is worth noting here that although both *R. palustris* f. *plena*-ARE accessions should belong to section *Carolinae*, they are likely hybrids, as

there is genetic evidence that they are closely related to *R. chinensis* (sect. *Indicae*) (see Chapter V).

II.5.2 Future directions

While one goal—that of developing large populations for genetic analyses—was achieved, the other—that of illuminating the breeding potential of seldom-used roses—was only achieved in part. In particular, much work is still needed to explore the breeding potential of *R. palustris*, *R. setigera*, and *R. rugosa*. A more systematic approach with multiple accessions of each species being crossed with multiple fertile breeding parents is needed. Reciprocal crosses, as in a diallel design, would allow the exploration of maternal and paternal effects. Closely tracking seedling survival for an extended period of time would give an indication of seedling vigor, which could function as another parameter of cross success. Finally, crossing in conjunction with pollen germination testing for each male parent would shed light on the role of pollen fertility in cross success.

CHAPTER III

HERITABILITY OF DISEASE RESISTANCE, DEFOLIATION, FLOWERING, AND ARCHITECTURE TRAITS IN DIPLOID ROSE POPULATIONS AND CULTIVARS

III.1 Synopsis

A total of 73 diploid rose cultivars and 330 genotypes from nine diploid rose families were assessed for black spot and cercospora leaf spot resistance, defoliation, flower intensity, and architecture traits in multiple environments (months, seasons, years, and locations). Architecture traits assessed were number of primary shoots, height, length, width, longest dimension, volume, apical dominance, and growth habit. Both cultivars and families included a mix of flowering and growth types. In both datasets, architectural traits varied between flowering and growth types. In general, once-flowering and climbing types were larger with less branching while continuous flowering and non-climbing types were smaller with more branching. Architecture traits had low to moderate broad-sense heritability when multiple seasons were considered; narrow-sense heritability estimates were low or zero. There was a high degree of genotype by environment interactions within a year, but lower genotype by environment interactions over years. Thus, while architecture traits may be stable over years, they are mostly under non-additive control. Narrow-sense heritability estimates for length, width, longest dimension, and apical dominance were slightly higher in once-flowering genotypes than continuous flowering genotypes, however, suggesting that some

germplasm likely has stronger additive effects for these traits; this germplasm should be identified and utilized for breeding. Most broad-sense heritability estimates for black spot, defoliation, and flower intensity were high, while they were low for cercospora. Narrow-sense heritability estimates for black spot, cercospora, defoliation, and flower intensity were low, again suggesting primarily non-additive effects. When flowering type was controlled for, the non-additive effects for flower intensity declined, reflecting the known gene for continuous flowering, though there was still moderate broad-sense heritability for flower intensity. This indicates that while flower intensity is affected by flowering type, there are genetic components to flower intensity beyond this major gene.

III.2 Introduction

Roses are among the most important ornamental crops: culturally, they have long been valued for their beauty and symbolic significance (Krüssman, 1981); economically, garden roses represent a substantial portion of ornamental plant sales in the United States (USDA, 2015). Roses belong to the genus *Rosa*, which comprises between 100 and 200 species (Cairns, 2003; Wissemann, 2003) and many thousands of inter- and intraspecific hybrid cultivars (Cairns, 2000). Due to the persistent popularity of roses, there is demand for cultivars superior in a range of traits including disease resistance, flower productivity, and plant architecture (Byrne et al., 2019; Chavez et al., 2019; Waliczek et al., 2018).

As garden roses are grown primarily for their flowers, abundant and consistent flowering throughout the growing season is highly desirable. Thus, though many rose species are once-flowering (OF), blooming only in the spring, many rose cultivars have

been selected to be of continuous flowering (CF) type, blooming throughout the growing season (Bendahmane et al., 2013). Flowering type is controlled by a single gene, *RoKSN*, which has been identified as a member of the *TERMINAL FLOWER 1* (*TFL1*) gene family (Iwata et al., 2012). Within CF roses, however, there is still variation in the degree of flowering which has possible explanations ranging from gibberellic acid biosynthesis genes (Choubane et al., 2012) to heat stress (Greyvenstein, 2013) and light intensity (Girault et al., 2008). Therefore, this critical trait needs further characterization and study.

Plant architecture greatly affects the visual quality of a rose plant (Boumaza et al., 2009). Plant architecture is determined by both genetics and the environment, and in roses, light (Khayat and Zieslin, 1982; Demotes-Mainard et al., 2013), water (Demotes-Mainard et al., 2013), mechanical stimulation (Morel et al. 2012), and nitrogen availability (Huché-Thélier et al., 2011) have all been shown to affect plant shape. Several studies have assessed the genetic control of architecture by examining a wide variety of traits, including number and length of axes (Morel et al., 2009; Crespel et al., 2013; Crespel et al., 2014; Li-Marchetti et al., 2017); number and length of metamers, a metamer being defined as an internode, a node, axillary bud(s), and a leaf (Morel et al., 2009; Demotes-Mainard et al., 2009; Crespel et al., 2013; Crespel et al., 2014; Li-Marchetti et al., 2017); number and length of determined axes (Crespel et al., 2013; Crespel et al., 2014; Li-Marchetti et al., 2017); number and length of primary shoots (Wu et al., 2019b; a); growth habit (Crespel et al., 2013; Kawamura et al., 2015); number of nodes per primary shoot (Wu et al., 2019b; a; Kawamura et al., 2015);

number of secondary and tertiary shoots per primary shoot (Wu et al., 2019a; b); plant height (Gitonga et al., 2014; Kawamura et al., 2015; Wu et al., 2019a; b); various branching angles (Crespel et al., 2014; Crespel et al., 2013; Li-Marchetti et al., 2017); and stem diameter (Crespel et al., 2013; Kawamura et al., 2015; Garbez et al., 2018). For some studies, the traits were examined with 3D digitization (Crespel et al., 2014; Crespel et al., 2013; Li-Marchetti et al., 2017), which unfortunately is unrealistic in a field setting. While heritability estimates vary with the trait, many architecture traits have moderate to high broad-sense heritability. Plant height, for instance, has been estimated to have a broad-sense heritability of 0.88 in one study (Kawamura et al., 2015) and 0.82 in two others (Wu et al., 2019b; Gitonga et al., 2014). Number of primary shoots was estimated to have a broad-sense heritability of 0.92 (Wu et al., 2019b) and the analogous trait of number of determined axes was estimated to have a broad-sense heritability ranging from 0.54 (Li-Marchetti et al., 2017) to 0.64 (Crespel et al., 2014). Thus, it is clear that rose plant architecture has large genetic components and should be a feasible breeding goal.

Roses are susceptible to many diseases, and for garden roses, the fungal disease black spot (*Diplocarpon rosae* Wolf) is among the most significant and well understood. Black spot is a hemibiotrophic ascomycete that, as the name suggests, causes black circular lesions on rose foliage, eventually leading to high rates of defoliation (Wolf, 1912; Horst and Cloyd, 2007). Many roses are susceptible (Horst and Cloyd, 2007). Thus far, four major genes for black spot resistance have been identified and there is evidence for partial resistance (Soufflet-Freslon et al., 2019; Yan et al., 2019).

While not as prominent as black spot, the fungal disease cercospora leaf spot (*Rosisphaerella rosicola* Pass., syn: *Cercospora rosicola* Pass. (Videira et al., 2017)) is also a concern for garden roses in warm humid environments. Similar to black spot, the disease manifests as dark foliar lesions, though cercospora lesions tend to have lighter necrotic centers as the disease progresses, and eventually defoliation results (Mangandi and Peres, 2009; Davis, 1938). Susceptibility appears to be common and the disease is currently controlled with fungicide application (Mangandi and Peres, 2009). No distinct races have been characterized and no resistance genes identified; however, it has been estimated to have high broad-sense heritability (Kang, 2020), indicating that resistance should be a feasible breeding goal.

This study sought to characterize a diploid cultivar panel and a set of diploid biparental families for architecture traits, black spot and cercospora resistance, flower productivity, and defoliation, and estimate the heritability of these traits. This marks the first time some of these architecture traits have been assessed in roses and the first time architecture has been explored in a cultivar panel of this size.

III.3 Materials and methods

III.3.1 Plant materials

A total of 96 commercially available cultivars, chosen for being known or possible diploids, were acquired as mature plants in one- to two-gallon pots from the Antique Rose Emporium, Independence, TX; Rogue Valley Roses, Phoenix, OR; and Chamblee's Rose Nursery, Winona, TX. When needed, ploidy levels were determined by mitotic root squashes using the method of Zlesak (2009) or by flow cytometry as

provided by Plant Cytometry Services, Didam, Netherlands, and subsequently 21 non-diploids were excluded, leaving 75 diploid genotypes (Table 9). The remaining cultivars were a mix of classes, including tea, China, shrub, polyantha, and others.

Table 9 Seventy-five diploid rose cultivar genotypes included in the study, the number of replications, and primary horticultural class (drawn from HelpMeFind.com). Number in parentheses indicates cultivar release year when there are multiple cultivars with the name. ARE = Antique Rose Emporium, RVR = Rogue Valley Roses, CHM = Chamblee's Rose Nursery.

Genotype	Abbreviation	Num. replications	Source	Class
Anemone (1896)	AM	3	ARE	H. Laevigata
Ballerina (1937)	BA	3	ARE	H. Musk
Borderer	BDR	3	ARE	Floribunda
Belinda	BE	3	ARE	H. Musk
Blush Noisette	BH	3	ARE	Noisette
Bermuda's Kathleen	BK	3	ARE	Bermuda
Bon Silene	BON	3	ARE	Tea
Blumenschmidt	BT	3	ARE	Tea
Cecile Brunner	CB	3	ARE	Polyantha
Celine Forestier	CF	3	ARE	Noisette
Clotilde Soupert (1890)	CL	3	ARE	Polyantha
Danae (1913)	DA	3	ARE	H. Musk
Duchesse de Brabant	DCH	3	ARE	Tea
Ducher	DU	3	ARE	China
Emmie Gray	EG	3	ARE	China
Fortunes Double Yellow	FY	3	ARE	China
Gipsy Boy	GB	3	ARE	Bourbon
Gardenia (1899)	GD	3	ARE	H. Wichurana
General Schablikine	GS	3	ARE	Tea
Happenstance	HA	3	ARE	H. Bracteata
Independence Musk	IM	3	ARE	H. Musk
Jeanne d'Arc (1848)	JA	3	ARE	Alba
Jaune Desprez	JD	3	ARE	Noisette
Jean Mermoz	JM	3	ARE	Polyantha
Katharina Zeimet	KZ	3	ARE	Polyantha
La Marne	LM	3	ARE	Polyantha

Table 9 Continued

Genotype	Abbreviation	Num. replications	Source	Class
Leontine Gervais	LO	3	ARE	H. Wichurana
Lavender Pink Parfait	LPP	3	ARE	H. Multiflora
Le Vesuve (1825)	LU	3	ARE	China
Mrs. Bosanquet	MB	3	ARE	Bourbon
Miss Caroline	MC	3	ARE	Tea
Mermaid (1917)	ME	3	ARE	H. Bracteata
Mevrouw Nathalie Nypels	MEV	3	ARE	Floribunda
Mademoiselle Franziska Kruger	MFK	3	ARE	Tea
Madame Joseph Schwartz	MJ	3	ARE	Tea
Marjorie Fair	MJF	3	ARE	Polyantha
Miss Lowe's Variety	MLV	2	RVR	China
Madame Laurette Messimy	MM	3	ARE	China
Marechal Niel (1864)	MNN	2	RVR	Noisette
Moonlight (1913)	MO	3	ARE	H. Musk
Monsieur Tillier	MT	3	ARE	Tea
Mutabilis	MU	3	ARE	China
Marie Van Houtte	MV	3	ARE	Tea
Mozart (1936)	MZ	3	ARE	H. Musk
Nastarana	NA	2	RVR	H. Musk
Old Blush	OB	3	ARE	China
Oakington Ruby	OR	2	RVR	Miniature
Phalaenopsis	PA	3	ARE	Floribunda
Porcelaine de Chine	PDC	2	RVR	H. Musk
Pink Grootendorst	PG	3	ARE	H. Rugosa
Perle des Jardins	PJ	3	ARE	Tea
Plaisanterie	PL	2	RVR	H. Musk
Petite Pink Scotch	PPS	3	ARE	H. Wichurana
Ma Paquerette	PQ	2	RVR	Polyantha
Pink Surprise (1987)	PS	2	RVR	H. Bracteata
Phyllis Bide	PY	3	ARE	Polyantha
Robin Hood (1927)	RBH	3	ARE	H. Musk
Red Drift	RD	3	CHM	Shrub
Rosa moschata	RCH	3	ARE	Species
Russelliana	RL	3	ARE	H. Multiflora

Table 9 Continued

Genotype	Abbreviation	Num. replications	Source	Class
Rouletii	ROU	3	RVR	China
Republic of Texas	RT	3	ARE	Shrub
Safrano	SA	3	ARE	Tea
Sarasota Spice	SAS	3	ARE	Noisette
Spice	SI	3	ARE	China
Sunshine (1927)	SUN	2	RVR	Polyantha
The Fairy	TFY	3	ARE	Polyantha
The Gift	TG	2	RVR	Polyantha
Trier	TI	2	RVR	H. Multiflora
Veilchenblau	VB	3	ARE	H. Multiflora
Vincent Godsiff	VF	3	ARE	China
Violette	VT	3	ARE	H. Multiflora
Climbing White Maman Cochet	WC	3	ARE	Tea
Windchimes	WI	3	ARE	H. Musk
Yesterday	Y	2	RVR	Polyantha

The ten populations developed in 2016 were propagated via stem cuttings. These populations were inter-related to varying degrees and ranged in size from one to 103 for a total of 373 genotypes (Table 10). The parents of the populations included a variety of flowering and growth types (Table 11).

Table 10 Diploid rose populations maintained in College Station and Overton, TX for phenotypic data collection.

Population	Abbreviation	College Station	Overton
J06-20-14-3 x Papa Hemeray	J14-3xPH	69	0
Papa Hemeray x *R. palustris* f. *plena* EB-ARE	PHxSEB-ARE	11	8
M4-4 x Srdce Europy	M4-4xSE	33	14
TAMU7-20 x Srdce Europy	T7-20xSE	103	92
TAMU7-30 x Srdce Europy	T7-30xSE	88	71
R. setigera-ARE x Lena	SET-ARExLN	1	0
R. setigera-ARE x Ole	SET-ARExOL	25	18
Ole x *R. palustris* f. *plena* EB-ARE	OLxSEB-ARE	23	12
Ole x *R. palustris* f. *plena* OB-ARE	OLxSOB-ARE	11	0
Lena x *R. palustris* f. *plena* OB-ARE	LNxSOB-ARE	11	2
Total		*373*	*217*

Table 11 Flowering and growth type (FlwgType and GType, respectively) of parents used to develop diploid rose populations. CF = continuous flowering, OF = once-flowering, ORF = occasional repeat flowering.

Parent	FlwgType	GType
J06-20-14-3	CF	Non-climber
Lena	CF	Non-climber
M4-4	CF	Non-climber
Ole	CF	Non-climber
Papa Hemeray	CF	Non-climber
R. palustris f. *plena* EB-ARE	CF	Non-climber
R. palustris f. *plena* OB-ARE	OF	Non-climber
R. setigera-ARE	OF	Climber
Srdce Europy	ORF	Climber
TAMU7-20	CF	Non-climber
TAMU7-30	CF	Non-climber

III.3.2 Growing conditions

Both cultivars and families were maintained at the Texas A&M University Horticulture Teaching Research and Extension Center in Somerville, TX (30.524591, -96.422479), approximately 10 miles from the campus of Texas A&M University, College Station, TX. This region has a subtropical climate with summer temperatures regularly above 30°C (Tables 12, 13; (NWS, 2019)). The soil in this field is primarily an

alkaline Weswood silty clay loam (NRCS, 2019). In addition, seven of the families (Table 2) were planted in spring 2018 at the Texas A&M AgriLife Research & Extension Center at Overton, TX (32.295920, -94.976125). This location has cooler average temperatures and greater rainfall than College Station (Table 14, (Historical temperatures, 2020)) and a soil type of Bowie fine sandy loam (B. Pemberton, personal communication). The families and number of genotypes at the Overton site were determined in large part by plant availability and by whether a given family was likely to be segregating for traits of interest.

Table 12 Temperature and precipitation for College Station, TX in 2018. Source: National Weather Service.

Month	Average minimum temperature (°C)	Average maximum temperature (°C)	Mean temperature (°C)	Total precipitation (mm)
January	2.7	15.2	8.9	26.9
February	9.1	17.8	13.4	47.2
March	12.7	24.5	18.6	156.5
April	11.9	24.8	18.4	37.6
May	20.4	31.9	26.2	52.8
June	23.9	34.3	29.2	51.1
July	23.9	35.8	29.9	40.6
August	23.7	36.6	30.2	5.3
September	22.4	30.8	26.6	209.3
October	16.5	25.7	21.1	297.9
November	8.0	18.5	13.2	100.8
December	6.8	16.5	11.7	243.8

Table 13 Temperature and precipitation for College Station, TX in 2019. Source: National Weather Service.

Month	Average minimum temperature (°C)	Average maximum temperature (°C)	Mean temperature (°C)	Total precipitation (mm)
January	5.0	15.7	10.3	122.7
February	8.9	17.4	13.2	53.3
March	10.2	20.8	15.5	31.8
April	14.2	26.0	20.1	141.0
May	20.3	29.8	25.1	200.7
June	22.6	32.6	27.6	125.7
July	24.1	34.8	29.4	4.6
August	25.4	36.8	31.1	53.3
September	23.8	34.9	29.4	64.5
October	15.8	27.9	21.8	77.7
November	8.3	21.6	14.9	32.3
December	6.4	20.2	13.3	14.2

Table 14 Temperature and precipitation for Overton, TX in 2019. Source: Texas A&M AgriLife Research and Extension Center at Overton.

Month	Average minimum temperature (°C)	Average maximum temperature (°C)	Mean temperature (°C)	Total precipitation (mm)
January	2.2	12.9	7.3	84.8
February	5.4	14.7	10.0	55.1
March	6.1	17.9	12.0	62.0
April	11.6	23.4	17.3	251.0
May	17.9	28.0	22.6	250.7
June	19.6	30.5	24.9	180.8
July	22.1	32.8	27.1	18.5
August	23.7	34.6	28.6	27.2
September	21.5	34.1	27.2	91.4
October	12.3	24.7	17.9	102.9
November	5.6	18.7	11.7	13.5
December	3.9	17.1	9.9	28.7

Cultivars were planted in March 2017 in a completely randomized design with two or three replications depending on plant availability (Table 9). Plants were arranged

in three raised double rows with four-foot inter-plant spacing and six-foot inter-row spacing. Black plastic weed barrier was used for weed suppression and the plants were watered with an overhead irrigation system to encourage disease development. As the cultivars came from multiple nurseries, the plants were grown for a year in the field to mitigate the effects of past growing conditions. Plants were pruned in February 2018 and 2019 to no more than 1.5 feet in all directions. Plants that were already smaller than this were only pruned lightly to stimulate growth. After this, plants were only pruned if they were substantially encroaching on another plant's space, and then only as needed to free the second plant. Select plants were treated with Malathion SEC (Cayman Chemical Company, Ann Arbor, MI) at a rate of 4.73 ml/gallon to control spider mites but no other pesticides or fungicides were applied throughout the growing season.

At the College Station location, two replications of the families were planted in December 2017 (first replication) and January 2018 (second replication) divided between two blocks. Within each block, plants were arranged in a completely randomized design of raised triple rows with four-foot inter-plant spacing and four-foot inter-row spacing. The beds were covered with black weed barrier and irrigated via drip. Due to the age of the plants, no pruning was performed prior to phenotypic data collection.

At the Overton location, two replications of the families were planted in spring 2018 in two blocks. Within each block, plants were arranged by families. Large plants (i.e., crosses with *R. setigera*-ARE as a parent) were planted in single rows with six-foot inter-plant spacing. All other plants were arranged in double rows with four-foot inter-

plant spacing and offset from each other by approximately two feet. Beds were covered with landscape fabric and irrigated via drip. Nitrogen was applied weekly during the growing season at a rate of 15 lbs/10,000 ft^2. Due to the age of the plants, no pruning was performed prior to phenotypic data collection.

III.3.3 Phenotyping

Phenotyping occurred at multiple times in 2018 and 2019, resulting in two year-location environments and three year-season environments (Table 15). In summary, at the College Station site, both cultivars and families were phenotyped in spring and winter of 2018 (2018-S and 2018-W, respectively) for architecture traits and monthly from April through November for disease, flowering, and defoliation (2018-CS). In 2019, the cultivars were phenotyped in winter for architecture traits (2019-W). Families at the Overton site were phenotyped for disease, flowering, and defoliation in June, September, and October in 2019 (2019-OV).

Table 15 Environments (season, month, year, and location) for diploid rose phenotypic data collection. CV = cultivar panel, FM = families.

	Location	
Evaluation, Year	College Station, TX	Overton, TX
Monthly, 2018	CV, FM	
Spring, 2018	CV, FM	
Winter, 2018	CV, FM	
Monthly, 2019		FM
Winter, 2019	CV	

All phenotypic data (Table 16) were recorded using the Field Book application (Rife and Poland, 2014). Black spot (BS) and cercospora leaf spot (CLS) resistance or

susceptibility was assessed visually using a scale of 0 to 9, where 0 indicates that the rose canopy is free of lesions; 1 indicates that 10% of the canopy bears lesions; 2, 20%; and so on. This data was collected monthly from April through November in College Station in 2018 (2018-CS) and in June, September, and October in Overton in 2019 (2019-OV). The monthly data was used to calculate the least squares means (ls means) disease rating and the maximum disease rating (BS_Max, CLS_Max). The disease scores were also used to calculate the area under the disease progress curve (BS_AUDPC, CLS_AUDPC) using the trapezoidal method (Madden et al., 2007):

$$AUDPC = \sum_{i=1}^{n} \frac{y_i + y_{i+1}}{2}(t_{i+1} - t_i)$$

in which y_i = BS or CLS score at the *i*-th observation, t_i = time (days) at the *i*-th observation, and *n* = total number of observations. Months were assumed to be 28 days long for ease of calculation.

Flower productivity throughout the growing season was quantified as flower intensity (FLI) on a scale of 0 to 9, where 0 indicates no flowers, 1 indicates that 10% of the canopy is covered in flowers, and so on. This data was collected monthly from April through November in 2018-CS and in three months in 2019-OV. This data was used to identify the flowering type (FlwgType): once-flowering (OF), occasional-repeat-flowering (ORF), or continuous-flowering (CF). In the families, genotypes that did not bloom at all in 2018-CS were assumed to be once-flowering (OF), as once-flowering roses do not bloom in their first year. The total flowering throughout the season for CF plants was quantified as the area under the flower intensity curve (AFLIC) using the trapezoidal method as described above. It was hypothesized that AFLIC would provide a

better estimation of the flowering productivity of CF plants than a simple average. Ls means and maximum score (FLI_Max) were also used to summarize flower intensity.

Plant defoliation (DEF) throughout the growing season was also assessed from April to November in 2018-CS and over three months in 2019-OV. DEF was quantified on a scale of 0 to 9, where 0 indicates no defoliation, 1 indicates that 10% of the plant is defoliated, and so on. DEF was summarized both as an ls means and as a maximum score (DEF_Max).

Table 16 Phenotypic traits assessed in diploid rose cultivars and families in 2018 and 2019.

Trait	Abbreviation	Cultivars	Families
Number of primary shoots	NPrimaries	2018, 2019	2018
Plant height (cm)	Height	2018, 2019	2018
Plant length (cm)	Length	2018, 2019	2018
Plant width (cm)	Width	2018, 2019	2018
Longest dimension (cm)	LDim	2018, 2019	2018
Plant volume (cm^3)	Volume	2018, 2019	2018
Apical dominance index (number secondary shoots/shoot length)	ADI	2018, 2019	2018
Growth habit	GHabit	2018	2018
Growth type	GType	2018	2018
Flowering type	FlwgType	2018	2018
Mean black spot	BS	2018	2018, 2019
Maximum black spot	BS_Max	2018	2018, 2019
Black spot area under the disease progress curve	BS_AUDPC	2018	2018, 2019
Mean cercospora leaf spot	CLS	2018	2018, 2019
Maximum cercospora leaf spot	CLS_Max	2018	2018, 2019
Cercospora leaf spot area under the disease progress curve	CLS_AUDPC	2018	2018, 2019
Average flower intensity	FLI	2018	2018, 2019
Maximum flower intensity	FLI_Max	2018	2018, 2019
Area under the flower intensity curve	AFLIC	2018	2018, 2019
Mean defoliation	DEF	2018	2018, 2019
Maximum defoliation	DEF_Max	2018	2018, 2019

Nine architectural traits were assessed on all plants in College Station, TX: number of primary shoots (NPrimaries); plant height, length, and width; longest dimension (LDim); volume; apical dominance index (ADI); growth habit (GHabit); and growth type (GType). Some of these traits were chosen for having high heritability in a previous study as in the case of NPrimaries (Wu et al., 2019b), height (Wu et al., 2019b; Kawamura et al., 2015), and growth habit (Kawamura et al., 2015), while others represent new avenues of exploration. In the cultivars, architecture data was collected in spring (March/April) 2018 (2018-S), December 2018 (2018-W), and December 2019 (2019-W), with the exceptions of ADI, GHabit, and GType, which were assessed in winter only. In the families, architecture data was collected in 2018-S and 2018-W; ADI, GHabit, and GType were collected in 2018-W only.

NPrimaries (Fig. 8a), was assessed in the spring one month after pruning and was defined as the living shoots at the base of the plant, similar to Wu et al. (2019b); however, if a primary shoot branched within approximately a centimeter of the soil level, both shoots were counted as separate primary shoots in an attempt to account for variation in planting depth. No distinction was made between flowering/nonflowering shoots, pruned/unpruned shoots, long/short shoots, etc.

Unlike NPrimaries, plant vigor traits--plant height, length, width, and the traits derived from them--were measured in April, approximately two months after pruning. Plant height (Fig. 8b) was defined as the distance in centimeters from the base of the plant to the highest living tissue. Plant length (Fig. 8c) was the longest horizontal distance in centimeters through the center of the plant, counting only living tissue, and

plant width (Fig. 8c) was the distance perpendicular to the length through the center of the plant. All measurements were taken to the nearest centimeter. These measurements also permitted determination of LDim, which was whichever of these measurements (height, length, or width) was the greatest. As the study included climbers and groundcovers, which frequently grow more horizontally than vertically when unsupported by a trellis, LDim was hypothesized to be a better measure of plant size when comparing a variety of growth types.

Plant volume (Fig. 8d, 8e) was calculated with an elliptical cylinder volume formula (Lyon, 1968; Peek, 1970):

$$V = \pi(Height)\left(\frac{Major\ axis\ length}{2} \times \frac{Minor\ axis\ length}{2}\right)$$

in which plant length and width were considered the major and minor axes, respectively. The elliptical cylinder volume was determined to be more suitable for roses than rectangular or spherical volume due to the natural shape of most rose plants. It will, however, tend to overestimate plant volume as it does not take into account variable plant widths at different heights (Thorne et al., 2002).

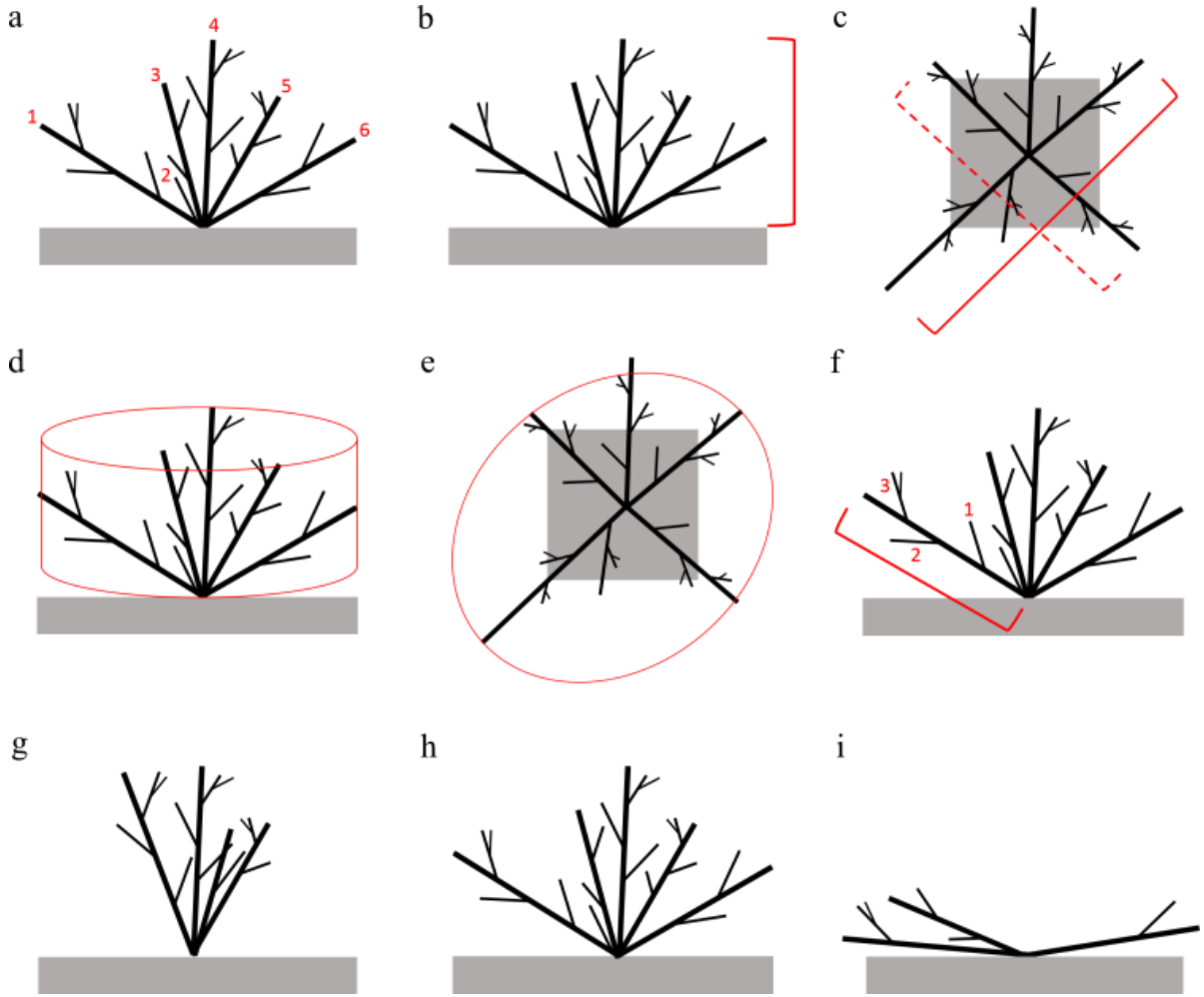

Figure 8 Plant architecture traits assessed on diploid roses in College Station, TX. a. Number of primary shoots (NPrimaries). b. Plant height. c. Plant length (solid line) and width (dashed line). d. Plant volume as estimated by an elliptical cylinder, side view. e. Plant volume as estimated by an elliptical cylinder, viewed from above. f. Apical dominance index (ADI) calculated as number of secondary shoots divided by the length of the primary shoot. g-i. Growth habit (GHabit) assessed on a scale of 1 to 9. g. GHabit of 1 (erect). h. GHabit of 4. i. GHabit of 9 (prostrate).

ADI (Fig. 8f) was used to quantify the degree of branching within a plant, as it was assumed that the fullness of a plant will be determined in part by the degree of branching. ADI was calculated on up to three primary shoots per plant. The shoots were required to show no signs of pruning (i.e., be new growth) and to extend to the exterior of the canopy, as these shoots were considered more representative of the plant architecture. In 2018, most of these shoots were primary shoots; in 2019, large secondary shoots arising from shoots which presumably developed the previous year were frequently used to avoid pruned shoots. The length in centimeters of each primary shoot was measured and the number of secondary shoots on each primary shoot counted. The ADI was calculated as the number of secondary shoots divided by the length of the primary shoot (Perez-Harguindeguy et al., 2016); thus, a low value indicates a low degree of branching (zero indicating no branching) and a high value indicates a high degree of branching. In cultivars in 2018-W, any living secondary shoot that was long enough to have at least one node was counted. For the families, two separate ADI values were calculated: one ADI in the same manner as the cultivars, and a modified ADI (MADI) in which only secondary shoots more than two to three centimeters long were included, as only longer secondary shoots will be contributing visually to plant architecture. As the ADI and MADI were highly correlated with each other (data not shown), they were considered effectively interchangeable for the purposes of this study. Family ADI values and 2019-W ADI values for cultivars are derived from the modified method.

GHabit was assessed at the end of the growing season as the post-spring pruning GHabit would not be an accurate portrayal of a plant. GHabit (Fig. 8g-8i) was determined using the subjective, ordinal scale from the International Union for the Protection of New Varieties of Plants (UPOV), where 1 = erect growth habit and 9 = prostrate growth habit (UPOV, 2010). At the end of the growing season plants were also classified into growth types (GTypes) of climber, groundcover, or non-climber.

III.3.4 Statistical analyses

Phenotypic statistical analyses were conducted in JMP Pro® 15 and SAS® 9.4 (SAS Institute Inc., Cary, NC). Prior to statistical analyses, individuals missing the majority of phenotypic data (i.e., plants that had died over the course of the growing season) were removed from the dataset. Progeny from the families that the genetic analysis (see Chapter V) indicated were outcrosses were likewise removed from the dataset if their true parents could not be determined. Impossible data (for example, a length of zero) was made missing. Least squares means (ls means) were used to combine the individual shoot measurements of ADI into a single value per plant.

Data were tested for the normal distribution in each environment and combined environment with the Shapiro-Wilk test. When data were non-normally distributed, a square root or natural logarithm (ln(x+1)) transformation was performed and data were tested for normality again. Calculated variables (ADI, Volume, BS_AUDPC, CLS_AUDPC, and AFLIC) were tested for normality but were not transformed in an attempt to limit error propagation.

Differences between environments (year-locations, year-seasons, and months), populations, growth types, and flowering types were investigated using an analysis of variance (ANOVA) that included block (that is, the physical blocks within the field) as an effect when applicable and the interaction between block and the various effects when degrees of freedom permitted. Means were compared with either a Student's t-test or Tukey's HSD test. Correlations between traits for each season were quantified with Pearson's product-moment correlation test.

Restricted maximum likelihood (REML) models were developed for all traits. The general model for both cultivars and families was

$$P_{ij} = \mu + G_i + E_j + GE_{ij} + \varepsilon_{ij}$$

in which P_{ij} is the phenotypic value of genotype *i* at environment *j*; μ is the overall mean; G_i is the random effect of genotype *i*; E_j is the random effect of environment *j*; GE_{ij} is the random interaction of environment *j* and genotype *i*; and ε_{ij} is the random residual error for genotype *i* at environment *j*.

In the cultivars, environment was defined as year-seasons or months, depending on the trait. Accordingly, the phenotypic variance (σ_P^2) was partitioned as

$$\sigma_P^2 = \sigma_G^2 + \sigma_{GE}^2 + \sigma_\varepsilon^2$$

in which σ_G^2 is the variance of genotypic effect, σ_{GE}^2 is the variance of genotype x environment effect, and σ_ε^2 is the residual error variance, which includes the error between replicated plants. Broad-sense heritability/repeatability was estimated from the variance components with the formula below:

$$H^2 = \frac{\sigma_G^2}{\sigma_G^2 + \sigma_{GE}^2 + \sigma_\varepsilon^2}$$

For single-season, area and maximum measures, and multi-season traits per season, the environment effect was removed from the model and repeatability was estimated with the formula below (Holland et al., 2003):

$$H^2 = \frac{\sigma_G^2}{\sigma_G^2 + \sigma_\varepsilon^2}$$

In the families, environment was defined as location, time (year, season, or month), or a combination of location and time as appropriate for the dataset. Accordingly, the phenotypic variance (σ_P^2) was partitioned as follows:

$$\sigma_P^2 = \sigma_{G[FM]}^2 + \sigma_F^2 + \sigma_M^2 + \sigma_E^2 + \sigma_{B[E]}^2 + \sigma_{FE}^2 + \sigma_{ME}^2 + \sigma_{G[FM]E}^2 + \sigma_\varepsilon^2$$

in which $\sigma_{G[FM]}^2$ is the variance of the genotype nested within the female and male parents; σ_F^2 and σ_M^2 are the variances of the female and male parents, respectively; σ_E^2 is the variance due to environment; $\sigma_{B[E]}^2$ is the variance of block nested within environment; σ_{FE}^2 and σ_{ME}^2 are the variances of the female parent x environment and male parent x environment, respectively; $\sigma_{G[FM]E}^2$ is the variance of genotype nested within female and male parents x environment; and σ_ε^2 is the residual error variance. Broad-sense heritability (H^2) was estimated from the variance components with the formula

$$H^2 = \frac{\sigma_{G[FM]}^2 + \sigma_F^2 + \sigma_M^2}{\sigma_{G[FM]}^2 + \sigma_F^2 + \sigma_M^2 + (\sigma_{FE}^2 + \sigma_{ME}^2 + \sigma_{G[FM]E}^2)/E + \sigma_\varepsilon^2/ER}$$

in which E = number of environments and R = number of replications.

Narrow-sense heritability (h^2) was estimated from the variance components with the formula below:

$$h^2 = \frac{\sigma_F^2 + \sigma_M^2}{\sigma_{G[FM]}^2 + \sigma_F^2 + \sigma_M^2 + (\sigma_{FE}^2 + \sigma_{ME}^2 + \sigma_{G[FM]E}^2)/E + \sigma_\varepsilon^2/ER}$$

For single-season, area and maximum measures, and multi-season traits per season, the environment effect was removed from the model.

III.4 Results

After removal of off-types and individuals with missing data, 330 genotypes from nine populations were retained in the families (Table 17). Two cultivars ('Anemone' and 'Phyllis Bide') were removed from the cultivars to maintain consistency with the genotypic analysis (see Chapter V).

III.4.1 Normality and phenotypic variability

No phenotypic traits except height (in cultivars only) were normally distributed. While square root and natural logarithm transformations improved the distribution of some traits in some environments, no transformation consistently improved the distribution of a trait in all environments. Therefore, the analyses were done with the raw data.

Table 17 Number of genotypes from diploid rose families retained for statistical analyses.

Population	Abbreviation	College Station	Overton
J06-20-14-3 x Papa Hemeray	J14-3xPH	68	0
Papa Hemeray x *R. palustris* f. *plena* EB-ARE	PHxSEB-ARE	10	8
M4-4 x Srdce Europy	M4-4xSE	33	14
TAMU7-20 x Srdce Europy	T7-20xSE	103	91
TAMU7-30 x Srdce Europy	T7-30xSE	88	71
R. setigera-ARE x Lena	SET-ARExLN	1	0
R. setigera-ARE x Ole	SET-ARExOL	24	16
Ole x *R. palustris* f. *plena* EB-ARE	OLxSEB-ARE	2	0
Lena x *R. palustris* f. *plena* OB-ARE	LNxSOB-ARE	1	0
Total		*330*	*200*

III.4.2 Differences between environments

III.4.2.1 Trends over months

Four traits were evaluated monthly: black spot (BS), cercospora (CLS), defoliation (DEF), and flower intensity (FLI). Each of these varied over the growing season.

III.4.2.1.1 Cultivar panel

In the cultivars, BS was at its lowest in April and highest in September, October, and November (Fig. 9a). CLS was low from April through September and highest in October and November (Fig. 9b). FLI, on the other hand, peaked in April, plateaued at a lower level from June through October, and was lowest in November (Fig. 9c). DEF increased over the course of the year (Fig. 9d), achieving its peak in November.

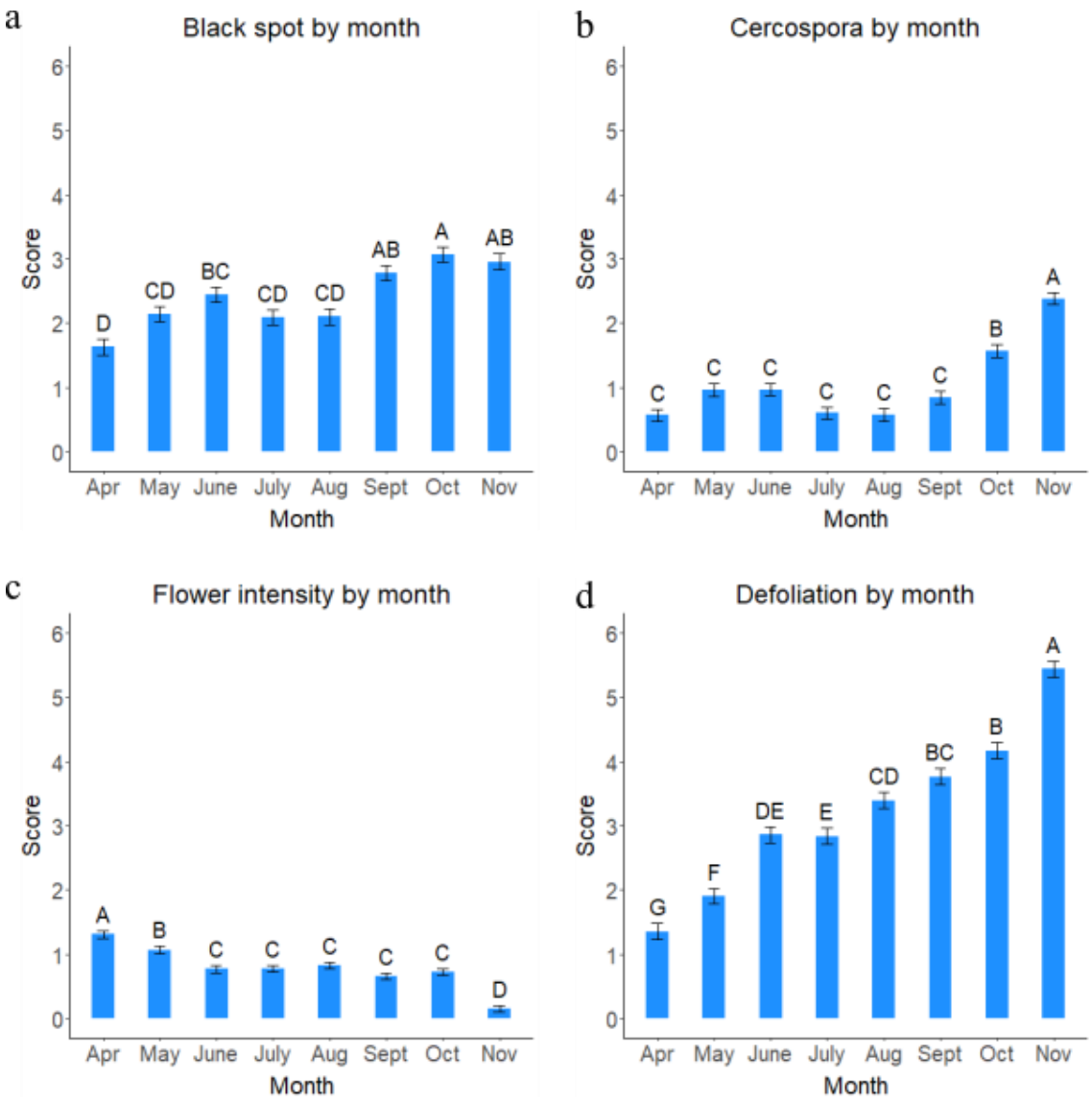

Figure 9 Mean ratings per month in diploid rose cultivar panel in 2018-CS environment. Traits were scored on a scale of 0-9 in which 0 = 0% of plant canopy affected (by disease, flowering, or defoliation), 1 =10% of plant canopy affected, and so on. Error bars reflect standard error of the mean. Months not connected by the same letter are significantly different ($p<0.05$) according to Tukey's HSD. a. Mean black spot severity per month. b. Mean cercospora severity per month. c. Mean flower intensity per month. d. Mean defoliation per month.

III.4.2.1.2 Families

In the families, BS followed a different pattern than in the cultivars. In the 2018-CS environment, the means in April and November were the highest (Fig. 10a). In 2019-OV, the mean in June was the highest, and October was lower than both June and September; however, with only three months of data from this environment the true pattern is hard to discern (Fig. 10b). As in the cultivars, CLS increased towards the end of the growing season in both environments (Fig. 10c, d). Flowering in 2018-CS peaked in May and again in July; in 2019-OV, it peaked in June and October (Fig. 10e, f). In 2018-CS, DEF followed a similar pattern as in the cultivars that same year, increasing throughout the year to its maximum in November; however, in 2019-OV, defoliation peaked in September and declined in October (Fig. 10g, h). For all traits in all year-locations, the block effect was significant; the block x month effect could not be tested.

Figure 10 Mean ratings per month in diploid rose families in College Station, TX in 2018 (2018-CS) and Overton, TX in 2019 (2019-OV) environments. Data was only collected in three months in 2019-OV. Traits were scored on a scale of 0-9 in which 0 = 0% of plant canopy affected (by disease, flowering, or defoliation), 1 = 10% of plant canopy affected, and so on. Error bars reflect standard error of the mean. Months not connected by the same letter are significantly different ($p<0.05$) according to Tukey's HSD. a. Mean black spot severity per month, 2018-CS. b. Mean black spot severity per month, 2019-OV. c. Mean cercospora severity per month, 2018-CS. d. Mean cercospora severity per month, 2019-OV. e. Mean flower intensity per month, 2018-CS. f. Mean flower intensity per month, 2019-OV. g. Mean defoliation per month, 2018-CS. h. Mean defoliation per month, 2019-OV.

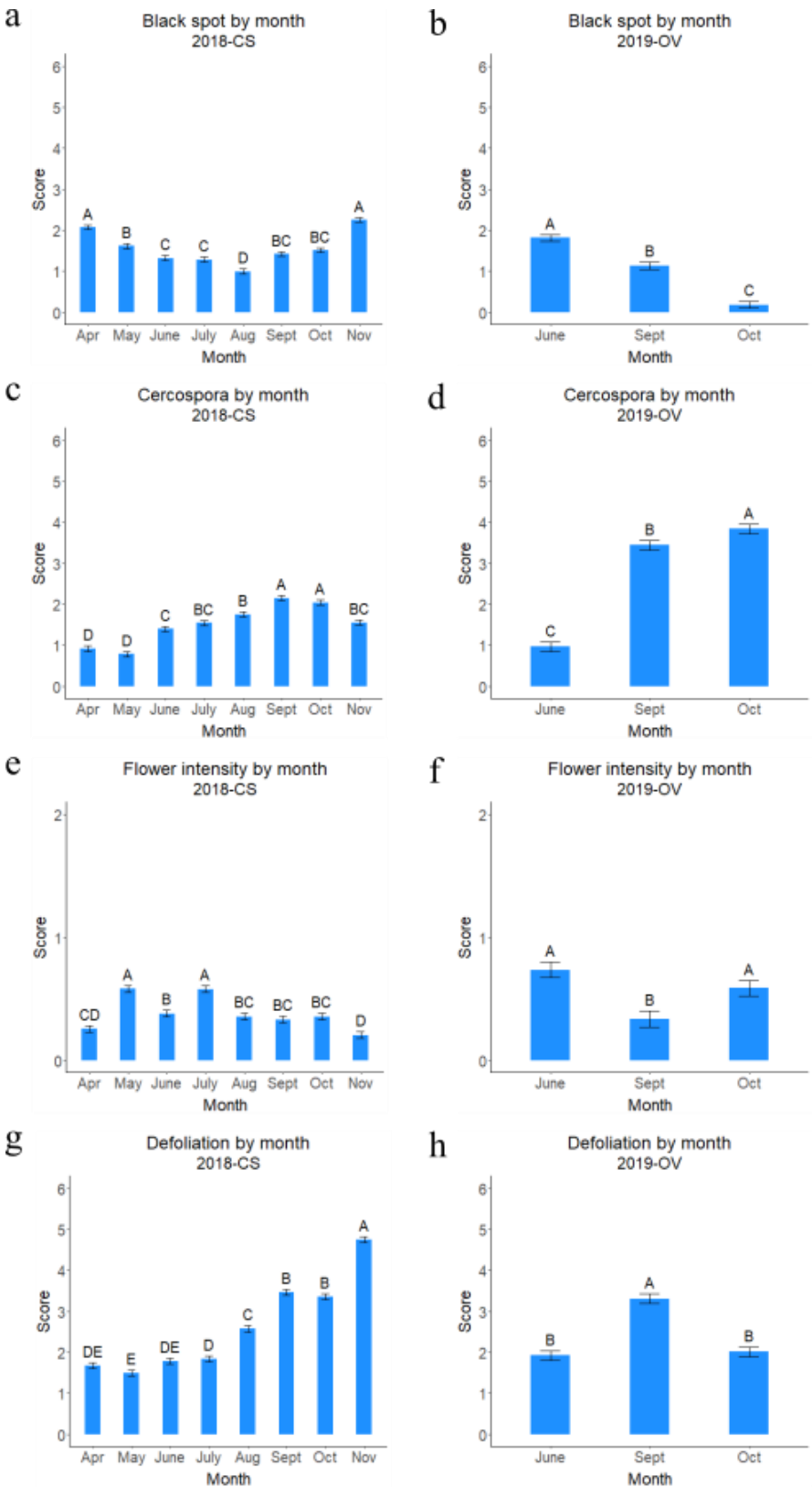
a
Black spot by month
2018-CS
Score
Month
Apr May June July Aug Sept Oct Nov
A B C C D BC BC A
b
Black spot by month
2019-OV
Score
Month
June Sept Oct
A B C
c
Cercospora by month
2018-CS
Score
Month
Apr May June July Aug Sept Oct Nov
D D C BC B A A BC
d
Cercospora by month
2019-OV
Score
Month
June Sept Oct
C B A
e
Flower intensity by month
2018-CS
Score
Month
Apr May June July Aug Sept Oct Nov
CD A B A BC BC BC D
f
Flower intensity by month
2019-OV
Score
Month
June Sept Oct
A B A
g
Defoliation by month
2018-CS
Score
Month
Apr May June July Aug Sept Oct Nov
DE E DE D C B B A
h
Defoliation by month
2019-OV
Score
Month
June Sept Oct
B A B

III.4.2.2 Year-location differences

BS, CLS, FLI, and DEF differed between 2018-CS and 2019-OV in the rose families (Fig. 11). 2019-OV had higher levels of cercospora and flowering, while 2018-CS had higher levels of black spot and defoliation. For all traits, the block effect was significant.

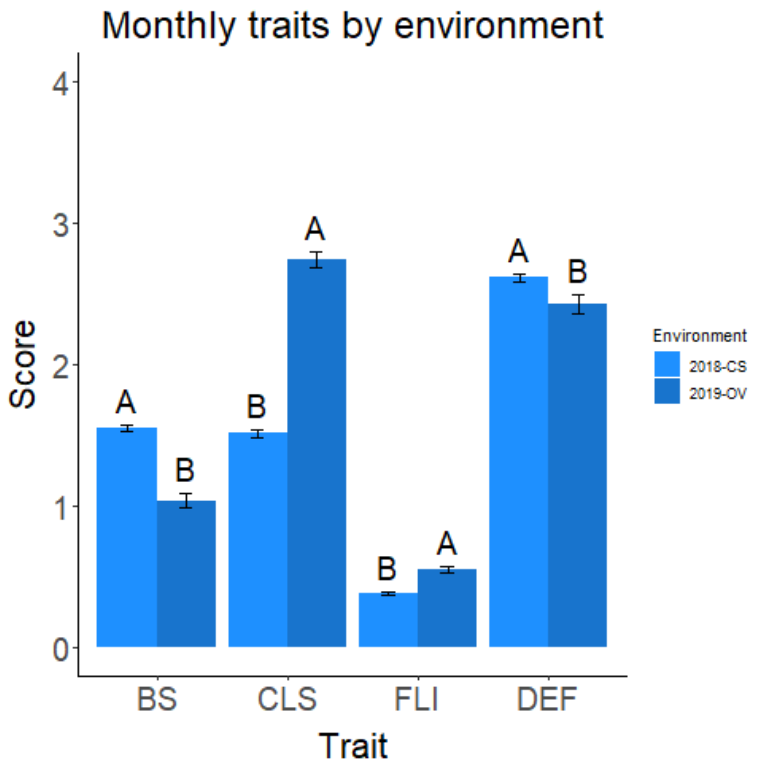

Figure 11 Mean ratings for black spot (BS), cercospora (CLS), flower intensity (FLI), and defoliation (DEF) in diploid rose families over the growing season in College Station, TX in 2018 (2018-CS) versus Overton, TX in 2019 (2019-OV). Traits were scored on a scale of 0-9 in which 0 = 0% of plant canopy affected (by disease, flowering, or defoliation), 1 = 10% of plant canopy affected, and so on. Means not connected by the same letter are significantly different ($p<0.05$) according to Student's t-test.

III.4.2.3 Year-season differences

III.4.2.3.1 Cultivar panel

In the cultivars, architecture data was collected over three year-seasons: 2018-S, 2018-W, and 2019-W. NPrimaries was higher in 2018-W, while the other two year-seasons did not differ from each other (Fig. 12). Plant vigor-related traits (height, LDim, length, width, and volume) were lower in 2018-S than in the two winter environments (Fig. 13, 14). 2018-W and 2019-W did not differ for any of these traits. ADI, which was only measured in winter, was higher (i.e., plants had more branching) in 2019-W than 2018-W (Fig. 15).

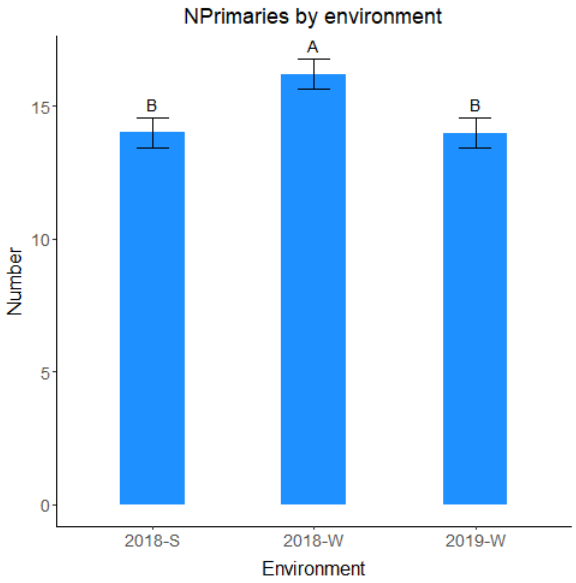

Figure 12 Mean number of primary shoots (NPrimaries) per year-season (environment) in diploid rose cultivar panel in College Station, TX. Error bars reflect standard error of the mean. Means not connected by the same letter are significantly different ($p<0.05$) according to Tukey's HSD.

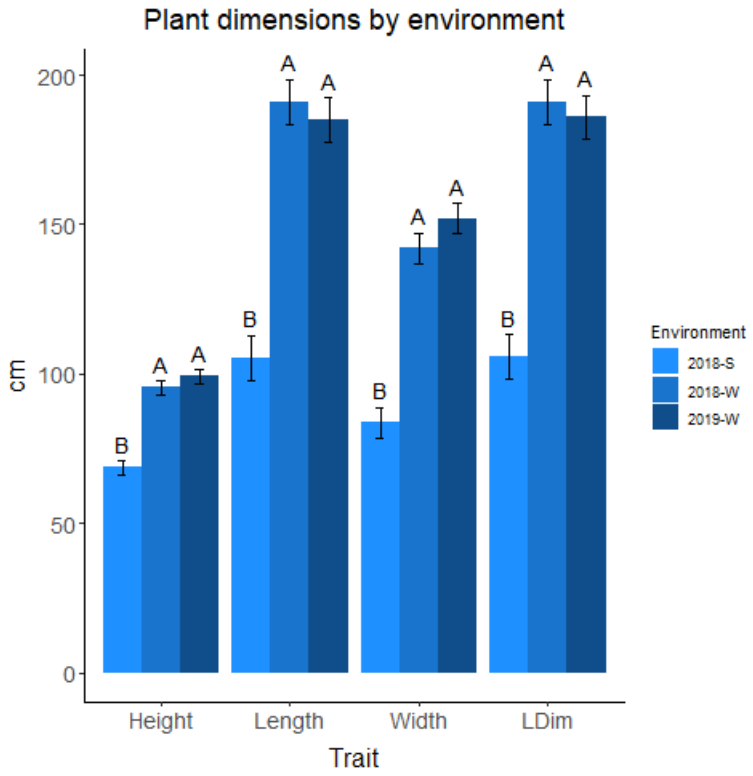

Figure 13 Mean height, length, width, and longest dimension (LDim) in cm per year-season (environment) in diploid rose cultivar panel in College Station, TX. Longest dimension was defined as the largest plant measurement (height, length, or width). Error bars reflect standard error of the mean. Means not connected by the same letter are significantly different ($p<0.05$) according to Tukey's HSD.

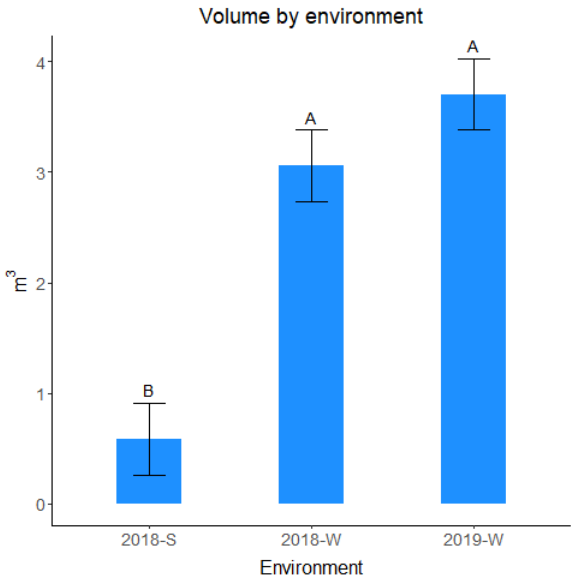

Figure 14 Mean volume in cubic meters per year-season (environment) in diploid rose cultivar panel in College Station, TX. Plant volume was determined as the volume of an elliptical cylinder. Error bars reflect standard error of the mean. Means not connected by the same letter are significantly different ($p<0.05$) according to Tukey's HSD.

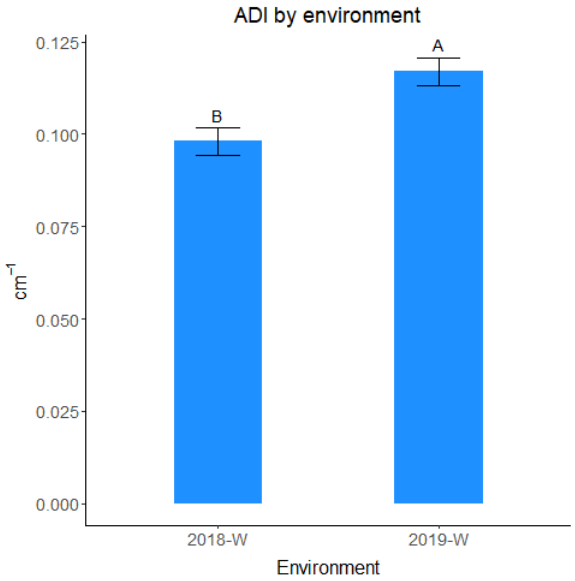

Figure 15 Mean apical dominance index (ADI) per year-season (environment) in diploid rose cultivar panel in College Station, TX. ADI was only measured in winter environments. Error bars reflect standard error of the mean. Means not connected by the same letter are significantly different ($p<0.05$) according to Student's t-test.

III.4.2.3.2 Families

In the families, architecture data was collected only in 2018-S and 2018-W. As in the cultivars, NPrimaries and the vigor traits were higher in the winter as compared to the summer measurement (Fig. 16-18). For all traits, the block effect was significant; the block x season effect could not be tested due to insufficient degrees of freedom.

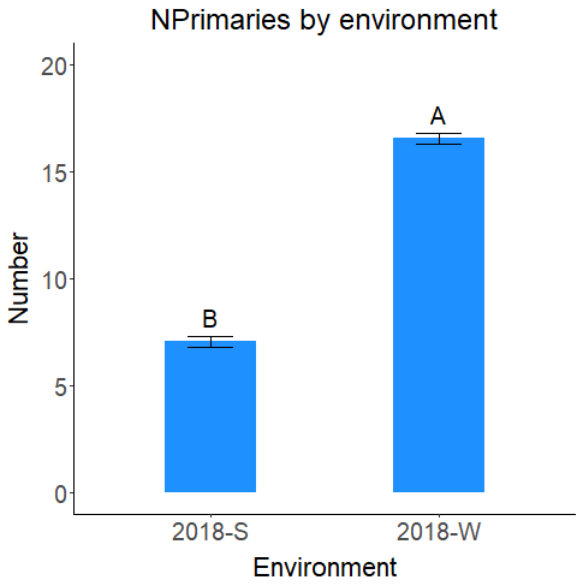

Figure 16 Mean number of primary shoots (NPrimaries) per year-season (environment) in nine diploid rose families in College Station, TX. Architecture data was only collected in 2018 in diploid families. Error bars reflect standard error of the mean. Means not connected by the same letter are significantly different ($p<0.05$) according to Student's t-test.

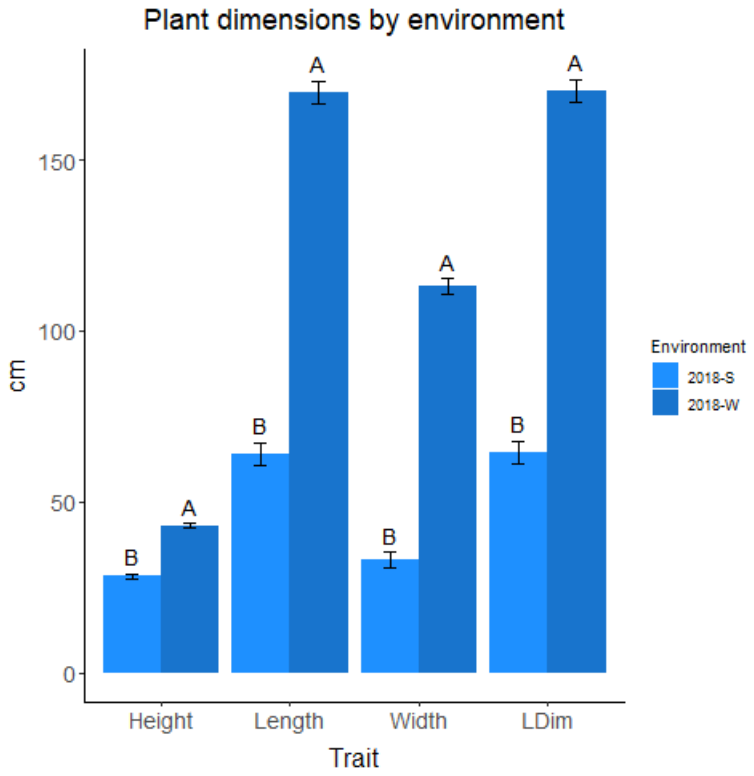

Figure 17 Mean height, length, width, and longest dimension (LDim) per year-season (environment) in nine diploid rose families in College Station, TX. Longest dimension was defined as the largest plant measurement (height, length, or width). Architecture data was only collected in 2018 in diploid families. Error bars reflect standard error of the mean. Means not connected by the same letter are significantly different ($p<0.05$) according to Student's t-test.

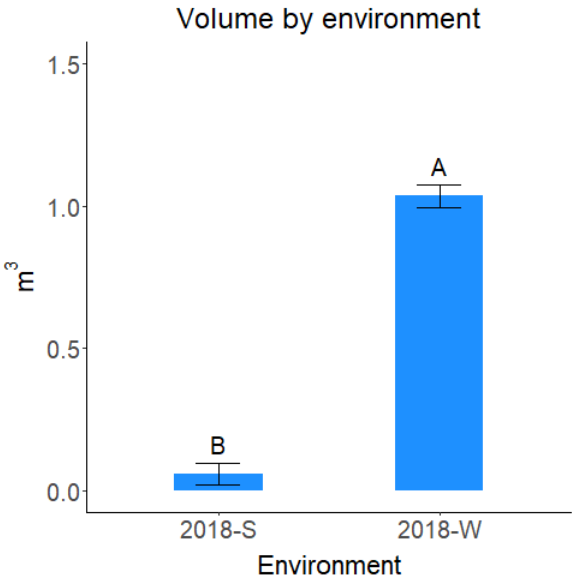

Figure 18 Mean volume in cubic meters per year-season (environment) in nine diploid rose families in College Station, TX. Plant volume was determined as the volume of an elliptical cylinder. Architecture data was only collected in 2018 in diploid families. Error bars reflect standard error of the mean. Means not connected by the same letter are significantly different ($p<0.05$) according to Student's t-test.

III.4.3 Differences between families

Black spot severity differed between populations in 2018-CS but not in 2019-OV. The least squares mean and AUDPC for BS indicated that population SET-ARExOL had the greatest amount of black spot in 2018-CS; however, in 2019-OV it did not differ from the other populations (Fig. 19, 20). Population SET-ARExLN had the highest BS_Max of all populations in 2018-CS (Fig. 21a). All measures of BS had significant block effects.

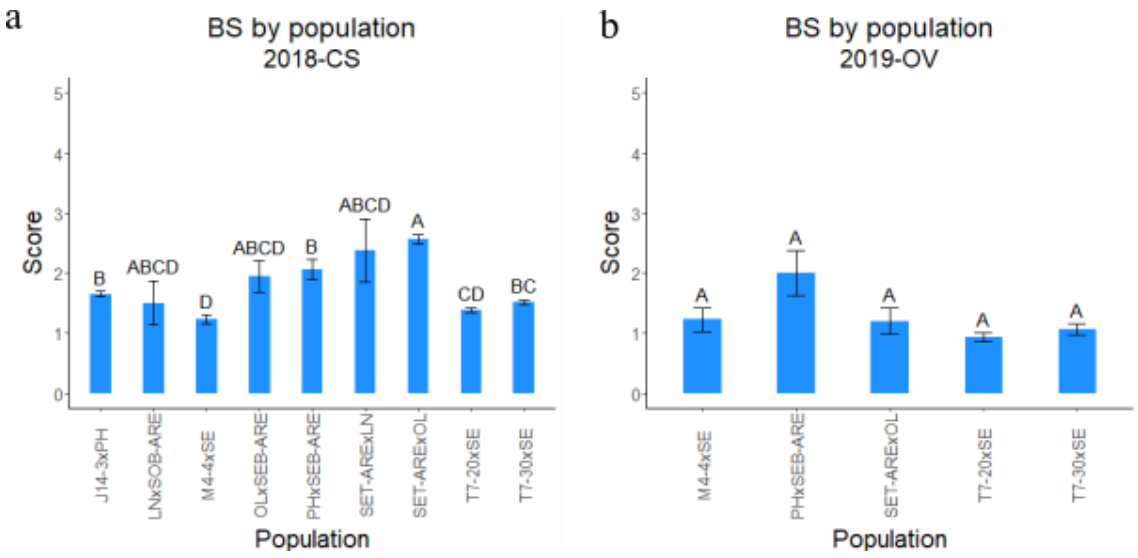

Figure 19 Mean black spot (BS) rating per diploid rose population in College Station, TX (2018-CS, a) and Overton, TX (2019-OV, b). Black spot was scored on a scale of 0-9 in which 0 = 0% of plant canopy covered in lesions, 1 = 10% of plant canopy covered in lesions, and so on. Error bars reflect standard error of the mean. Means not connected by the same letter are significantly different ($p<0.05$) according to Tukey's HSD.

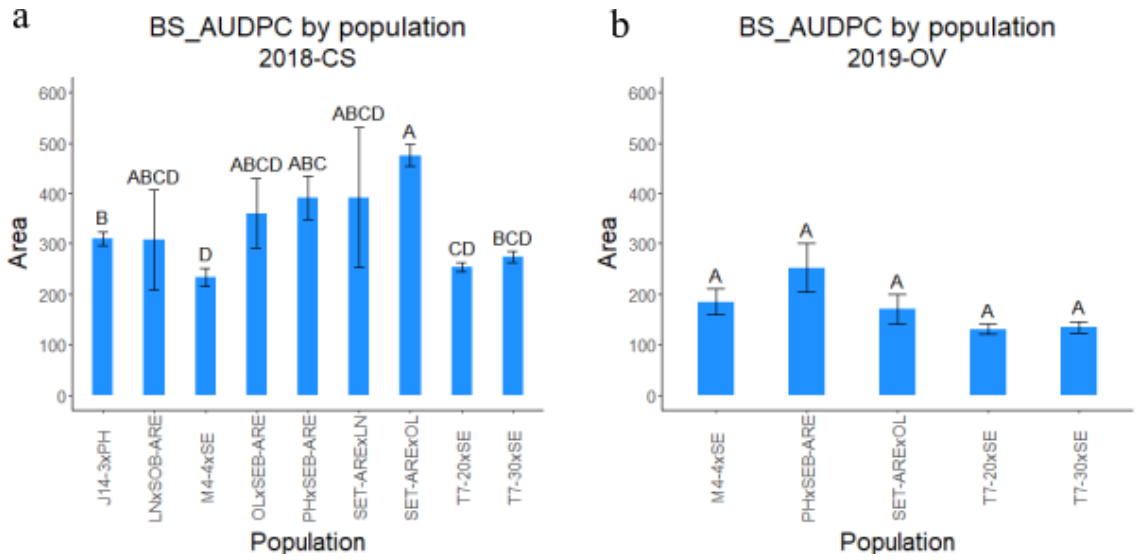

Figure 20 Mean black spot area under the disease progress curve (BS_AUDPC) per diploid rose population in College Station, TX (2018-CS, a) and Overton, TX (2019-OV, b). AUDPC was calculated with the trapezoidal method. Error bars reflect standard error of the mean. Means not connected by the same letter are significantly different ($p<0.05$) according to Tukey's HSD.

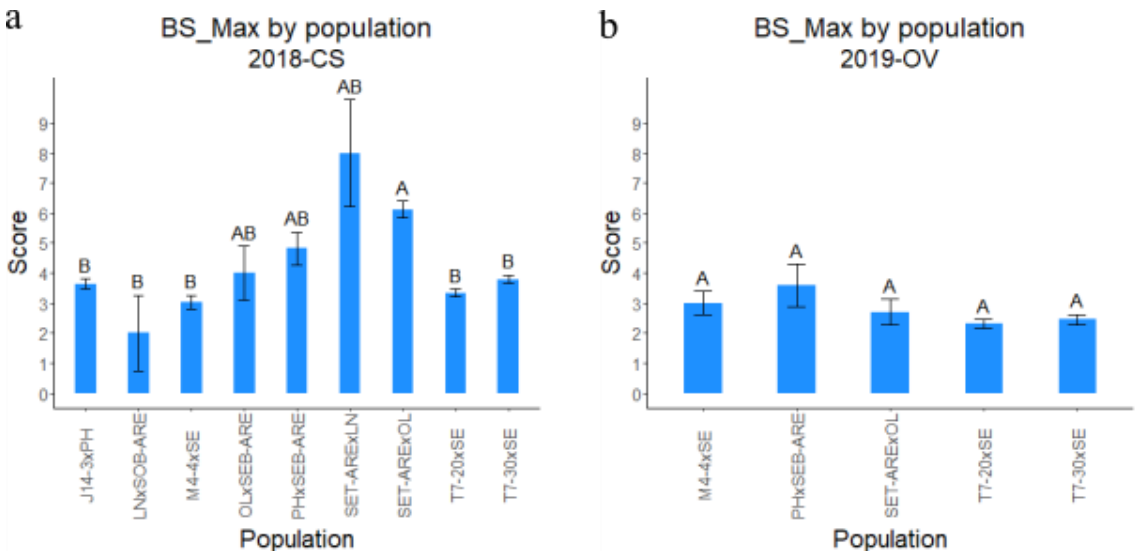

Figure 21 Mean black spot maximum score (BS_Max) per diploid rose population in College Station, TX (2018-CS, a) and Overton, TX (2019-OV, b). Black spot was scored on a scale of 0-9 in which 0 = 0% of plant canopy covered in lesions, 1 = 10% of plant canopy covered in lesions, and so on. Error bars reflect standard error of the mean. Means not connected by the same letter are significantly different ($p<0.05$) according to Tukey's HSD.

Populations differed in CLS severity in both year-locations, though this was not consistent (Fig. 22-24). For instance, while SET-ARExOL had one of the smallest CLS and CLS_AUDPC values in 2018-CS, it had one of the largest values in 2019-OV (Fig. 15, 16). PHxSEB-ARE had some of the lowest levels of CLS and population T7-20xSE had some of the highest levels of CLS in both year-locations by all three measures of CLS severity. All measures of CLS had significant block effects in 2018-CS, whereas only CLS_Max had a significant block effect in 2019-OV.

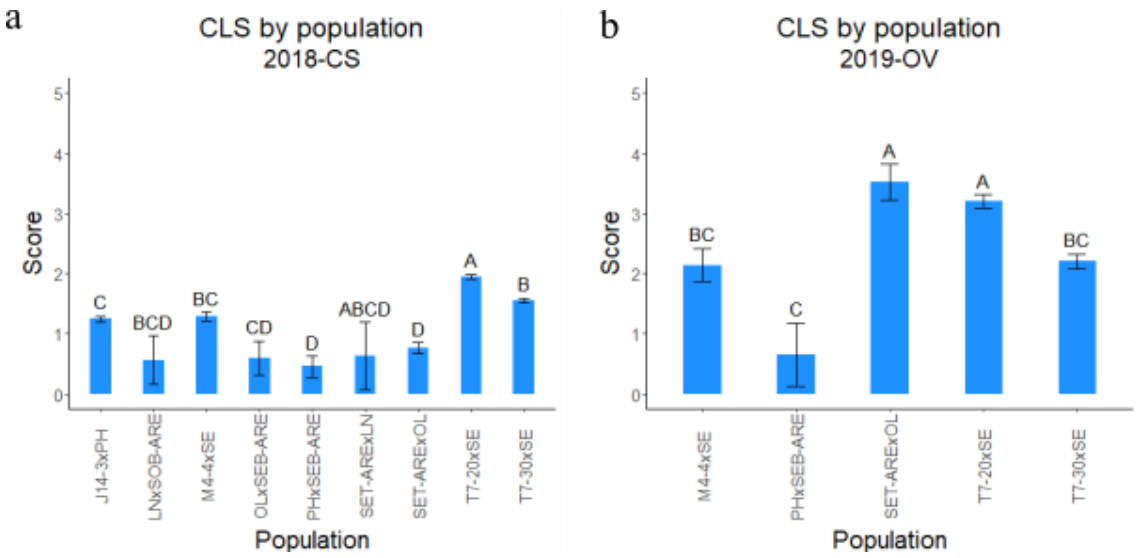

Figure 22 Mean cercospora (CLS) rating per diploid rose population in College Station, TX (2018-CS, a) and Overton, TX (2019-OV, b). Cercospora was scored on a scale of 0-9 in which 0 = 0% of plant canopy covered in lesions, 1 = 10% of plant canopy covered in lesions, and so on. Error bars reflect standard error of the mean. Means not connected by the same letter are significantly different ($p<0.05$) according to Tukey's HSD.

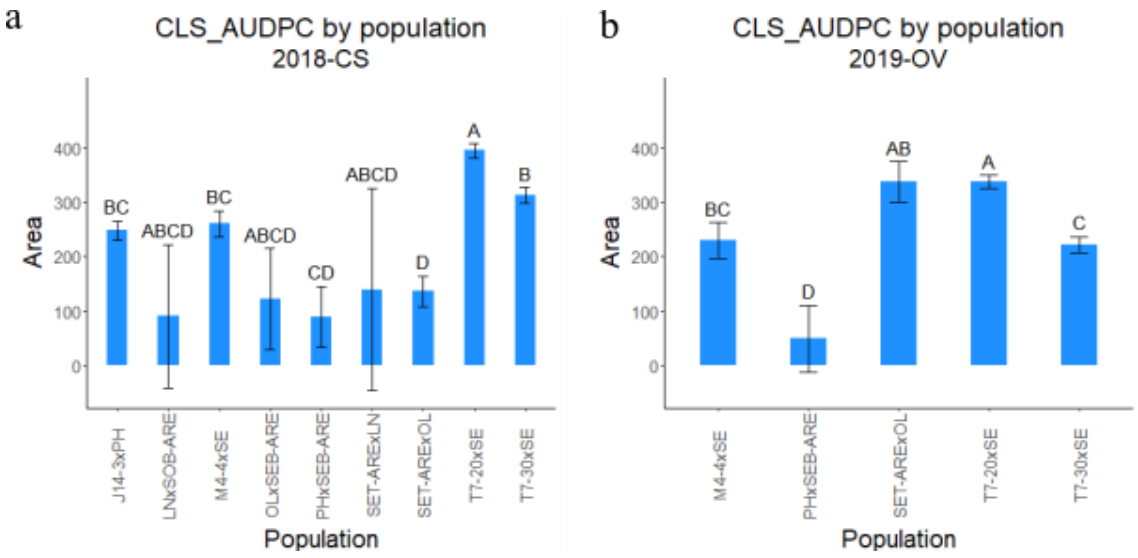

Figure 23 Mean cercospora area under the disease progress curve (CLS_AUDPC) per diploid rose population in College Station, TX (2018-CS, a) and Overton, TX (2019-OV, b). AUDPC was calculated with the trapezoidal method. Error bars reflect standard error of the mean. Means not connected by the same letter are significantly different ($p<0.05$) according to Tukey's HSD.

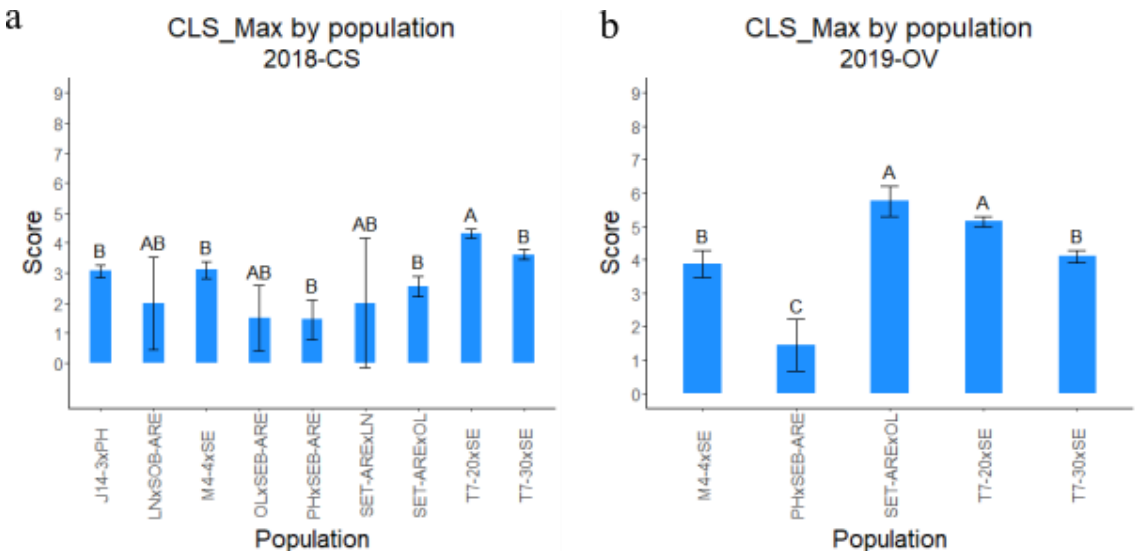

Figure 24 Mean cercospora maximum score (CLS_Max) per diploid rose population in College Station, TX (2018-CS, a) and Overton, TX (2019-OV, b). Cercospora was scored on a scale of 0-9 in which 0 = 0% of plant canopy covered in lesions, 1 = 10% of plant canopy covered in lesions, and so on. Error bars reflect standard error of the mean. Means not connected by the same letter are significantly different ($p<0.05$) according to Tukey's HSD.

Flowering intensity differed between populations in both year-locations (Fig. 25-27). SET-ARExOL, which contains mostly OF flowering types, had the least flowering in both year-locations; J14-3xPH, which is primarily CF types, had the most flowering of the populations in 2018-CS but was not present in 2019-OV. FLI ls means (2018-CS), FLI_Max (both year-locations), AFLIC (2018-CS), and CLS_AUDPC (2019-OV) did not have significant block effects.

Defoliation differed between populations only in 2018-CS (Fig. 28, 29). M4-4xSE had the least defoliation by both measures of DEF. Block effects were not significant for DEF in 2018-CS.

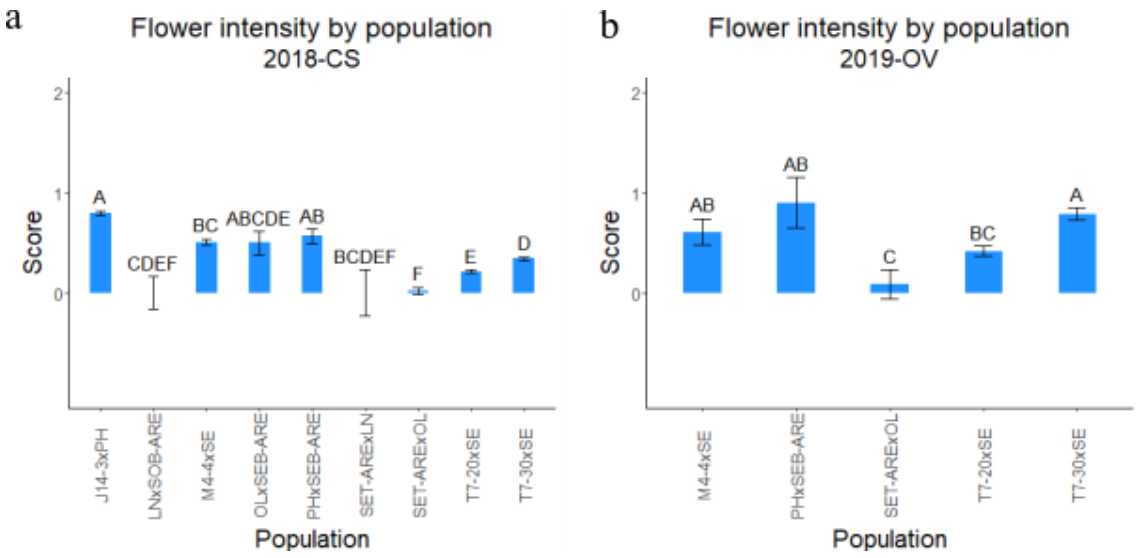

Figure 25 Mean flower intensity rating per diploid rose population in College Station, TX (2018-CS, a) and Overton, TX (2019-OV, b). Flower intensity was scored on a scale of 0-9 in which 0 = 0% of plant canopy covered in flowers, 1 = 10% of plant canopy covered in flowers, and so on. Error bars reflect standard error of the mean. Means not connected by the same letter are significantly different ($p<0.05$) according to Tukey's HSD.

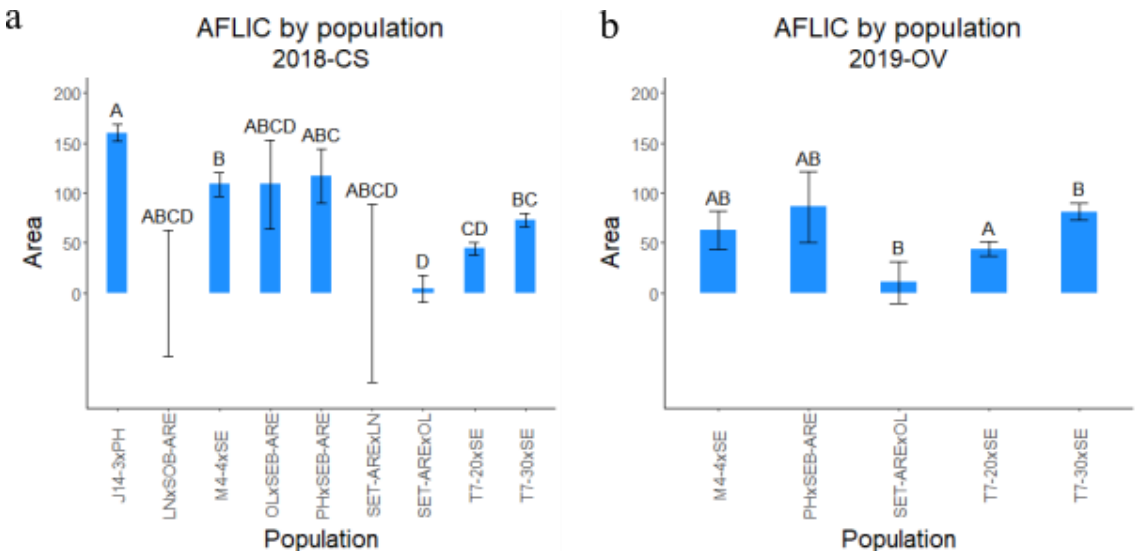

Figure 26 Mean area under the flower intensity curve (AFLIC) per diploid rose population in College Station, TX (2018-CS, a) and Overton, TX (2019-OV, b). AFLIC was calculated with the trapezoidal method. Error bars reflect standard error of the mean. Means not connected by the same letter are significantly different ($p<0.05$) according to Tukey's HSD.

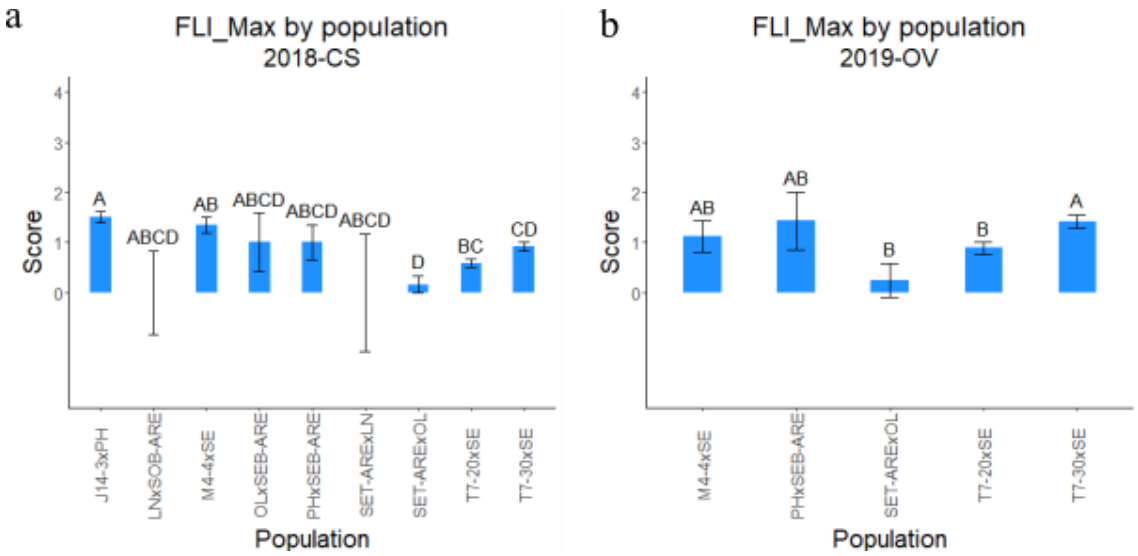

Figure 27 Mean flower intensity maximum score (FLI_Max) per diploid rose population in College Station, TX (2018-CS, a) and Overton, TX (2019-OV, b). Flower intensity was scored on a scale of 0-9 in which 0 = 0% of plant canopy covered in flowers, 1 = 10% of plant canopy covered in flowers, and so on. Error bars reflect standard error of the mean. Means not connected by the same letter are significantly different ($p<0.05$) according to Tukey's HSD.

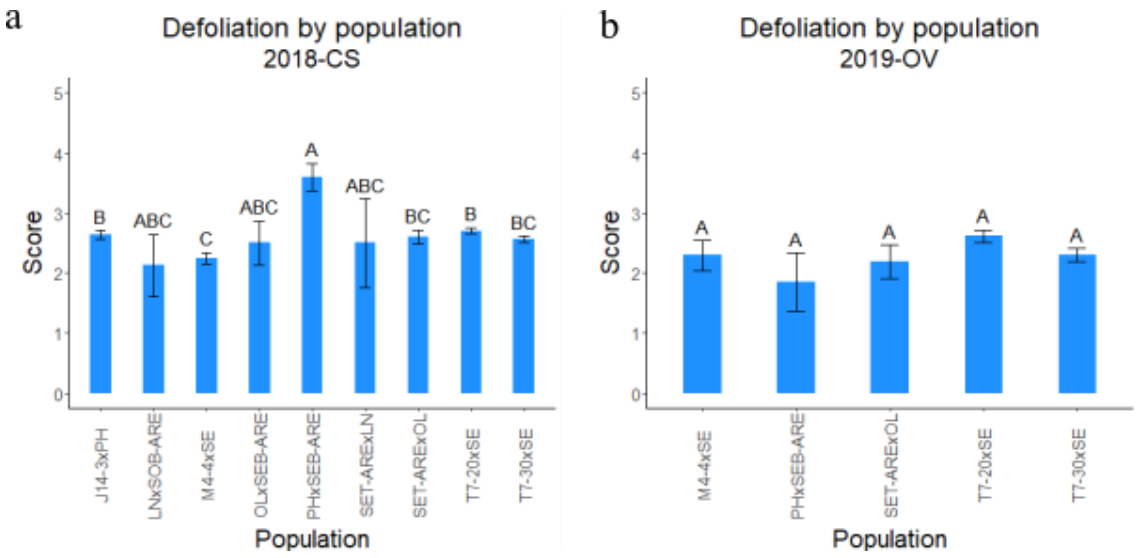

Figure 28 Mean defoliation rating per diploid rose population in College Station, TX (2018-CS, a) and Overton, TX (2019-OV, b). Defoliation was scored on a scale of 0-9 in which 0 = 0% of plant defoliated, 1 = 10% of plant defoliated, and so on. Error bars reflect standard error of the mean. Means not connected by the same letter are significantly different ($p<0.05$) according to Tukey's HSD.

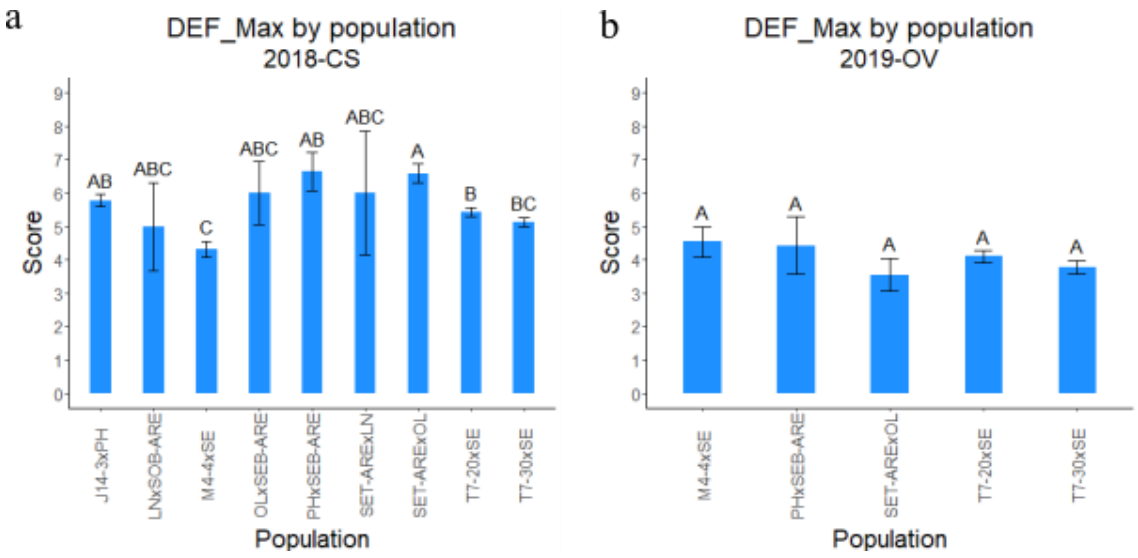

Figure 29 Mean defoliation maximum score (DEF_Max) per diploid rose population in College Station, TX (2018-CS, a) and Overton, TX (2019-OV, b). Defoliation was scored on a scale of 0-9 in which 0 = 0% of plant defoliated, 1 = 10% of plant defoliated, and so on. Error bars reflect standard error of the mean. Error bars reflect standard error of the mean. Means not connected by the same letter are significantly different ($p<0.05$) according to Tukey's HSD.

Architecture traits also varied between populations; however, the differences between populations were not always consistent between seasons. For instance, in 2018-S, population J14-3xPH had a lower NPrimaries than T7-20xSE and T7-30xSE; however, in 2018-W, J14-3xPH was different from T7-30xSE but not T7-20xSE (Fig. 30). Generally, populations M4-4xSE and PHxSEB-ARE had lower NPrimaries than T7-20xSE and T7-30xSE. Plants from J14-3xPH were usually smaller than those of the other populations as measured by the various plant vigor traits; plants from SET-ARExLN were frequently among the largest (Fig. 31-35). J14-3xPH, M4-4xSE, and PHxSEB-ARE had a greater degree of branching (higher ADI) while SET-ARExOL had less branching (Fig. 36a). Four populations (M4-4xSE, SET-ARExOL, T7-20xSE, and

T7-30xSE) were more prostrate (higher GHabit) while J14-3xPH and PHxSEB-ARE were more erect (Fig. 36b). The remaining populations were not different from either group. GHabit, height, length, and LDim did not have significant block effects in 2018-W.

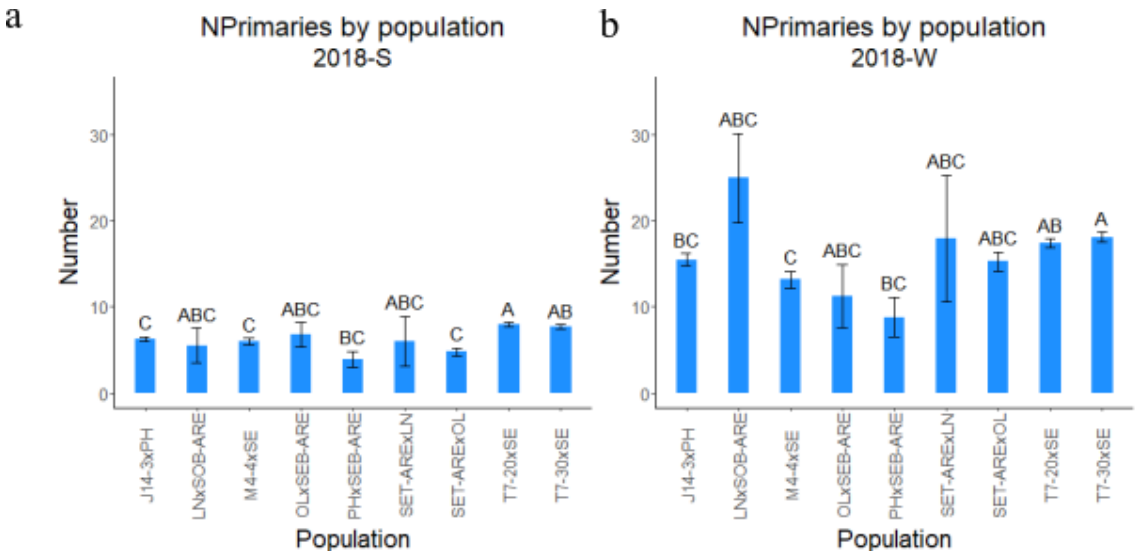

Figure 30 Mean number of primary shoots (NPrimaries) per diploid rose population in spring (2018-S, a) and winter (2018-W, b) 2018 in College Station, TX. Error bars reflect standard error of the mean. Means not connected by the same letter are significantly different ($p<0.05$) according to Tukey's HSD.

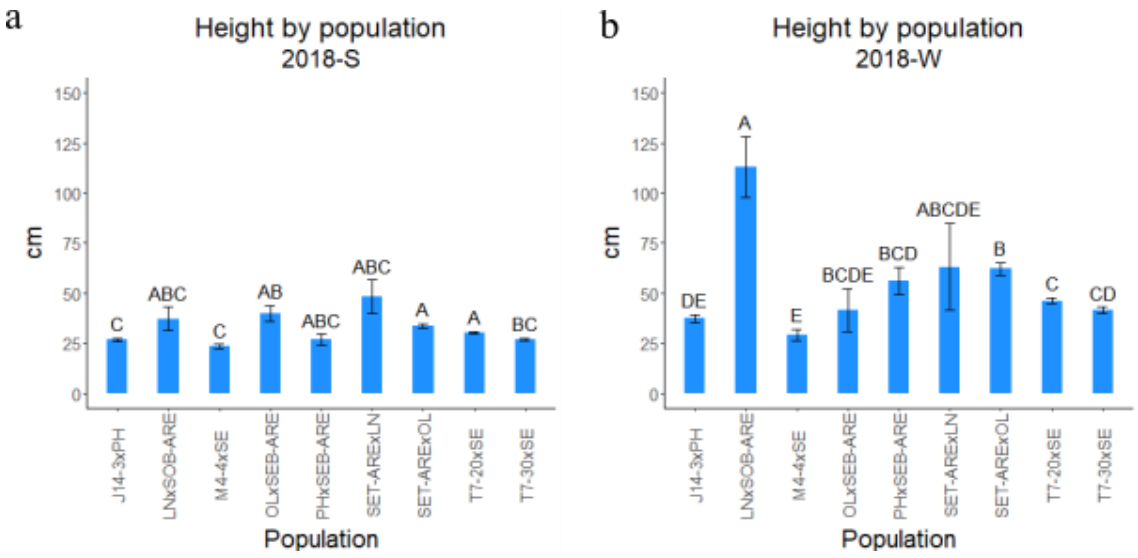

Figure 31 Mean plant height per diploid rose population in spring (2018-S, a) and winter (2018-W, b) 2018 in College Station, TX. Error bars reflect standard error of the mean. Means not connected by the same letter are significantly different ($p<0.05$) according to Tukey's HSD.

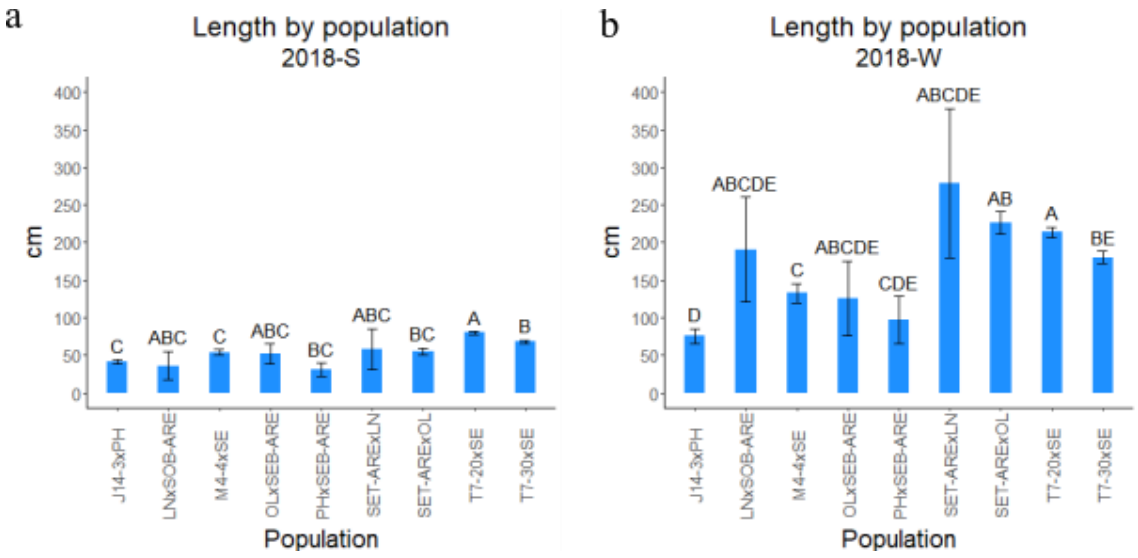

Figure 32 Mean plant length per diploid rose population in spring (2018-S, a) and winter (2018-W, b) 2018 in College Station, TX. Error bars reflect standard error of the mean. Means not connected by the same letter are significantly different ($p<0.05$) according to Tukey's HSD.

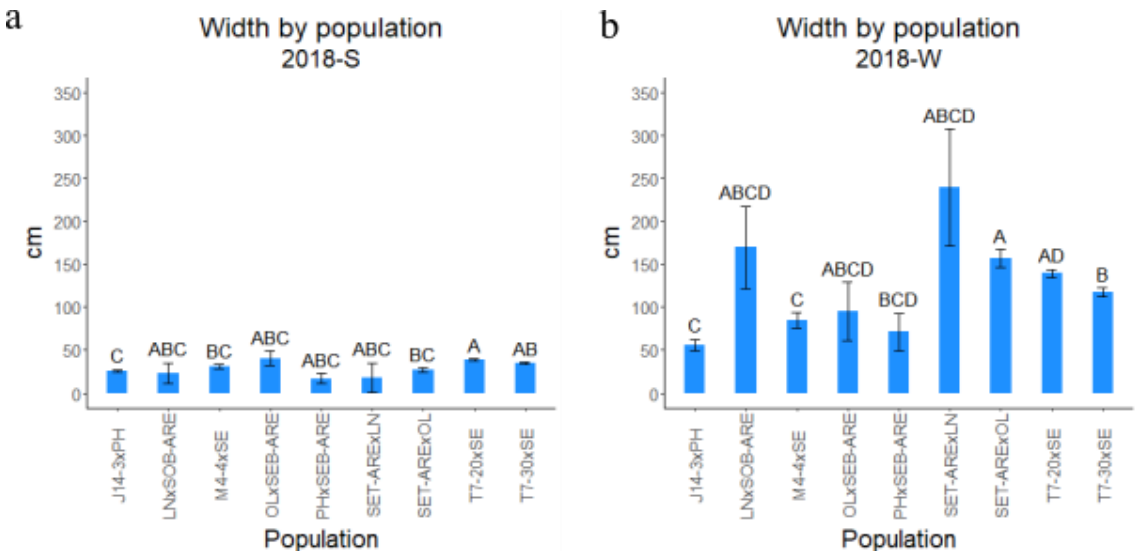

Figure 33 Mean plant width per diploid rose population in spring (2018-S, a) and winter (2018-W, b) 2018 in College Station, TX. Error bars reflect standard error of the mean. Means not connected by the same letter are significantly different ($p<0.05$) according to Tukey's HSD.

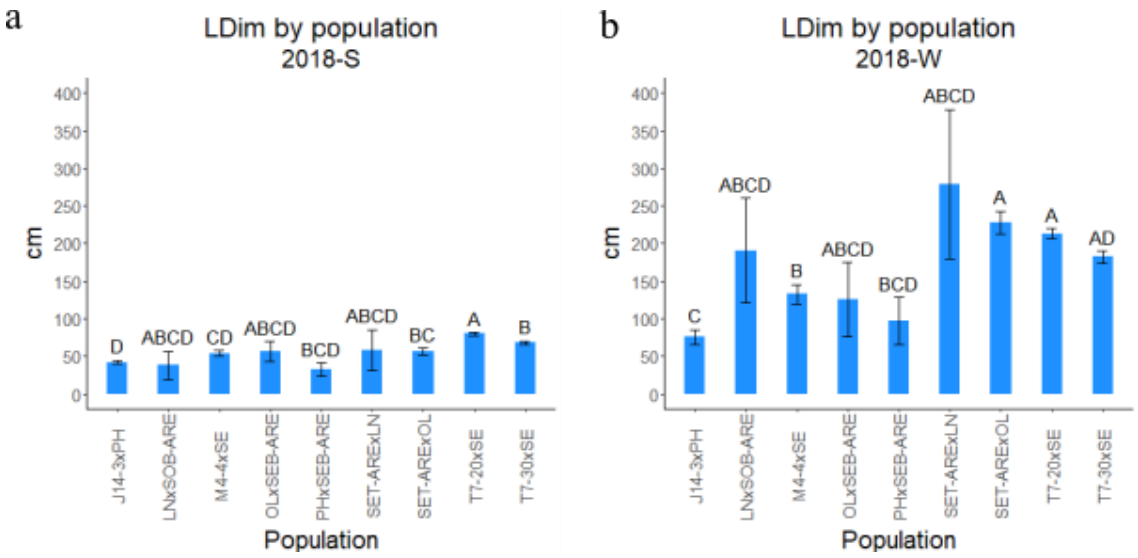

Figure 34 Mean plant longest dimension (LDim) per diploid rose population in spring (2018-S, a) and winter (2018-W, b) 2018 in College Station, TX. Longest dimension was defined as the largest plant measurement (height, length, or width). Error bars reflect standard error of the mean. Means not connected by the same letter are significantly different ($p<0.05$) according to Tukey's HSD.

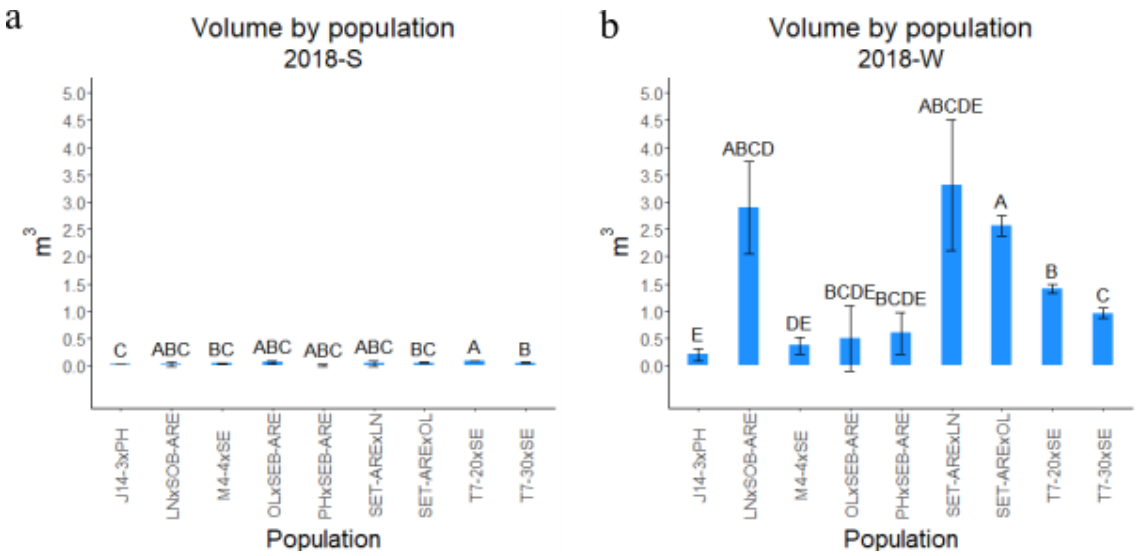

Figure 35 Mean plant volume (in cubic meters) per diploid rose population in spring (2018-S, a) and winter (2018-W, b) 2018 in College Station, TX. Plant volume was determined as the volume of an elliptical cylinder. Error bars reflect standard error of the mean. Means not connected by the same letter are significantly different ($p<0.05$) according to Tukey's HSD.

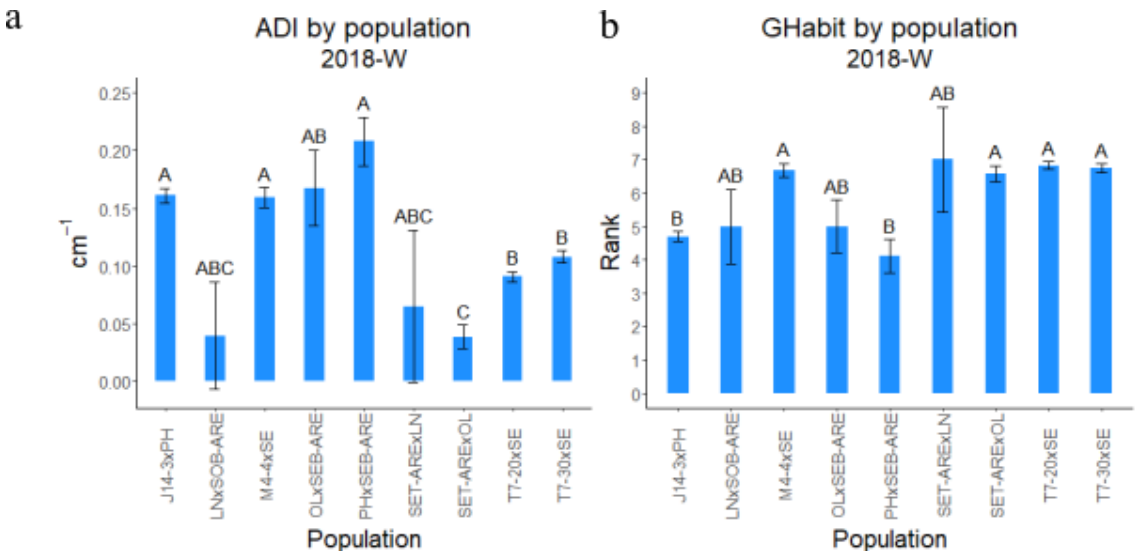

Figure 36 a. Mean apical dominance index (number of secondary shoots / length of primary shoot) per diploid rose population in winter 2018 (2018-W) in College Station, TX. b. Mean growth habit (GHabit) per diploid rose population in winter 2018 (2018-W) in College Station, TX. GHabit was ranked on a scale of 1 (erect) to 9 (prostrate) in 2018-W. Error bars reflect standard error of the mean. Means not connected by the same letter are significantly different ($p<0.05$) according to Tukey's HSD.

III.4.4 Differences between growth and flowering types

III.4.4.1 Cultivar panel

The majority of genotypes in the cultivar panel were found to be CF shrubs (Table 18). 21 genotypes were identified as climbers, two as groundcovers, and 50 as non-climbers. 61 genotypes were identified as CF, 11 as OF, and one as ORF. The FlwgType of 10 genotypes (14%) differed from that on record (Table 19). Three genotypes on record as CF and three on record as ORF were all identified as OF, and four genotypes on record as ORF were identified as CF. The field-determined FlwgType was used for subsequent analyses. Due to the low number of groundcover growth types and the difficulties of distinguishing between groundcover and climber growth types in

the field, climbers and groundcovers were grouped together. Similarly, the only ORF genotype was included with the OF genotypes for analysis.

Table 18 Number of each growth type (climber, groundcover, non-climber) and flowering type (once-flowering, OF; occasional repeat flowering, ORF; continuous flowering, CF) within the diploid rose cultivar panel as determined by visual assessment in 2018 in College Station, TX.

	OF	ORF	CF	Total
Climber	6	1	14	21
Groundcover	2	0	0	2
Non-climber	3	0	47	50
Total	11	1	61	73

*Table 19 Flowering type (FlwgType: once-flowering, OF; occasional repeat flowering, ORF; continuous flowering, CF) and growth type (GType, climber, groundcover, non-climber) for each diploid rose cultivar used in phenotypic analysis as determined by visual assessment in 2018 in College Station, TX. * indicates the FlwgType of record (drawn from HelpMeFind.com) is CF; † indicates FlwgType of record is ORF.*

Genotype	FlwgType	GType
Ballerina (1937)	CF	climber
Borderer	CF	non-climber
Belinda	CF	climber
Blush Noisette	CF	non-climber
Bermudas Kathleen	CF	non-climber
Bon Silene	CF	non-climber
Blumenschmidt	CF	non-climber
Cecile Brunner	CF	non-climber
Celine Forestier	CF	non-climber
Clotilde Soupert (1890)	CF	non-climber
Danae (1913)	CF	climber
Duchesse de Brabant	CF	non-climber
Ducher	CF	non-climber
Emmie Gray	CF	non-climber
Fortunes Double Yellow	OF	climber
Gipsy Boy	OF	climber
Gardenia (1899)	OF†	groundcover
General Schablikine	CF	non-climber

Table 19 Continued

Genotype	FlwgType	GType
Happenstance	OF*	non-climber
Independence Musk	CF†	non-climber
Jeanne dArc (1848)	CF	non-climber
Jaune Desprez	CF	non-climber
Jean Mermoz	CF	non-climber
Katharina Zeimet	CF	non-climber
La Marne	CF	non-climber
Leontine Gervais	OF†	groundcover
Lavender Pink Parfait	CF	non-climber
Le Vesuve (1825)	CF	non-climber
Mrs. Bosanquet	CF	non-climber
Miss Caroline	CF	non-climber
Mermaid (1917)	CF	climber
Mevrouw Nathalie Nypels	CF	non-climber
Mademoiselle Franziska Kruger	CF	non-climber
Madame Joseph Schwartz	CF	non-climber
Marjorie Fair	OF*	climber
Miss Lowes Variety	CF	non-climber
Madame Laurette Messimy	CF	non-climber
Marechal Niel (1864)	CF	climber
Moonlight (1913)	CF†	climber
Monsieur Tillier	CF	non-climber
Mutabilis	CF	non-climber
Marie Van Houtte	CF	non-climber
Mozart (1936)	CF	climber
Nastarana	CF	non-climber
Old Blush	CF	non-climber
Oakington Ruby	CF	non-climber
Phalaenopsis	CF	non-climber
Porcelaine de Chine	ORF	climber
Pink Grootendorst	CF†	non-climber
Perle des Jardins	CF	non-climber
Plaisanterie	CF	climber
Petite Pink Scotch	OF†	non-climber
Ma Paquerette	CF	non-climber
Pink Surprise (1987)	CF†	climber

Table 19 Continued

Genotype	FlwgType	GType
Robin Hood (1927)	CF	climber
Red Drift	CF	non-climber
Rosa moschata	CF	non-climber
Russelliana	OF	climber
Rouletii	CF	non-climber
Republic of Texas	CF	non-climber
Safrano	CF	non-climber
Sarasota Spice	CF	non-climber
Spice	CF	non-climber
Sunshine (1927)	OF*	non-climber
The Fairy	CF	non-climber
The Gift	CF	climber
Trier	CF	climber
Veilchenblau	OF	climber
Vincent Godsiff	CF	non-climber
Violette	OF	climber
Climbing White Maman Cochet	CF	climber
Windchimes	CF	climber
Yesterday	CF	non-climber

In the cultivars, most architecture traits differed significantly between both growth types and flowering types (Fig. 37-41). NPrimaries did not differ between growth types, and height did not differ between flowering types, however. OF cultivars had a higher NPrimaries and were usually larger (except by height) with less branching than CF cultivars. Climbing cultivars were likewise larger with less branching than non-climbers but did not differ from non-climbers in NPrimaries.

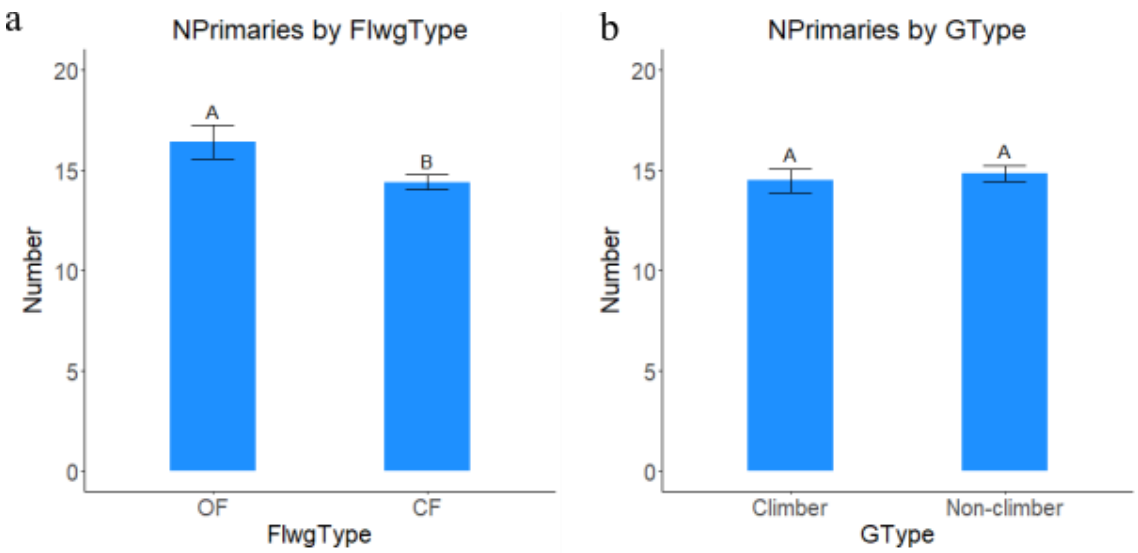

Figure 37 a. Mean NPrimaries, year-seasons combined, per flowering type (FlwgType) in diploid rose cultivars. OF = once-flowering, CF = continuous flowering. b. Mean NPrimaries, year-seasons combined, per growth type (GType) in diploid rose cultivars. Error bars reflect standard error of the mean. Means not connected by the same letter are significantly different ($p<0.05$) according to Student's t-test.

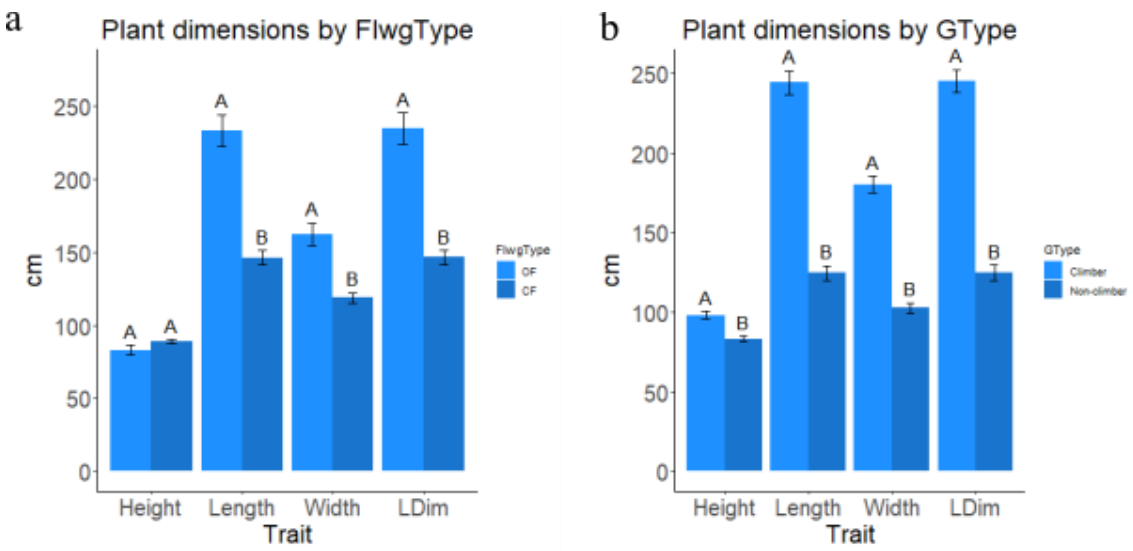

Figure 38 a. Mean plant height, length, width, and longest dimension (LDim), year-seasons combined, per flowering type (FlwgType) in diploid rose cultivars. OF = once-flowering, CF = continuous flowering. b. Mean plant height, length, width, and longest dimension (LDim), year-seasons combined, per growth type (GType) in diploid rose cultivars. Longest dimension was defined as the largest plant measurement (height, length, or width). Error bars reflect standard error of the mean. Means not connected by the same letter are significantly different ($p<0.05$) according to Student's t-test.

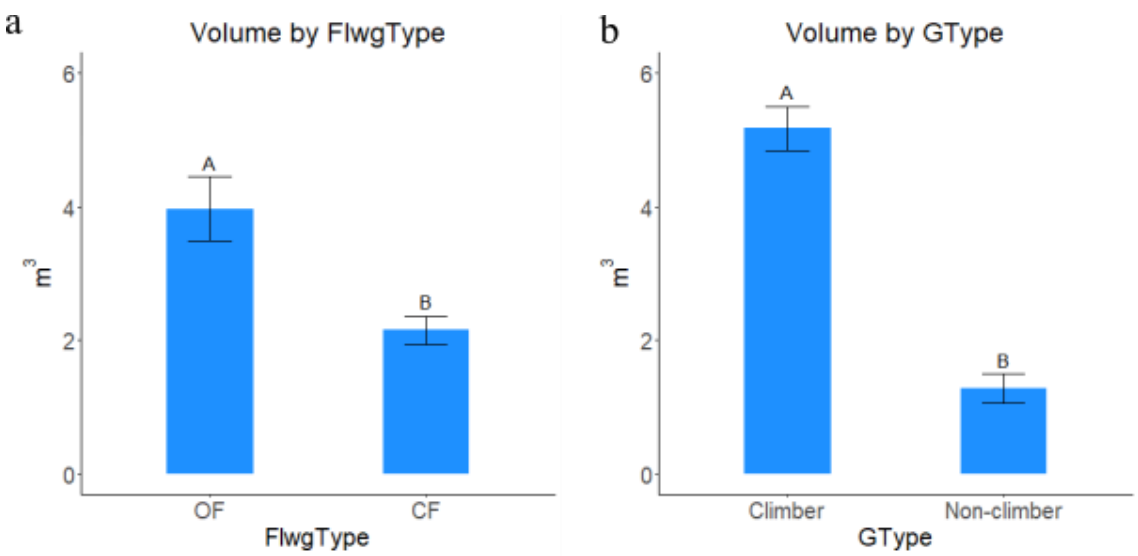

Figure 39 a. Mean plant volume, year-seasons combined, per flowering type (FlwgType) in diploid rose cultivars. OF = once-flowering, CF = continuous flowering. b. Mean plant volume, year-seasons combined, per growth type (GType) in diploid rose cultivars. Plant volume was determined as the volume of an elliptical cylinder. Error bars reflect standard error of the mean. Means not connected by the same letter are significantly different ($p<0.05$) according to Student's t-test.

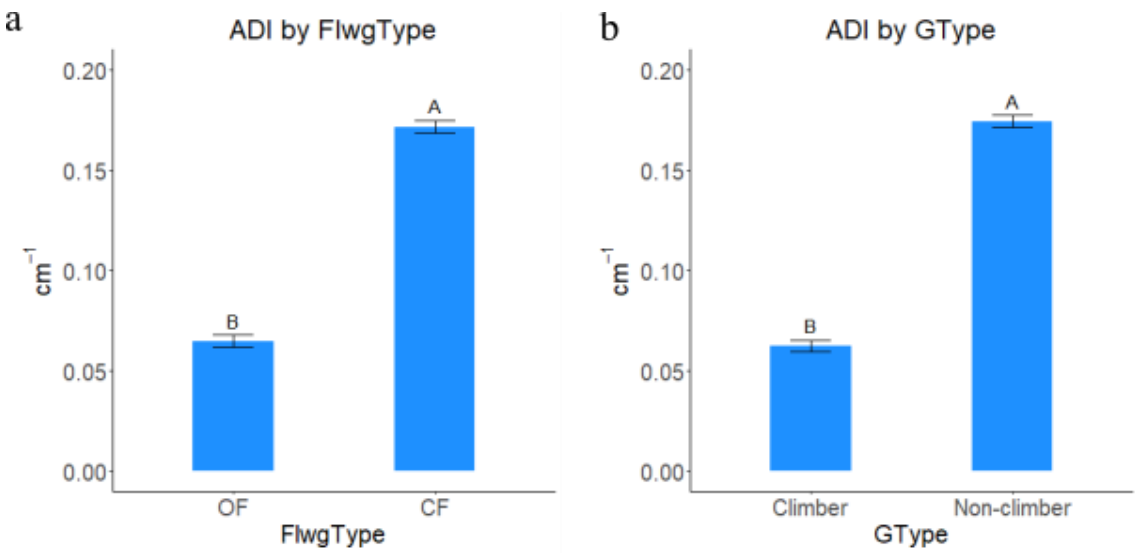

Figure 40 a. Mean apical dominance index (ADI), year-seasons combined, per flowering type (FlwgType) in diploid rose cultivars. OF = once-flowering, CF = continuous flowering. b. Mean apical dominance index (ADI), year-seasons combined, per growth type (GType) in diploid rose cultivars. ADI = number of secondary shoots / length of primary shoot. Error bars reflect standard error of the mean. Means not connected by the same letter are significantly different ($p<0.05$) according to Student's t-test.

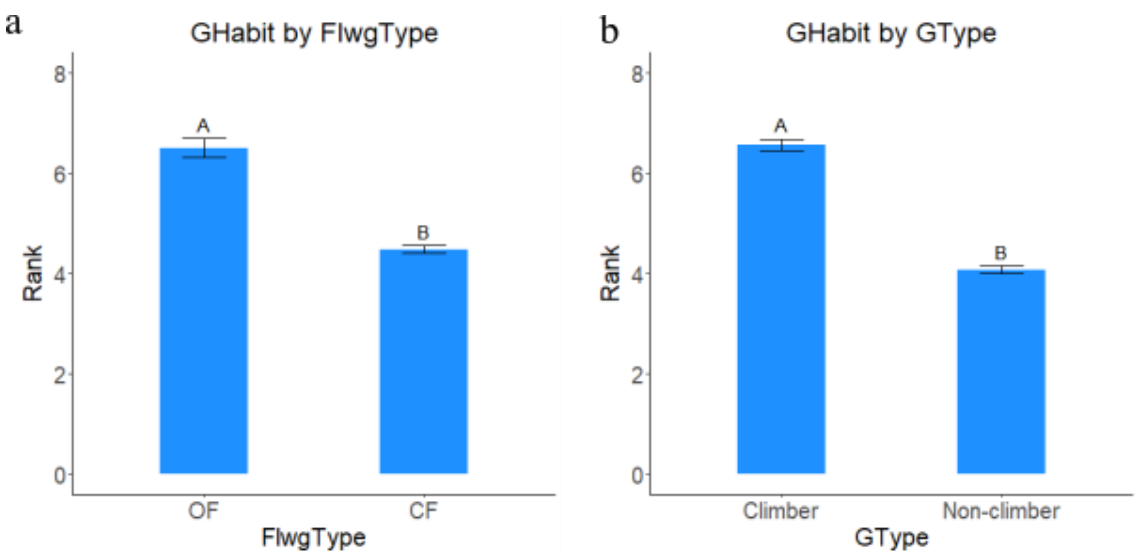

Figure 41 a. Mean GHabit per flowering type (FlwgType) in diploid rose cultivars. OF = once-flowering, CF = continuous flowering. b. Mean GHabit per growth type (GType) in diploid rose cultivars. GHabit was ranked on a scale of 1 (erect) to 9 (prostrate) in 2018-W. Error bars reflect standard error of the mean. Means not connected by the same letter are significantly different ($p<0.05$) according to Student's t-test.

III.4.4.2 Families

The seedlings in the nine diploid rose families were approximately evenly divided between OF and CF flowering types and climber/groundcover and non-climber growth types (Tables 20, 21). Four genotypes, however, were determined to have different growth types between the two replications, and these were excluded from the subsequent analysis. As flowering type and growth type were not perfectly correlated, the effects of both on architecture were investigated as in the cultivars.

In the families, all architecture traits differed between flowering types (Fig. 42-46). Similar to the cultivars, OF and climbing genotypes had a higher NPrimaries than CF and non-climbers. OF and climbing genotypes were larger by all measures of plant

vigor, had less branching, and were more prostrate. The block x flowering type and block x growth type effects were not significant for any traits. All traits had a significant block effect when both flowering and growth types were investigated.

Table 20 Growth type (climber, non-climber) and flowering type (once-flowering, OF; continuous flowering, CF) in diploid rose families as determined by visual assessment in 2018 in College Station, TX. Growth types that conflicted between replications have been excluded.

	OF	CF	Total
Climber	164	4	168
Non-climber	6	149	155
Total	170	153	323

Table 21 Growth type (Gtype: climber, non-climber) and flowering type (once-flowering, OF; continuous flowering, CF) per diploid rose family as determined by visual assessment in 2018 in College Station, TX. GTypes that were in conflict between replications have been excluded.

	FlwgType		GType	
	OF	CF	Climber	Non-climber
J14-3xPH	4	64	0	65
PHxSEB-ARE	2	8	2	8
M4-4xSE	11	22	11	21
T7-20xSE	76	27	79	24
T7-30xSE	54	34	54	33
SET-ARExLN	1	0	1	0
SET-ARExOL	23	1	20	3
OLxSEB-ARE	0	2	0	1
LNxSOB-ARE	1	0	1	0

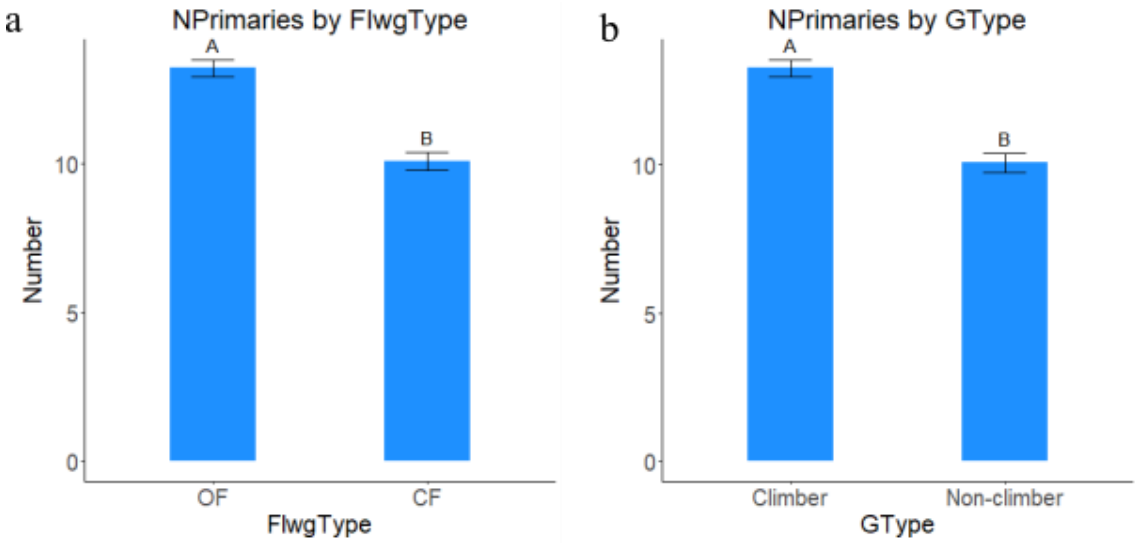

Figure 42 a. Mean number of primary shoots (NPrimaries), year-seasons combined, per flowering type (FlwgType) in nine diploid rose families. OF = once-flowering, CF = continuous flowering. b. Mean number of primary shoots (NPrimaries), year-seaosns combined, per growth type (GType) in nine diploid rose families. Error bars reflect standard error of the mean. Means not connected by the same letter are significantly different ($p<0.05$) according to Student's t-test.

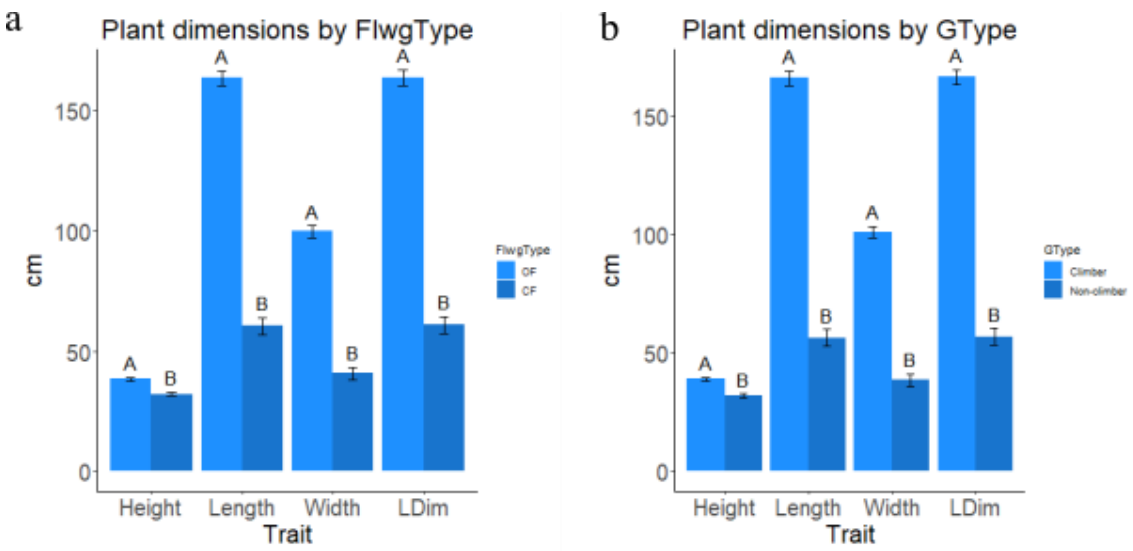

Figure 43 a. Mean plant height, length, width, and longest dimension (LDim), year-seasons combined, per flowering type (FlwgType) in nine diploid rose families. OF = once-flowering, CF = continuous flowering. b. Mean plant height, length, width, and longest dimension (LDim), year-seasons combined, per growth type (GType) in nine diploid rose families. Longest dimension was defined as the largest plant measurement (height, length, or width). Error bars reflect standard error of the mean. Means not connected by the same letter are significantly different ($p<0.05$) according to Student's t-test.

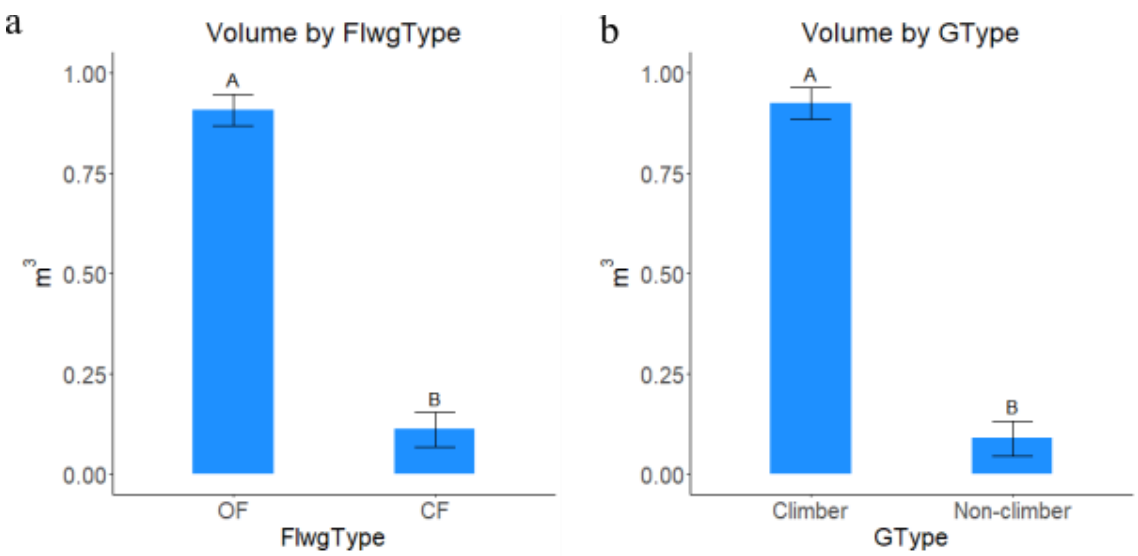

Figure 44 a. Mean plant volume, year-seasons combined, per flowering type (FlwgType) in nine diploid rose families. OF = once-flowering, CF = continuous flowering. b. Mean plant volume, year-seasons combined, per growth type (GType) in nine diploid rose families. Plant volume was determined as the volume of an elliptical cylinder. Error bars reflect standard error of the mean. Means not connected by the same letter are significantly different ($p<0.05$) according to Student's t-test.

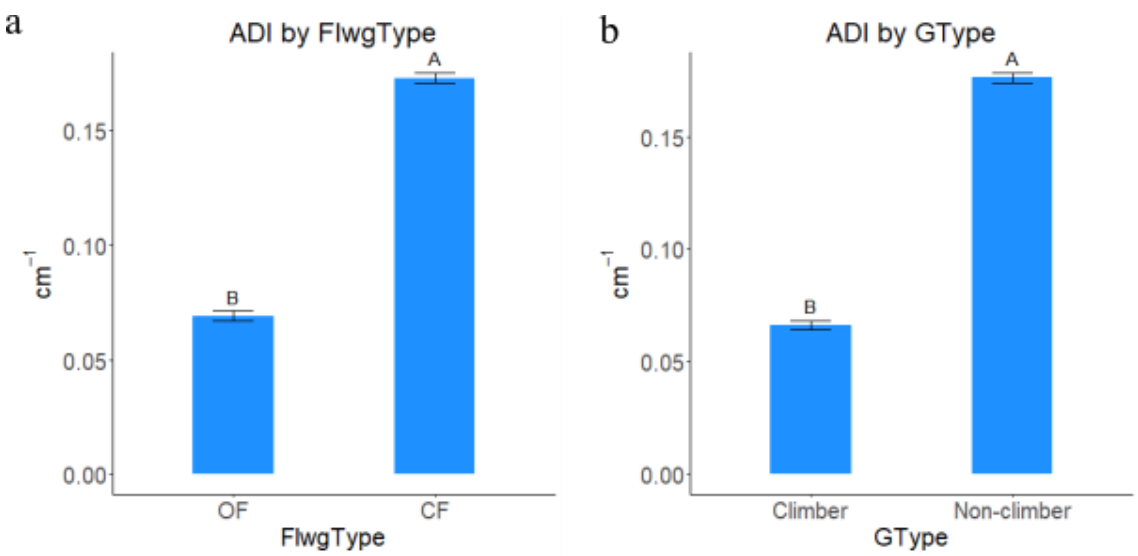

Figure 45 a. Mean apical dominance index (ADI) in 2018-W per flowering type (FlwgType) in nine diploid rose families. OF = once-flowering, CF = continuous flowering. b. Mean ADI in 2018-W per growth type (GType) in nine diploid rose families. ADI = number of secondary shoots / length of primary shoot. Error bars reflect standard error of the mean. Means not connected by the same letter are significantly different ($p<0.05$) according to Student's t-test.

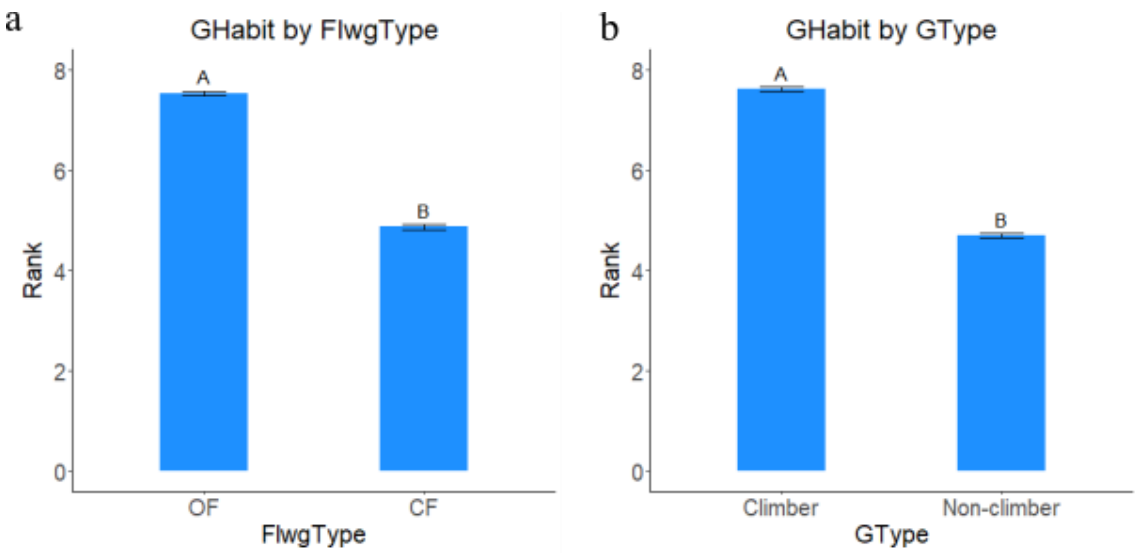

Figure 46 a. Mean growth habit (GHabit) per flowering type (FlwgType) in nine diploid rose families. OF = once-flowering, CF = continuous flowering. b. Mean GHabit per growth type (GType) in nine diploid rose families. GHabit was ranked on a scale of 1 (erect) to 9 (prostrate) in 2018-W. Error bars reflect standard error of the mean. Means not connected by the same letter are significantly different ($p<0.05$) according to Student's t-test.

III.4.5 Correlations between traits

III.4.5.1 Architecture traits

III.4.5.1.1 Cultivar panel

In the cultivars, plant vigor traits were strongly correlated with each other (Table 22, Fig. 47). Notably, LDim was perfectly correlated with Length and almost perfectly correlated with width (r = 0.9); however, the correlation between height and LDim was only 0.49. NPrimaries was only weakly correlated with plant vigor traits and was not correlated with ADI and GHabit. Plant vigor traits and GHabit had a weak negative correlation with ADI. All plant vigor traits had a moderately weak positive correlation with GHabit except height, which had a weak negative correlation.

*Table 22 Correlation coefficients from Pearson's product-moment correlation test between architecture traits in diploid rose cultivars, year-seasons combined. NPrimaries = number of primary shoots, LDim = longest dimension, ADI = apical dominance index, GHabit = growth habit. ns, p >0.05; *, 0.01 ≤ p ≤ 0.05; **, 0.00 ≤ p≤ 0.01; ***, 0.0001 ≤ p ≤ 0.001; ****, p < 0.0001.*

	NPrimaries	Height	Length	Width	LDim	Volume	ADI	GHabit
NPrimaries	1							
Height	0.25****	1						
Length	0.17****	0.49****	1					
Width	0.24****	0.61****	0.9****	1				
LDim	0.17****	0.49****	1****	0.9****	1			
Volume	0.15***	0.54****	0.82****	0.86****	0.82****	1		
ADI	-0.05^{ns}	-0.19***	-0.3****	-0.25****	-0.3****	-0.26****	1	
GHabit	-0.09^{ns}	-0.1*	0.46****	0.4****	0.46****	0.32****	-0.21**	1

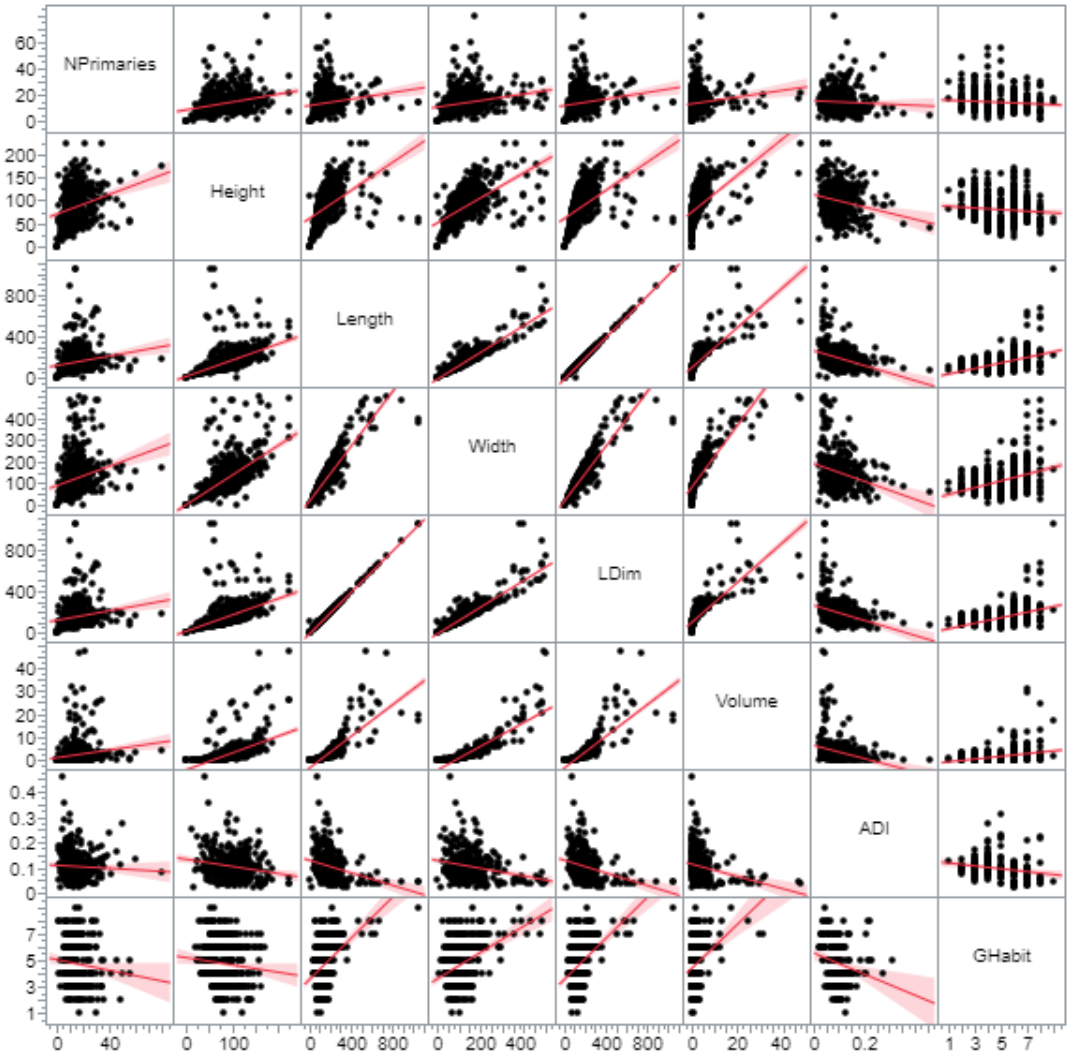

Figure 47 Scatterplots of relationships between architecture traits in diploid rose cultivars, year-seasons combined. Line indicates line of best fit. NPrimaries = number of primary shoots, LDim = longest dimension, ADI = apical dominance index, GHabit = growth habit.

III.4.5.1.2 Families

Similar relationships were seen in the families, though they differed in degree (Table 23, Fig. 48). Again, LDim was perfectly correlated with length and very strongly correlated with width. Vigor traits were moderately to very strongly correlated with each

other. Unlike in the cultivars, NPrimaries was moderately to very strongly correlated with vigor. Vigor traits (except height) and GHabit had moderately strong negative correlations with ADI. Vigor traits except height were moderately correlated with GHabit.

Correlations between architecture traits were also investigated within OF and CF flowering types. In OF types, height was moderately weakly correlated with length, width, and LDim (Table 24, Fig. 49); in CF types, correlations between plant vigor traits were moderate to very strong (Table 25, Fig. 50). In OF types, NPrimaries was moderately to very strongly correlated with plant vigor traits. In CF types, the correlation was reduced, ranging from r = 0.39 for NPrimaries to volume to r = 0.61 for NPrimaries to width. Correlations between ADI and other architecture traits were weak or nonsignificant for both flowering types. GHabit was weakly correlated with length and LDim in CF types only.

III.4.5.2 Disease, defoliation, and flower intensity

The correlations between area, maximum scores, and ls means of BS, CLS, DEF, and FLI were likewise investigated (Tables 26-32; Fig. 40-51). Ls means, areas, and maximum scores were very strongly correlated within each trait for cultivars and families. In cultivars, families in both year-locations, OF types within families, and CF types within families in both year-locations, correlations between flower intensity and disease/defoliation measures were weak or nonsignificant. CLS and BS frequently had weak to moderately weak negative correlations with each other. Correlations between diseases and defoliation were weak or nonsignificant.

*Table 23 Correlation coefficients from Pearson's product-moment correlation test between architecture traits in nine diploid rose families, year-seasons combined, in College Station, TX in 2018. NPrimaries = number of primary shoots, LDim = longest dimension, ADI = apical dominance index, GHabit = growth habit. ns, $p > 0.05$; *, $0.01 \leq p \leq 0.05$; **, $0.00 \leq p \leq 0.01$; ***, $0.0001 \leq p \leq 0.001$; ****, $p < 0.0001$.*

	NPrimaries	Height	Length	Width	LDim	Volume	ADI	GHabit
NPrimaries	1							
Height	0.54****	1						
Length	0.61****	0.44****	1					
Width	0.67****	0.52****	0.88****	1				
LDim	0.61****	0.45****	1****	0.89****	1			
Volume	0.59****	0.7****	0.79****	0.83****	0.79****	1		
ADI	-0.34****	-0.29****	-0.59****	-0.55****	-0.59****	-0.49****	1	
GHabit	0.13****	-0.03^{ns}	0.52****	0.41****	0.52****	0.26****	-0.52****	1

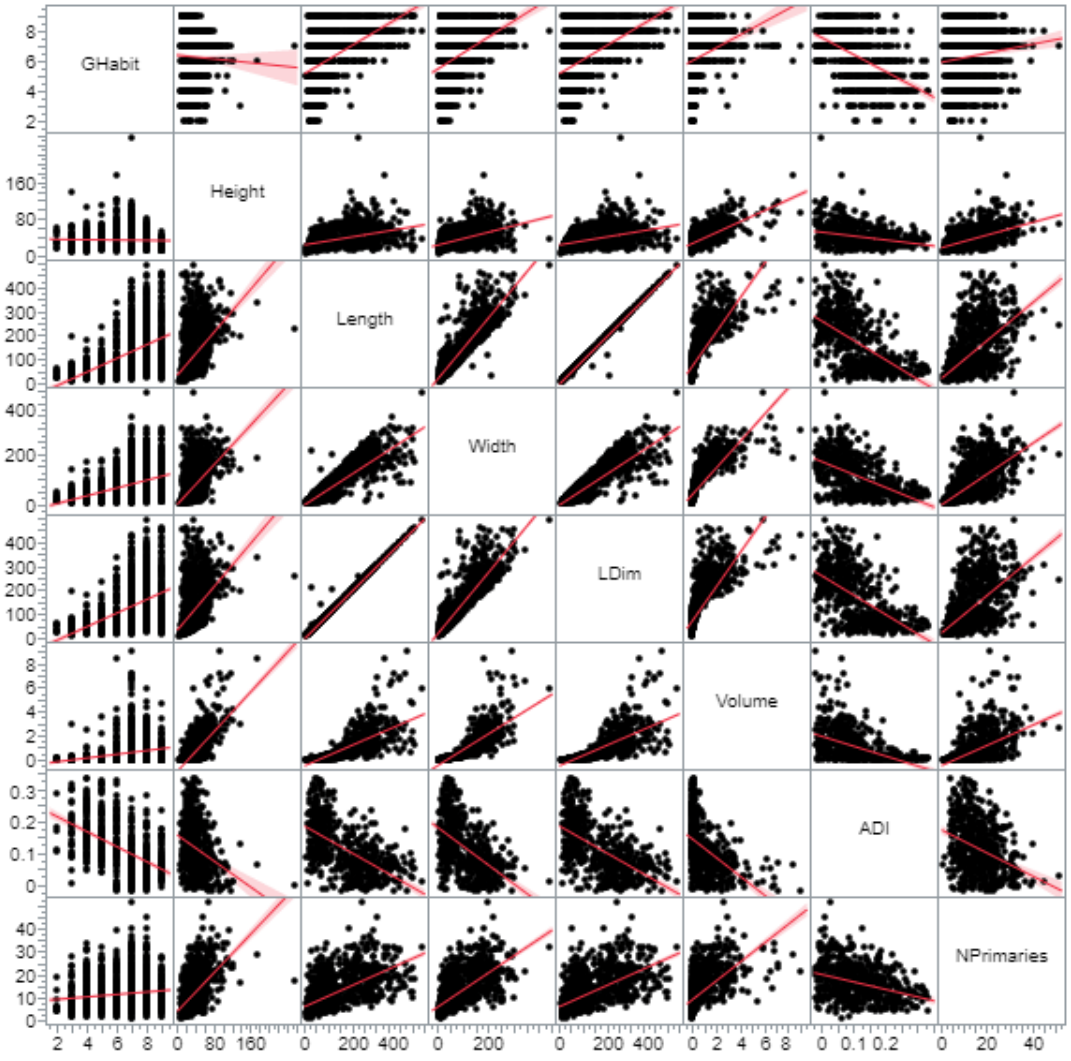

Figure 48 Scatterplots of relationships between architecture traits in nine diploid rose families, year-seasons combined, in College Station, TX in 2018. Line indicates line of best fit. NPrimaries = number of primary shoots, LDim = longest dimension, ADI = apical dominance index, GHabit = growth habit.

*Table 24 Correlation coefficients from Pearson's product-moment correlation test between architecture traits in once-flowering genotypes from nine diploid rose families, year-seasons combined, in College Station, TX in 2018. NPrimaries = number of primary shoots, LDim = longest dimension, ADI = apical dominance index, GHabit = growth habit. ns, $p > 0.05$; *, $0.01 \leq p \leq 0.05$; **, $0.00 \leq p \leq 0.01$; ***, $0.0001 \leq p \leq 0.001$; ****, $p < 0.0001$.*

	NPrimaries	Height	Length	Width	LDim	Volume	ADI	GHabit
NPrimaries	1							
Height	0.54****	1						
Length	0.66****	0.4****	1					
Width	0.71****	0.49****	0.85****	1				
LDim	0.66****	0.41****	1****	0.86****	1			
Volume	0.65****	0.74****	0.75****	0.81****	0.75****	1		
ADI	-0.21***	-0.22****	-0.17**	-0.19***	-0.16**	-0.24****	1	
GHabit	-0.04^{ns}	-0.33****	0.23****	0.13**	0.22****	-0.07^{ns}	-0.03^{ns}	1

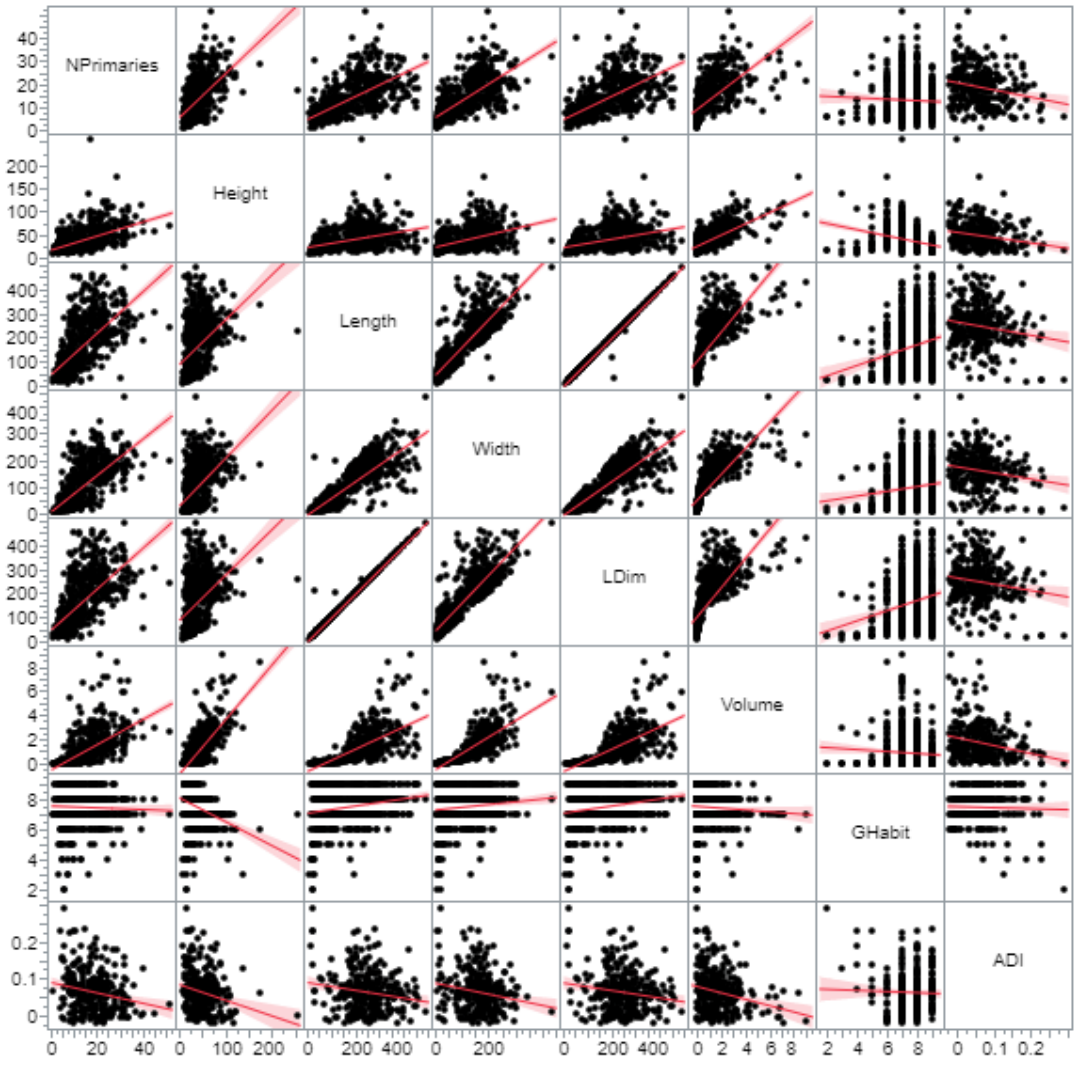

Figure 49 Scatterplots of relationships between architecture traits in once-flowering genotypes from nine diploid rose families, year-seasons combined, in College Station, TX in 2018. Line indicates line of best fit. NPrimaries = number of primary shoots, LDim = longest dimension, ADI = apical dominance index, GHabit = growth habit.

*Table 25 Correlation coefficients from Pearson's product-moment correlation test between architecture traits in continuous flowering genotypes from nine diploid rose families, year-seasons combined, in College Station, TX in 2018. NPrimaries = number of primary shoots, LDim = longest dimension, ADI = apical dominance index, GHabit = growth habit. ns, $p > 0.05$; *, $0.01 \leq p \leq 0.05$; **, $0.00 \leq p \leq 0.01$; ***, $0.0001 \leq p \leq 0.001$; ****, $p < 0.0001$.*

	NPrimaries	Height	Length	Width	LDim	Volume	ADI	GHabit
NPrimaries	1							
Height	0.5****	1						
Length	0.49****	0.61****	1					
Width	0.61****	0.66****	0.89****	1				
LDim	0.48****	0.62****	1****	0.9****	1			
Volume	0.39****	0.59****	0.84****	0.8****	0.84****	1		
ADI	-0.18**	-0.09^{ns}	-0.19**	-0.15*	-0.21***	-0.24****	1	
GHabit	-0.03^{ns}	-0.08^{ns}	0.39****	0.27****	0.39****	0.24****	-0.07^{ns}	1

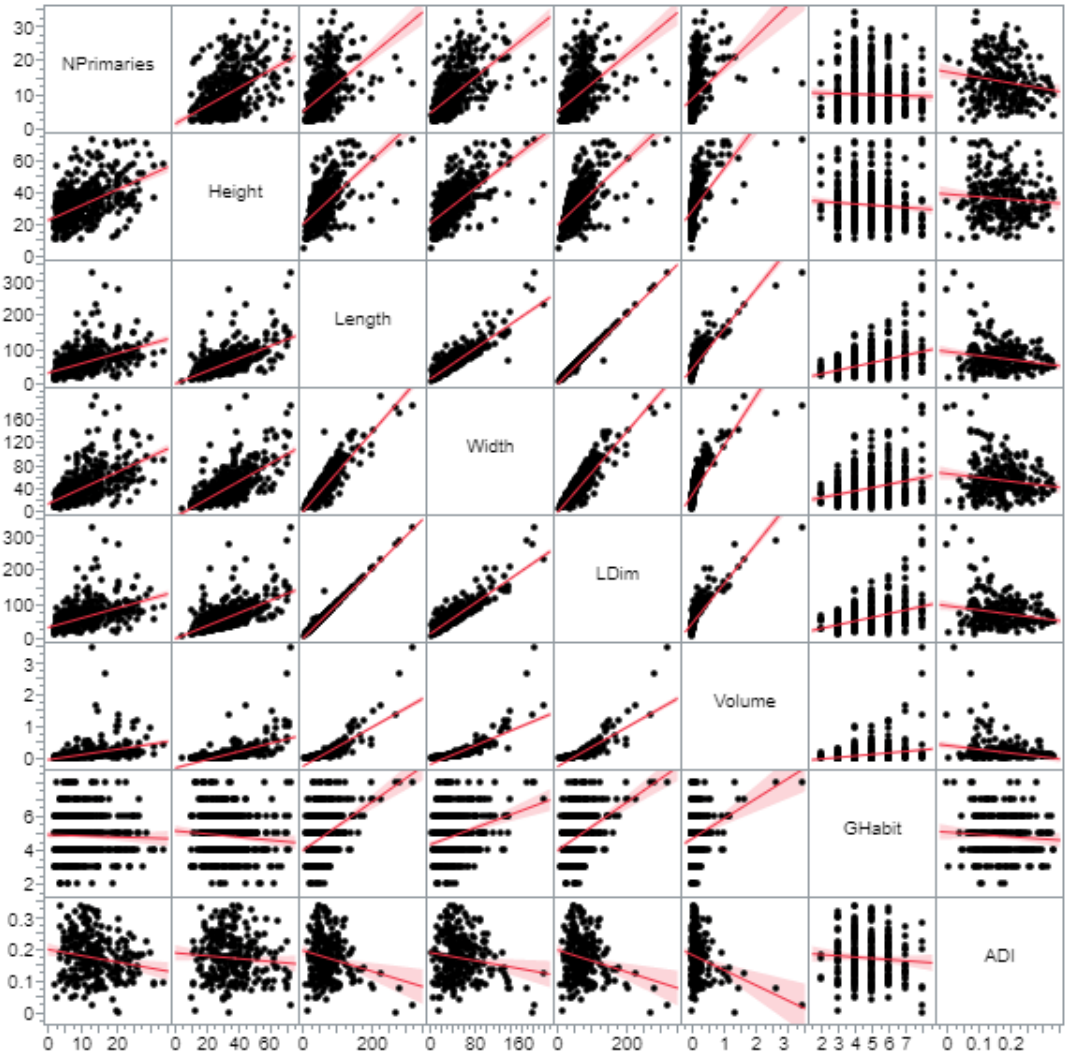

Figure 50 Scatterplots of relationships between architecture traits in continuous flowering genotypes from nine diploid rose families, year-seasons combined, in College Station, TX in 2018. Line indicates line of best fit. NPrimaries = number of primary shoots, LDim = longest dimension, ADI = apical dominance index, GHabit = growth habit.

*Table 26 Correlation coefficients from Pearson's product-moment correlation test between black spot (BS) severity, cercospora (CLS) severity, flower intensity (FLI), and defoliation (DEF) in diploid rose cultivars. BS, CLS, FLI, and DEF refer to the least squares means of each trait. AUDPC indicates the area under the disease progress curve for BS and CLS; AFLIC indicates the area under the flower intensity curve for FLI. _Max indicates the maximum score for BS, CLS, FLI, and DEF over the course of the growing season (2018-CS). ns, p >0.05; *, 0.01 ≤ p ≤ 0.05; **, 0.00 ≤ p≤ 0.01; ***, 0.0001 ≤ p ≤ 0.001; ****, p < 0.0001.*

	BS	BS_ AUDPC	BS_Max	CLS	CLS_ AUDPC	CLS_ Max	FLI	AFLIC	FLI_ Max	DEF	DEF_ Max
BS	1										
BS_ AUDPC	0.97****	1									
BS_Max	0.79****	0.75****	1								
CLS	-0.38****	-0.34****	-0.22**	1							
CLS_ AUDPC	-0.36****	-0.31****	-0.16*	0.98****	1						
CLS_Max	-0.3****	-0.22**	-0.2**	0.81****	0.75****	1					
FLI	0.08^{ns}	0.09^{ns}	0^{ns}	0.06^{ns}	0.05^{ns}	0.07^{ns}	1				
AFLIC	0.11^{ns}	0.14^{ns}	0.05^{ns}	0.06^{ns}	0.07^{ns}	0.09^{ns}	0.99****	1			
FLI_Max	0^{ns}	0.03^{ns}	-0.04^{ns}	0.07^{ns}	0.08^{ns}	0.05^{ns}	0.83****	0.78****	1		
DEF	0.44****	0.39****	0.4****	-0.03^{ns}	-0.01^{ns}	-0.03^{ns}	-0.28****	-0.29****	-0.22**	1	
DEF_Max	0.33****	0.32****	0.36****	0.1^{ns}	0.13^{ns}	0.06^{ns}	-0.3****	-0.29****	-0.21**	0.79****	1

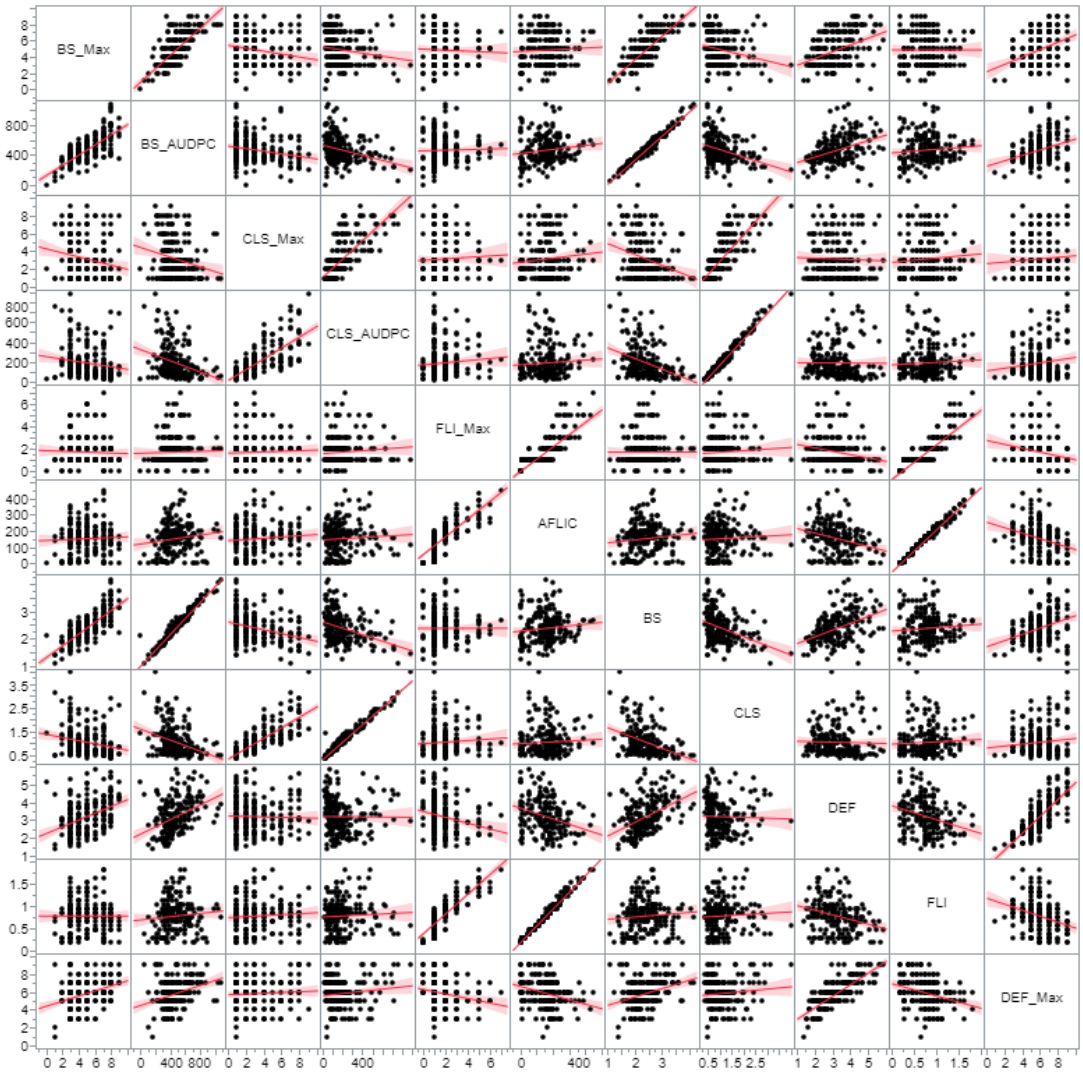

Figure 51 Scatterplots of relationships between black spot (BS) severity, cercospora (CLS) severity, flower intensity (FLI), and defoliation (DEF) in diploid rose cultivars. BS, CLS, FLI, and DEF refer to the least squares means of each trait. AUDPC indicates the area under the disease progress curve for BS and CLS; AFLIC indicates the area under the flower intensity curve for FLI. _Max indicates the maximum score for BS, CLS, FLI, and DEF over the course of the growing season (2018-CS). Line indicates line of best fit.

*Table 27 Correlation coefficients from Pearson's product-moment correlation test between black spot (BS) severity, cercospora (CLS) severity, flower intensity (FLI), and defoliation (DEF) in nine diploid rose families in College Station, TX in 2018. BS, CLS, FLI, and DEF refer to the least squares means of each trait. AUDPC indicates the area under the disease progress curve for BS and CLS; AFLIC indicates the area under the flower intensity curve for FLI. _Max indicates the maximum score for BS, CLS, FLI, and DEF over the course of the growing season. ns, $p > 0.05$; *, $0.01 \leq p \leq 0.05$; **, $0.00 \leq p \leq 0.01$; ***, $0.0001 \leq p \leq 0.001$; ****, $p < 0.0001$.*

	BS	BS_ AUDPC	BS_Max	CLS	CLS_ AUDPC	CLS_Max	FLI	AFLIC	FLI_Max	DEF	DEF_ Max
BS	1										
BS_ AUDPC	0.91****	1									
BS_Max	0.74****	0.75****	1								
CLS	-0.41****	-0.39****	-0.22****	1							
CLS_ AUDPC	-0.34****	-0.47****	-0.28****	0.91****	1						
CLS_Max	-0.3****	-0.36****	-0.23****	0.83****	0.87****	1					
FLI	0.18****	0.15***	0.17****	0.34****	0.33****	0.26****	1				
AFLIC	0.15***	0.12**	0.1*	0.3****	0.23****	0.17****	0.89****	1			
FLI_Max	0.2****	0.15***	0.13**	0.25****	0.22****	0.17****	0.84****	0.89****	1		
DEF	0.3****	0.3****	0.25****	0.06^{ns}	0.08^{ns}	0.1*	0.37****	0.32****	0.38****	1	
DEF_ Max	0.31****	0.37****	0.34****	0.07^{ns}	0.03^{ns}	0.08*	0.27****	0.23****	0.26****	0.77****	1

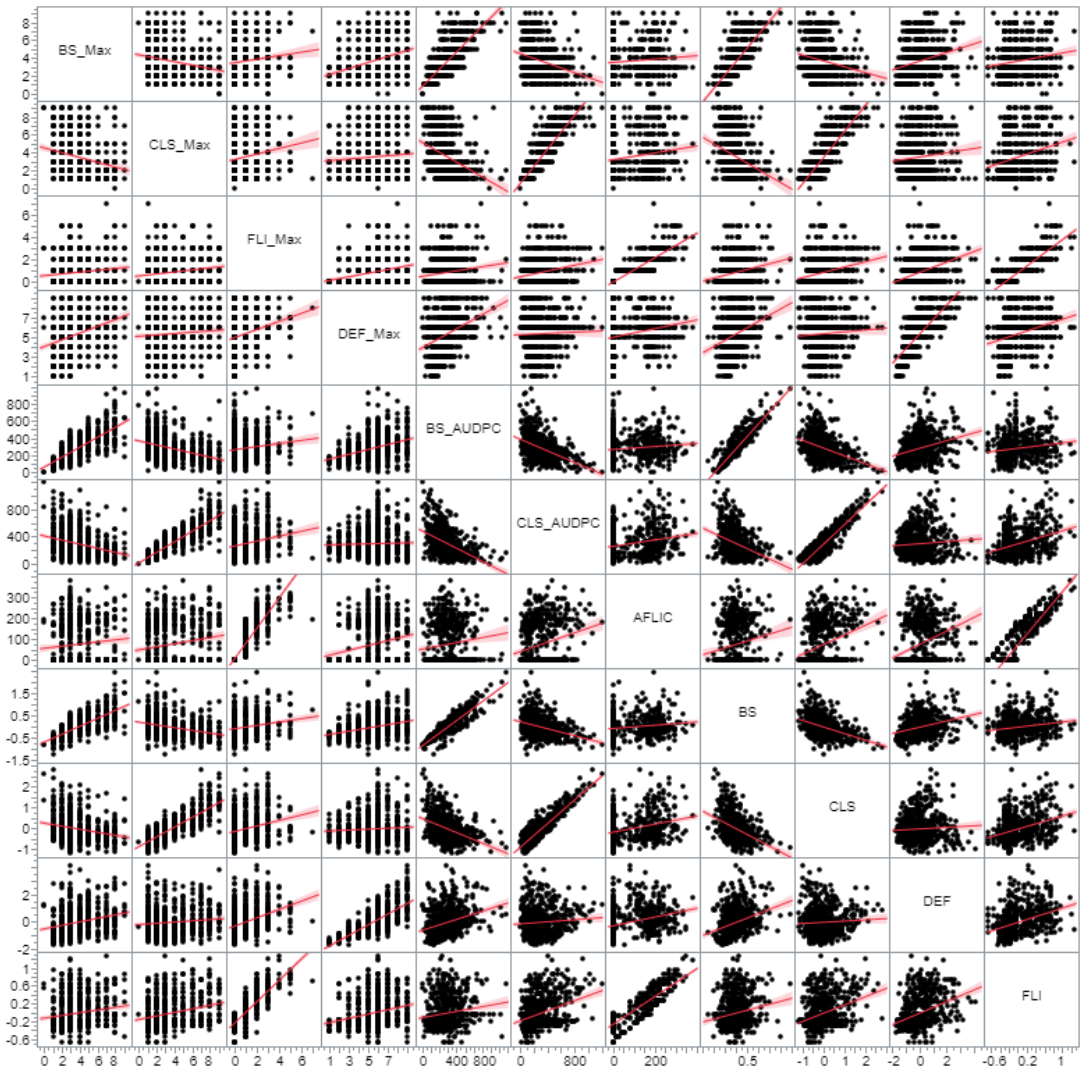

Figure 52 Scatterplots of relationships between black spot (BS) severity, cercospora (CLS) severity, flower intensity (FLI), and defoliation (DEF) in nine diploid rose families in College Station, TX in 2018. BS, CLS, FLI, and DEF refer to the least squares means of each trait. AUDPC indicates the area under the disease progress curve for BS and CLS; AFLIC indicates the area under the flower intensity curve for FLI. _Max indicates the maximum score for BS, CLS, FLI, and DEF over the course of the growing season. Line indicates line of best fit.

*Table 28 Correlation coefficients from Pearson's product-moment correlation test between black spot (BS) severity, cercospora (CLS) severity, flower intensity (FLI), and defoliation (DEF) in nine diploid rose families in Overton, TX in 2019. BS, CLS, FLI, and DEF refer to the least squares means of each trait. AUDPC indicates the area under the disease progress curve for BS and CLS; AFLIC indicates the area under the flower intensity curve for FLI. _Max indicates the maximum score for BS, CLS, FLI, and DEF over the course of the growing season. ns, p >0.05; *, 0.01 ≤ p ≤ 0.05; **, 0.00 ≤ p≤ 0.01; ***, 0.0001 ≤ p ≤ 0.001; ****, p < 0.0001.*

	BS	BS_ AUDPC	BS_Max	CLS	CLS_ AUDPC	CLS_Max	FLI	AFLIC	FLI_Max	DEF	DEF_ Max
BS	1										
BS_AUDPC	0.9****	1									
BS_Max	0.85****	0.92****	1								
CLS	-0.1^{ns}	-0.07^{ns}	-0.09^{ns}	1							
CLS_AUDPC	-0.11*	-0.08^{ns}	-0.1^{ns}	0.88****	1						
CLS_Max	-0.07^{ns}	-0.02^{ns}	-0.04^{ns}	0.84****	0.86****	1					
FLI	0.26****	0.23****	0.19***	-0.03^{ns}	0.01^{ns}	-0.06^{ns}	1				
AFLIC	0.22****	0.23****	0.19***	-0.04^{ns}	-0.04^{ns}	-0.1^{ns}	0.95****	1			
FLI_Max	0.24****	0.22****	0.2***	-0.02^{ns}	-0.02^{ns}	-0.08^{ns}	0.93****	0.9****	1		
DEF	0.39****	0.38****	0.35****	0.29****	0.29****	0.27****	0.23****	0.21***	0.19***	1	
DEF_Max	0.28****	0.37****	0.36****	0.22****	0.25****	0.24****	0.19***	0.18***	0.17**	0.88****	1

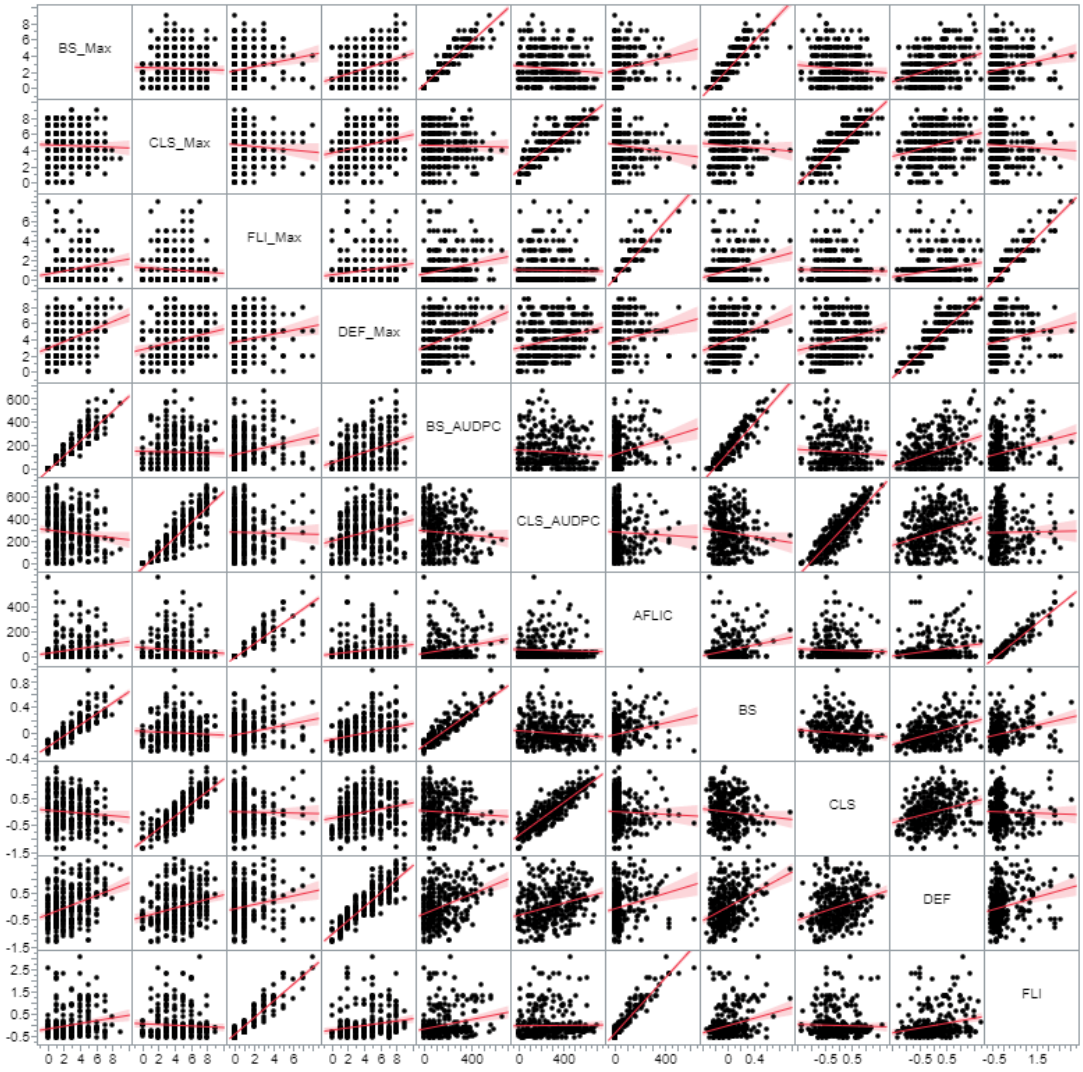

Figure 53 Scatterplots of relationships between black spot (BS) severity, cercospora (CLS) severity, flower intensity (FLI), and defoliation (DEF) in nine diploid rose families in Overton, TX in 2019. BS, CLS, FLI, and DEF refer to the least squares means of each trait. AUDPC indicates the area under the disease progress curve for BS and CLS; AFLIC indicates the area under the flower intensity curve for FLI. _Max indicates the maximum score for BS, CLS, FLI, and DEF over the course of the growing season. Line indicates line of best fit.

*Table 29 Correlation coefficients from Pearson's product-moment correlation test between black spot (BS) severity, cercospora (CLS) severity, and defoliation (DEF) in once-flowering genotypes from nine diploid rose families in College Station, TX in 2018. Flowering data was not available for once-flowering genotypes in 2018-CS. BS, CLS, and DEF refer to the least squares means of each trait. AUDPC indicates the area under the disease progress curve for BS and CLS; _Max indicates the maximum score for BS, CLS, and DEF over the course of the growing season. ns, p >0.05; *, 0.01 ≤ p ≤ 0.05; **, 0.00 ≤ p≤ 0.01; ***, 0.0001 ≤ p ≤ 0.001; ****, p < 0.0001.*

	BS	BS_AUDPC	BS_Max	CLS	CLS_AUDPC	CLS_Max	DEF	DEF_Max
BS	1							
BS_AUDPC	0.86****	1						
BS_Max	0.71****	0.78****	1					
CLS	-0.41****	-0.32****	-0.16**	1				
CLS_AUDPC	-0.36****	-0.5****	-0.34****	0.85****	1			
CLS_Max	-0.3****	-0.34****	-0.22****	0.83****	0.85****	1		
DEF	0.31****	0.37****	0.34****	-0.04^{ns}	-0.07^{ns}	-0.01^{ns}	1	
DEF_Max	0.36****	0.47****	0.44****	0.03^{ns}	-0.04ns	0.03^{ns}	0.81****	1

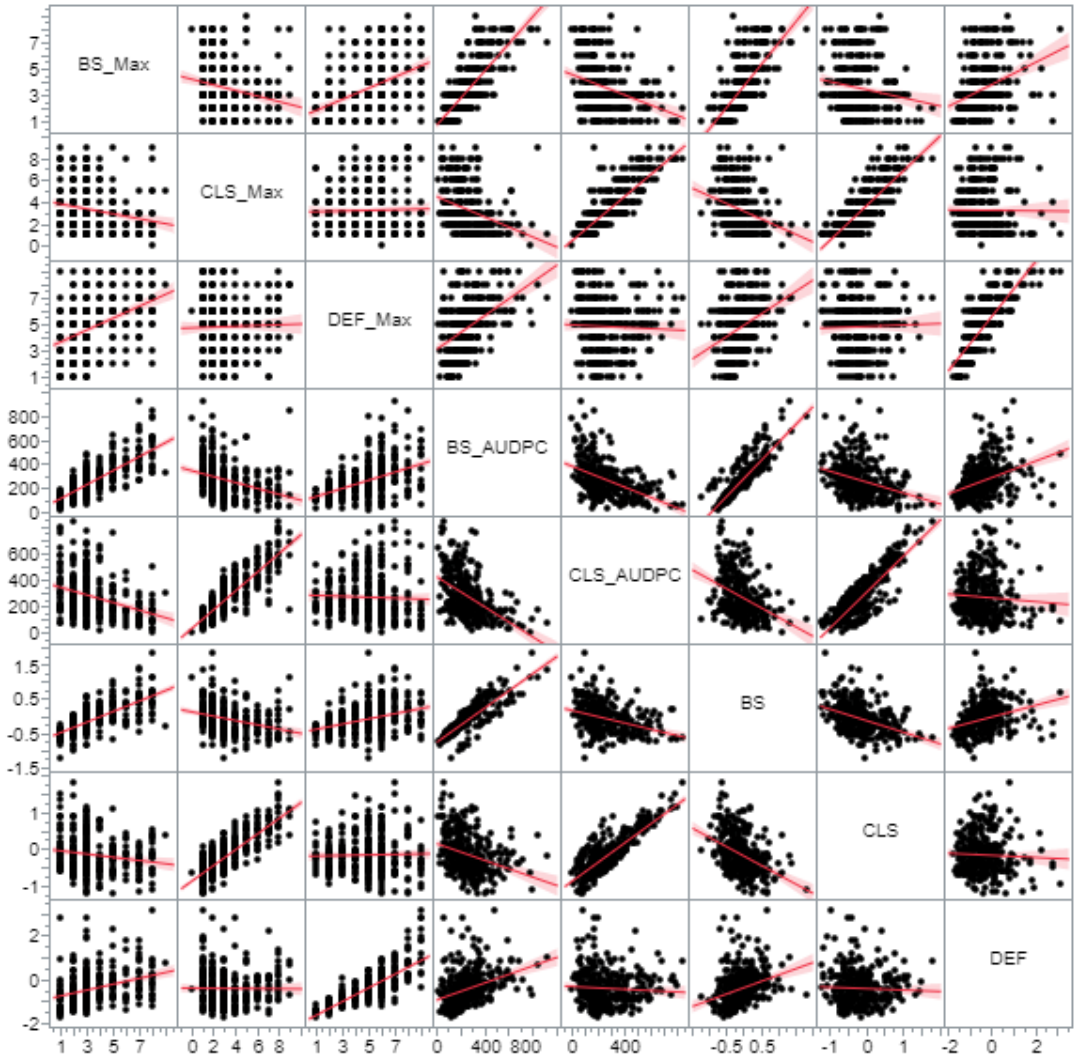

Figure 54 Scatterplots of relationships between black spot (BS) severity, cercospora (CLS) severity, and defoliation (DEF) in once-flowering genotypes from nine diploid rose families in College Station, TX in 2018. Flowering data was not available for once-flowering genotypes in 2018-CS. BS, CLS, and DEF refer to the least squares means of each trait. AUDPC indicates the area under the disease progress curve for BS and CLS; _Max indicates the maximum score for BS, CLS, and DEF over the course of the growing season. Line indicates line of best fit.

*Table 30 Correlation coefficients from Pearson's product-moment correlation test between black spot (BS) severity, cercospora (CLS) severity, flower intensity (FLI), and defoliation (DEF) in continuous flowering genotypes from nine diploid rose families in College Station, TX in 2018. BS, CLS, FLI, and DEF refer to the least squares means of each trait. AUDPC indicates the area under the disease progress curve for BS and CLS; AFLIC indicates the area under the flower intensity curve for FLI. _Max indicates the maximum score for BS, CLS, FLI, and DEF over the course of the growing season. ns, p >0.05; *, 0.01 ≤ p ≤ 0.05; **, 0.00 ≤ p≤ 0.01; ***, 0.0001 ≤ p ≤ 0.001; ****, p < 0.0001.*

	BS	BS_ AUDPC	BS_Max	CLS	CLS_ AUDPC	CLS_Max	FLI	AFLIC	FLI_Max	DEF	DEF_ Max
BS	1										
BS_ AUDPC	0.95****	1									
BS_Max	0.77****	0.72****	1								
CLS	-0.5****	-0.56****	-0.33****	1							
CLS_ AUDPC	-0.4****	-0.51****	-0.29****	0.94****	1						
CLS_Max	-0.35****	-0.44****	-0.27****	0.83****	0.87****	1					
FLI	0.11^{ns}	0^{ns}	0.11^{ns}	0.3****	0.4****	0.3****	1				
AFLIC	0.05^{ns}	-0.01^{ns}	0.06^{ns}	0.24****	0.24****	0.15*	0.86****	1			
FLI_Max	0.17**	0.09^{ns}	0.14*	0.13*	0.19**	0.14*	0.71****	0.68****	1		
DEF	0.22***	0.18**	0.14*	-0.05^{ns}	0.07^{ns}	0.1^{ns}	0.12*	-0.13*	0.1^{ns}	1	
DEF_Max	0.18**	0.18**	0.17**	-0.05^{ns}	0.01^{ns}	0.06^{ns}	0.02^{ns}	-0.13*	0.05^{ns}	0.7****	1

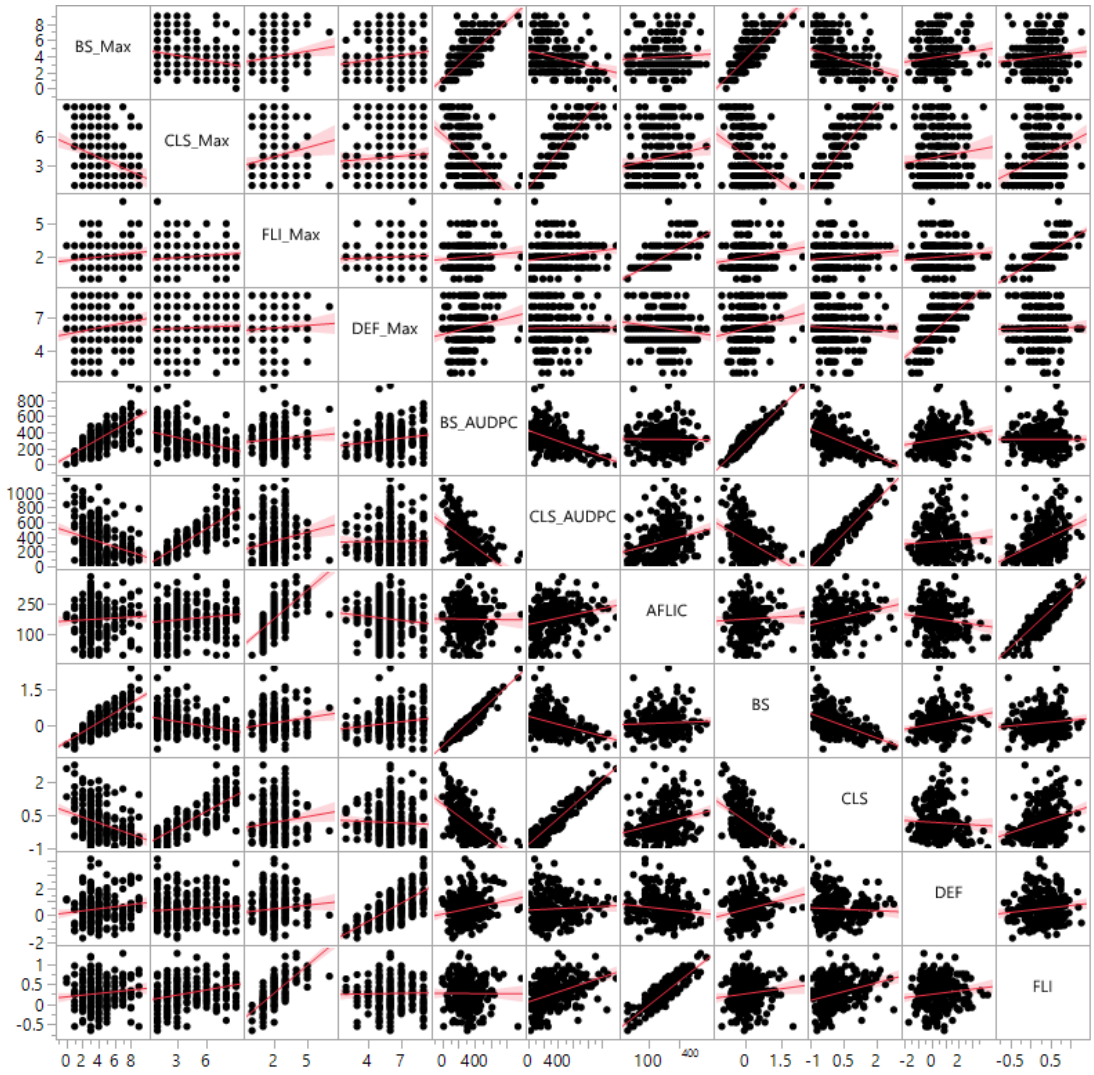

Figure 55 Scatterplots of relationships between black spot (BS) severity, cercospora (CLS) severity, flower intensity (FLI), and defoliation (DEF) in continuous flowering genotypes from nine diploid rose families in College Station, TX in 2018. BS, CLS, FLI, and DEF refer to the least squares means of each trait. AUDPC indicates the area under the disease progress curve for BS and CLS; AFLIC indicates the area under the flower intensity curve for FLI. _Max indicates the maximum score for BS, CLS, FLI, and DEF over the course of the growing season. Line indicates line of best fit.

*Table 31 Correlation coefficients from Pearson's product-moment correlation test between black spot (BS) severity, cercospora (CLS) severity, flower intensity (FLI), and defoliation (DEF) in once-flowering genotypes from nine diploid rose families in Overton, TX in 2019. BS, CLS, FLI, and DEF refer to the least squares means of each trait. AUDPC indicates the area under the disease progress curve for BS and CLS; AFLIC indicates the area under the flower intensity curve for FLI. _Max indicates the maximum score for BS, CLS, FLI, and DEF over the course of the growing season. ns, $p > 0.05$; *, $0.01 \leq p \leq 0.05$; **, $0.00 \leq p \leq 0.01$; ***, $0.0001 \leq p \leq 0.001$; ****, $p < 0.0001$.*

	BS	BS_ AUDPC	BS_Max	CLS	CLS_ AUDPC	CLS_Max	FLI	AFLIC	FLI_Max	DEF	DEF_ Max
BS	1										
BS_AUDPC	0.88****	1									
BS_Max	0.87****	0.93****	1								
CLS	-0.04^{ns}	0.02^{ns}	-0.02^{ns}	1							
CLS_AUDPC	-0.08^{ns}	-0.02^{ns}	-0.07^{ns}	0.89****	1						
CLS_Max	-0.02^{ns}	0.06^{ns}	0.03^{ns}	0.87****	0.84****	1					
FLI	-0.01^{ns}	-0.05^{ns}	-0.06^{ns}	0.07^{ns}	0.22***	0.14*	1				
AFLIC	-0.05^{ns}	-0.01^{ns}	0^{ns}	0.1^{ns}	0.08^{ns}	0.05^{ns}	0.77****	1			
FLI_Max	-0.02^{ns}	0.01^{ns}	0.03^{ns}	0.07^{ns}	0.08^{ns}	0.05^{ns}	0.74****	0.93****	1		
DEF	0.29****	0.26****	0.27****	0.42****	0.43****	0.4****	0.08^{ns}	-0.01^{ns}	-0.02^{ns}	1	
DEF_Max	0.19**	0.25****	0.26****	0.33****	0.39****	0.38****	0.08^{ns}	0.07^{ns}	0.06^{ns}	0.89****	1

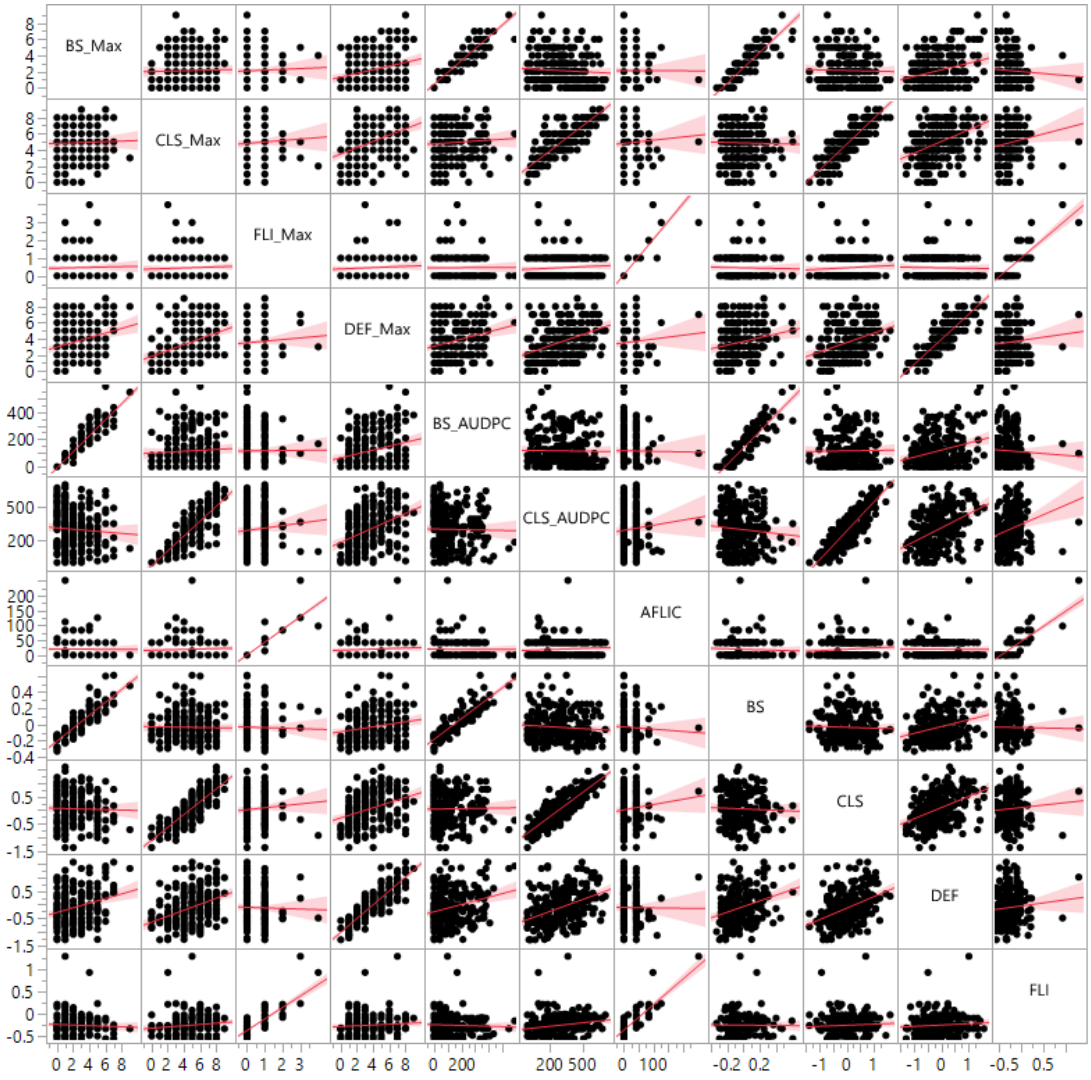

Figure 56 Scatterplots of relationships between black spot (BS) severity, cercospora (CLS) severity, flower intensity (FLI), and defoliation (DEF) in once-flowering genotypes from nine diploid rose families in Overton, TX in 2019. BS, CLS, FLI, and DEF refer to the least squares means of each trait. AUDPC indicates the area under the disease progress curve for BS and CLS; AFLIC indicates the area under the flower intensity curve for FLI. _Max indicates the maximum score for BS, CLS, FLI, and DEF over the course of the growing season. Line indicates line of best fit.

*Table 32 Correlation coefficients from Pearson's product-moment correlation test between black spot (BS) severity, cercospora (CLS) severity, flower intensity (FLI), and defoliation (DEF) in continuous flowering genotypes from nine diploid rose families in Overton, TX in 2019. BS, CLS, FLI, and DEF refer to the least squares means of each trait. AUDPC indicates the area under the disease progress curve for BS and CLS; AFLIC indicates the area under the flower intensity curve for FLI. _Max indicates the maximum score for BS, CLS, FLI, and DEF over the course of the growing season. ns, $p > 0.05$; *, $0.01 \leq p \leq 0.05$; **, $0.00 \leq p \leq 0.01$; ***, $0.0001 \leq p \leq 0.001$; ****, $p < 0.0001$.*

	BS	BS_ AUDPC	BS_Max	CLS	CLS_ AUDPC	CLS_Max	FLI	AFLIC	FLI_Max	DEF	DEF_ Max
BS	1										
BS_AUDPC	0.9****	1									
BS_Max	0.8****	0.88****	1								
CLS	-0.08^{ns}	-0.11^{ns}	-0.1^{ns}	1							
CLS_AUDPC	-0.03^{ns}	-0.06^{ns}	-0.04^{ns}	0.84****	1						
CLS_Max	0.03^{ns}	-0.01^{ns}	0^{ns}	0.72****	0.89****	1					
FLI	0.12^{ns}	0.03^{ns}	-0.01^{ns}	0.25*	0.26*	0.19^{ns}	1				
AFLIC	0.05^{ns}	0.04^{ns}	-0.02^{ns}	0.17^{ns}	0.18^{ns}	0.09^{ns}	0.91****	1			
FLI_Max	0.09^{ns}	-0.01^{ns}	-0.04^{ns}	0.25*	0.23*	0.16^{ns}	0.89****	0.78****	1		
DEF	0.42****	0.43****	0.37***	0.18^{ns}	0.14^{ns}	0.2^{ns}	-0.01^{ns}	0.02^{ns}	-0.02^{ns}	1	
DEF_Max	0.26*	0.41	0.41***	0.15^{ns}	0.12^{ns}	0.17^{ns}	-0.2^{ns}	-0.15^{ns}	-0.21^{ns}	0.84****	1

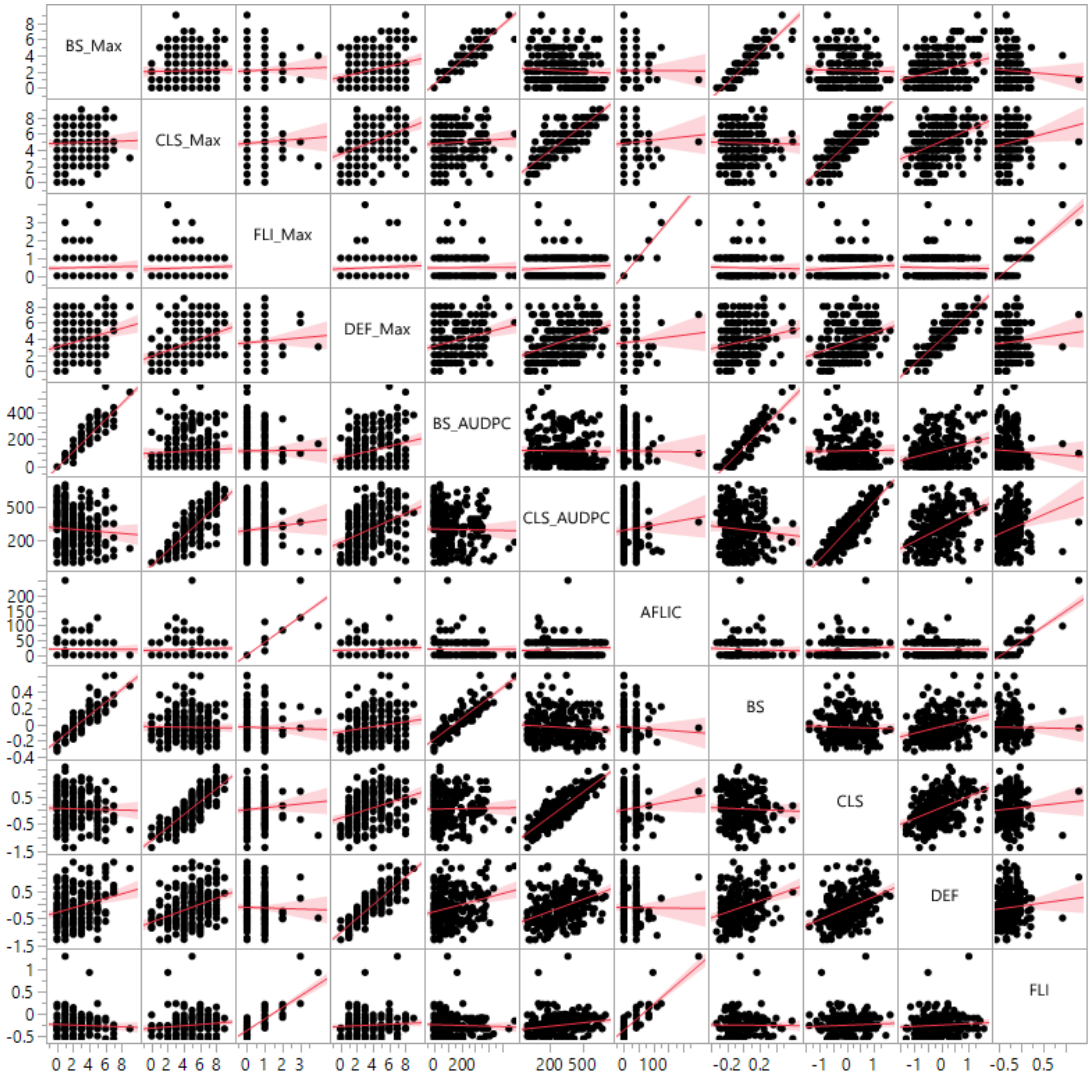

Figure 57 Scatterplots of relationships between black spot (BS) severity, cercospora (CLS) severity, flower intensity (FLI), and defoliation (DEF) in continuous flowering genotypes from nine diploid rose families in Overton, TX in 2019. BS, CLS, FLI, and DEF refer to the least squares means of each trait. AUDPC indicates the area under the disease progress curve for BS and CLS; AFLIC indicates the area under the flower intensity curve for FLI. _Max indicates the maximum score for BS, CLS, FLI, and DEF over the course of the growing season. Line indicates line of best fit.

III.4.6 Variances and heritability

III.4.6.1 Architectural traits

Combined year-seasons repeatability for architecture traits in cultivars was low to moderate, ranging from 0.43 for volume to 0.61 for LDim (Table 33). Repeatabilities were higher in the winters-only estimates (2018-W and 2019-W), ranging from 0.57 for NPrimaries to 0.77 for length. ADI, which was only measured in the winter environments, had a repeatability of 0.38. 2019-W had lower repeatabilities for all traits relative to the other year-seasons, which may be due to differences between individual data collectors. V_{GxE}/V_G was zero or very low for all traits in winters-only estimates with ADI having highest V_{GxE}/V_G at 0.25. The combined year-seasons estimates all had higher V_{GxE}/V_G ratios (0.07 to 0.67). Together this indicates that architecture traits are relatively stable from year to year, but that there is a high degree of genotype by season interaction within a year.

Table 33 Variance components and broad-sense heritability/repeatability for architecture traits in diploid rose cultivars per season (2018-S, 2018-W, 2019-W), over winters (Winters), and over all seasons (All yr-seasons). V_G = variance due to genotype, V_E = variance due to environment, V_{GxE} = variance due to genotype-environment interactions, V_{GxE}/V_G = ratio of genotype-environment effects to genotype effects, and $V\varepsilon$ = error variance. NPrimaries = number of primary shoots, LDim = longest dimension, ADI = apical dominance index, and GHabit = growth habit.

			NPrimaries	Height	Length	Width	LDim	Volume	ADI	GHabit
% of total variance	2018-S	Genotype	73.0	72.8	83.8	82.6	84.2	82.0		
		Residual	27.0	27.2	16.2	17.4	15.8	18.0		
	2018-W	Genotype	57.1	82.9	87.9	85.3	87.9	85.3	49.6	85.3
		Residual	42.9	17.1	12.1	14.7	12.1	14.7	50.4	14.7
	2019-W	Genotype	54.4	61.6	66.1	60.1	69.4	63.1	44.8	
		Residual	45.6	38.4	33.9	39.9	30.6	36.9	55.2	
	Winters	Genotype	55.1	66.3	76.8	69.9	78.5	71.9	35.8	
		Environment	2.8	0.3	0.0	0.6	0.0	0.5	5.8	
		Genotype x Environment	0	4.2	0	1.054	0	0	9.1	
		Residual	42.1	29.2	23.2	28.5	21.5	27.6	49.3	
	All yr-seasons	Genotype	55.0	47.1	49.7	46.9	50.6	38.6		
		Environment	2.0	19.4	16.3	19.7	16.4	10.8		
		Genotype x Environment	3.9	10.0	14.2	11.1	14.7	25.9		
		Residual	39.1	23.5	19.7	22.3	18.2	24.7		
Variance	2018-S	V_G	35.88	274.45	11883.27	938.32	1275.07	0.30		
		V_ε	13.29	102.41	6081.34	197.44	238.88	0.07		
	2018-W	V_G	37.57	1008.39	12986.48	5754.37	12972.26	22.56	0.001	2.38
		V_ε	28.23	207.87	1788.29	994.75	1784.87	3.88	0.001	0.41
	2019-W	V_G	48.39	1083.44	1281.65	5149.81	12305.44	23.78	0.002	
		V_ε	40.60	676.33	248.17	3422.61	5436.70	13.91	0.002	
	Winters	V_G	45.14	997.80	12902.65	5414.82	13070.39	23.45	0.0011	
		V_E	2.27	5.16	0.93	43.09	0.00	0.18	0.0002	

Table 33 Continued

		NPrimaries	Height	Length	Width	LDim	Volume	ADI	GHabit
	V_{GxE}	0.00	63.26	0.00	81.63	0.00	0.00	0.0003	
	V_{GxE}/V_G	0.00	0.06	0.00	0.02	0.00	0.00	0.25	
	V_ε	34.45	439.78	3891.17	2204.30	3572.43	8.99	0.0015	
All yr-seasons	V_G	38.21	657.82	6808.11	3217.53	6879.00	9.33		
	V_E	1.41	270.76	2230.97	1351.69	2228.26	2.61		
	V_{GxE}	2.69	140.29	1943.93	760.02	2003.38	6.27		
	V_{GxE}/V_G	0.07	0.21	0.29	0.24	0.29	0.67		
	V_ε	27.18	327.54	2702.37	1533.38	2478.88	5.96		
2018-S	H^2	0.73	0.73	0.84	0.83	0.84	0.82		
2018-W	H^2	0.57	0.83	0.88	0.85	0.88	0.85	0.50	0.85
2019-W	H^2	0.54	0.62	0.66	0.60	0.69	0.63	0.45	
Winters	H^2	0.57	0.66	0.77	0.70	0.79	0.72	0.38	
All yr-seasons	H^2	0.56	0.58	0.59	0.58	0.61	0.43		

The broad-sense heritability for architecture traits in the families (Tables 34-36) likewise ranged from low to moderate when seasons were combined. Volume was less heritable than in the cultivars (0.05 vs 0.43, all seasons combined), as was width. NPrimaries had the highest broad-sense heritability at 0.6. ADI, which was only measured in 2018-W in the families, had a H^2 of 0.90, which is more than double either the 2018-W or 2019-W estimate in the cultivars. Narrow-sense heritability was low for all traits in the combined-seasons estimates. Height had the highest h^2 at 0.32. For all traits over seasons, parental effects contributed only up to 13% of the total variance. NPrimaries had the lowest V_{GxE}/V_G ratio of 0.69. The other traits had V_{GxE}/V_G ratios ranging from 1.07 (height) to 29.73 (volume), indicating high genotype x season interactions.

Architecture heritabilities were also estimated for OF and CF types in the families.

III.4.6.1.1 Families: once-flowering types

Broad-sense heritabilities for OF types ranged from very low (0.03, volume) to moderate (0.59, NPrimaries) (Tables 37-39). Narrow-sense heritabilities were substantially higher for length, width, and LDim in OF types than in the combined flowering types, but were still relatively low. The V_{GxE}/V_G ratios were similar to the combined flowering types except for length, which was reduced by approximately half. Broad-sense heritabilities for ADI and GHabit were comparable between OF and combined types, but the narrow-sense heritabilities were considerably higher in the OF types compared to the combined types and CF types.

Table 34 Variance components, broad-sense heritability (H^2), and narrow-sense heritability (h^2) for architecture traits in nine diploid rose families over all seasons. FP = female parent and MP = male parent. V_G = variance due to genotype, V_E = variance due to environment, V_{GxE} = variance due to genotype-environment interactions, V_{GxE}/V_G = ratio of genotype-environment effects to genotype effects, and V_ε = error variance. NPrimaries = number of primary shoots, LDim = longest dimension, ADI = apical dominance index, and GHabit = growth habit.

		NPrimaries	Height	Length	Width	LDim	Volume
% of total variance	Genotype (FP,MP)	8.9	10.9	10.5	5.5	10.6	1.0
	Block (Season)	3.0	1.7	1.4	2.1	1.4	1.6
	FP	2.0	3.1	1.2	1.7	1.6	0.6
	MP	1.1	9.9	2.8	0.0	2.5	0.0
	Season	60.5	32.0	42.6	46.0	41.9	30.5
	FP x Season	0.6	2.5	13.5	9.7	13.6	21.4
	MP x Season	0.0	9.7	0.0	0.0	0.0	0.0
	Season x Genotype (FP,MP)	7.7	13.4	18.1	21.3	17.7	25.2
	Residual	16.2	16.7	9.7	13.7	10.7	19.8
Variance	V_a	2.9	87.1	548.3	100.0	544.4	0.01
	V_d	8.5	73.4	1428.1	331.4	1404.0	0.02
	V_E	57.5	215.1	5777.6	2780.6	5535.7	0.5
	V_{GxE}	7.9	172.3	4288.6	1872.1	4135.7	0.7
	V_ε	15.4	112.3	1321.8	828.6	1420.3	0.3
	V_{GxE}/V_G	0.69	1.07	2.17	4.34	2.12	29.73
	H^2	0.59	0.58	0.44	0.27	0.45	0.05
	h^2	0.15	0.32	0.12	0.06	0.12	0.02

Table 35 Variance components, broad-sense heritability (H^2), and narrow-sense heritability (h^2) for architecture traits in nine diploid rose families in 2018-S. FP = female parent and MP = male parent. V_a = variance due to additive effects (female parent + male parent), V_d = variance due to non-additive effects (genotype), V_E = variance due to environment, V_{GxE} = variance due to genotype-environment interactions, V_{GxE}/V_G = ratio of genotype-environment effects to genotype effects, and V_ε = error variance. NPrimaries = number of primary shoots, LDim = longest dimension, ADI = apical dominance index, and GHabit = growth habit.

		NPrimaries	Height	Length	Width	LDim	Volume
% of total variance	Genotype (FP,MP)	21.8	21.1	24.1	17.4	24.1	10.7
	Block	18.0	15.6	21.2	23.1	21.6	27.1
	FP	7.0	13.2	10.8	3.5	11.2	8.4
	MP	5.0	4.5	6.7	3.8	5.9	0.0
	Residual	48.2	45.6	37.1	52.2	37.3	53.8
Variance	V_a	1.4	18.9	210.2	31.8	201.3	0.0005
	V_d	2.6	22.4	288.7	76.0	283.2	0.001
	V_ε	5.7	48.6	443.9	227.3	438.7	0.003
	H^2	0.58	0.63	0.69	0.49	0.69	0.41
	h^2	0.21	0.29	0.29	0.14	0.29	0.18

Table 36 Variance components, broad-sense heritability (H^2), and narrow-sense heritability (h^2) for architecture traits in nine diploid rose families in 2018-W. FP = female parent and MP = male parent. V_a = variance due to additive effects (female parent + male parent), V_d = variance due to non-additive effects (genotype), V_E = variance due to environment, V_{GxE} = variance due to genotype-environment interactions, V_{GxE}/V_G = ratio of genotype- environment effects to genotype effects, and V_ε = error variance. NPrimaries = number of primary shoots, LDim = longest dimension, ADI = apical dominance index, and GHabit = growth habit.

		NPrimaries	Height	Length	Width	LDim	Volume	ADI	GHabit
% of total variance	Genotype (FP,MP)	46.0	35.7	53.9	45.9	52.0	37.6	33.2	53.7
	Block	5.8	0.5	0.8	2.2	0.6	2.2	21.1	0.3
	FP	6.9	7.7	29.4	30.2	30.0	31.8	14.7	0.0
	MP	1.5	34.8	0.0	0.0	0.0	0.0	16.9	32.8
	Residual	39.8	21.2	16.0	21.7	17.5	28.4	14.1	13.1
Variance	V_a	5.3	357.4	4065.6	2043.8	4132.1	0.7	0.003	1.2
	V_d	29.0	300.1	7461.5	3110.5	7176.1	0.8	0.003	2.0
	V_ε	25.1	177.9	2208.2	1469.2	2410.6	0.6	0.001	0.5
	H^2	0.73	0.88	0.91	0.88	0.90	0.83	0.90	0.93
	h^2	0.11	0.48	0.32	0.35	0.33	0.38	0.44	0.35

III.4.6.1.2 Families: continuous flowering types

In CF types, broad-sense heritabilities were substantially lower than OF and combined types for all traits except NPrimaries and height. Narrow-sense heritabilities were low (0 to 0.27). While the V_{GxE}/V_G ratios for NPrimaries and height were similar to or lower than those for OF and combined types, the ratios for length, width, LDim, and volume were several times higher. The broad-sense heritability of ADI was moderately high (0.57) with little narrow-sense heritability (0.01), considerably lower than OF and combined types (Table 40). Heritabilities for GHabit were also lower than in the OF and combined types.

Table 37 Variance components, broad-sense heritability (H^2), and narrow-sense heritability (h^2) for architecture traits in nine diploid rose families over all seasons separated by flowering type (OF, once-flowering; CF, continuous flowering). FP = female parent and MP = male parent. V_a = variance due to additive effects (female parent + male parent), V_d = variance due to non-additive effects (genotype), V_E = variance due to environment, V_{GxE} = variance due to genotype-environment interactions, V_{GxE}/V_G = ratio of genotype-environment effects to genotype effects, and V_ε = error variance. NPrimaries = number of primary shoots, LDim = longest dimension, ADI = apical dominance index, and GHabit = growth habit.

		OF						CF					
		NPrimaries	Height	Length	Width	LDim	Volume	NPrimaries	Height	Length	Width	LDim	Volume
% of total variance	Genotype (FP,MP)	8.0	8.0	4.3	1.1	4.1	0.4	10.3	19.9	5.1	5.3	5.2	0.3
	Block (Season)	2.9	1.0	1.7	1.9	1.5	2.2	6.3	3.6	1.2	2.2	1.2	0.3
	FP	3.0	4.0	0.1	0.0	0.1	0.3	0.0	3.2	0.8	0.0	0.7	0.1
	MP	1.9	11.5	9.8	6.2	9.8	0.0	1.1	10.7	0.0	0.0	0.0	0.0
	Season	57.2	32.9	57.8	59.1	56.9	47.2	49.7	21.4	30.8	39.8	27.0	15.0
	FP x Season	2.8	1.3	0.0	1.0	0.0	10.2	0.0	0.0	0.1	0.0	0.0	0.0
	MP x Season	0.0	21.5	10.4	9.8	10.3	0.0	3.6	4.3	53.6	39.1	57.4	79.1
	Season x Genotype (FP,MP)	6.4	8.0	4.3	7.9	4.8	18.8	7.8	16.0	4.4	6.9	4.3	1.8
	Residual	17.8	11.9	11.7	12.9	12.5	20.9	21.2	20.9	4.0	6.8	4.2	3.5
Variance	V_a	5.1	211.3	1743.8	628.1	1758.3	0.01	0.6	28.2	52.0	0.0	44.8	0.001
	V_d	8.4	109.6	750.0	113.9	722.5	0.0099	5.4	40.4	341.1	151.5	348.9	0.0019
	V_E	60.1	449.2	10151.0	5986.6	10100.8	1.2	26.0	43.5	2080.7	1135.6	1816.1	0.1
	V_{GxE}	9.7	420.6	2570.2	1899.6	2685.8	0.7	5.9	41.3	3919.2	1312.3	4147.0	0.6
	V_ε	18.6	162.3	2047.6	1305.3	2222.6	0.5	11.1	42.4	270.2	194.2	280.1	0.03
	V_{GxE}/V_G	0.72	1.31	1.03	2.56	1.08	43.09	0.99	0.60	9.97	8.66	10.53	219.86
	H^2	0.59	0.56	0.58	0.37	0.57	0.03	0.51	0.69	0.16	0.18	0.16	0.01
	h^2	0.22	0.37	0.41	0.31	0.40	0.01	0.05	0.28	0.02	0.00	0.02	0.003

Table 38 Variance components, broad-sense heritability (H^2), and narrow-sense heritability (h^2) for architecture traits in nine diploid rose families in 2018-S separated by flowering type (OF, once-flowering; CF, continuous flowering). FP = female parent and MP = male parent. V_a = variance due to additive effects (female parent + male parent), V_d = variance due to non-additive effects (genotype), and V_ε = error variance. NPrimaries = number of primary shoots, LDim = longest dimension, ADI = apical dominance index, and GHabit = growth habit.

		OF						CF					
		NPrimaries	Height	Length	Width	LDim	Volume	NPrimaries	Height	Length	Width	LDim	Volume
% of total variance	Genotype (FP,MP)	20.6	16.1	14.1	12.6	14.1	8.5	22.2	24.4	15.0	17.5	14.0	8.6
	Block	21.5	16.8	26.1	23.2	26.1	33.8	15.7	10.5	18.7	26.9	19.5	27.0
	FP	6.3	27.1	3.1	0.2	3.2	3.7	0.6	19.8	7.9	3.5	9.9	9.3
	MP	8.6	0.0	25.4	16.6	25.3	7.3	0.9	0.0	1.7	0.0	0.0	0.0
	Residual	43.0	40.1	31.3	47.4	31.3	46.7	60.7	45.4	56.6	52.1	56.5	55.1
Variance	V_a	2.3	38.2	501.2	113.4	496.1	0.001	0.1	16.3	39.2	6.3	39.3	0.0001
	V_d	3.2	22.6	248.2	84.7	246.2	0.001	1.5	20.0	61.1	31.9	55.6	0.0001
	V_ε	6.7	56.5	548.8	319.3	546.1	0.004	4.0	37.2	229.9	95.2	224.0	0.001
	H^2	0.62	0.68	0.73	0.55	0.73	0.45	0.44	0.66	0.47	0.45	0.46	0.39
	h^2	0.26	0.43	0.49	0.32	0.49	0.26	0.03	0.30	0.18	0.07	0.19	0.21

Table 39 Variance components, broad-sense heritability (H^2), and narrow-sense heritability (h^2) for architecture traits in once-flowering genotypes from nine diploid rose families in 2018-W. FP = female parent and MP = male parent. V_a = variance due to additive effects (female parent + male parent), V_d = variance due to non-additive effects (genotype), and V_ε = error variance. NPrimaries = number of primary shoots, LDim = longest dimension, ADI = apical dominance index, and GHabit = growth habit.

		NPrimaries	Height	Length	Width	LDim	Volume	ADI	GHabit
% of total variance	Genotype (FP,MP)	36.9	24.3	23.8	22.2	21.1	34.7	9.1	15.7
	Block	3.8	0.3	1.0	2.8	0.6	4.0	20.2	0.8
	FP	16.4	7.5	0.0	0.3	0.0	8.3	3.8	6.5
	MP	1.0	51.8	49.5	45.2	50.2	14.6	58.8	66.0
	Residual	41.9	16.1	25.7	29.5	28.2	38.5	8.1	10.9
Variance	V_a	12.7	996.8	6880.3	3558.6	6944.6	0.6	0.005	2.3
	V_d	26.9	408.8	3307.4	1737.6	2915.0	0.9	0.001	0.5
	V_ε	30.5	271.2	3572.6	2306.4	3895.4	1.0	0.001	0.3
	H^2	0.72	0.91	0.85	0.82	0.84	0.75	0.95	0.94
	h^2	0.23	0.65	0.57	0.55	0.59	0.30	0.83	0.77

Table 40 Variance components, broad-sense heritability (H^2), and narrow-sense heritability (h^2) for architecture traits in nine diploid rose families in 2018-W divided by flowering type (OF, once-flowering; CF, continuous flowering). FP = female parent and MP = male parent. V_a = variance due to additive effects (female parent + male parent), V_d = variance due to non-additive effects (genotype), and V_ε = error variance. NPrimaries = number of primary shoots, LDim = longest dimension, ADI = apical dominance index, and GHabit = growth habit.

		NPrimaries	Height	Length	Width	LDim	Volume	ADI	GHabit
% of total variance	Genotype (FP,MP)	39.1	52.9	13.2	23.1	13.1	2.4	23.4	47.7
	Block	12.3	1.8	0.6	2.4	0.7	0.3	38.8	0.0
	FP	0.0	0.0	0.5	0.0	0.5	0.2	1.6	13.1
	MP	8.7	25.2	81.9	64.4	81.8	93.1	0.4	0.0
	Residual	39.9	20.2	3.7	10.2	3.9	4.0	35.8	39.3
Variance	V_a	3.9	60.7	7457.3	1842.5	7433.6	1.2	0.00002	0.2
	V_d	17.7	127.7	1196.1	660.3	1188.3	0.0	0.001	0.8
	V_ε	18.0	48.6	336.8	291.2	352.9	0.0	0.002	0.7
	H^2	0.71	0.89	0.98	0.95	0.98	0.98	0.57	0.76
	h^2	0.13	0.29	0.85	0.70	0.84	0.96	0.01	0.16

III.4.6.2 Disease, defoliation, and flower intensity

III.4.6.2.1 Cultivar panel

Disease, defoliation, and flowering in the cultivars had moderate to high H^2 as estimated from the area and maximum scores, but low H^2 when based upon the ls means (Table 41). Presumably, this is because area and maximum scores inherently simplify these traits by removing the variance over time. For the ls means for BS, CLS, and FLI, the residual contributed the greatest amount of variance of all effects; for defoliation, however, the greatest contribution came from the month effect, indicating that time of year has a stronger impact on defoliation than genetic effects. The V_{GxE}/V_G ratios for all four traits was greater than 1, indicating a high degree of genotype x environment (months considered as environments) interaction for these traits.

III.4.6.2.2 Families

The H^2 of BS, FLI, and defoliation in the families was considerably higher than in the cultivars (Table 42). FLI had the highest H^2 of 0.82, and BS and defoliation had broad-sense heritabilities of 0.66 and 0.67, respectively. The H^2 of CLS was 0.3. The h^2 of all of these traits was low, ranging from 0.004 for defoliation to 0.22 for FLI. For all four traits, the residual contributed the most to the total variance and the V_a, or additive variance, was low. BS, CLS, and DEF had high V_{GxE}/V_G ratios (>1) while FLI had a V_{GxE}/V_G ratio of 0.59, indicating less genotype x environment interaction for flowering.

Table 41 Variance components and broad-sense heritability/repeatability for black spot (BS) severity, cercospora (CLS) severity, flower intensity (FLI), and defoliation (DEF) in diploid rose cultivars in 2018-CS. _AUDPC indicates the area under the disease progress curve for BS and CLS; AFLIC indicates the area under the flower intensity curve for FLI. _Max indicates the maximum score for BS, CLS, FLI, and DEF over the course of the growing season. V_G = variance due to genotype, V_E = variance due to environment, V_{GxE} = variance due to genotype-environment interactions, V_{GxE}/V_G = ratio of genotype-environment effects to genotype effects, and $V\varepsilon$ = error variance.

		BS	BS_Max	BS_AUDPC	CLS	CLS_Max	CLS_AUDPC	FLI	FLI_Max	AFLIC	DEF	DEF_Max
% of total variance	Genotype	15.1	63.9	79.4	19.8	54.5	74.4	22.9	78.2	86.2	20.9	74.2
	Month	6.7			16.2			15.9			33.3	
	Genotype* Month	38.4			20.4			32.7			26.3	
	Residual	39.7	36.1	20.6	43.6	45.5	25.6	28.5	21.8	13.8	19.4	25.9
Variance	V_G	0.48	2.56	25827.76	0.46	2.74	19993.28	0.15	1.28	7024.29	1.02	1.84
	V_E	0.22			0.37			0.11			1.62	
	V_{GxE}	1.23			0.47			0.22			1.28	
	V_{GxE}/V_G	2.55			1.03			1.43			1.26	
	V_ε	1.27	1.44	6687.07	1.01	2.29	6876.22	0.19	0.36	1124.54	0.94	0.64
	H^2	0.16	0.64	0.79	0.24	0.55	0.74	0.27	0.78	0.86	0.31	0.74

Notable differences were observed for disease, flowering, and defoliation heritabilities between 2018-CS and 2019-OV. Both broad and narrow-sense heritabilities were higher in 2018-CS than in the combined year-locations with the exception of h^2 for defoliation (Table 43). In 2018-CS, only BS had a V_{GxE}/V_G ratio over 1. In 2019-OV, the broad-sense heritability for FLI was comparable to the combined year-locations estimate (Table 44). Both broad and narrow-sense heritability estimates for CLS were higher in 2019-OV than in the combined year-locations. CLS and FLI had low V_{GxE}/V_G ratios, whereas the genotype x environment interactions were high (>2) for BS and DEF. The maximum and area measures of CLS and FLI had moderately high to high broad-sense heritability in both 2018-CS and 2019-OV (Tables 45, 46). The narrow-sense heritabilities for CLS_Max and CLS_AUDPC were moderately high (0.59 and 0.5, respectively) in 2019-OV but low in 2018-CS. BS and DEF had high broad-sense heritability and low narrow-sense heritability in 2018-CS but low broad-sense and low or zero narrow-sense heritability in 2019-OV. Differences between 2018-CS and 2019-OV may be due in part to differences in individual data collectors.

Table 42 Variance components, broad-sense heritability (H^2), and narrow-sense heritability (h^2) for black spot (BS) severity, cercospora (CLS) severity, flower intensity (FLI), and defoliation (DEF) in nine diploid rose families combined over year-locations (Yr_location). FP = female parent, MP = male parent. V_a = variance due to additive effects (female parent + male parent), V_d = variance due to non-additive effects (genotype), V_E = variance due to environment, V_{GxE} = variance due to genotype-environment interactions, V_{GxE}/V_G = ratio of genotype-environment effects to genotype effects, and V_ε = error variance.

		BS	CLS	FLI	DEF
% of total variance	Genotype (FP x MP)	9.2	1.8	26.5	12.9
	FP	0.0	2.6	4.7	0.1
	MP	1.7	1.1	5.1	0.0
	Block (Yr_location x Month)	5.3	2.2	1.1	2.6
	Month	0.0	3.3	0.2	0.0
	Yr_location	3.2	12.5	4.2	0.0
	Yr_location x Month	6.7	5.7	1.2	25.3
	FP x Yr_location	0.0	0.7	1.4	0.0
	FP x Yr_location x Month	6.8	0.0	0.5	0.5
	MP x Yr_location	3.5	8.0	0.3	0.3
	MP x Yr_location x Month	0.0	3.7	0.2	6.6
	Yr_location x Genotype (FP x MP)	1.8	12.2	10.6	7.6
	Month x Genotype (FP x MP)	1.1	1.7	0.9	3.1
	Yr_location x Month x Genotype (FP x MP)	12.9	6.8	6.9	8.4
	FP x Month	0.0	0.4	0.0	0.4
	MP x Month	0.0	0.4	0.5	0.0
	Residual	47.8	36.9	35.7	32.3
Variance	V_a	0.05	0.16	0.07	0.004
	V_d	0.25	0.08	0.19	0.65
	V_E	0.27	0.93	0.04	1.28
	V_{GxE}	0.72	1.46	0.16	1.35
	V_ε	1.31	1.59	0.26	1.63
	V_{GxE}/V_G	2.40	6.17	0.59	2.06
	H^2	0.66	0.30	0.82	0.67
	h^2	0.10	0.20	0.22	0.004

Table 43 Variance components, broad-sense heritability (H^2), and narrow-sense heritability (h^2) for black spot (BS) severity, cercospora (CLS) severity, flower intensity (FLI), and defoliation (DEF) in nine diploid rose families in 2018-CS. FP = female parent, MP = male parent. V_a = variance due to additive effects (female parent + male parent), V_d = variance due to non-additive effects (genotype), V_E = variance due to environment (month), V_{GxE} = variance due to genotype-environment interactions, V_{GxE}/V_G = ratio of genotype-environment effects to genotype effects, and V_ε = error variance.

		BS	CLS	FLI	DEF
% of total variance	Genotype (FP x MP)	12.2	19.3	31.5	21.9
	FP	0.0	2.7	12.2	0.0
	MP	6.7	4.5	0.0	0.0
	Block (Month)	2.1	3.0	0.5	0.4
	Month	6.8	0.0	2.2	33.9
	Month x Genotype (FP x MP)	16.0	15.7	11.0	13.7
	FP x Month	1.6	0.5	1.0	0.8
	MP x Month	5.4	5.2	0.9	2.8
	Residual	49.0	49.0	40.8	26.5
Variance	V_a	0.17	0.20	0.06	0.000
	V_d	0.31	0.53	0.15	1.09
	V_E	0.17	0.00	0.01	1.69
	V_{GxE}	0.59	0.58	0.06	0.86
	V_ε	1.26	1.33	0.20	1.32
	V_{GxE}/V_G	1.21	0.81	0.29	0.79
	H^2	0.76	0.82	0.91	0.85
	h^2	0.53	0.56	0.75	0.00

Table 44 Variance components, broad-sense heritability (H^2), and narrow-sense heritability (h^2) for black spot (BS) severity, cercospora (CLS) severity, flower intensity (FLI), and defoliation (DEF) in diploid rose families in 2019-OV. FP = female parent, MP = male parent. V_a = variance due to additive effects (female parent + male parent), V_d = variance due to non-additive effects (genotype), V_E = variance due to environment (month), V_{GxE} = variance due to genotype-environment interactions, V_{GxE}/V_G = ratio of genotype-environment effects to genotype effects, and V_ε = error variance.

		BS	CLS	FLI	DEF
% of total variance	Genotype (FP x MP)	6.2	9.2	40.5	9.7
	FP	0	5.0	3.4	0.1
	MP	3.9	12.5	3.7	0
	Block (Month)	11.6	1.4	1.6	8.0
	Month	8.9	26.2	1.1	0
	Month x Genotype (FP x MP)	7.1	0.9	6.8	0
	FP x Month	17.7	0	0	1.0
	MP x Month	0	7.1	0.6	28.9
	Residual	44.7	37.8	42.4	52.4
Variance	V_a	0.14	1.37	0.10	0.009
	V_d	0.22	0.72	0.57	0.63
	V_E	0.32	2.05	0.02	-0.51
	V_{GxE}	0.89	0.63	0.10	1.95
	V_ε	1.61	2.95	0.60	3.42
	V_{GxE}/V_G	2.46	0.30	0.15	3.05
	H^2	0.39	0.75	0.83	0.34
	h^2	0.15	0.66	0.42	0.01

Table 45 Variance components, broad-sense heritability (H^2), and narrow-sense heritability (h^2) for black spot (BS) severity, cercospora (CLS) severity, flower intensity (FLI), and defoliation (DEF) in diploid rose families in 2018-CS. _AUDPC indicates the area under the disease progress curve for BS and CLS; AFLIC indicates the area under the flower intensity curve for FLI. _Max indicates the maximum score for BS, CLS, FLI, and DEF over the course of the growing season. FP = female parent, MP = male parent. V_a = variance due to additive effects (female parent + male parent), V_d = variance due to non-additive effects (genotype), and V_ε = error variance.

		BS_ Max	BS_ AUDPC	CLS_ Max	CLS_ AUDPC	FLI_ Max	AFLIC	DEF_ Max
% of total variance	Genotype (FP,MP)	28.0	44.5	47.9	51.3	57.0	65.7	55.9
	Block	1.1	1.1	4.5	5.3	0.0	0.0	0.0
	FP	1.9	0.0	4.1	6.4	13.2	23.3	3.9
	MP	34.7	24.7	7.3	13.9	0.0	0.0	8.9
	Residual	34.2	29.6	36.1	23.1	29.8	11.0	31.3
Variance	V_a	1.86	6475.47	0.64	9225.19	0.21	2451.85	0.50
	V_d	1.43	11634.52	2.66	23296.30	0.89	6904.34	2.19
	V_ε	1.74	7733.48	2.00	10498.42	0.47	1154.30	1.22
	H^2	0.79	0.82	0.77	0.86	0.82	0.94	0.81
	h^2	0.45	0.29	0.15	0.24	0.16	0.25	0.15

Table 46 Variance components, broad-sense heritability (H^2), and narrow-sense heritability (h^2) for black spot (BS) severity, cercospora (CLS) severity, flower intensity (FLI), and defoliation (DEF) in diploid rose families in 2019-OV. _AUDPC indicates the area under the disease progress curve for BS and CLS; AFLIC indicates the area under the flower intensity curve for FLI. _Max indicates the maximum score for BS, CLS, FLI, and DEF over the course of the growing season. FP = female parent, MP = male parent. V_a = variance due to additive effects (female parent + male parent), V_d = variance due to non-additive effects (genotype), and V_ε = error variance.

		BS_ Max	BS_ AUDPC	CLS_ Max	CLS_ AUDPC	FLI_ Max	AFLIC	DEF_ Max
% of total variance	Genotype (FP,MP)	17.8	16.0	15.0	17.8	54.2	52.5	6.7
	Block	19.5	39.0	1.9	1.2	0.1	1.9	8.9
	FP	0.0	0.0	5.6	10.7	3.1	4.3	0.5
	MP	0.0	3.5	42.2	27.8	6.4	6.0	0.2
	Residual	62.7	41.5	35.3	42.5	36.1	35.3	83.8
Variance	V_a		978.38	3.91	16334.25	0.24	1019.59	0.04
	V_d	0.78	4475.22	1.22	7538.72	1.38	5171.15	0.37
	V_ε	2.77	11595.21	2.88	18016.88	0.92	3475.05	4.59
	H^2	0.36	0.48	0.78	0.73	0.78	0.78	0.15
	h^2	0.00	0.09	0.59	0.50	0.12	0.13	0.01

The family dataset was split by flowering type in both year-locations to investigate the changes in the heritability of FLI. In 2018-CS, this effectively excluded OF types, as OF types did not bloom in 2018-CS; in 2019-OV, heritability could be estimated for both flowering types. Changes in the heritability of FLI were observed in both year-locations as a result (Table 47). Generally, broad-sense heritability for all measures of FLI decreased in the split analyses relative to the combined analysis; the only exception to this was AFLIC in OF types in 2019-OV. For FLI ls means, the narrow-sense heritability decreased in both locations in the split analysis; for FLI_Max, narrow-sense heritability either remained similar or increased; for AFLIC, narrow-sense heritability decreased in 2018-CS and increased in 2019-OV. V_{GxE}/V_G increased in the split analyses relative to the combined analysis. In 2018-CS, the V_{GxE}/V_G ratio increased from 0.29 in the combined analysis to 2.41 in the CF types. In 2019-OV, the ratio increased from 0.15 in the combined analysis to 0.44 in the CF types and 0.9 in the OF types. For each measure of FLI in each year-location, V_d declined, sometimes to almost zero, when the analysis was split by flowering type, indicating the loss of considerable non-additive gene action when controlling for flowering type.

Table 47 Changes in variance components, broad-sense heritability (H^2), and narrow-sense heritability (h^2) for flower intensity (FLI) in nine diploid rose families across year-locations (2018-CS, 2019-OV) when divided by flowering type (OF, once-flowering; CF, continuous flowering) or when flowering types are combined (Comb.). Flowering data was not available for OF types in 2018-CS. AFLIC indicates the area under the flower intensity curve. _Max indicates the maximum score FLI over the course of the growing season. V_a = variance due to additive effects (female parent + male parent), V_d = variance due to non-additive effects (genotype), V_E = variance due to environment (month), V_{GxE} = variance due to genotype-environment interactions, V_{GxE}/V_G = ratio of genotype-environment effects to genotype effects, and V_ε = error variance.

	FLI					FLI_Max					AFLIC				
	2018-CS		2019-OV			2018-CS		2019-OV			2018-CS		2019-OV		
	CF	Comb.	OF	CF	Comb.	CF	Comb.	OF	CF	Comb.	CF	Comb.	OF	CF	Comb.
V_a	0.00	0.06	0.0001	0.21	0.10	0.53	0.21	0.32	0.37	0.24	174.67	2451.85	1548.19	2531.80	1019.59
V_d	0.07	0.15	0.01	0.33	0.57	0.03	0.89	0.03	0.80	1.38	2824.10	6904.34	145.44	1033.87	5171.15
V_E	0.03	0.01	0.03	0.43	0.02										
V_{GxE}	0.16	0.06	0.01	0.24	0.10										
V_e	0.45	0.20	0.14	1.85	0.60	1.08	0.47	0.40	2.76	0.92	2844.85	1154.30	831.75	13961.07	3475.05
V_{GxE}/V_G	2.41	0.29	0.90	0.44	0.15										
H^2	0.58	0.91	0.53	0.79	0.83	0.51	0.82	0.64	0.46	0.78	0.68	0.94	0.80	0.34	0.78
h^2	0.00	0.75	0.01	0.31	0.42	0.48	0.16	0.58	0.14	0.12	0.04	0.25	0.73	0.24	0.13

III.5 Discussion

III.5.1 Architecture traits

As expected, plant vigor traits increased significantly between spring and winter in 2018, reflecting the plants' growth over the year. Plant vigor traits were similar in 2018-W and 2019-W in the cultivars, indicating that the ability of a plant to grow back after pruning is stable over time. Interestingly, NPrimaries increased in both families and cultivars between spring and winter, which is contrary to the finding of Wu et al. (2019b); however, at least for the cultivars, this may be due to data collection timing differences. This study assessed NPrimaries four weeks after pruning, while Wu et al. (2019b) assessed this trait two to three months after pruning. As the families in this study were relatively young compared to the plants of Wu et al. (2019b), it may also be the case that young plants produce new primary shoots as they mature. In the cultivars, NPrimaries decreased in 2019-W, which may be due to winterkill of primary shoots, as only live shoots were counted, or due to differences between data collectors. The amount of branching (ADI) increased between years, indicating that this trait may not be stable over time; however, more work is needed to illuminate the effect of time on this trait.

This study highlights the importance of distinguishing plants according to their growth or flowering type, particularly for future genetic studies, as all architecture traits except height (cultivars only) varied between flowering types and all except NPrimaries (cultivars only) varied between growth types. This is consistent with the findings of Kawamura et al. (2015) in which there were significant differences in growth habit, height, and stem elevation angle between once-flowering and continuous flowering

genotypes. That study did not investigate differences between growth types, presumably due to limited variability within their single biparental family. As the results between flowering and growth types were so similar in this study, in many cases they could be used interchangeably; i.e., if flowering data cannot be collected on a set of plants, growth type, which is easily assessed, could be used as an approximation.

Several architecture traits were strongly correlated with one another, particularly those related to plant vigor (height, length, width, LDim, and volume). While the plant vigor to ADI and plant vigor to NPrimaries correlations were weak in the cultivars, these correlations were moderately strong in the families, suggesting possible linkage between plant vigor and NPrimaries in the families. The moderately strong correlations in the families were consistent with the findings that ADI and NPrimaries differed between flowering/growth types. Together, this suggests that climber growth types (which are larger) tend to have less branching and more NPrimaries than non-climber growth types. The differences in NPrimaries were small, however; in the families, climbers on average had 13.3 primary shoots compared to 10 in non-climbers. Thus, climbers may not be especially useful for breeding for an increased number of primary shoots.

The moderate heritabilities for most architecture traits in both cultivars and families indicate that breeding for superior architecture should be feasible; however, the fact that the genetic variances are mostly non-additive will be crucial to designing a breeding scheme for these traits: most likely, backcrossing of genotypes with desirable architecture to genotypes with other desirable traits followed by clonal propagation will be necessary. Since narrow-sense heritabilities for length, width, LDim, and ADI were

greater in OF types than CF types, it is possible that in certain germplasm there are stronger additive effects for these traits, and this germplasm could be identified and utilized for breeding for these traits.

As the cultivars (which were assessed over two years) indicate a lower proportion of environment and genotype x environment effects (as indicated by the V_{GxE}/V_G ratio in the winters-only analysis) than the families, it would be beneficial to continue evaluating these traits over time in the families to confirm that these traits are stable over years. The high V_{GxE}/V_G ratios for plant vigor traits in the families indicate that selection for these traits cannot be performed in the spring alone, as spring size does not necessarily reflect end-of-season size. Moreover, the heritability estimates combined with the correlation results suggest that plant width and especially plant volume may be less achievable breeding goals and do not contribute any new architecture information relative to height, length, and LDim. Therefore, if future architecture studies aim to streamline the phenotypic data collection process, these two traits could be eliminated.

Only three architecture traits in this study have been directly examined in roses: NPrimaries, height, and GHabit. Branching in roses has been studied by way of number of secondary/side shoots per primary shoot (Wu et al., 2019b; Gitonga et al., 2014) and the ratio between the number of secondary shoots and the total number of buds on the primary shoot (Djennane et al., 2014); these measures of branching may be considered comparable to ADI.

Wu et al. (2019b) examined NPrimaries (defined similarly to this study) and height (as well as other traits) in 13 diploid garden rose biparental families and found

that the two traits had a correlation of 0.39. In this study, NPrimaries and height were weakly correlated (r = 0.25) in the cultivars and moderately strongly correlated in the families (r = 0.54 for all flowering types; r = 0.5 for CF types). Thus, there appears to be a relationship, though not extremely strong, between NPrimaries and height. Wu et al. Wu et al. (2019b) estimated the broad-sense heritability of NPrimaries to be 0.92, whereas in this study it ranged from 0.56 (cultivars, combined year-seasons) to 0.59 (families, combined seasons). While the CF types within families may be more comparable to the populations of Wu et al. (2019b), this heritability was still only 0.51, considerably lower than the estimate of Wu et al. (2019b), and the V_{GxE}/V_G ratio of 0.99 (CF types, combined seasons) was much higher than the estimate of 0.18 reported by Wu et al. (2019b). Narrow-sense heritability estimates were also lower in the current study. This difference is likely due to differences in germplasm. Some of the parents used in this study were parents of the populations of Wu et al. (2019b) (M4-4, J14-3) or developed from those populations (T7-20, T7-30). The other parents in the present study's populations ('Papa Hemeray', *R. palustris* f. *plena*, *R. setigera*-ARE, 'Srdce Europy, 'Lena', and 'Ole'), however, are unique to this study.

Previous studies have estimated high broad-sense heritabilities for plant height: $H^2 = 0.82$ in a tetraploid cut flower biparental population (Gitonga et al., 2014), $H^2 = 0.88$ in a diploid garden rose biparental population (Kawamura et al., 2015), and $H^2 = 0.82$ in a set of inter-related diploid garden rose biparental populations (Wu et al., 2019b). In this study, combined-season estimates of H^2 ranged from 0.58 (families, combined seasons) to 0.66 (cultivars, winters only). Individual season estimates of H^2

were more similar to previous reports. The narrow-sense heritability in this study (0.32, families, combined seasons) was lower than the estimate of 0.50 reported by Wu et al. (2019b). Dividing the families by flowering type did not substantially increase the heritability estimates for height; thus, differences in flowering types cannot be responsible for this discrepancy. Differences in germplasm may be responsible.

GHabit was previously studied over two years in the biparental population of Kawamura et al. (2015), where it was called plant form, and was found to have high broad-sense heritability ($H^2 = 0.89$). This is comparable to the estimates in this study ($H^2 = 0.85$-0.93); however, GHabit was only assessed once in this study and it unknown if in this germplasm these estimates would change over time. Kawamura et al. (2015) also found that GHabit was very strongly positively correlated with height, whereas in this study the correlation was weak or nonsignificant and negative. As Kawamura et al. (2015) used an inverted growth habit score relative to this study (i.e., a prostrate growth habit was scored as a 1 and an erect growth habit was scored as a 9), the difference in sign is expected. The difference in correlation presence/strength may be due to differences in germplasm, inclusion of a wider range of growth types, and/or the fact that GHabit is a subjective trait and scoring may not be consistent.

Branching as measured by number of secondary shoots per primary shoot has been estimated to have a low broad-sense heritability of 0.34 to 0.4 as estimated over multiple seasons (Wu et al., 2019b) or multiple year-locations (Gitonga et al., 2014), respectively. These estimates are similar to the winters-only estimate of ADI heritability in the cultivars of $H^2 = 0.38$. Gitonga et al. (2014) estimated a per-environment H^2

ranging from 0.63-0.74 which is lower than the per-season estimates of this study (H^2 = 0.85 and 0.90, cultivars and families, respectively). The V_{GxE}/V_G ratio of 0.25 in this study is considerably lower than that of the other studies, which both estimated a V_{GxE}/V_G ratio >3; however, in present study the V_{GxE}/V_G ratio was calculated over multiple winters rather than over multiple flushes as in Wu et al. (2019b) and Gitonga et al. (2014). Additional years of ADI data are needed to confirm that ADI is stable over time (as in the cultivars) and to explain the low heritability of ADI in CF types.

III.5.2 Disease resistance, flowering, and defoliation

Generally, both black spot and cercospora increased over the course of the growing season. BS in 2019-OV did not follow this pattern; however, 2019-OV had less black spot occurrence overall as indicated by the ls means. In 2018-CS in both cultivars and families, defoliation increased over the growing season and flower intensity decreased, but this pattern was not observed in 2019-OV. The differences between year-locations is likely due to climate differences, differences in populations present at each site, and differences in individual data collectors.

To explore various methods of describing disease resistance and flowering intensity, black spot, cercospora, and flowering intensity were summarized by ls means, area under a progress curve, and maximum value. Ls means and area measures were usually well-correlated with one another. In 2018-CS, BS was usually negatively correlated with CLS, but this was not the case in 2019-OV; again, the lower incidence of BS in 2019-OV could be playing a role. An inverse relationship between black spot and cercospora has been previously observed (r = -0.55 in College Station, TX, r = -0.12 to -

0.29 in Overton) (Kang, 2020). It is unclear whether this is due to linkage between two distinct resistance genes, competition between the two pathogens, or other factors. Moderately weak correlations between defoliation and the two foliar diseases have also been previously observed, though the relationship between cercospora and defoliation is less consistent (Kang, 2020).

All estimates of heritability based on the ls means were lower in the cultivars than in the families. Heritabilities based on the ls means were usually lower than that of the maximum and areas. Of disease, flowering, and defoliation traits, flower intensity had the highest broad-sense heritability in the families and a low narrow-sense heritability. Some of the high broad-sense heritability likely reflects the known gene for continuous flowering in roses (Iwata et al., 2012), as the non-additive effects declined when the analysis was performed for each flowering type. As there was still moderate broad-sense heritability and low to moderate narrow-sense heritability for FLI when flowering type was controlled for, however, there are genetic components to FLI beyond flowering type that should be explored further. This will likely necessitate studying FLI in populations that are entirely OF or CF.

The broad-sense heritability for BS in the families is comparable to the estimate of 0.51 from 15 diploid biparental families (Yan et al., 2019), though the narrow-sense heritability in this study is lower, indicating mostly non-additive genetic effects in these families. A previous estimate of cercospora resistance in 15 families resulted in H^2 = 0.83 and h^2 = 0.57, which is considerably higher than this study's estimate (Kang, 2020) although the levels of cercospora infection were similar. In general, cercospora and

cercospora resistance are less well understood than black spot, and further work on cercospora in these and other populations is needed.

III.5.3 Future directions

While the results from the cultivars indicate that architecture traits are relatively stable from year to year, additional years of data in different germplasm (i.e., the families) are needed to confirm this. Moreover, all architecture data in this study was collected in a single location. Bud burst in roses is known to be impacted by environmental factors such as light (Khayat and Zieslin, 1982; Demotes-Mainard et al., 2013) and water (Demotes-Mainard et al., 2013), and previous studies found that branching had large genotype x environment effects (Wu et al., 2019b; Gitonga et al., 2014). Thus, it is possible that branching will vary by location, and this effect should be explored in future studies. Additional years of data should also be collected for black spot and cercospora on these families. As the families were only planted in 2018, it is likely they were under less disease pressure due to lower levels of inoculum. More years and locations of data could provide better estimates of heritability and illuminate the relationship between black spot, cercospora, and defoliation.

Due to the effects of flowering type on architecture and flower intensity, future genetic studies should characterize genotypes for flowering type (or growth type if flowering data is not available) to control for this effect.

CHAPTER IV

DEVELOPMENT OF AN INTEGRATED CONSENSUS MAP FOR DIPLOID ROSE POPULATIONS

IV.1 Synopsis

Three diploid rose populations—J06-20-14-3 x ‘Papa Hemeray’, TAMU7-20 x ‘Srdce Europy’, and TAMU7-30 x ‘Srdce Europy’—were genotyped for single nucleotide polymorphisms (SNPs) via genotyping by sequencing. After initial filtration, 12,000-27,000 SNPs per population were retained for mapping; curation for segregation distortion left approximately 9,000 markers per population. Population maps were developed that had approximately 6,000-7,700 markers per map with an average density of 8-10 unique positions per cM. Highly distorted regions were found on linkage groups 2, 3, and 6. The distorted regions on linkage group 3 likely correspond to known self-incompatibility genes while the other regions have yet to be explained. Population maps had high collinearity with the rose genome. Each population map was binned to one marker per 0.5 cM and these binned maps were used to construct an integrated consensus map (ICM). The final ICM had 2,871 SNPs over 828.3 cM with an average density of 1.5 unique positions per cM. The ICM had high collinearity with the rose genome ($\rho = 0.9997$). In marker number and density, the ICM was comparable to recent diploid rose maps and should be adequate for discovery of quantitative trait loci in future studies.

IV.2 Introduction

Roses are among the most important ornamental crops: culturally, they have long been valued for their beauty and symbolic significance (Krüssman, 1981); economically, garden roses represent a substantial portion of ornamental plant sales in the United States (USDA, 2015). Genetically, roses are complicated. While roses belong to the genus *Rosa*, which comprises between 100 and 200 species (Cairns, 2003), they effectively form a multispecies complex (Debener and Byrne, 2014) due to the frequent hybridization between species, which has resulted in thousands of cultivars (Cairns, 2000). While many rose species are diploid (2n = 2x = 14), ploidy levels in species and cultivars can range from diploid to decaploid (Wissemann, 2003; Zlesak, 2009; Jian et al., 2010) with most cultivars being triploid or tetraploid (Zlesak, 2009). The genome of roses is relatively small: most diploid species studied have 2C values of 0.78 (Yokoya et al., 2000) to 1.33 pg (Roberts et al., 2009), and the *Rosa chinensis* Jacq. cultivar 'Old Blush' is estimated to have a haploid genome size of 512 Mbp (Hibrand Saint-Oyant et al., 2018).

To map the many phenotypic traits of interest in rose, a number of linkage maps have been created for both diploid and tetraploid roses. Initially, many of these maps were low-density (100 to 200 markers total) due to the types of markers used. Common marker choices included amplified fragment length polymorphisms (AFLPs) (Rajapakse et al., 2001; Yan et al., 2005a; Yu et al., 2015; Linde et al., 2006; Moghaddam et al., 2012; Gar et al., 2011; Crespel et al., 2002; Debener and Mattiesch, 1999) and simple sequence repeats (SSRs) (Rajapakse et al., 2001; Yan et al., 2005a; Yu et al., 2015;

Dugo et al., 2005; Kawamura et al., 2011; Li-Marchetti et al., 2017; Gar et al., 2011), though other molecular markers as well as morphological markers have also been used. Most of these studies also employed one or two populations of approximately 100 individuals each. The first integrated consensus map for diploid roses represented a considerable step forward, using 597 markers over 530 cM to unify four populations, each of 80-170 individuals (Spiller et al., 2011). This map was then used to locate several major genes and several quantitative trait loci (QTLs), illustrating the usefulness of consensus linkage maps for further genetic analyses.

Recent advances in genotyping and genomics have opened doors for future studies in roses. Genotyping by sequencing, which can produce tens or hundreds of thousands of single nucleotide polymorphisms (SNPs) in relatively little time and for a relatively low cost, has been successfully used in plants (He et al., 2014) including roses (Yan et al., 2018; Heo et al., 2017). The development of the WagRhSNP 68K Axiom array for rose has also enabled high-throughput genotyping of roses of various ploidy levels (Koning-Boucoiran et al., 2015). Finally, the release of three rose genomes—a fragmented genome of *Rosa multiflora* Thunb. (Nakamura et al., 2018) and two genomes of *R. chinensis* ‘Old Blush’ (Hibrand Saint-Oyant et al., 2018; Raymond et al., 2018)—means that markers can be linked to candidate genes and the function of these genes can be more fully explored.

With these new technologies, recent rose linkage maps have included considerably more markers than early maps. Vukosavljev et al. (2016) used the 68K array to develop tetraploid maps with 1,700-2,500 SNPs each. Yan et al. (2018)

produced a new consensus map for diploid rose with 3,527 SNPs produced by genotyping by sequencing. Li et al. (2019) created a single-population map using over 2,000 SNPs that was shown to have good collinearity with the Hibrand Saint-Oyant et al. (2018) rose genome. While these maps are aptly described as high-density, two ultra-high-density maps for tetraploid roses have also been produced: one employed 25,695 SNPs (Bourke et al., 2017) and the other 10,835 SNPs (Zurn et al., 2018). Theoretically, this high number of mapped markers should enable more precise mapping of trait loci.

This study seeks to create an integrated consensus map uniting three diploid rose populations comparable to the previous consensus map of Yan et al. (2018), which used related populations. The new consensus map will be used for future QTL analyses in diploid roses.

IV.3 Materials and methods

IV.3.1 Genotyping

Diploid rose populations were developed as described in Chapter II. Three of the largest populations—J06-20-14-3 x 'Papa Hemeray' (J14-3xPH), TAMU7-20 x 'Srdce Europy' (T7-20xSE), and TAMU7-30 x 'Srdce Europy' (T7-30xSE)—were selected for the development of a consensus map (Table 48). Genomic DNA was extracted from new rose leaves with a CTAB extraction method as described in Yan et al. (2018). Genotyping by sequencing was then performed using the digital genotyping procedure of Morishige et al. (2013). In brief, DNA was digested with the restriction enzyme *Ngo*MIV. After ligation of a barcoded adapter, samples were grouped into pools of 75 samples and sheared via sonication to fragments of approximately 300 bp; fragments

subsequently were purified using the Mag-Bind® Plant DNA kit (Omega Bio-Tek, Norcross, GA). Fragments of the desired size were selected via separation on a 2% agarose gel and extracted with the QIAquick Gel Purification kit (QIAGEN, Boston, MA). The adapter 5'-overhang was filled in in a reaction with *Bst* DNA polymerase; the sheared ends of the DNA fragments were repaired with the Quick Blunting™ kit (New England BioLab, Ipswich, MA); and an A-tailed adapter was added. A T-tailed adapter was ligated to the fragments and PCR with Phusion® high-fidelity polymerase (New England BioLab, Ipswich, MA) was performed to amplify fragments with both adapters. Dynabeads (Invitrogen, Carlsbad, CA), were used to select single-stranded fragments with both adapters. A final PCR with the Phusion® polymerase was performed to incorporate Illumina bridge amplification sequences.

Table 48 Diploid rose populations used for linkage mapping.

Population	Abbreviation	Num. genotyped	Num. mapped
J06-20-14-3 x 'Papa Hemeray'	J14-3xPH	140	138
TAMU7-20 x 'Srdce Europy'	T7-20xSE	103	94
TAMU7-30 x 'Srdce Europy'	T7-30xSE	86	82

Single-end sequencing was performed on the templates on an Illumina HiSeq 2500 with Illumina protocols and filtered initially with FastQC (Illumina, San Diego, CA). Reads were sorted by barcode using a custom python script; only reads with a full match to the barcode and to the partial *Ngo*MIV restriction site were continued through the pipeline. After trimming the barcodes, the CLC Genomics Workbench v9.0 (Qiagen, Boston, MA) was used to align the reads to the *Rosa chinensis* v1.0 genome (Hibrand

Saint-Oyant et al., 2018) with the following parameters: mismatch cost = 2, insertion and deletion cost = 3, a 50% minimum read length required to match the reference, and a minimum 75% similarity between reads and the reference genome. Reads that did not align to the genome or aligned at multiple locations were excluded. SNP detection was also performed in the CLC Genomics Workbench using the Variant Detection Tool with the following parameters: 90% probability of detection, minimum read coverage of 15, minimum SNP count of 3, neighborhood radius of 5, minimum central quality of 20, and minimum neighborhood quality of 15. The mapping and SNP files were exported as SAM and comma-separated-value (.csv) formats, respectively. Further SNP call analysis was performed using custom scripts written in python and perl. Markers were named based on their physical position in the rose genome. Alleles were converted to the CP population segregation types described in the JoinMap® v5.0 manual (www.kyazma.nl) using a custom python script. Markers were grouped into bins based on their proximity to a given restriction enzyme cut site in the reference genome, a procedure hereafter referred to as REbinning.

An examination of the parental genotypes revealed that the parent 'Srdce Europy' as genotyped did not explain the progeny genotypes well. Therefore, the male parent of the T7-20xSE and T7-30xSE populations was considered unknown; however, for the purposes of internal consistency, 'SE' was retained as part of the population name. The parental genotype was imputed via custom scripts that identified loci where an allele was segregating but the maternal parent was homozygous; the paternal parent was assumed to be heterozygous at these loci and homozygous otherwise. Ambiguous

markers were removed. Genotypes with excessively high recombination rates were removed as part of this process.

IV.3.2 Linkage mapping

Prior to mapping, data were filtered as followed. Markers that were not biallelic, markers that mapped to chromosome 0 (contigs from the rose genome that were unassigned to a chromosome), and markers missing >10% were removed. For population J14-3xPH, which had far more markers than the others, markers with read depths below 20 or above 150 were removed. Segregation distortion was calculated via a chi-squared test implemented in JoinMap® v5.0. In general, markers that were distorted at a level of $p \geq 0.0005$ were removed. For some chromosomes in certain populations, however, this would have entailed removing all or most markers; therefore, these chromosomes were not filtered for segregation distortion. Markers that were mapped successfully in a previous consensus map (unpublished data) for related populations were identified. The datasets were simplified by choosing one marker per segregation type per REbin, giving preference to markers that were in the previous map, had little missing data, and which fit expected segregation ratios.

To map the high number of markers remaining after the above filtration, the R package polymapR v.1.0.20 (Bourke et al., 2018) was used to develop individual population maps. polymapR, which was designed for use in polyploids but can be used for diploids, can implement both regression mapping and the multi-dimensional scaling method of MDSMap (Preedy and Hackett, 2016), and automatically phases the final map. A custom script used the reference genome call at a given locus to convert marker

calls into nulliplex (homozygous, matching the reference genome), simplex (heterozygous), or duplex (homozygous for the alternate allele). In polymapR, individuals with over 10% missing data were removed and markers with identical segregation patterns were merged. Homologs were identified with the simplex x nulliplex markers in coupling phase at LOD values ranging from five to 26, depending on the population and parent. Other marker types were assigned to homologs based on their linkage to the simplex x nulliplex markers. The two-dimensional method of MDSMap was used to construct maps for all homologs and linkage groups. Markers that mapped to a different linkage group than the reference genome indicated were removed, as were markers that showed high nearest-neighbor stress, and the map recalculated. Population maps were compared and summarized with the R Shiny application Genetic Map Comparator (Holtz et al., 2017).

The consensus map was developed using the R package LPmerge (Endelman and Plomion, 2014) as implemented in the R package Mapfuser (van Muijen et al., 2017). To reduce computation time, population maps were binned to one marker per 0.5 cM with the representative markers being those that were most common between populations and had less missing data. These thinned maps were then used to develop the consensus map. The best maps, as determined by the lowest root mean square error (RMSE), were chosen automatically from six different interval sizes (1:10, 11:20, 21:30, 31:40, 41:50, and 51:60), and the best map of these six was chosen by manual comparison of map length and overall quality. Markers that mapped far from their expected position based on the rose genome were removed or replaced with an alternative marker from the same

bin. The map was re-calculated, and the best map chosen by the same method. The consensus map was visualized with the R package LinkageMapView (Ouellette et al., 2018) and MapChart 2.32 (Voorrips, 2002). The Genetic Map Comparator was used to compare the consensus map to previous rose maps.

IV.4 Results

IV.4.1 SNP discovery and curation

Approximately 192,000 SNPs were identified by the digital genotyping method. After filtration and the SE imputation process, 12,000 to 27,000 SNPs per population were retained. Filtration for segregation distortion removed 150, 2,457, and 1,292 markers for J14-3xPH, T7-20xSE, and T7-30xSE, respectively. Frequently, markers segregating for the male parent on chromosomes 2, 3, and 6 were not filtered for segregation distortion (Table 49). In all, approximately 9,000 SNPs per population were retained for linkage mapping. Furthermore, during the SE imputation process, nine genotypes were removed from T7-20xSE and four were removed from T7-30xSE; two genotypes were removed from J14-3xPH during the mapping process (Table 48).

IV.4.2 Maps developed

Maps are summarized in Table 50. J14-3xPH had 6,204 markers over a length of 736.8 cM. One parental homolog for chromosome 6 was missing, as were large portions of parental homologs for chromosomes 1, 2, 3, and 5. The map had 5,763 unique positions resulting in an average density of 7.8 unique positions/cM. T7-20xSE had the most markers of all three populations (7,724) over the shortest length (701.7 cM) and consequently had the highest density (9.9 unique positions/cM). T7-30xSE had 7,444

markers over 843.6 cM, 6,810 unique positions, and a density of 8.1 unique positions/cM. For all three maps, LG2 had the highest number of markers and was consistently one of the longest linkage groups. All three maps had high collinearity with the rose genome as indicated by a Spearman's correlation coefficient of approximately 0.99 (Table 51, Fig. 58). 1,191 markers were common to the three maps; 4,373 markers were shared between two maps.

Table 49 Chromosomes not filtered for segregation distortion per diploid rose population. J14-3xPH indicates J06-20-14-3 x 'Papa Hemeray'; T7-20xSE indicates TAMU7-20 x 'Srdce Europy'; and T7-30xSE indicates TAMU7-30 x 'Srdce Europy'. 'Class" refers to which parent was heterozygous for the markers; i.e., in population J14-3xPH, markers heterozygous in the male parent were not filtered for segregation distortion.

J14-3xPH		T7-20xSE		T7-30xSE	
chromosome	class	chromosome	class	chromosome	class
3	all	2	paternal	2	paternal
6	paternal	3	paternal	6	paternal
		6	maternal		

Table 50 Summary of three unbinned diploid population maps and the integrated consensus map (ICM). Marker distortion was based on a chi-squared test (p<0.05). J14-3xPH indicates J06-20-14-3 x 'Papa Hemeray'; T7-20xSE indicates TAMU7-20 x 'Srdce Europy'; and T7-30xSE indicates TAMU7-30 x 'Srdce Europy'. Pop. = population.

		Linkage group							
Pop.	Map	1	2	3	4	5	6	7	overall
J14-3 xPH	Num. markers	768	1210	884	825	994	641	882	6204
	Length (cM)	94.7	138.9	85.6	82.4	129.5	94.7	111.1	736.8
	Maximum gap (cM)	2.3	2.8	1.4	0.9	3.7	2.2	1.8	3.7
	Distorted markers (%)	15.0	36.9	89.0	20.5	33.7	45.7	37.5	39.9
	Num. unique positions	715	1111	810	766	931	594	836	5763
	Density (unique positions/cM)	7.6	8.0	9.5	9.3	7.2	6.3	7.5	7.8
T7-20x SE	Num. markers	757	1398	1022	943	1118	1175	1311	7724
	Length (cM)	85.4	107.5	105.0	85.5	111.6	113.7	93.0	701.7
	Maximum gap (cM)	4.4	3.1	3.4	2.6	3.3	2.1	2.0	4.4
	Distorted markers (%)	43.9	82.1	51.7	12.4	27.4	51.8	23.0	43.3
	Num. unique positions	701	1175	917	897	1043	1034	1167	6934
	Density (unique positions/cM)	8.2	10.9	8.7	10.5	9.3	9.1	12.5	9.9
T7-30x SE	Num. markers	926	1342	947	827	973	1156	1273	7444
	Length (cM)	104.5	151.5	101.0	102.6	117.7	134.6	131.7	843.6
	Maximum gap (cM)	4.8	3.8	2.8	2.2	3.7	3.0	5.4	5.4
	Distorted markers (%)	29.0	69.2	21.5	9.7	29.5	71.4	22.0	38.6
	Num. unique positions	856	1225	871	768	913	1016	1161	6810
	Density (unique positions/cM)	8.2	8.1	8.6	7.5	7.8	7.5	8.8	8.1
ICM	Num. markers	362	493	394	357	433	408	424	2871
	Length (cM)	94.7	141.8	107.3	102.6	126.2	128.4	127.3	828.3
	Maximum gap (cM)	3.1	5.7	4.2	9.3	4.1	14.2	18.6	18.6
	Num. unique positions	162	202	186	167	199	165	188	1269
	Density (unique positions/cM)	1.7	1.4	1.7	1.6	1.6	1.3	1.5	1.5

Table 51 Collinearity of unbinned individual diploid rose population maps and the integrated consensus map (ICM) to the rose genome as indicated by correlation coefficients from a Spearman's rank-order test. J14-3xPH indicates J06-20-14-3 x 'Papa Hemeray'; T7-20xSE indicates TAMU7-20 x 'Srdce Europy'; and T7-30xSE indicates TAMU7-30 x 'Srdce Europy'.

	Collinearity with rose genome			
Linkage group	J14-3xPH	T7-20xSE	T7-30xSE	ICM
1	0.9835	0.9818	0.9897	0.9860
2	0.9878	0.9697	0.9881	0.9915
3	0.9515	0.9589	0.8023	0.9569
4	0.9795	0.9897	0.9829	0.9891
5	0.9923	0.9913	0.9907	0.9927
6	0.9843	0.9608	0.9681	0.9895
7	0.9733	0.9857	0.9921	0.9928
overall	0.9996	0.9995	0.9993	0.9997

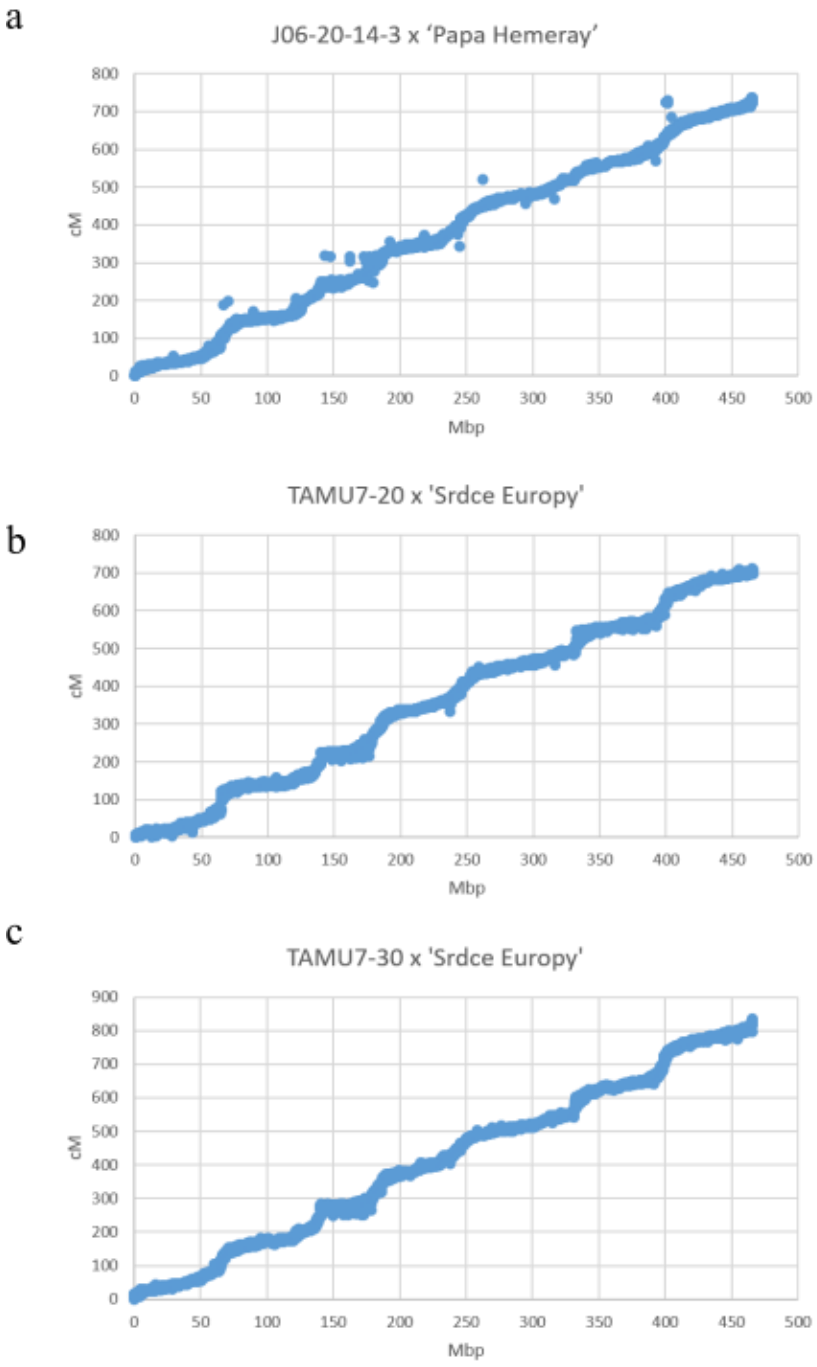

Figure 58 Collinearity of unbinned individual diploid rose population maps with the diploid rose genome. Y-axes indicate total centimorgan (cM) positions within maps; x-axes indicate total mega base pairs (Mbp) across the rose genome of Hibrand Saint-Oyant et al. (2018).a. J06-20-14-3 x 'Papa Hemeray'. b. TAMU7-20 x 'Srdce Europy'. c. TAMU7-30 x 'Srdce Europy'.

Approximately 40% of all markers in the unbinned maps had some level of distortion ($0.0005 < p < 0.05$). While distortion was found throughout all linkage groups, several linkage groups had highly concentrated regions of distortion, some of which were consistent across populations (Fig. 59). Both T7-20xSE and T7-30xSE had a distorted region on LG1, though the region was around 40-60 cM in the former and 70-80 cM in the latter. All three populations had a highly distorted region on LG2. In J14-3xPH, the region was at 50-60 cM; in T7-20xSE, 20-50 cM; and in T7-30xSE, 50-90 cM. LG2 was also the most distorted linkage group for T7-20xSE with 82% of markers having some level of distortion. T7-20xSE and T7-30xSE had a highly distorted region on the first half of LG3, and in J14-3xPH almost all markers on LG3 had distorted segregation. Highly distorted regions were also found on the second half of LG6 and the first half of LG7 in all populations.

The large number of markers per population map was determined to be unnecessary for a QTL analysis (Ronin et al., 2017), so to save computational time markers were binned in each population map. After binning to 1 marker per 0.5 cM, J14-3xPH had 1,320 markers, T7-20xSE had 1,268 markers, and T7-30xSE had 1,450 markers.

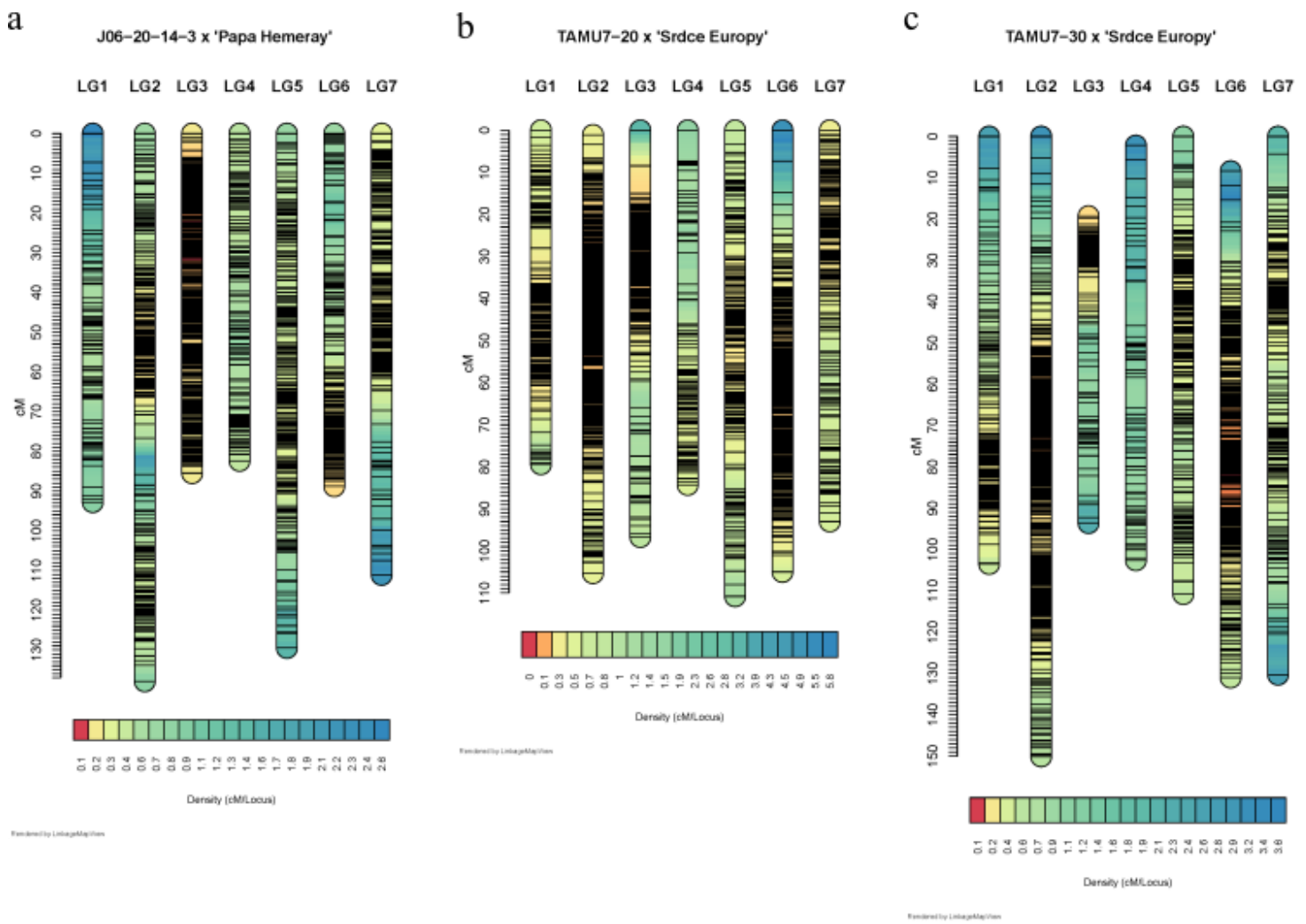

Figure 59 Density of distorted markers across unbinned diploid rose population maps. Distortion was determined by a chi-squared test ($p<0.05$). a. J06-20-14-3 x 'Papa Hemeray'. b. TAMU7-20 x 'Srdce Europy'. c. TAMU7-30 x 'Srdce Europy'.

The integrated consensus map (ICM) incorporated 2,871 markers over 828.3 cM (Table 3, Appendix B). Similar to the population maps, LG2 had the most markers and was the longest linkage group. The largest gap (18.6 cM) was on LG7; interestingly, a similarly placed gap on LG7 was present in a preliminary consensus map that was not binned, indicating that the gap is not due to the binning process. The gap may be due to genotyping errors causing the appearance of recombination between the involved markers (Appels et al., 1998). In all, there were 1,269 unique positions, resulting in a density of 1.5 unique positions/cM. Overall, the ICM had high collinearity to the rose genome (Table 51, Fig. 60) as indicated by a Spearman's correlation coefficient of 0.9997. LG3 was less collinear ($\rho = 0.9569$), particularly the first half of LG3, which coincides with the highly distorted region evident in the population maps and overlaps with a known rearrangement on chromosome 3 (Smulders et al., 2019). While not large, a gap near the end of LG5 is worth mentioning, as it was also present in all population maps. This gap is not due to mapping or filtration methods, as no SNPs were identified in this region during genotyping.

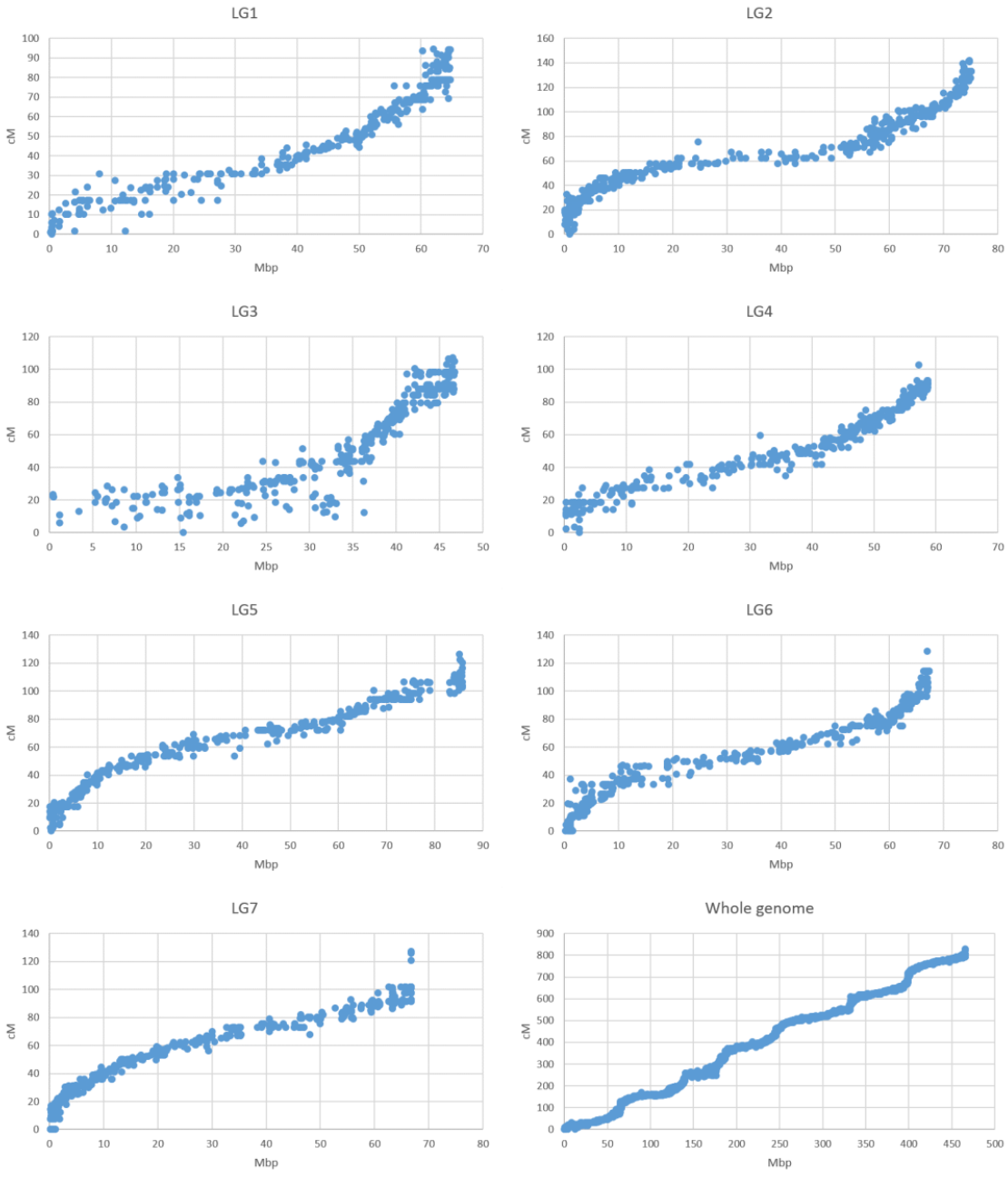

Figure 60 Collinearity between the rose genome (x-axis, in Mbp) and the diploid rose integrated consensus map (y-axis, cM).

IV.5 Discussion

The construction of a high-density integrated consensus map for these diploid rose populations will enable future genetic studies. Furthermore, this map demonstrates the usefulness of alternative linkage mapping programs. polymapR and MDSMap enabled the use of high numbers of markers on the population maps, meaning that high-quality markers were not filtered out prior to development of the consensus map. MDSMap also proved an efficient approach, mapping several thousand markers in minutes, which is considerably faster than programs such as JoinMap (Preedy and Hackett, 2016). mapfuser and LPmerge successfully produced a consensus map without the inflation noted by Yan et al. (2018) in MergeMap.

IV.5.1 Segregation distortion

A previous map on related diploid populations (Yan et al., 2018) reported that 14% of mapped markers were distorted ($p<0.05$), which is much lower than in this study. This could be due to a difference in germplasm. Using a diploid rose population related to that of Yan et al. (2018), Li et al. (2019) reported 76.09% of their markers were at least mildly distorted ($p<0.05$). Furthermore, they reported that LG1 (equivalent to LG3 in this study) contained the most blocks of segregation distortion, one of which contains seven potential self-incompatibility-related genes in the 40-45 Mbp region of chromosome 3 (Hibrand Saint-Oyant et al., 2018). This is consistent with the findings of the first consensus map of rose as well (Spiller et al., 2011). The region of the rose genome identified with the self-incompatibility genes roughly corresponds to the 60-75 cM region of LG3 in J14-3xPH, the 75-90 cM region of LG3 in T7-20xSE, and the 65-

85 cM region of LG3 in T7-30xSE. In J14-3xPH and T7-30xSE these regions are also highly distorted; thus, self-incompatibility genes on LG3 are reasonable culprits for the segregation distortion seen in this study. Interestingly, while the populations of Yan et al. (2018) are somewhat related to those in this study, the highly distorted regions on LG3 were not observed in that study.

Li et al. (2019) also found a distorted region on the end of LG6 (equivalent to LG6 in this study) which is similar to that found here, particularly in population J14-3xPH. In J14-3xPH, it is only the paternal markers of LG6 that are extremely distorted. Moreover, one paternal homolog was missing during the mapping process. Technically, one possible explanation is that this is a case of aneuploidy (specifically, trisomy) for chromosome 6 in the parent PH. However, the ploidy of PH was verified (see Chapter II), making aneuploidy unlikely but not impossible. The distortion was present in T7-20xSE (maternal) and T7-30xSE (paternal), though, indicating that it is not due to a PH-specific problem. A more likely explanation is the presence of a deleterious allele in that region on LG6 with an effect strong enough to prevent the transmission of an entire parental homolog. To date there is little research on roses that suggests what sort of deleterious allele this would be; however, considering that multiple rose species are represented in the pedigrees of these populations, chromosomal abnormalities such as translocations or large deletions may be to blame.

IV.5.2 Comparison to previous maps

The first consensus map for rose was developed from four diploid populations with 597 markers, including AFLPs, SSRs, and gene-based markers (Spiller et al.,

2011). While the average density of this first ICM was ~1.2 markers/cM, similar to the density of this map, the coverage of the rose genome has improved considerably in the ICM from this study, likely due to technological improvements in the past decade such as the development of effective SNP genotyping pipelines.

More recent maps include those of Yan et al. (2018), Li et al. (2019), Bourke et al. (2017), and Zurn et al. (2018) (Table 52). The maps of Yan et al. (2018) and Li et al. (2019) are the most similar to the present map. The map of Yan et al. (2018) was primarily developed with SNPs in three diploid rose populations related to the populations used in this study. Similar numbers of markers were mapped to each linkage group with the notable exception of LG2, which had 753 markers versus 493 in this study. Many of these markers were cosegregating, however, resulting in 161 unique positions versus 202 in this study. The average density (0.92 unique positions/cM) was slightly lower and the map longer (892.2 cM) than the current study (828.3 cM). The maximum gap (11.19 cM on LG5) was smaller than that of the current map. Li et al. (2019) mapped a single BC_1F_1 diploid population with fewer markers and unique positions than the present ICM, resulting in an average density of 0.99 unique positions/cM, which is comparable to the ICM of this study and considerably lower than the individual population maps.

Zurn et al. (2018) and Bourke et al. (2017) both mapped single tetraploid rose populations using polymapR. The map of Zurn et al. (2018) is the shortest of the maps summarized here at 421.92 cM. The map had an average density of 8.59 unique positions/cM, which is denser than the consensus map in this study but is comparable to the individual population maps constructed with polymapR in this study. Bourke et al. (2017) produced the densest map by far with 26.31 unique positions/cM and a total length of 573.66 cM. The length of these maps may be at least partially explained by the studies' use of the WagRhSNP 68K Axiom array for genotyping. Genotyping errors are known to contribute to map inflation, and SNP arrays are generally less error-prone than GBS or RAD-seq genotyping methods.

In short, while the recent ultra-high-density maps in tetraploid populations far exceed the ICM of this study in marker number and density, the ICM of this study is comparable to two recent diploid maps, having a larger maximum gap but higher density. Thus, it should be of use for future QTL analyses in these diploid rose populations.

Table 52 Comparison of the diploid rose ICM of this study ('Current') to other recent rose linkage maps. Number of unique positions and density were estimated by the Genetic Map Comparator if not provided within the study referenced.

		Linkage group							
Study	Map	1	2	3	4	5	6	7	overall
Current	Num. markers	362	493	394	357	433	408	424	2871
	Length (cM)	94.69	141.78	107.29	102.61	126.19	128.42	127.29	828.27
	Maximum gap (cM)	3.07	5.70	4.23	9.33	4.07	14.21	18.64	18.64
	Num. unique positions	162	202	186	167	199	165	188	1269
	Density (unique positions/cM)	1.71	1.42	1.73	1.63	1.58	1.28	1.48	1.53
Yan et al. 2018	Num. markers	348	753	340	520	564	472	530	3527
	Length (cM)	94.61	133.01	118.21	117.3	152.71	109.49	166.87	892.2
	Maximum gap (cM)	3.77	4.45	8.51	4.18	11.19	3.6	5.89	11.19
	Num. unique positions	93	161	91	120	121	109	125	820
	Density (unique positions/cM)	0.98	1.21	0.77	1.02	0.79	1.00	0.75	0.92
Li et al. 2019 (Version 2.0)	Num. markers	196	503	386	167	503	243	325	2213
	Length (cM)	103.95	208.63	140.20	77.73	190.96	129.58	176.38	1027.43
	Maximum gap (cM)	5.62	9.95	6.08	4.52	3.79	7.97	5.01	9.95
	Num. unique positions	97	196	145	191	191	122	158	1022
	Density (unique positions/cM)	0.93	0.94	1.03	2.46	1.00	0.94	0.90	0.99
Zurn et al. 2018	Num. markers	1164	1975	1118	1442	1861	1568	1707	10835
	Length (cM)	51.13	76.17	48.46	60.19	64.56	61.65	59.76	421.92
	Maximum gap (cM)	0.89	2.41	1.34	1.35	1.37	3.60	1.78	3.60
	Num. unique positions	472	678	369	494	645	428	537	3623
	Density (unique positions/cM)	9.23	8.90	7.61	8.21	9.99	6.94	8.99	8.59

Table 52 Continued

Study	Map	Linkage group							
		1	2	3	4	5	6	7	overall
Bourke et al. 2017	Num. markers	1865	6154	2912	2866	3799	4193	3906	25695
	Length (cM)	79.19	108.67	72.16	77.3	89.76	71.82	74.76	573.66
	Maximum gap (cM)	4.32	1	1.18	3.48	0.7	2.02	0.53	4.32
	Num. unique positions	1191	3575	1744	1791	2426	2111	2254	15092
	Density (unique positions/cM)	15.04	32.90	24.17	23.17	27.03	29.39	30.15	26.31

CHAPTER V

ASSOCIATION MAPPING FOR DISEASE RESISTANCE, DEFOLIATION, FLOWERING, AND ARCHITECTURE TRAITS IN DIPLOID ROSE CULTIVARS AND FAMILIES

V.1 Synopsis

A genome-wide association study in 73 diploid rose cultivars and a single marker analysis in 321 genotypes from eight diploid rose families was performed to identify markers associated with black spot and cercospora resistance, defoliation, flower intensity, and architecture traits. The cultivars were found to form two main subpopulations that corresponded to their known pedigrees and horticultural classes. In the families, many associations were found for the traits of interest, some of which fell into small genomic regions (termed ‘clusters’). Three clusters of associations were identified for black spot and three for cercospora on chromosomes 2, 3, and 6; however, only the cluster on chromosome 3 overlapped between black spot and cercospora. The chromosome 3 cluster may coincide with previously identified QTLs for black spot and cercospora. The clusters on chromosomes 2 and 6 are novel and encompass several NBS-LRR genes. When flowering type was controlled for, five clusters associated with flower intensity were identified on chromosomes 2, 4, and 5. Ten clusters associated with plant vigor traits (height, length, width, longest dimension, and volume) were identified. Vigor clusters on chromosomes 1 and 2 may coincide with previously identified QTLs, but the other clusters are novel. Presumably due to its small size, no

marker-trait associations were found in the cultivars for disease, defoliation, or flowering; a few associations were found for architectural traits. Some of these associations overlapped with the vigor clusters in the families. Thus, novel genomic regions associated with disease resistance and architecture have been identified; further work is needed to narrow down the regions and validate them in different and/or larger datasets.

V.2 Introduction

Roses are among the most important ornamental crops: culturally, they have long been valued for their beauty and symbolic significance (Krüssman, 1981); economically, garden roses represent a substantial portion of ornamental plant sales in the United States (Chavez et al., 2019; USDA, 2015). Roses belong to the genus *Rosa*, which comprises between 100 and 200 species (Cairns, 2003) and many thousands of inter- and intraspecific hybrid cultivars (Cairns, 2000). While many rose species are diploid (2n = 2x = 14), ploidy levels in species and cultivars alike can range from diploid to decaploid (Jian et al., 2010; Wissemann, 2003; Zlesak, 2009). Due to the persistent popularity of roses, there is demand for cultivars with superior disease resistance, increased flower productivity, and more attractive shape. Breeding efforts have been hampered, however, by the complex genetics of roses of varying ploidies, a shortage of genomic resources, a relatively long generation time, and insufficient understanding of the genetic control of traits of interest. With the recent availability of the rose genome (Hibrand Saint-Oyant et al., 2018; Raymond et al., 2018; Nakamura et al., 2018) and the advent of more

affordable genotyping techniques, it is more feasible to study and breed for the various desirable traits of roses.

Roses are susceptible to many diseases, and for garden roses, the fungal disease black spot (*Diplocarpon rosae* Wolf) is among the most significant and well understood. Black spot is a hemibiotrophic ascomycete that, as the name suggests, causes black circular lesions on rose foliage, eventually leading to high rates of defoliation (Horst and Cloyd, 2007; Wolf, 1912). Many roses are susceptible (Horst and Cloyd, 2007); however, four major genes for black spot resistance have been identified. *Rdr1* on chromosome 1 confers resistance to race 5 (Von Malek et al., 2000; Spiller et al., 2011); *Rdr2* confers resistance to race 4 (Hattendorf et al., 2003) and is also on chromosome 1 (Zurn et al., 2018); *Rdr3* confers resistance to race 8 but has not been successfully mapped (Whitaker et al., 2010); and *Rdr4* on chromosome 5 confers resistance to 12 of the 13 identified black spot races (Zurn et al., 2018). Partial resistance to black spot does seem to exist (reviewed in Debener (2019)) and quantitative trait loci (QTLs) for black spot have been identified on chromosomes 3 and 5 in various populations (Soufflet-Freslon et al., 2019; Yan et al., 2019). The QTL on chromosome 5 has yet to be validated in other populations, however, and more QTLs may still be identified.

While not as prominent as black spot, the fungal disease cercospora leaf spot (caused by *Rosisphaerella rosicola* Pass., syn: *Cercospora rosicola* Pass. (Videira et al., 2017) is also a concern for garden roses. Similar to black spot, this disease manifests as dark foliar lesions, though cercospora lesions tend to have lighter necrotic centers as the disease progresses, and eventually defoliation results (Mangandi and Peres, 2009; Davis,

1938). Susceptibility appears to be common and the disease is currently controlled with fungicide application (Mangandi and Peres, 2009). No distinct races have been characterized and no major resistance genes identified; however, resistance has been estimated to have high broad-sense heritability, indicating that it should be a feasible breeding goal, and QTLs have been identified on chromosomes 1, 3, and 7 (Kang, 2020). Further work is needed to validate these QTLs and/or identify other genetic components of cercospora resistance.

As garden roses are grown primarily for their flowers, abundant and consistent flowering throughout the growing season is highly desirable. Thus, though many rose species are once-flowering (OF), blooming only in the spring, many rose cultivars have been selected to be of continuous flowering (CF) type, blooming throughout the growing season (Bendahmane et al., 2013). Flowering type is controlled by a single gene, *RoKSN*, which has been identified as a member of the *TERMINAL FLOWER 1* (*TFL1*) gene family (Iwata et al., 2012). Within CF roses, however, there is still variation in the degree of flowering. Possible genetic explanations include MADS-box genes encoding transcription factors that are crucial for floral organogenesis (Liu et al., 2018) and gibberellic acid biosynthesis genes that have been shown to be upregulated during bud burst (Choubane et al., 2012). Flower productivity is also known to be affected by heat stress (Greyvenstein, 2013) and light intensity (Girault et al., 2008). A disconnect remains between the molecular understanding of flowering and the flower productivity observed in the field, meaning that while flower productivity is assumed by breeders to

be additive (Gudin, 2003), this critical trait is in need of further characterization and study.

Plant architecture greatly affects the visual quality of a rose plant (Boumaza et al., 2009). Generally, architecture is determined by both genetics and the environment, and in roses, light (Khayat and Zieslin, 1982; Demotes-Mainard et al., 2013), water (Demotes-Mainard et al., 2013), mechanical stimulation (Morel et al., 2012), and nitrogen availability (Huché-Thélier et al., 2011) have all been shown to affect plant shape. The genetic control of architecture has been studied by examining a wide variety of traits, including number and length of axes (Morel et al., 2009; Crespel et al., 2014; Crespel et al., 2013; Li-Marchetti et al., 2017); number and length of metamers, a metamer being defined as an internode, a node, axillary bud(s), and a leaf (Crespel et al., 2014; Crespel et al., 2013; Li-Marchetti et al., 2017; Morel et al., 2009; Demotes-Mainard et al., 2009); number and length of determined axes (Crespel et al., 2014; Crespel et al., 2013; Li-Marchetti et al., 2017); number and length of primary shoots (Wu et al., 2019b; a); growth habit (Crespel et al., 2013; Kawamura et al., 2015); number of nodes per primary shoot (Kawamura et al., 2015; Wu et al., 2019b; a); number of secondary and tertiary shoots per primary shoot (Wu et al., 2019b; a); plant height (Wu et al., 2019b; a; Kawamura et al., 2015; Gitonga et al., 2014); various branching angles (Crespel et al., 2014; Crespel et al., 2013; Li-Marchetti et al., 2017); and stem diameter (Crespel et al., 2013; Kawamura et al., 2015; Garbez et al., 2018). Some studies have employed 3D digitization to measure multiple traits (Crespel et al., 2014; Crespel et al., 2013; Li-Marchetti et al., 2017) which unfortunately is unrealistic in

a field setting. While heritability estimates vary with the trait, many architecture traits have moderate to high broad-sense heritability. Accordingly, many QTLs have been identified for architecture traits, including growth habit, height (Kawamura et al., 2015), number of determined axes, length of long axes (Li-Marchetti et al., 2017), shoot length, number of internodes (Yan et al., 2007), branching intensity (Djennane et al., 2014), number of nodes per primary shoot (Kawamura et al., 2011), and internode length (Kawamura et al., 2011; Kawamura et al., 2015). These results are promising and merit further exploration in a wide range of germplasm.

Association mapping provides a way to explore the genetic control of such traits in diverse germplasm, making it potentially well-suited to a crop with a complex history such as roses. As implemented in genome-wide association studies (GWAS), association mapping employs linkage disequilibrium in an unstructured population to identify marker-trait associations. By using a panel of unrelated genotypes, GWAS can exploit many generations of meiotic events rather than the single meiosis permitted by traditional QTL mapping in a biparental family. The resulting higher resolution means that a GWAS can potentially identify a single nucleotide associated with the trait of interest while QTL mapping will potentially identify a large genomic region that may contain many genes. Moreover, since GWAS rely on diverse germplasm, the results are theoretically more applicable to a wide range of germplasm (Oraguzie et al., 2007). The success of a GWAS will depend on a variety of factors, however, including the level of linkage disequilibrium, the degree of relatedness within the panel, and the panel size used (Myles et al., 2009). GWAS have been successfully performed in roses to

determine the genetic basis of adventitious root formation (Nguyen et al., 2017; Nguyen et al., 2020) and petal color (Schulz et al., 2016).

This study seeks to expand the knowledge of the genetic control of flower intensity, plant architecture, and resistance to black spot and cercospora by identifying molecular markers associated with these traits through two methods. The first method is a genome-wide association study in a diverse set of diploid rose cultivars; the second, a marker-trait association analysis in a set of interrelated biparental diploid rose families. Previous studies for these traits often employed one or a few biparental families; it is hoped that by using several biparental families drawing from diverse germplasm in conjunction with a cultivar panel more accurate and more widely applicable results will be obtained. The ultimate goal is to identify markers for future marker-assisted selection.

V.3 Materials and methods

V.3.1 Plant materials

A total of 73 diploid rose cultivars and 373 individuals (Tables 53, 54) from ten diploid rose biparental families was phenotyped for plant architecture, black spot and cercospora resistance, defoliation, and flower intensity in multiple environments as described in Chapter III and summarized in Tables 55 and 56. One family, *R. setigera*-ARE x 'Lena', was phenotyped but not genotyped, resulting in nine populations and 372 individuals. Least squares means (ls means) and best linear unbiased predictions (BLUPs) were estimated from the restricted maximum likelihood (REML) models for each environment and for combined environments (described in Chapter III), keeping the cultivars and families separate.

Table 53 Diploid rose cultivar genotypes included in the study, the number of replications, and primary horticultural class (drawn from HelpMeFind.com). Number in parentheses indicates cultivar release year when there are multiple cultivars with the name. ARE = Antique Rose Emporium, RVR = Rogue Valley Roses, CHM = Chamblee's Rose Nursery.

Genotype	Abbreviation	Num. replications	Source	Class
Anemone (1896)	AM	3	ARE	H. Laevigata
Ballerina (1937)	BA	3	ARE	H. Musk
Borderer	BDR	3	ARE	Floribunda
Belinda	BE	3	ARE	H. Musk
Blush Noisette	BH	3	ARE	Noisette
Bermuda's Kathleen	BK	3	ARE	China
Bon Silene	BON	3	ARE	Tea
Blumenschmidt	BT	3	ARE	Tea
Cecile Brunner	CB	3	ARE	Polyantha
Celine Forestier	CF	3	ARE	Noisette
Clotilde Soupert (1890)	CL	3	ARE	Polyantha
Danae (1913)	DA	3	ARE	H. Musk
Duchesse de Brabant	DCH	3	ARE	Tea
Ducher	DU	3	ARE	China
Emmie Gray	EG	3	ARE	China
Fortunes Double Yellow	FY	3	ARE	China
Gipsy Boy	GB	3	ARE	Bourbon
Gardenia (1899)	GD	3	ARE	H. Wichurana
General Schablikine	GS	3	ARE	Tea
Happenstance	HA	3	ARE	H. Bracteata
Independence Musk	IM	3	ARE	H. Musk
Jeanne d'Arc (1848)	JA	3	ARE	Alba
Jaune Desprez	JD	3	ARE	Noisette
Jean Mermoz	JM	3	ARE	Polyantha
Katharina Zeimet	KZ	3	ARE	Polyantha
La Marne	LM	3	ARE	Polyantha
Leontine Gervais	LO	3	ARE	H. Wichurana
Lavender Pink Parfait	LPP	3	ARE	H. Multiflora
Le Vesuve (1825)	LU	3	ARE	China
Mrs. Bosanquet	MB	3	ARE	Bourbon
Miss Caroline	MC	3	ARE	Tea
Mermaid (1917)	ME	3	ARE	H. Bracteata
Mevrouw Nathalie Nypels	MEV	3	ARE	Floribunda
Mademoiselle Franziska Kruger	MFK	3	ARE	Tea
Madame Joseph Schwartz	MJ	3	ARE	Tea
Marjorie Fair	MJF	3	ARE	Polyantha

Table 53 Continued

Genotype	Abbreviation	Num. replications	Source	Class
Miss Lowe's Variety	MLV	2	RVR	China
Madame Laurette Messimy	MM	3	ARE	China
Marechal Niel (1864)	MNN	2	RVR	Noisette
Moonlight (1913)	MO	3	ARE	H. Musk
Monsieur Tillier	MT	3	ARE	Tea
Mutabilis	MU	3	ARE	China
Marie Van Houtte	MV	3	ARE	Tea
Mozart (1936)	MZ	3	ARE	H. Musk
Nastarana	NA	2	RVR	H. Musk
Old Blush	OB	3	ARE	China
Oakington Ruby	OR	2	RVR	Miniature
Phalaenopsis	PA	3	ARE	Floribunda
Porcelaine de Chine	PDC	2	RVR	H. Musk
Pink Grootendorst	PG	3	ARE	H. Rugosa
Perle des Jardins	PJ	3	ARE	Tea
Plaisanterie	PL	2	RVR	H. Musk
Petite Pink Scotch	PPS	3	ARE	H. Wichurana
Ma Paquerette	PQ	2	RVR	Polyantha
Pink Surprise (1987)	PS	2	RVR	H. Bracteata
Phyllis Bide	PY	3	ARE	Polyantha
Robin Hood (1927)	RBH	3	ARE	H. Musk
Red Drift	RD	3	CHM	Shrub
Rosa moschata	RCH	3	ARE	Species
Russelliana	RL	3	ARE	H. Multiflora
Rouletii	ROU	3	RVR	China
Republic of Texas	RT	3	ARE	Shrub
Safrano	SA	3	ARE	Tea
Sarasota Spice	SAS	3	ARE	Noisette
Spice	SI	3	ARE	China
Sunshine (1927)	SUN	2	RVR	Polyantha
The Fairy	TFY	3	ARE	Polyantha
The Gift	TG	2	RVR	Polyantha
Trier	TI	2	RVR	H. Multiflora
Veilchenblau	VB	3	ARE	H. Multiflora
Vincent Godsiff	VF	3	ARE	China
Violette	VT	3	ARE	H. Multiflora

Table 53 Continued

Genotype	Abbreviation	Num. replications	Source	Class
Climbing White Maman Cochet	WC	3	ARE	Tea
Windchimes	WI	3	ARE	H. Musk
Yesterday	Y	2	RVR	Polyantha

Table 54 Diploid rose populations maintained in College Station and Overton, TX for phenotypic data collection.

Population	Abbreviation	College Station	Overton
J06-20-14-3 x Papa Hemeray	J14-3xPH	69	0
Papa Hemeray x *R. palustris* f. *plena* EB-ARE	PHxSEB-ARE	11	8
M4-4 x Srdce Europy	M4-4xSE	33	14
TAMU7-20 x Srdce Europy	T7-20xSE	103	92
TAMU7-30 x Srdce Europy	T7-30xSE	88	71
R. setigera-ARE x Lena	SET-ARExLN	1	0
R. setigera-ARE x Ole	SET-ARExOL	25	18
Ole x *R. palustris* f. *plena* EB-ARE	OLxSEB-ARE	23	12
Ole x *R. palustris* f. *plena* OB-ARE	OLxSOB-ARE	11	0
Lena x *R. palustris* f. *plena* OB-ARE	LNxSOB-ARE	11	2
Total		*373*	*217*

Table 55 Phenotypic traits assessed in diploid rose cultivars and families each year in College Station, TX and Overton, TX. 2018-CS and 2019-CS indicate data taken in 2018 and 2019, respectively, in College Station, TX. 2019-OV indicates data taken in 2019 in Overton, TX.

Trait	Abbreviation	Cultivars	Families
Number of primary shoots	NPrimaries	2018-CS, 2019-CS	2018-CS
Plant height (cm)	Height	2018-CS, 2019-CS	2018-CS
Plant length (cm)	Length	2018-CS, 2019-CS	2018-CS
Plant width (cm)	Width	2018-CS, 2019-CS	2018-CS
Longest dimension (cm)	LDim	2018-CS, 2019-CS	2018-CS
Plant volume (cm^3)	Volume	2018-CS, 2019-CS	2018-CS
Apical dominance index (number secondary shoots/shoot length)	ADI	2018-CS, 2019-CS	2018-CS
Growth habit	GHabit	2018-CS	2018-CS
Growth type	GType	2018-CS	2018-CS
Flowering type	FlwgType	2018-CS	2018-CS
Mean black spot	BS	2018-CS	2018-CS, 2019-OV
Maximum black spot	BS_Max	2018-CS	2018-CS, 2019-OV
Black spot area under the disease progress curve	BS_AUDPC	2018-CS	2018-CS, 2019-OV
Mean cercospora leaf spot	CLS	2018-CS	2018-CS, 2019-OV
Maximum cercospora leaf spot	CLS_Max	2018-CS	2018-CS, 2019-OV
Cercospora leaf spot area under the disease progress curve	CLS_AUDPC	2018-CS	2018-CS, 2019-OV
Average flower intensity	FLI	2018-CS	2018-CS, 2019-OV
Maximum flower intensity	FLI_Max	2018-CS	2018-CS, 2019-OV
Area under the flower intensity curve	AFLIC	2018-CS	2018-CS, 2019-OV
Mean defoliation	DEF	2018-CS	2018-CS, 2019-OV
Maximum defoliation	DEF_Max	2018-CS	2018-CS, 2019-OV

Table 56 Season, month, year, and location combinations for phenotypic data collected on diploid rose cultivars and families. CV = cultivar panel, FM = families.

	Location	
Evaluation, Year	College Station, TX	Overton, TX
Monthly, 2018	CV, FM	
Spring, 2018	CV, FM	
Winter, 2018	CV, FM	
Monthly, 2019		FM
Winter, 2019	CV	

V.3.2 Genotyping and curation

Genomic DNA was extracted from new rose leaves with a CTAB extraction method as described in Yan et al. (2018). Genotyping by sequencing using the digital

genotyping procedure of Morishige et al. (2013) was performed. In brief, DNA was digested with the restriction enzyme *Ngo*MIV. After ligation of a barcoded adapter, samples were grouped into pools of 75 samples and sheared via sonication to fragments of approximately 300 bp; fragments subsequently were purified using the Mag-Bind® Plant DNA kit (Omega Bio-Tek, Norcross, GA). Fragments of the desired size were selected via separation on a 2% agarose gel and extracted with the QIAquick Gel Purification kit (QIAGEN, Boston, MA). The adapter 5'-overhang was filled in in a reaction with *Bst* DNA polymerase; the sheared ends of the DNA fragments were repaired with the Quick Blunting™ kit (New England BioLab, Ipswich, MA); and an A-tailed adapter was added. A T-tailed adapter was ligated to the fragments and PCR with Phusion® high-fidelity polymerase (New England BioLab, Ipswich, MA) was performed to amplify fragments with both adapters. Dynabeads (Invitrogen, Carlsbad, CA), were used to select single-stranded fragments with both adapters. A final PCR with the Phusion® polymerase was performed to incorporate Illumina bridge amplification sequences.

Single-end sequencing was performed on the templates on an Illumina HiSeq 2500 with Illumina protocols and filtered initially with FastQC (Illumina, San Diego, CA). Reads were sorted by barcode using a custom python script; only reads with a full match to the barcode and to the partial *Ngo*MIV restriction site were continued through the pipeline. After trimming the barcodes, the CLC Genomics Workbench v9.0 (Qiagen, Boston, MA) was used to align the reads to the *Rosa chinensis* v1.0 genome with the following parameters: mismatch cost = 2, insertion and deletion cost = 3, a 50%

minimum read length required to match the reference, and a minimum 75% similarity between reads and the reference genome. Reads that did not align to the genome or aligned at multiple locations were excluded. SNP detection was also performed in the CLC Genomics Workbench with the Variant Detection Tool with the following parameters: 90% probability of detection, minimum read coverage of 15, minimum SNP count of 3, neighborhood radius of 5, minimum central quality of 20, and minimum neighborhood quality of 15. The mapping and SNP files were exported as SAM and comma-separated-value (.csv) formats, respectively, and further SNP call analysis was performed using custom scripts written in python and perl. Markers were named based on their physical position in the genome and genotypes were exported as a comma-separated file.

Curation steps for families and cultivars were then separated. Between 180,000 and 192,000 SNPs were identified for the two datasets for further curation and analysis. Curation proceeded as follows. Markers that were from unassigned contigs from the rose genome (chromosome 0) were removed, as were markers that had a large number of the - allele. Average read depth was calculated and markers with an average read depth below 20 were removed, as these were determined to be less reliable. Similarly, a histogram of average read depth was created and the markers in the extreme of the right-hand tail (approximately the 99.9th percentile) were removed. The data was then used to create .map and .ped files for use in PLINK 1.9 (Purcell and Chang, 2015; Purcell et al., 2007). In PLINK, markers were removed if they had missing data >10%, had very low

minor allele frequency (<1%), or were not biallelic. In the families, genotypes missing more than 20% of the markers were removed (5 genotypes).

In the cultivar panel, further curation was performed. Linkage disequilibrium (LD) was estimated with a window of 1 Mb and 1 kb and visualized in the R package ggplot2 (Wickham, 2009). Based on this visualization, the data was pruned for excessive LD with the indep-pairwise command using a window of 25 SNPs, a shift of 5 SNPs, and an r^2 threshold of 0.5. LD was re-visualized with ggplot2. At this point, genotypes (2 total) missing more than 20% of the markers were removed and the curation steps redone with the addition of distance-based marker thinning so that SNPs had a minimum gap of 10 bp. The LD pruning window was also adjusted to 50 SNPs based on the LD visualization.

V.3.3 Population structure and genetic diversity

Population structure (K) in the cultivar panel was estimated using the admixture model in STRUCTURE 2.3.4, which uses a Bayesian approach to determine population structure (Pritchard et al., 2000). A burn in of 10,000 cycles was used followed by a run length of 50,000 cycles. Ten iterations were performed for each value of K from 1 to 10. The optimal value of K was determined with the method of Evanno et al. (2005) as implemented in STRUCTURE HARVESTER (Earl and vonHoldt, 2012). To validate the results of STRUCTURE, ADMIXTURE 1.3, which uses maximum likelihood estimates rather than Bayesian (Alexander et al., 2009), was also used to estimate population structure. K 1-20 were tested with a 5-fold cross-validation (CV). The CV error was plotted in R and the optimal K identified by minimization of the CV error. The

results of both programs were visualized as barplots with R. Results were also compared by assigning genotypes to subpopulations with a cutoff probability of 0.5 for optimal K > 2 and a cutoff probability of 0.6 for optimal K = 2.

Relationships between cultivars were also investigated via genetic distance and a phylogenetic tree. SNP alleles were alphabetized and concatenated to form a pseudo-sequence for each genotype (Bentley et al., 2019) and entered into MEGA X (Kumar et al., 2018) as a non-protein encoding nucleotide sequence. The maximum likelihood (ML) model selection feature with no branch swap filter and using all sites was used to determine the best-fitting model, which was the General Time Reversible (GTR) model where gamma = 1.03. An unrooted phylogenetic tree was created with the GTR model with the following settings: gamma = 2 (minimum gamma value permitted), no branch swap filter, missing data treated with pairwise deletion; and 1000 bootstrap replications performed.

Kinship using GBS with depth adjustment (KGD) (Dodds et al., 2015) was used to investigate relatedness between genotypes and verify pedigrees when possible for both the cultivar panel and the families. KGD is designed for use with GBS data and takes read depth into account when estimating kinship (Dodds et al., 2015). In the cultivar panel, the curated set of SNPs was used; in the families, minimally curated SNPs were used. Scripts developed by Bentley et al. (2019) were used to format the data for KGD. A Hardy-Weinberg disequilibrium cutoff of 0.05 was used.

Finally, a principal component analysis in PLINK was used to identify population structure in the families. The best number of principal components was determined by visual inspection of the resulting scree plot.

V.3.4 Association mapping

Association mapping was performed in the R package GAPIT (Lipka et al., 2012) with all SNPs that were retained from the curation process. Families were analyzed separately from the cultivar panel, as it was assumed that since the families so outnumbered the cultivars any signal from the cultivars would be drowned out by the families. Environments (seasons, locations) were analyzed separately and as combined-environments (year-seasons, year-locations). Two primary models were used: mixed linear model (MLM) (Lipka et al., 2012; Yu et al., 2006) and fixed and random model circulating probability unification (FarmCPU) (Liu et al., 2016). In order to investigate the effects of population structure (Q) and kinship (K) in the cultivars, a variety of Q and K matrices were used (Table 57). Q matrices used included both STRUCTURE and ADMIXTURE results as well as population structure with the additional covariate of growth type. The use of covariates instead of population structure was also tested: either growth type or principal components (PCs) with the number of PCs corresponding to number of subpopulations. The KGD kinship matrix as well as the GAPIT-provided kinship matrix calculated with the VanRaden method (VanRaden, 2008) were used as K matrices. In all, 26 different variations on the two base models were assessed for goodness of fit for the cultivars.

In the families, both FarmCPU and MLM were employed (Table 58). MLM variants used PCs of zero, four (based on the PCs estimated by PLINK), or up to eight with the setting Model.selection = T, which permits GAPIT to determine and use the best number of PCs. The VanRaden kinship matrix was used for all models. FarmCPU was tested at PCs of zero and four through eight PCs. In order to test the effect of flowering type on architecture and flowering traits, the family dataset was divided by flowering type and single-marker analysis performed again. In this analysis, FarmCPU and MLM were both tested with PCs of zero through five.

Goodness of fit was determined by visual inspection of the QQ plots for each model and trait combination. A single model that fit all traits well was chosen for each dataset, giving preference to models with a lower number of parameters. Markers from the best-fitting model were determined to be significant based on a false discovery rate (FDR) of 10% estimated with the Benjamini-Hochberg procedure (Benjamini and Hochberg, 1995) as well as a LOD score of 5 or greater. Markers were tested for contribution to the relevant phenotype via ANOVA when appropriate. The Genome Database for Rosaceae (Jung et al., 2018) was used to compare significant markers to previously identified QTLs and genes.

Table 57 Models and variations tested for use in association mapping in diploid rose cultivars. Variants are named according to Model (Q+K). MLM indicates mixed linear model; FarmCPU indicates fixed and random model circulating probability unification. ADMIX and STRUCT indicate ADMIXTURE and STRUCTURE results were used as a Q matrix, respectively; _gtype indicates an extra covariate of growth type was added to these Q matrices. PCA indicates principle components were used as covariates. KGD and VanRaden indicate kinships estimated by the KGD method and the VanRaden method, respectively, were used as K matrices in those models.

Model	Variant name
FarmCPU	FarmCPU (PCA0)
FarmCPU	FarmCPU (PCA2)
FarmCPU	FarmCPU (PCA5)
FarmCPU	FarmCPU (PCA6)
MLM	MLM (ADMIX_gtype+KGD)
MLM	MLM (ADMIX_gtype+VanRaden)
MLM	MLM (ADMIX+KGD)
MLM	MLM (ADMIX+VanRaden)
MLM	MLM (Gtype+KGD)
MLM	MLM (Gtype+VanRaden)
MLM	MLM (PCA0+KGD)
MLM	MLM (PCA0+VanRaden)
MLM	MLM (PCA2 +KGD)
MLM	MLM (PCA2+VanRaden)
MLM	MLM (PCA5+KGD)
MLM	MLM (PCA5+VanRaden)
MLM	MLM (PCA6+KGD)
MLM	MLM (PCA6+VanRaden)
MLM	MLM (STRUCT2_gtype+KGD)
MLM	MLM (STRUCT2_gtype+VanRaden)
MLM	MLM (STRUCT2+KGD)
MLM	MLM (STRUCT2+VanRaden)
MLM	MLM (STRUCT6_gtype+KGD)
MLM	MLM (STRUCT6_gtype+VanRaden)
MLM	MLM (STRUCT6+KGD)
MLM	MLM (STRUCT6+VanRaden)

Table 58 Models and variations tested for association mapping in eight diploid rose families. Variants are named according to Model (Q+K). PCA indicates principle components were used as covariates. PCAT indicates GAPIT chose the best number of PCs from one to eight.

Model	Variant name
FarmCPU	FarmCPU (PCA0)
FarmCPU	FarmCPU (PCA4)
FarmCPU	FarmCPU (PCA5)
FarmCPU	FarmCPU (PCA6)
FarmCPU	FarmCPU (PCA7)
FarmCPU	FarmCPU (PCA8)
MLM	MLM (FlwgType)
MLM	MLM (PCA0+VanRaden)
MLM	MLM (PCA4+VanRaden)
MLM	MLM (PCA8+VanRaden)
MLM	MLM (PCAT+VanRaden)

V.4 Results

V.4.1 Genotypic data

A total of 11,884 and 58,075 SNPs was retained for association mapping in the cultivars and families, respectively. While the SNPs were not evenly distributed across the genome, the entire genome was represented (Fig. 61, 62). Linkage disequilibrium in the cultivars was found to decay to an r^2 of 0.2 within ~200 bp (Fig. 63). 73 cultivars and 321 progeny were retained after curation.

Figure 61 Distribution of 11,884 SNP markers retained after data curation per chromosome and over the full genome in diploid rose cultivars.

Figure 62 Distribution of 58,075 SNP markers retained after data curation per chromosome and over the full genome in eight diploid rose families.

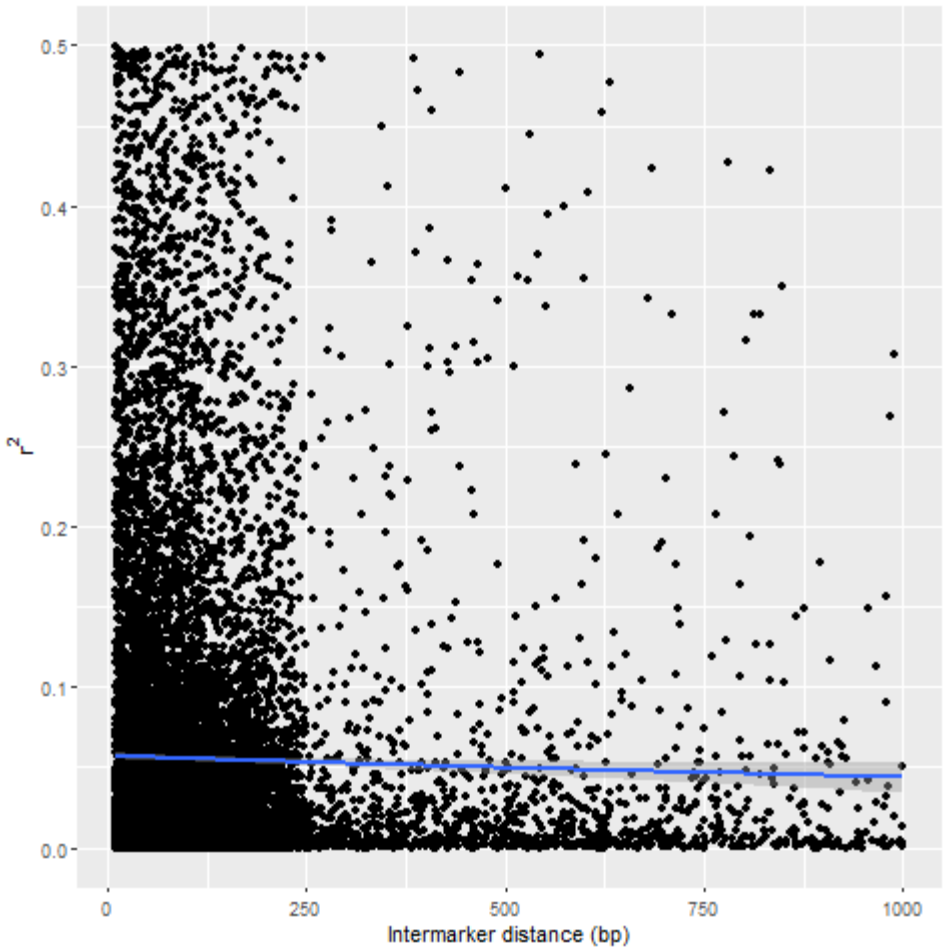

Figure 63 Linkage disequilibrium (r^2) decay over 1 kb in 73 diploid rose cultivars. Line reflects linkage disequilibrium decay over distance and is calculated with the generalized additive model (GAM).

V.4.2 Population structure and genetic diversity

Based upon the ΔK value from STRUCTURE, there were two subpopulations within the 73 cultivars (Fig. 64). There was, however, good support for K = 6. ADMIXTURE CV error was minimized at K = 5 (Fig. 65), further supporting the possibility of more than two subpopulations.

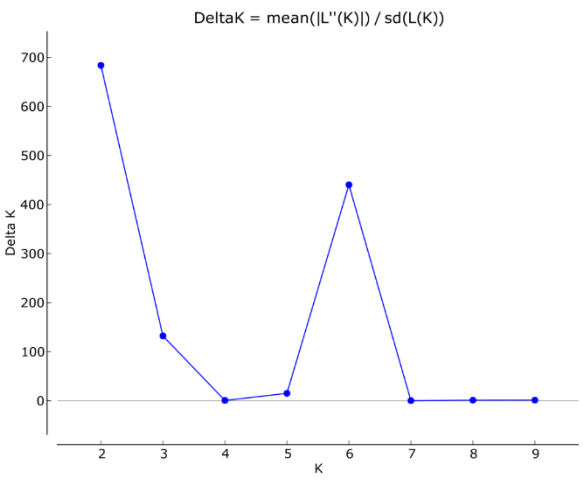

Figure 64 Population substructure in 73 diploid rose cultivars as estimated by STRUCTURE. K = number of subpopulations. The highest Delta K value indicates the most likely number of subpopulations.

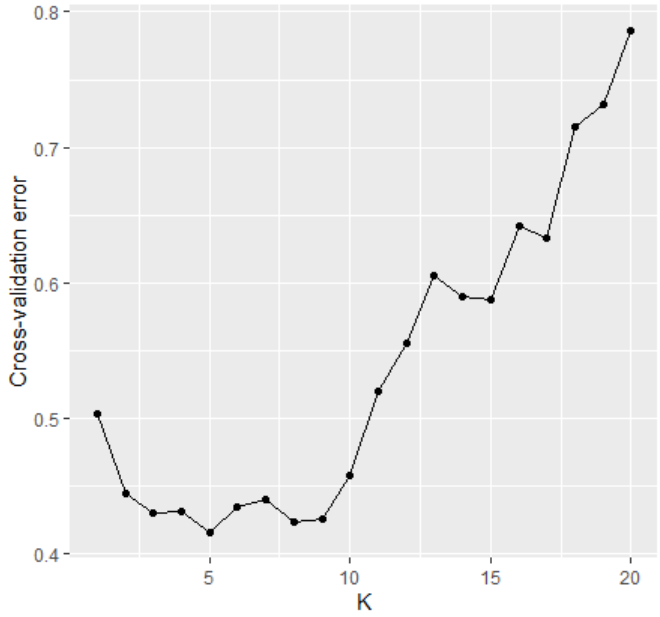

Figure 65 Population substructure in 73 diploid rose cultivars as estimated by ADMIXTURE. K = number of subpopulations. The lowest cross-validation error indicates the most likely number of subpopulations.

STRUCTURE at K = 2 (STRUCT2) identified two major groups of 40 and 24 genotypes with nine admixed individuals (Table 7, Fig. 6). The larger group is defined primarily by China and tea roses, but the smaller group is initially less clearly identifiable, being a mix of polyantha, *Rosa multiflora* Thunb. ex Murr. hybrids, and various other species hybrids. *Rosa polyantha* Sieb et Zucc., however, derives from *R. multiflora* (Cairns, 2000), and many of the other genotypes also include *R. multiflora* in their pedigrees. Thus, STRUCT2 indicates a Tea/China subpopulation and a Multiflora subpopulation. This understanding sheds some light on the admixed individuals. Several of them contain both tea/China roses and *R. multiflora* in their immediate ancestry. One, 'Leontine Gervais', is a hybrid between the species *Rosa luciae* Franch. & Rochebr. and a China rose (Cairns, 2000). The admixed genotypes, however, only make up ~12% of the total genotypes.

The Tea/China and Multiflora distinction is maintained, to an extent, in the STRUCTURE at K = 6 (STRUCT6) and ADMIXTURE at K = 5 (ADMIX5) results (Table 59, Fig. 6). The largest groups for both STRUCT6 and ADMIX5 are defined by tea roses and multiflora roses. A core set of 23 genotypes are common to the Tea/China group across all three K-values. Similarly, 21 genotypes are common to the Multiflora group across all three K-values. Both STRUCT6 and ADMIX5 separate several of the China genotypes from the Tea/China group, including 'Old Blush', which is often considered the quintessential China rose (green-colored group). Likewise, both separate several hybrid musk/noisette type roses from the Tea/China group (yellow-colored group). The division of the Multiflora group is less consistent, however. For instance,

STRUCT6 considers admixed several Multiflora-group genotypes that ADMIX5 assigns fairly strongly to a unique population; on the other hand, both STRUCT6 and ADMIX5 parse out several hybrid *R. wichurana* genotypes from the Multiflora group. On the whole, however, both of the K>2 divisions provide additional details rather than directly contradicting STRUCT2.

Table 59 Subpopulation assignment for three population substructure estimates in 73 diploid rose cultivars. Genotypes are sorted by the subpopulation assignment of STRUCT2. ADMIX5 = 5 subpopulations as estimated by ADMIXTURE; STRUCT2 indicates 2 subpopulations as estimated by STRUCTURE; STRUCT6 indicates 6 subpopulations as estimated by STRUCTURE. 'Class' indicates primary horticultural class and is not necessarily indicative of ancestry. Red indicates the Tea/China group; blue indicates the Multiflora group; yellow indicates the musk/noisette group; green indicates the China group; orange indicates the hybrid wichurana/miscellaneous group; purple indicates a subpopulation comprised of only 'Pink Surprise'; gray indicates admixed (i.e., not belonging to a group with a probability >0.5 or >0.6 for K>2 or K = 2, respectively). Numbers indicate probability that each genotype belongs to the subpopulation.

Genotype	Abbreviation	Class	ADMIX5	STRUCT2	STRUCT6
Bon Silene	BON	Tea	1.00	1.00	1.00
Blumenschmidt	BT	Tea	1.00	1.00	1.00
Mademoiselle Franziska Kruger	MFK	Tea	1.00	1.00	1.00
Miss Lowe's Variety	MLV	China	1.00	1.00	1.00
Marie Van Houtte	MV	Tea	1.00	1.00	1.00
Safrano	SA	Tea	1.00	1.00	1.00
Climbing White Maman Cochet	WC	Tea	1.00	1.00	1.00
Monsieur Tillier	MT	Tea	1.00	1.00	0.99
General Schablikine	GS	Tea	1.00	1.00	0.99
Perle des Jardins	PJ	Tea	1.00	1.00	0.96
Marechal Niel (1864)	MNN	Noisette	0.95	1.00	0.94
Miss Caroline	MC	Tea	0.68	1.00	0.81
Madame Joseph Schwartz	MJ	Tea	0.68	1.00	0.80
Duchesse de Brabant	DCH	Tea	0.67	1.00	0.79
Le Vesuve (1825)	LU	China	0.80	1.00	0.78
Mrs. Bosanquet	MB	Bourbon	0.66	1.00	0.77

Table 59 Continued

Genotype	Abbreviation	Class	ADMIX5	STRUCT2	STRUCT6
Ducher	DU	China	0.62	1.00	0.76
Spice	SI	China	0.55	1.00	0.73
Celine Forestier	CF	Noisette		1.00	0.53
Independence Musk	IM	H. Musk	0.58	0.99	0.53
Jaune Desprez	JD	Noisette	0.51	0.99	0.51
Emmie Gray	EG	China	1.00	0.98	0.54
Mutabilis	MU	China	0.53	0.94	0.50
Old Blush	OB	China	1.00	0.92	0.56
Cecile Brunner	CB	Polyantha	0.56	0.91	0.56
Rouletii	ROU	China	1.00	0.91	0.58
Vincent Godsiff	VF	China	1.00	0.90	0.53
Fortunes Double Yellow	FY	China		0.86	0.56
Oakington Ruby	OR	Miniature	1.00	0.85	0.61
Mermaid (1917)	ME	H. Bracteata	0.61	0.82	0.59
Rosa moschata	RCH	Species	1.00	0.81	1.00
Bermuda's Kathleen	BK	China	0.52	0.81	
Happenstance	HA	H. Bracteata	0.59	0.81	0.57
Nastarana	NAS	H. Musk	0.63	0.80	0.51
Jeanne d'Arc (1848)	JA	Alba	0.66	0.77	0.58
Blush Noisette	BH	Noisette	0.64	0.75	0.55
Madame Laurette Messimy	MM	China	0.52	0.74	
Sunshine (1927)	SUN	Polyantha	0.64	0.69	0.64
Clotilde Soupert (1890)	CL	Polyantha		0.63	0.52
Borderer	BDR	Floribunda		0.60	0.53
Marjorie Fair	MJF	Polyantha	1.00	1.00	0.97
The Fairy	TFY	Polyantha	0.69	1.00	0.63
Petite Pink Scotch	PPS	H. Wichurana	0.52	1.00	0.52
Belinda	BE	H. Musk	0.97	1.00	0.93
Lavender Pink Parfait	LPP	H. Multiflora	1.00	1.00	0.92
Ballerina (1937)	BA	H. Musk	0.89	1.00	0.88
Robin Hood (1927)	RBH	H. Musk	0.84	1.00	0.84
The Gift	TG	Polyantha	0.86	1.00	0.76
Ma Paquerette	PQ	Polyantha	1.00	0.99	0.95
Jean Mermoz	JM	Polyantha	0.61	0.94	0.55

Table 59 Continued

Genotype	Abbreviation	Class	ADMIX5	STRUCT2	STRUCT6
Mozart (1936)	MZ	H. Musk	0.90	0.91	0.88
Porcelaine de Chine	PDC	H. Musk	0.58	0.88	0.65
Yesterday	Y	Polyantha	0.80	0.87	0.75
Violette	VT	H. Multiflora	0.77	0.87	0.70
Pink Grootendorst	PG	H. Rugosa	0.61	0.87	0.55
Phalaenopsis	PA	Floribunda	0.72	0.86	0.71
Windchimes	WI	H. Musk	0.83	0.84	0.81
Russelliana	RL	H. Multiflora	0.82	0.84	
Katharina Zeimet	KZ	Polyantha	0.83	0.83	0.79
Veilchenblau	VB	H. Multiflora	0.69	0.81	0.63
Red Drift	RD	Shrub		0.75	
Trier	TI	H. Multiflora	0.72	0.72	0.70
Sarasota Spice	SAS	Noisette	0.51	0.71	
Gipsy Boy	GB	Bourbon	0.63	0.62	
Pink Surprise (1987)	PS	H. Bracteata	0.89		0.74
Republic of Texas	RT	Shrub	0.70		
Mevrouw Nathalie Nypels	MEV	Floribunda	0.54		0.53
La Marne	LM	Polyantha	0.51		0.50
Gardenia (1899)	GD	H. Wichurana	0.58		0.51
Moonlight (1913)	MO	H. Musk	0.52		0.50
Danae (1913)	DA	H. Musk	0.51		0.50
Plaisanterie	PL	H. Musk	0.57		
Leontine Gervais	LO	H. Wichurana	0.55		0.52

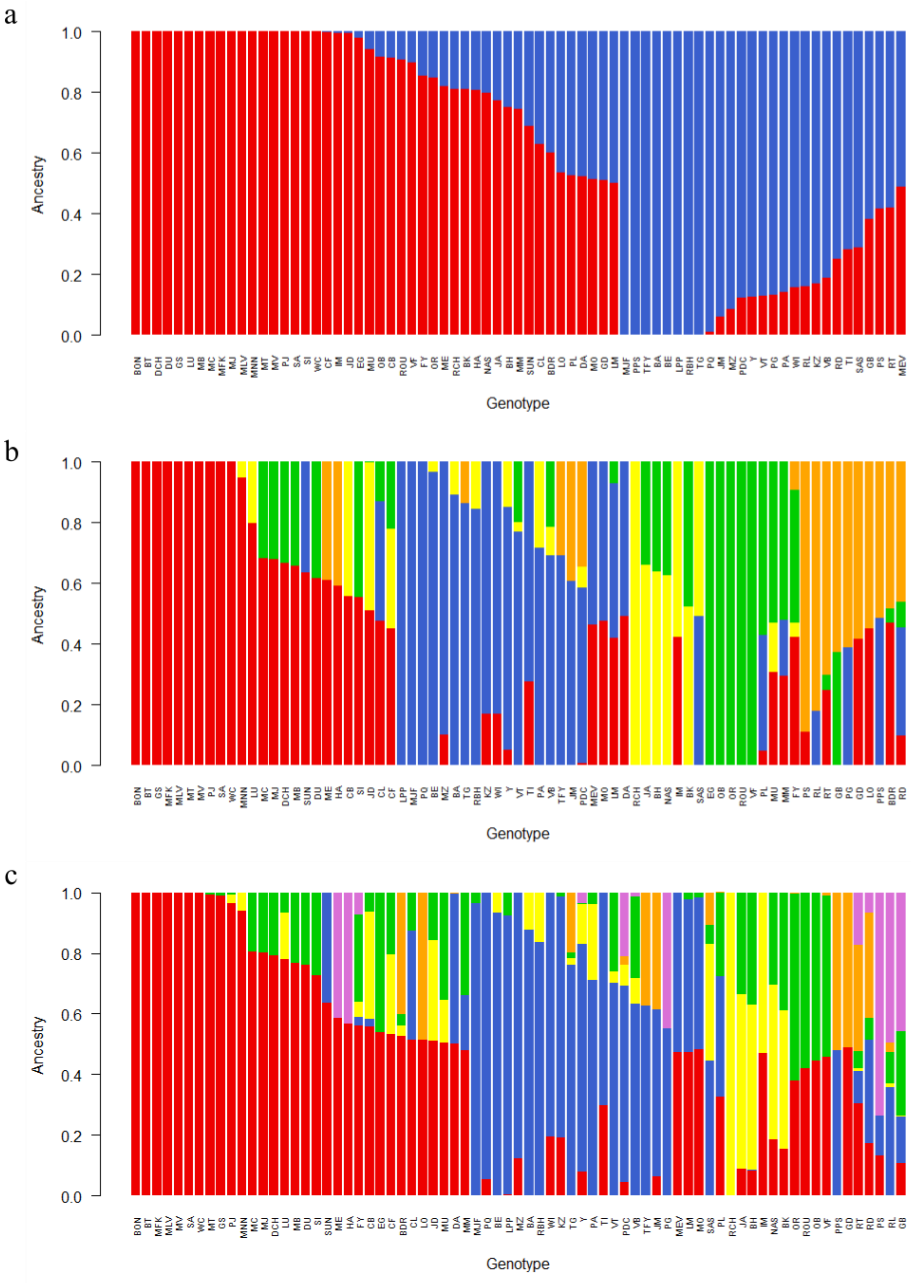

Figure 66 Comparison between three population substructure estimates in 73 diploid rose cultivars. (a) STRUCT2. (b) ADMIX5. (c) STRUCT6. Red indicates the Tea/China group; blue indicates the Multiflora group; yellow indicates the musk/noisette group; green indicates the China group; orange indicates the hybrid wichurana/miscellaneous group; purple indicates a subpopulation comprised of only 'Pink Surprise'.

The phylogenetic tree (Fig. 67) supports some aspects of the population structure findings. The two largest groups in the tree are consistent with the Tea/China subpopulation and the Multiflora subpopulation. While the bootstrap values for these branches are relatively low (50 and 63, respectively), the separation is reasonable in light of the STRUCT2 results and what is known of the pedigrees of these individuals. The separation of China and hybrid musk/noisette genotypes from the Tea/China group in ADMIX5 and STRUCT6 is reflected in the tree; however, ADMIX5's division encompasses the entire branch in each case, while STRUCT6 does not. Interestingly, while all three population structures assigned 'Pink Surprise' in a different way (admixed in STRUCT2, hybrid wichurana/miscellaneous group in ADMIX5, unique group in STRUCT6), the tree indicates a connection between 'Pink Surprise' and the hybrid bracteatas 'Mermaid' and 'Happenstance'. This was not observed in the population structure divisions, though it is consistent with the pedigree of record.

Figure 67 Comparison between three population substructure estimates and the phylogeny of 73 diploid rose cultivars. Numbers at branching points indicate bootstrap values. 'K' = number of subpopulations. Red indicates the Tea/China group; blue indicates the Multiflora group; yellow indicates the musk/noisette group; green indicates the China group; orange indicates the hybrid wichurana/miscellaneous group; purple indicates a subpopulation comprised of only 'Pink Surprise'; gray indicates admixed (i.e., not belonging to a group with a probability >0.5 or >0.6 for K>2 or K = 2, respectively).

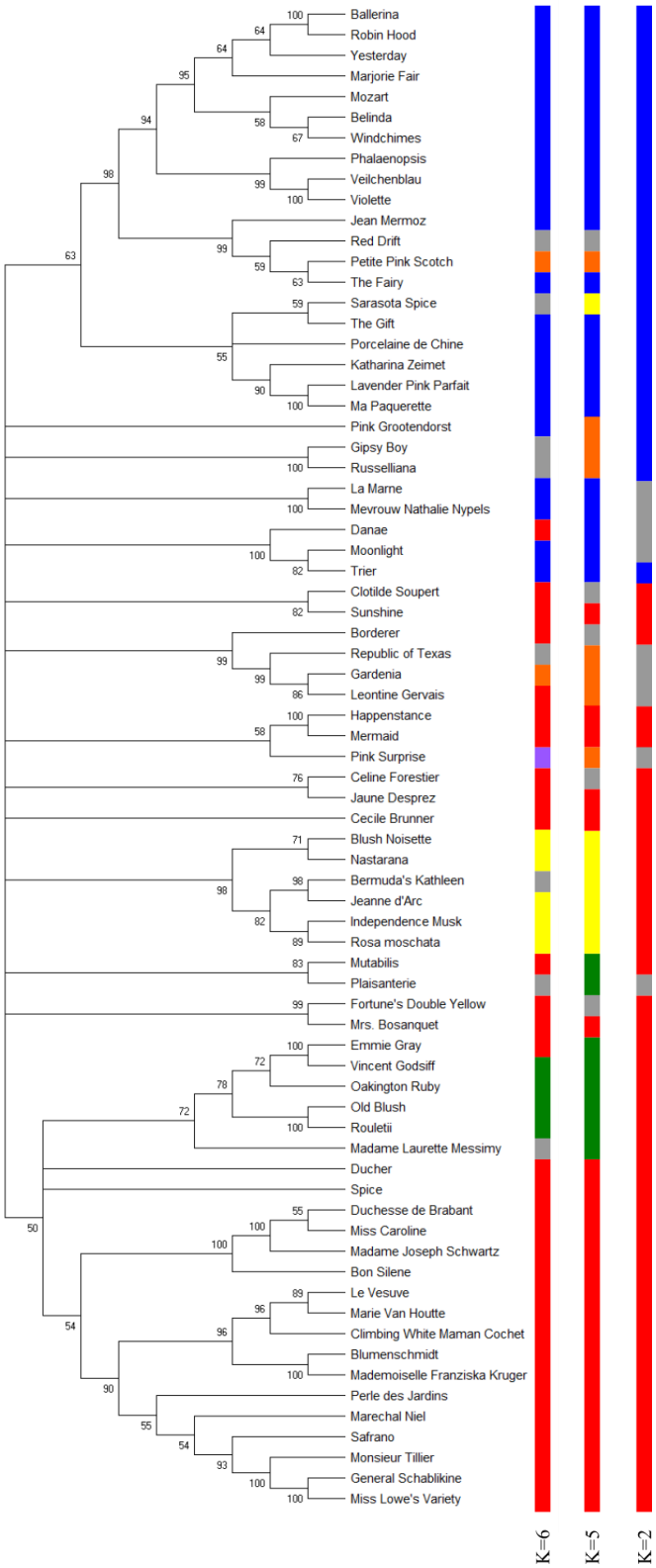
Ballerina
Robin Hood
Yesterday
Marjorie Fair
Mozart
Belinda
Windchimes
Phalaenopsis
Veilchenblau
Violette
Jean Mermoz
Red Drift
Petite Pink Scotch
The Fairy
Sarasota Spice
The Gift
Porcelaine de Chine
Katharina Zeimet
Lavender Pink Parfait
Ma Paquerette
Pink Grootendorst
Gipsy Boy
Russelliana
La Marne
Mevrouw Nathalie Nypels
Danae
Moonlight
Trier
Clotilde Soupert
Sunshine
Borderer
Republic of Texas
Gardenia
Leontine Gervais
Happenstance
Mermaid
Pink Surprise
Celine Forestier
Jaune Desprez
Cecile Brunner
Blush Noisette
Nastarana
Bermuda's Kathleen
Jeanne d'Arc
Independence Musk
Rosa moschata
Mutabilis
Plaisanterie
Fortune's Double Yellow
Mrs. Bosanquet
Emmie Gray
Vincent Godsiff
Oakington Ruby
Old Blush
Rouletii
Madame Laurette Messimy
Ducher
Spice
Duchesse de Brabant
Miss Caroline
Madame Joseph Schwartz
Bon Silene
Le Vesuve
Marie Van Houtte
Climbing White Maman Cochet
Blumenschmidt
Mademoiselle Franziska Kruger
Perle des Jardins
Marechal Niel
Safrano
Monsieur Tillier
General Schablikine
Miss Lowe's Variety
K=6
K=5
K=2

While there are 21 parent-progeny relationships and three sport (cultivars arising from the somatic mutation of another cultivar) pairs within the 73 genotypes of the study according to the pedigrees, KGD suggests that not all of these pedigrees may be accurate, as the kinship values are considerably lower than expected. Specifically, it appears that 'Perle des Jardins' is not the parent of 'Gardenia' and 'Rouletii' is not the parent of 'Porcelaine de Chine' (Table 60), as these kinship values are well below the theoretical value of 0.5 (Dodds et al., 2015). This absence of relationship is also supported by the phylogenetic tree. When these parent-progeny combinations were removed, the average parent-progeny kinship value was 0.53 with a standard deviation of 0.17. All other parent-progeny relationships had good support (data not shown). Of the three alleged sport pairs, only one, 'Mermaid'/'Happenstance' appears to be a true sport with a kinship value near to that of self-relatedness. The kinship values for the other pairs, 'Mademoiselle Franziska Kruger'/'Blumenschmidt' and 'Old Blush'/'Rouletii', are closer to that of parent-progeny or sibling relationships (Table 61). These pairs grouped closely together in the phylogenetic tree with bootstrap values of 100 although this does not necessarily indicate that they are identical. Finally, many other genotype pairs had kinship values that indicated kinship although the available pedigree information did not indicate relatedness (data not shown). Many of these relationships are compatible with the phylogenetic tree and population structure.

The KGD analysis identified unexpected relationships in the families (data not shown). All but one genotype from the family 'Lena' x *R. palustris* f. *plena* OB-ARE were shown to be off-types. Similarly, all but two genotypes from the family 'Ole' x *R.*

palustris f. *plena* EB-ARE were off-types. All genotypes from the family ‘Ole’ x *R. palustris* f. *plena* OB-ARE were identified as off-types. For all three of these families, the off-types showed a high degree of relatedness with both ‘Lena’ and ‘Ole’ (which are closely related), indicating that they may be selfs. These off-types were excluded from subsequent analyses. Furthermore, although *R. palustris* f. *plena* EB-ARE and OB-ARE should belong to section *Carolinae*, both accessions showed a high degree of relatedness (average 1.06) to ‘Old Blush’, which belongs to section *Indicae*. This supports the hypothesis that *R. palustris* f. *plena* may be at best a hybrid with *R. palustris* rather than a species form (J. Windham, personal communication) though it may be a selection from within *Indicae*.

Table 60 Kinship values of select parent-progeny relationships from 73 diploid rose cultivars. Values are estimated by the KGD method. Values for disproven parent-progeny relationships are in bold. The theoretical parent-child kinship value is 0.5. The average parent-progeny kinship value without these relationships is 0.53 with a standard deviation of 0.17.

	Gardenia (1899)	Porcelaine de Chine	Perle des Jardins	Rouletii
Gardenia (1899)				
Porcelaine de Chine	0.12			
Perle des Jardins	**0.11**	-0.10		
Rouletii	-0.05	**-0.05**	0.05	

Table 61 Kinship values of alleged sport relationships from 73 diploid rose cultivars. Values are estimated by the KGD method. Values for relevant relationships are in bold.

	Blumenschmidt	Happenstance	Mermaid (1917)	Mademoiselle Franziska Kruger	Old Blush	Rouletii
Blumenschmidt						
Happenstance	0.12					
Mermaid (1917)	0.15	**1.10**				
Mademoiselle Franziska Kruger	**0.54**	0.17	0.20			
Old Blush	0.13	-0.07	-0.05	0.14		
Rouletii	0.13	-0.10	-0.07	0.14	**0.50**	

V.4.3 Association mapping

V.4.3.1 Cultivar panel

Most traits had multiple models that fit equally well (data not shown). The models FarmCPU (PCA5), FarmCPU (PCA6), and MLM (Gtype+VanRaden) fit all traits reasonably well, and MLM (Gtype+VanRaden) was chosen as the final model.

In the cultivar panel, significant marker-trait associations were found for ADI, LDim, length, NPrimaries, and volume (Table 62), though not for any disease, defoliation, or flowering measures. Many associations were consistent over environments, including over the combined-winter and combined-seasons analyses. An exception to this was the single marker significant for apical dominance, which was only significant in the combined-winter analysis. This marker, chr06_50911143, explained 53% of the phenotypic variation. Two markers, both on chromosome 3, were associated with both LDim and length. One of them, chr03_32531179, was significantly associated with LDim in all environments. These two markers explained between 54% and 70% of

the phenotypic variation for LDim and length, depending on the environment considered. Multiple marker-trait associations were found for NPrimaries on chromosomes 3, 4, 5, and 7. The associations on chromosomes 3, 5, and 7 were only significant in one environment each, whereas the association on chromosome 4 was significant in all environments except 2018-S. This marker, chr04_57543705, explained 57% of the phenotypic variation in the combined-seasons analysis. Similarly, many significant marker-trait associations were found for volume on all chromosomes except 3 and 7. All were significant in at least two environments and all were significant in the combined-winters and combined-seasons analyses. These markers explained between 52 and 65% of the phenotypic variation for volume.

Due to the small size of the cultivar panel, however, these results must be interpreted with caution. Many genotype classes were represented by only one or two individuals (Table 63), meaning that the associations above are due to the influence of only a handful of cultivars. Specifically, associations for length and LDim in multiple seasons appear to be due entirely to the effects of ‘Gardenia’ and ‘Leontine Gervais’; volume in multiple seasons is due primarily to the effect of ‘Mermaid’; ADI is due primarily to the effect of ‘Oakington Ruby’ and ‘Petite Pink Scotch’; and NPrimaries is due primarily to the effect of ‘Petite Pink Scotch’. Thus, though the associations explained 50-70% of the phenotypic variation and were associated with significant differences in phenotypic means, these results must be interpreted in conjunction with the family analysis below.

Table 62 Significant marker-trait associations in 73 diploid rose cultivars for spring 2018 (2018-S), winter 2018 (2018-W), winter 2019 (2019-W), 2018 and 2019 winters combined (Winters), and all three seasons combined (Comb.). MAF = minor allele frequency, LOD = logarithm of the odds, R^2 = proportion of phenotypic variation explained by the marker. A LOD of 5 was used as the significance threshold.

			LOD per environment					R^2 per environment				
Trait	Marker	MAF	2018-S	2018-W	2019-W	Winters	Comb.	2018-S	2018-W	2019-W	Winters	Comb.
ADI	chr06_50911143	0.01				6.1					0.53	
LDim	chr03_27076869	0.03		6.0		5.4	5.5		0.66		0.59	0.60
	chr03_32531179	0.01	5.7	6.9	5.4	6.2	6.3	0.58	0.70	0.54	0.63	0.64
Length	chr03_27076869	0.03		6.0		5.2	5.4		0.66		0.58	0.59
	chr03_32531179	0.01	5.6	6.9		6.0	6.2	0.58	0.70		0.62	0.64
NPrimaries	chr03_34139226	0.02	5.2					0.54				
	chr04_57543705	0.08		5.3	5.6	5.9	5.8		0.54	0.49	0.56	0.57
	chr05_24876741	0.03			5.5	5.0				0.49	0.50	
	chr05_29686214	0.05	5.5					0.56				
	chr07_12989436	0.02	5.5					0.56				
Volume	chr01_23990571	0.03		5.9	5.4	6.0	5.9		0.55	0.53	0.58	0.57
	chr01_46639111	0.03		6.1	5.7	6.2	6.1		0.57	0.55	0.59	0.58
	chr02_7015157	0.03			5.3	5.2	5.1			0.53	0.53	0.52
	chr02_65955155	0.03		6.0	5.4	6.1	5.9		0.56	0.53	0.58	0.57
Volume	chr04_55543431	0.02		6.0	5.6	6.2	6.0		0.56	0.55	0.59	0.58
	chr05_2158693	0.03		6.9	6.4	7.1	6.9		0.62	0.60	0.65	0.64
	chr05_52346762	0.04		5.9		5.6	5.6		0.55		0.55	0.55
	chr05_74101141	0.05			5.3	5.2	5.1			0.53	0.53	0.52
	chr06_64689987	0.04			5.7	5.4	5.3			0.55	0.54	0.54

*Table 63 Phenotypic means and number of observations for each genotypic class from significant marker-trait associations in 73 diploid rose cultivars in multiple environments (Environ.): spring 2018 (2018-S), winter 2018 (2018-W), winter 2019 (2019-W), 2018 and 2019 winters combined (Winters), and all three seasons combined (Comb.). Means were tested for significant differences using an analysis of variance (ANOVA). ****, $p < 0.0001$.*

					Num. obs			Phenotypic mean			
Trait	Units	Environ.	Marker	Allele	AA	AB	BB	AA	AB	BB	Sig.
ADI	cm^{-1}	Winters	chr06_50911143	A/G	0	2	71		0.21	0.11	****
LDim	cm	2018-S	chr03_32531179	C/T	0	2	71		237.29	102.03	****
	cm	2018-W	chr03_27076869	A/G	70	0	2	178.96		643.40	****
	cm	2018-W	chr03_32531179	C/T	0	2	71		643.40	177.75	****
	cm	2019-W	chr03_32531179	C/T	0	2	71		569.19	174.89	****
	cm	Winters	chr03_27076869	A/G	70	0	2	176.68		630.68	****
	cm	Winters	chr03_32531179	C/T	0	2	71		630.68	175.42	****
	cm	Comb.	chr03_27076869	A/G	70	0	2	152.77		469.43	****
	cm	Comb.	chr03_32531179	C/T	0	2	71		469.43	151.92	****
Length	cm	2018-S	chr03_32531179	C/T	0	2	71		237.00	101.52	****
	cm	2018-W	chr03_27076869	A/G	70	0	2	178.86		643.38	****
	cm	2018-W	chr03_32531179	C/T	0	2	71		643.38	177.64	****
	cm	Winters	chr03_27076869	A/G	70	0	2	176.48		620.52	****
	cm	Winters	chr03_32531179	C/T	0	2	71		620.52	175.24	****
	cm	Comb.	chr03_27076869	A/G	70	0	2	152.44		463.52	****
	cm	Comb.	chr03_32531179	C/T	0	2	71		463.52	151.59	****
NPrimaries	Num.	2018-S	chr03_34139226	A/T	1	1	71	48.10	19.46	13.30	****
	Num.	2018-S	chr05_29686214	G/T	66	5	1	13.05	17.62	48.10	****
	Num.	2018-S	chr07_12989436	G/T	71	1	1	13.30	19.62	48.10	****
	Num.	2018-W	chr04_57543705	A/G	2	7	63	35.20	22.20	14.63	****
	Num.	2019-W	chr04_57543705	A/G	2	7	63	39.77	18.09	12.54	****
	Num.	2019-W	chr05_24876741	A/G	1	2	68	46.28	21.92	12.96	****
	Num.	Winters	chr04_57543705	A/G	2	7	63	40.84	20.90	13.34	****

Table 63 Continued

					Num. obs			Phenotypic mean			
Trait	Units	Environ.	Marker	Allele	AA	AB	BB	AA	AB	BB	Sig.
	Num.	Winters	chr05_24876741	A/G	1	2	68	44.47	24.14	13.98	****
	Num.	Comb.	chr04_57543705	A/G	2	7	63	38.69	19.67	13.14	****
Volume	m^3	2018-W	chr02_23990571	C/T	69	2	1	2.57	4.81	34.43	****
	m^3	2018-W	chr01_46639111	A/T	69	3	1	2.56	3.67	34.43	****
	m^3	2018-W	chr02_65955155	C/T	69	2	1	2.56	4.81	34.43	****
	m^3	2018-W	chr04_55543431	C/G	69	1	1	2.52	8.93	34.43	****
	m^3	2018-W	chr05_2158693	A/C	70	2	1	2.54	4.81	34.43	****
	m^3	2018-W	chr05_52346762	C/G	65	3	1	2.42	3.31	34.43	****
	m^3	2019-W	chr01_23990571	C/T	69	2	1	3.23	9.36	29.38	****
	m^3	2019-W	chr01_46639111	A/T	69	3	1	3.22	6.91	29.38	****
	m^3	2019-W	chr02_7015157	A/G	66	2	1	2.98	4.97	29.38	****
	m^3	2019-W	chr02_65955155	C/T	69	2	1	3.23	9.36	29.38	****
	m^3	2019-W	chr04_55543431	C/G	69	1	1	3.17	18.07	29.38	****
	m^3	2019-W	chr05_2158693	A/C	70	2	1	3.20	9.36	29.38	****
	m^3	2019-W	chr05_74101141	C/T	66	3	2	3.20	2.08	23.73	****
	m^3	2019-W	chr06_64689987	A/C	63	1	2	2.96	0.66	23.73	****
	m^3	Winters	chr01_23990571	C/T	69	2	1	2.86	7.61	33.62	****
	m^3	Winters	chr01_46639111	A/T	69	3	1	2.85	5.59	33.62	****
	m^3	Winters	chr02_7015157	A/G	66	2	1	2.65	4.73	33.62	****
	m^3	Winters	chr02_65955155	C/T	69	2	1	2.86	7.61	33.62	****
	m^3	Winters	chr04_55543431	C/G	69	1	1	2.80	14.84	33.62	****
	m^3	Winters	chr05_2158693	A/C	70	2	1	2.84	7.61	33.62	****
	m^3	Winters	chr05_52346762	C/G	65	3	1	2.75	5.17	33.62	****

Table 63 Continued

					Num. obs			Phenotypic mean			
Trait	Units	Environ.	Marker	Allele	AA	AB	BB	AA	AB	BB	Sig.
	m^3	Winters	chr05_74101141	C/T	66	3	2	2.84	1.63	24.23	****
	m^3	Winters	chr06_64689987	A/C	63	1	2	2.62	0.37	24.23	****
	m^3	Comb.	chr01_23990571	C/T	69	2	1	2.16	4.92	19.39	****
	m^3	Comb.	chr01_46639111	A/T	69	3	1	2.15	3.74	19.39	****
	m^3	Comb.	chr02_7015157	A/G	66	2	1	2.04	3.24	19.39	****
	m^3	Comb.	chr02_65955155	C/T	69	2	1	2.16	4.92	19.39	****
	m^3	Comb.	chr04_55543431	C/G	69	1	1	2.13	9.11	19.39	****
	m^3	Comb.	chr05_2158693	A/C	70	2	1	2.14	4.92	19.39	****
	m^3	Comb.	chr05_52346762	C/G	65	3	1	2.09	3.49	19.39	****
	m^3	Comb.	chr05_74101141	C/T	66	3	2	2.14	1.47	14.25	****
	m^3	Comb.	chr06_64689987	A/C	63	1	2	2.02	0.73	14.25	****

V.4.3.2 Families

Most traits had multiple models that fit equally well (data not shown), but only FarmCPU (PCA5) fit all traits. Thus, this model was initially used for all traits, most of which had significant marker-trait associations. Due to the high number of marker-trait associations, this study focused on genomic regions spanning 5-10 Mbp, termed clusters, that had high concentrations of marker-trait associations. A cluster could be comprised of multiple associations for the same trait in the same or different environments or of multiple associations for highly correlated traits (i.e., plant vigor traits) in the same or different environments. A cluster could also include multiple associations for the same trait summarized in different ways (i.e., ls means, AUDPC, and maximum score), or associations for the same trait across different flowering types. While marker-trait associations not occurring in clusters may still be real associations, clusters were deemed to be of particular interest for downstream analysis.

BS measures had marker-trait associations on all chromosomes (Table 64, Fig. 68). Three clusters of significant marker-trait associations were observed, however (Table 65). The first (BS 1) was from approximately 64 to 72 Mbp on chromosome 2 and included associations from 2018-CS, 2019-OV, and the combined-environments analysis. Most of the markers in this cluster explained only 1-2% of the phenotypic variation with the exception of chr02_64089392, which had an R^2 of 0.37. A cluster on chromosome 3 (BS 2) from approximately 43 to 46 Mbp likewise included associations from 2018-CS, 2019-OV, and the combined-environments analysis. Two markers in this cluster, chr03_42864258 and chr03_42864279, each explained 65% of the phenotypic

variation. The third cluster (BS 3) encompassed the 58-66 Mbp region of chromosome 6 and included associations from 2018-CS and 2019-OV. While most of the markers in BS 3 explained 3% or less of the phenotypic variation, chr06_58256136 and chr06_58612618 explained 54 and 18%, respectively.

Table 64 Significant marker-trait associations for black spot (BS), cercospora leaf spot (CLS), and defoliation (DEF) in eight diploid rose families in College Station, TX in 2018 (2018-CS), Overton, TX in 2019 (2019-OV), and combined year-locations (Comb.). Traits were summarized with least square means (BS, CLS, DEF), area under the disease progress curve (BS_AUDPC, CLS_AUDPC), and maximum values (BS_Max, CLS_Max, DEF_Max). Chr. = chromosome, MAF = minor allele frequency, LOD = logarithm of the odds. A LOD of 5 was used as the significance threshold.

					LOD per environment		
Trait	Marker	Chr.	Position	MAF	2018-CS	2019-OV	Comb.
BS	chr01_18812824	1	18812824	0.35			6.3
	chr01_29899030	1	29899030	0.02	5.0		
	chr02_42306276	2	42306276	0.21		19.8	
	chr02_64089392	2	64089392	0.34		8.4	
	chr02_67440445	2	67440445	0.01	9.2		9.9
	chr02_72315206	2	72315206	0.32			5.2
	chr02_72316791	2	72316791	0.32	6.1		
	chr03_16133530	3	16133530	0.29			5.3
	chr03_26216248	3	26216248	0.42		12.2	
	chr03_42864258	3	42864258	0.43		5.8	
	chr03_42864279	3	42864279	0.42		6.1	
	chr03_45571653	3	45571653	0.32			5.5
	chr03_45709227	3	45709227	0.24	5.5		
	chr04_25002782	4	25002782	0.14	7.8		
	chr04_42252514	4	42252514	0.04		6.8	
	chr04_45733652	4	45733652	0.42			5.6
	chr05_31237324	5	31237324	0.04			5.6
	chr05_44849987	5	44849987	0.20	7.3		
	chr05_52834935	5	52834935	0.35			8.4
	chr06_38202295	6	38202295	0.08		17.8	
	chr06_55787498	6	55787498	0.05			6.4
	chr06_58256136	6	58256136	0.24		10.4	

Table 64 Continued

Trait	Marker	Chr.	Position	MAF	LOD per environment		
					2018-CS	2019-OV	Comb.
	chr06_58612618	6	58612618	0.09		5.3	
	chr06_64212881	6	64212881	0.41	6.0		
	chr06_66058634	6	66058634	0.06		6.8	
	chr07_2400758	7	2400758	0.08		8.7	
	chr07_9514320	7	9514320	0.48		10.3	
	chr07_64926275	7	64926275	0.11		10.5	
BS_AUDPC	chr01_58788798	1	58788798	0.14		6.7	
	chr01_60420561	1	60420561	0.40		11.1	
	chr02_10321800	2	10321800	0.05		6.4	
	chr02_36074618	2	36074618	0.01		5.1	
	chr02_60383408	2	60383408	0.13		5.4	
	chr02_67440445	2	67440445	0.01	7.1		
	chr04_14707213	4	14707213	0.48		9.7	
	chr06_17640444	6	17640444	0.04	5.4		
	chr06_46575735	6	46575735	0.31		5.9	
	chr06_54584248	6	54584248	0.09		6.2	
	chr06_64212881	6	64212881	0.41	6.4		
BS_Max	chr02_5368417	2	5368417	0.42	5.4		
	chr02_26633116	2	26633116	0.20	5.2		
	chr03_15054375	3	15054375	0.32		5.5	
	chr06_50357303	6	50357303	0.12		9.4	
	chr06_63917472	6	63917472	0.47	10.5		
	chr07_19164802	7	19164802	0.06		5.5	
	chr07_30889068	7	30889068	0.17		9.8	
	chr07_66607015	7	66607015	0.26	5.4		
CLS	chr01_4832558	1	4832558	0.02	8.2		
	chr02_2004912	2	2004912	0.02	5.1		
	chr02_18593200	2	18593200	0.45	5.5		
	chr02_61961197	2	61961197	0.35	5.7		
	chr03_42935798	3	42935798	0.02	5.9		
	chr03_44488035	3	44488035	0.11		6.6	
	chr03_45708789	3	45708789	0.02		5.2	
	chr04_54994483	4	54994483	0.26	6.9		
	chr05_28744305	5	28744305	0.24	6.2		
	chr05_65387530	5	65387530	0.29		5.8	

Table 64 Continued

Trait	Marker	Chr.	Position	MAF	LOD per environment		
					2018-CS	2019-OV	Comb.
	chr06_39699180	6	39699180	0.38		6.0	
	chr06_46575723	6	46575723	0.28		8.4	
	chr07_14670151	7	14670151	0.42	7.6		
CLS_AUDPC	chr03_32413893	3	32413893	0.22	6.5		
	chr04_39712105	4	39712105	0.43	6.6		
	chr06_35611239	6	35611239	0.37	7.5		
	chr07_14873914	7	14873914	0.26	6.3		
CLS_Max	chr01_42156624	1	42156624	0.04		5.2	
	chr01_56362651	1	56362651	0.30		5.2	
	chr01_61767790	1	61767790	0.42		5.3	
	chr02_2004912	2	2004912	0.02	5.6		
	chr02_7538487	2	7538487	0.41	5.1		
	chr02_9416719	2	9416719	0.35		5.2	
	chr02_21732308	2	21732308	0.40		6.1	
	chr02_61187370	2	61187370	0.14		5.2	
	chr03_5292917	3	5292917	0.46	5.5		
	chr03_22894283	3	22894283	0.02		7.3	
	chr03_24652176	3	24652176	0.02		5.5	
	chr03_32413893	3	32413893	0.22	9.1		
	chr03_38508321	3	38508321	0.10		5.4	
	chr04_32585847	4	32585847	0.07	6.0		
	chr05_15387152	5	15387152	0.06		5.9	
	chr06_46575723	6	46575723	0.28		7.4	
	chr06_59655327	6	59655327	0.39		7.6	
	chr07_1662879	7	1662879	0.24	6.8		
	chr07_6190034	7	6190034	0.02		5.4	
DEF	chr01_18812714	1	18812714	0.30	8.1		
	chr01_44614998	1	44614998	0.12			5.2
	chr01_64389769	1	64389769	0.18			6.5
	chr02_6397050	2	6397050	0.07		5.2	
	chr02_63669639	2	63669639	0.12	5.2		
	chr02_75051828	2	75051828	0.02		5.6	
	chr03_28196728	3	28196728	0.37	15.2		
	chr03_30707689	3	30707689	0.33			6.2
	chr03_32413776	3	32413776	0.27			8.0
	chr03_37132029	3	37132029	0.47			5.6
	chr03_46391099	3	46391099	0.01	5.0		

Table 64 Continued

Trait	Marker	Chr.	Position	MAF	LOD per environment		
					2018-CS	2019-OV	Comb.
	chr05_27037450	5	27037450	0.41	5.4		
	chr05_76951469	5	76951469	0.03	5.1		
	chr06_11790348	6	11790348	0.45			6.6
	chr06_35227087	6	35227087	0.14	8.7		
	chr06_50112751	6	50112751	0.27			5.8
	chr06_53136875	6	53136875	0.10		7.7	
	chr07_11543159	7	11543159	0.24			6.1
	chr07_11845663	7	11845663	0.16		7.4	
	chr07_14556636	7	14556636	0.42			10.2
	chr07_15462015	7	15462015	0.05	6.5		
DEF_Max	chr01_43821789	1	43821789	0.09		7.9	
	chr01_64389899	1	64389899	0.16	5.2		
	chr02_15896752	2	15896752	0.26	5.3		
	chr02_23654625	2	23654625	0.26		7.4	
	chr03_28196632	3	28196632	0.39	7.6		
	chr03_32413776	3	32413776	0.27		9.5	
	chr05_48662503	5	48662503	0.30	6.2		
	chr05_71587331	5	71587331	0.21	5.7		
	chr07_18806136	7	18806136	0.33	7.0		
	chr07_55930466	7	55930466	0.03	8.4		

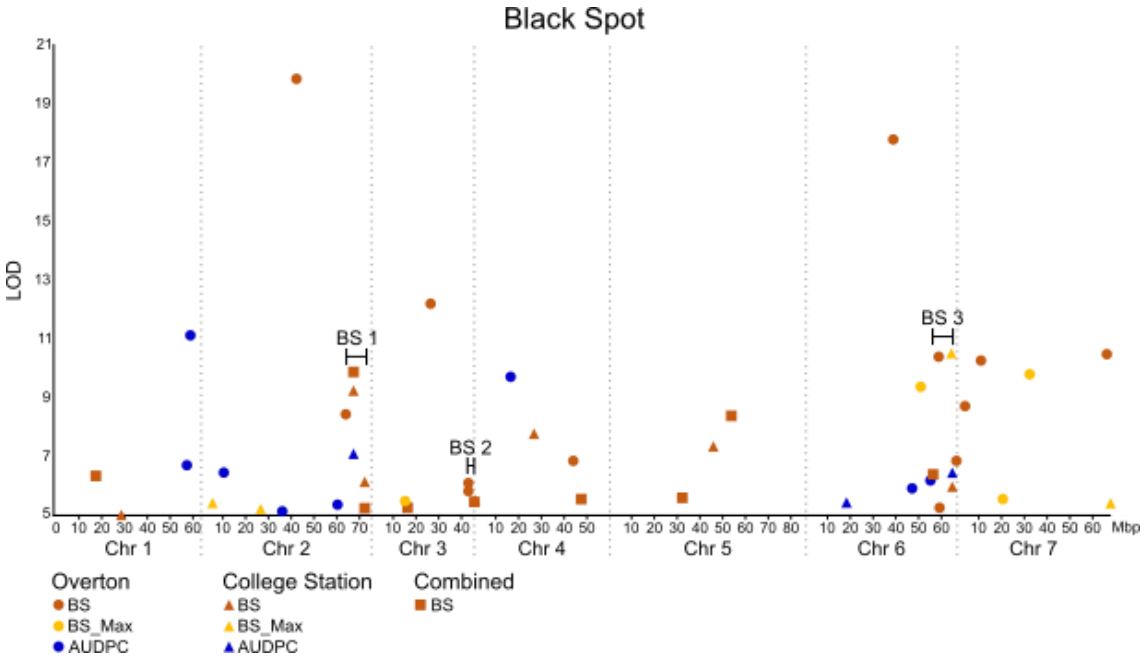

Figure 68 Overlaid Manhattan plots of significant marker-trait associations for black spot measures in College Station, TX in 2018 (2018-CS), Overton, TX in 2019 (2019-OV), and combined year-locations (Comb.) in eight diploid rose families. Black spot was summarized with least square means (BS), area under the disease progress curve (AUDPC), and maximum value (BS_Max). LOD = logarithm of the odds. Vertical lines indicate ends of chromosomes. Brackets indicate clusters of marker-trait associations. A LOD of 5 was used as the significance threshold.

Table 65 Genomic regions (Cluster) associated with flower intensity, black spot, cercospora leaf spot, and plant vigor in diploid rose families. Analyses were run separately for each flowering type (FlwgType, once-flowering (OF) and continuous flowering (CF)) for flower intensity and plant vigor. Flower intensity, black spot, and cercospora were assessed in College Station, TX in 2018 (2018-CS) and in Overton, TX in 2019 (2019-OV). 2018-CS and 2019-OV data were combined into one analysis in Comb. yr-locations. Flower intensity, black spot, and cercospora were summarized with least square means (FLI, BS, CLS), area (AFLIC, BS_AUDPC, CLS_AUDPC), and maximum values (FLI_Max, BS_Max, CLS_Max). Vigor traits were assessed in spring 2018 (2018-S) and winter 2018 (2018-W) in College Station, TX. 2018-S and 2018-W were combined into one analysis in Comb. yr-seasons. Height, length, width, longest dimension (LDim), and volume were considered vigor traits. 'Start' and 'End' indicate the position in base pairs of the first and last marker in a given cluster. R^2 indicates the proportion of phenotypic variation explained by a single marker.

							R^2 per environment					
Cluster	Chr.	Start	End	Traits	FlwgType	Marker	2018-S	2018-W	Comb. yr-seasons	2018-CS	2019-OV	Comb. yr-locations
FLI 1	2	32917842	32917909	FLI_Max	CF	chr02_32917842				0.03		
						chr02_32917909				0.09		
FLI 2	2	62161051	64842128	FLI	CF	chr02_62161051					0.15	
				AFLIC	CF	chr02_64842128					0.59	
				FLI_Max	CF	chr02_64698081				0.10		
FLI 3	4	5280553	9205067	AFLIC	CF	chr04_8506995					0.10	
				FLI_Max	CF	chr04_5280553				0.85		
						chr04_9205052				0.03		
						chr04_9205067				0.78		
FLI 4	4	41580898	46491727	FLI_Max	CF	chr04_41580898				0.12		
						chr04_41580910				0.11		
						chr04_46491687				0.03		
						chr04_46491727				0.03		
FLI 5	5	791715	791768	FLI_Max	CF	chr05_791715				0.03		
						chr05_791768				0.03		
BS 1	2	64089392	72316791	BS		chr02_64089392					0.37	
						chr02_67440445				0.01		0.01
						chr02_72315206						0.02

Table 65 Continued

Cluster	Chr.	Start	End	Traits	FlwgType	Marker	R^2 per environment					
							2018-S	2018-W	Comb. yr-seasons	2018-CS	2019-OV	Comb. yr-locations
						chr02_72316791				0.02		
				BS_AUDPC		chr02_67440445				0.003		
BS 2	3	42864258	45709227	BS		chr03_42864258					0.65	
						chr03_42864279					0.65	
						chr03_45571653						0.01
						chr03_45709227				0.01		
BS 3	6	58256136	66058634	BS		chr06_58256136					0.54	
						chr06_58612618					0.18	
						chr06_64212881				0.03		
						chr06_66058634					0.01	
				BS_AUDPC		chr06_64212881				0.0003		
				BS_Max		chr06_63917472				0.05		
CLS 1	2	2004912	9416719	CLS		chr02_2004912				0.0002		
				CLS_Max		chr02_2004912				0.02		
						chr02_7538487				0.01		
						chr02_9416719					0.09	
CLS 2	3	32413893	45708789	CLS		chr03_42935798				0.002		
						chr03_44488035					0.20	
						chr03_45708789					0.001	
				CLS_AUDPC		chr03_32413893				0.01		

Table 65 Continued

Cluster	Chr.	Start	End	Traits	FlwgType	Marker	R^2 per environment					
							2018-S	2018-W	Comb. yr-seasons	2018-CS	2019-OV	Comb. yr-locations
				CLS_Max		chr03_32413893				0.005		
						chr03_38508321					0.19	
CLS 3	6	35611239	46575723	CLS		chr06_39699180					0.01	
						chr06_46575723					0.0001	
				CLS_ AUDPC		chr06_35611239				0.08		
				CLS_Max		chr06_46575723					0.001	
Vigor 1	1	55173851	64419951	Height	CF	chr01_57213102			0.07			
						chr01_57245697			0.06			
				Height	OF	chr01_56298735		0.1	0.08			
						chr01_60277909			0.03			
						chr01_64419951			0.07			
				Length	OF	chr01_57180307	0.07					
				Width	CF	chr01_57980644		0.005				
						chr01_59761205		0.04				
				Width	OF	chr01_55198318			0.001			
						chr01_59594088		0.02				
				LDim	CF	chr01_60174454			0.01			
						chr01_58014993	0.02					
						chr01_64419847	0.001					
				Volume	CF	chr01_59761205		0.1	0.25			
				Volume	OF	chr01_55173851		0.2				
						chr01_62032017		0.1				
Vigor 2	2	46445953	55999281	Height	CF	chr02_52856512		0.1				

Table 65 Continued

Cluster	Chr.	Start	End	Traits	FlwgType	Marker	R^2 per environment					
							2018-S	2018-W	Comb. yr-seasons	2018-CS	2019-OV	Comb. yr-locations
				Height	OF	chr02_49406894		0.05				
				Length	CF	chr02_46445953			0.16			
						chr02_53575455			0.11			
				Length	OF	chr02_55288059		0.01				
				Width	CF	chr02_51140600			0.09			
				Width	OF	chr02_50240388	0.003					
						chr02_55999271			0.05			
				LDim	CF	chr02_46445953		0.2				
				LDim	OF	chr02_55999281		0.1	0.16			
				Volume	CF	chr02_54644667			0.02			
Vigor 3	2	70741591	72596610	Length	OF	chr02_70741591	0.41					
				Width	OF	chr02_72213994		0.03				
						chr02_72315287			0.03			
				LDim	OF	chr02_70741591	0.41					
						chr02_72596610			0.01			
Vigor 4	3	27333946	36062671	Length	CF	chr03_28196647			0.16			
						chr03_32497673	0.40					
						chr03_36062671	0.04					
				Width	CF	chr03_27333946			0.08			
						chr03_36062671		0.04				
				LDim	CF	chr03_28181482			0.12			
						chr03_32497673		0.40				
						chr03_36062671		0.04				
				Volume	CF	chr03_31563795			0.33			

Table 65 Continued

Cluster	Chr.	Start	End	Traits	FlwgType	Marker	R^2 per environment					
							2018-S	2018-W	Comb. yr-seasons	2018-CS	2019-OV	Comb. yr-locations
						chr03_36062671		0.001				
Vigor 5	3	42103736	42933515	Length	CF	chr03_42103736			0.05			
						chr03_42933515		0.1				
				Width	CF	chr03_42103736		0.1				
				LDim	CF	chr03_42933515		0.1				
				Volume	CF	chr03_42103736		0.04				
Vigor 6	4	53789486	58007999	LDim	OF	chr04_54976573		0.1	0.04			
				Volume	OF	chr04_53789486		0.01				
						chr04_58007989			0.02			
						chr04_58007999		0.01				
Vigor 7	5	176358	7757177	Height	CF	chr05_7757177		0.1	0.07			
				Length	CF	chr05_176358			0.003			
						chr05_2761965		0.05				
				LDim	CF	chr05_2174967			0.03			
						chr05_2761965		0.05				
				Volume	CF	chr05_3858006		0.05				
Vigor 8	5	82463436	85600362	Width	OF	chr05_85463559	0.08					
						chr05_85600362			0.36			
				Volume	OF	chr05_82463436			0.12			
Vigor 9	6	51821545	52890285	Width	OF	chr06_51821545			0.03			
						chr06_52890285	0.01					
				Volume	OF	chr06_52890265	0.01					
Vigor 10	7	34140989	35307487	Length	OF	chr07_34140989		0.00				
				Width	OF	chr07_35307487		0.05				

Table 65 Continued

Cluster	Chr.	Start	End	Traits	FlwgType	Marker	R^2 per environment					
							2018-S	2018-W	Comb. yr-seasons	2018-CS	2019-OV	Comb. yr-locations
				Volume	OF	chr07_35307487		0.01				

CLS measures likewise had marker-trait associations on all chromosomes (Table 64, Fig. 69) and three main clusters of associations were observed on chromosomes 2, 3, and 6 (Table 65). All three clusters included associations from both year-locations; no significant associations were found for the combined-environments analysis. On chromosome 2, the cluster CLS 1 spanned the 2-9 Mbp region. No marker in this cluster explained more than 2% of the phenotypic variation. The chromosome 3 cluster, CLS 2, partially overlapped with the BS cluster on chromosome 3. In this cluster, chr03_44488035 explained the greatest amount of phenotypic variation (20%). The chromosome 6 cluster, CLS 3, did not overlap with the BS cluster, covering the 36-47 Mbp region instead. The most phenotypic variation explained by a marker in this cluster was 8% (chr06_35611239).

Defoliation had significant marker-trait associations on all chromosomes except chromosome 4; however, two clusters of associations were prominent (Table 64). The first spanned the 28-32 Mbp region of chromosome 3 and included associations from both year-locations and the combined analysis. The second covered the 11-19 Mbp region of chromosome 7. While these clusters do not overlap with the disease clusters described above, two individual associations did fall within the disease clusters. Chr03_46391099 was associated with DEF in 2018-CS and fell within the BS 2/CLS 2 cluster. The association of chr02_6397050 with DEF in 2019-OV fell within the CLS 1 cluster.

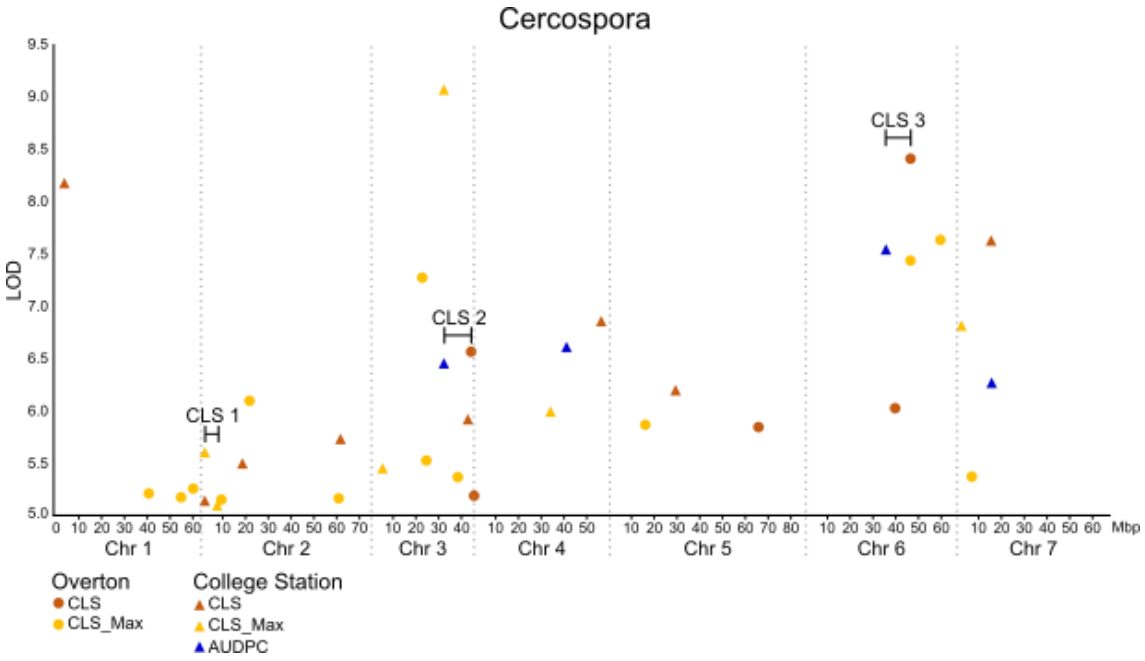

Figure 69 Overlaid Manhattan plots of significant marker-trait associations for cercospora leaf spot measures in College Station, TX in 2018 (2018-CS) and Overton, TX in 2019 (2019-OV) in eight diploid rose families. No significant associations were found for the combined environments. Cercospora was summarized with least square means (CLS), area under the disease progress curve (AUDPC), and maximum value (CLS_Max). LOD = logarithm of the odds. Brackets indicate clusters of marker-trait associations. Vertical lines indicate ends of chromosomes. A LOD of 5 was used as the significance threshold.

Flowering traits (AFLIC, FLI ls means, FLI_Max, and FlwgType) had significant marker-trait associations on all chromosomes (data not shown). Three markers spanning 117 bp on chromosome 3 (chr03_32413776, chr03_32413888, chr03_32413893) were significant for multiple traits in multiple environments and frequently had LOD scores of >10. These markers overlapped with the BS 2/CLS 2 cluster. Chr03_32413776 was also associated with defoliation. While many other associations were present, those in the 32 Mbp region of chromosome 3 had the highest LOD scores by far and eclipsed the other

signals. This region is the approximate location of the continuous flowering gene *RoKSN* (Hibrand Saint-Oyant et al., 2018).

All architecture traits had significant associations in the 27-34 Mbp region of chromosome 3 (i.e., in the vicinity of *RoKSN*). As the abundant associations in this area tended to drown out associations elsewhere in the genome, and architecture traits can vary between flowering types (see Chapter III), the single-marker analysis of architecture and flowering traits was modified to take flowering type into account.

V.4.3.2.1 Flowering type split analysis

A model using FlwgType as a covariate did not fit the data well based on visual assessment of the QQ plots; therefore, the data was split by FlwgType and two separate analyses performed. For the CF types, the model FarmCPU (PCA1) was used; for the OF types, the model FarmCPU (PCA4) was used.

In OF types, associations for flower intensity were found on all chromosomes (Table 66). One marker was common between FLI and FLI_Max (chr02_42306276). As OF types only bloomed in 2019-OV and would not be expected to bloom throughout the season anyhow, the usefulness of FLI as a trait in OF types is limited.

Table 66 Significant marker-trait associations for flower intensity in once-flowering genotypes from diploid rose families in Overton, TX in 2019 (2019-OV) and combined year-locations (Comb.). No flowering occurred in College Station, TX in 2018. Flower intensity was summarized with least square means (FLI), area under the disease progress curve (AFLIC), and maximum values (FLI_Max). Chr. = chromosome, MAF = minor allele frequency, LOD = logarithm of the odds. A LOD of 5 was used as the significance threshold.

					LOD per environment	
Trait	Marker	Chr.	Position	MAF	2019-OV	Comb.
FLI	chr01_59513365	1	59513365	0.01		5.9
	chr02_19501323	2	19501323	0.16		5.5
	chr02_42306276	2	42306276	0.25	7.2	
	chr02_69761274	2	69761274	0.02		5.4
	chr03_8235661	3	8235661	0.23		6.3
	chr03_39518309	3	39518309	0.02	6.2	
	chr05_13050736	5	13050736	0.02	6.9	
	chr06_10400751	6	10400751	0.34	5.5	
	chr06_61807468	6	61807468	0.13	8.9	
	chr07_18806077	7	18806077	0.34	5.0	
	chr07_45675031	7	45675031	0.01	6.7	
AFLIC	chr01_20074477	1	20074477	0.01	9.6	
	chr04_48298754	4	48298754	0.05	7.4	
	chr07_1962840	7	1962840	0.09	6.6	
FLI_Max	chr02_42306276	2	42306276	0.25	6.4	
	chr05_58116918	5	58116918	0.02	7.1	
	chr07_2400758	7	2400758	0.11	9.1	
	chr07_10047556	7	10047556	0.02	6.4	

In CF types, associations for flower intensity were also found on all chromosomes (Table 67, Fig. 70). Several small clusters of FLI associations were observed over year-locations and the three measures of FLI (ls means, AFLIC, and FLI_Max), however (Table 65). Two of these, FLI 1 and FLI 2 respectively, were on chromosome 2 at approximately 33 Mbp (2018-CS only) and 64 Mbp (2018-CS and 2019-OV). In FLI 1, no marker explained more than 10% of the phenotypic variation. In FLI 2, chr02_64842129 explained 59% of the phenotypic variation. Two clusters were

also observed on chromosome 4. FLI3 was at 5-9 Mbp (2018-CS and 2019-OV); two markers in this cluster, chr04_5280553 and chr04_9205067, explained 85 and 78% of the phenotypic variation, respectively. FLI 4 was at 41-46 Mbp (2018-CS only) and the markers in this cluster explained between 3 and 12% of the phenotypic variation. Finally, two markers at approximately 792 kb on chromosome 5 were associated with FLI_Max in 2018-CS (FLI 5), though each only explained 3% of the phenotypic variation.

Table 67 Significant marker-trait associations for flower intensity in continuous flowering genotypes from diploid rose families in College Station, TX in 2018 (2018-CS), Overton, TX in 2019 (2019-OV), and combined year-locations (Comb.). Flower intensity was summarized with least square means (FLI), area under the disease progress curve (AFLIC), and maximum values (FLI_Max). Chr. = chromosome, MAF = minor allele frequency, LOD = logarithm of the odds. A LOD of 5 was used as the significance threshold.

					LOD per environment		
Trait	Marker	Chr.	Position	MAF	2018-CS	2019-OV	Comb.
FLI	chr01_56735535	1	56735535	0.14			6.0
	chr02_12196094	2	12196094	0.34			5.2
	chr02_29780438	2	29780438	0.33		5.5	
	chr02_47221463	2	47221463	0.04			8.0
	chr02_62161051	2	62161051	0.02		5.3	
	chr02_70324204	2	70324204	0.19			5.4
	chr03_29610671	3	29610671	0.01			9.3
	chr05_36656412	5	36656412	0.31		12.3	
	chr06_11790307	6	11790307	0.30			8.6
	chr07_53961302	7	53961302	0.23		5.3	
AFLIC	chr02_64842128	2	64842128	0.34		15.5	
	chr03_29610671	3	29610671	0.01		6.3	
	chr04_8506995	4	8506995	0.32		8.4	
	chr04_11949335	4	11949335	0.01		5.8	
	chr05_24321254	5	24321254	0.12		6.7	
	chr07_52108249	7	52108249	0.12		5.4	
FLI_Max	chr01_497117	1	497117	0.003	35.1		
	chr02_6162200	2	6162200	0.003	7.8		

Table 67 Continued

					LOD per environment		
Trait	Marker	Chr.	Position	MAF	2018-CS	2019-OV	Comb.
	chr02_9022512	2	9022512	0.01	6.4		
	chr02_32917842	2	32917842	0.003	7.8		
	chr02_32917909	2	32917909	0.02	6.0		
	chr02_53879167	2	53879167	0.47	5.8		
	chr02_64698081	2	64698081	0.03	28.8		
	chr04_5280553	4	5280553	0.20	6.2		
	chr04_9205052	4	9205052	0.003	7.8		
	chr04_9205067	4	9205067	0.22	5.3		
	chr04_24488671	4	24488671	0.47	17.2		
	chr04_41580898	4	41580898	0.02	5.2		
	chr04_41580910	4	41580910	0.02	5.2		
	chr04_46491687	4	46491687	0.01	7.8		
	chr04_46491727	4	46491727	0.01	7.8		
	chr04_51431469	4	51431469	0.003	7.8		
	chr04_56435699	4	56435699	0.01	8.6		
	chr05_791715	5	791715	0.01	10.5		
	chr05_791768	5	791768	0.01	6.5		
	chr05_10381939	5	10381939	0.01	6.4		
	chr05_70025827	5	70025827	0.44	6.4		
	chr06_46575572	6	46575572	0.003	7.8		
	chr07_152381	7	152381	0.01	5.0		

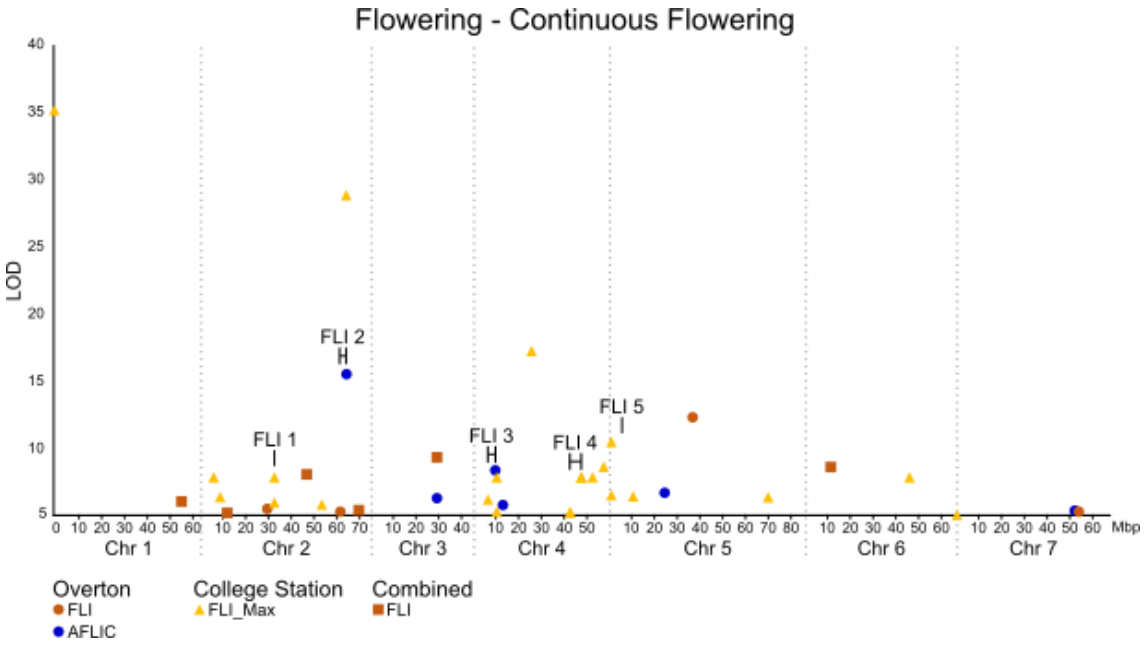

Figure 70 Overlaid Manhattan plots of significant marker-trait associations for flower intensity in continuous flowering genotypes from diploid rose families in College Station, TX in 2018 (2018-CS), Overton, TX in 2019 (2019-OV), and combined year-locations (Comb.). Flower intensity was summarized with least square means (FLI), area under the disease progress curve (AFLIC), and maximum values (FLI_Max). LOD = logarithm of the odds. Brackets indicate clusters of marker-trait associations. Vertical lines indicate ends of chromosomes. A LOD of 5 was used as the significance threshold.

In OF types, all plant vigor traits (height, length, width, LDim, and volume) had significant marker-trait associations in one or both seasons (Table 68, Fig. 71). While associations between individual traits and markers were rarely constant over seasons or the combined-season analysis, several clusters associated with multiple vigor traits were observed (Table 65). Significant associations for all plant vigor traits were observed on chromosome 1 from approximately 55 to 65 Mbp (Vigor 1). The strongest association in this region was between height and marker chr01_56298735 with a LOD of 17.7 in the combined-seasons analysis; however, this marker only explained 8% of the phenotypic variation for height. Two regions on chromosome 2, one from approximately 49 to 56

Mbp (Vigor 2) and the second from 70 to 72 Mbp (Vigor 3), were associated with height, width, length, and LDim. Most of the markers in Vigor 2 explained 10% or less of the variation in a trait, with the exception of chr02_55999281 (16%, LDim). Associations for volume and LDim were found from 54 to 58 Mbp on chromosome 4 (Vigor 6), though no marker explained more than 10% of the phenotypic variation. Associations for volume and width clustered in the 82-86 Mbp region of chromosome 5 (Vigor 8), including an association with a LOD of 42.8 for width. This marker, chr05_85600362, explained 36% of the phenotypic variation. Smaller clusters were also found on chromosomes 6 and 7 (Vigor 9, Vigor 10). Associations were found on chromosome 3 but did not form a prominent cluster.

Table 68 Significant marker-trait associations for plant vigor traits in once-flowering genotypes from diploid rose families in spring 2018 (2018-S), winter 2018 (2018-W), and combined seasons (Comb.). LDim indicates longest plant dimension. Chr. = chromosome, MAF = minor allele frequency, LOD = logarithm of the odds. A LOD of 5 was used as the significance threshold.

					LOD per environment		
Trait	Marker	Chr.	Position	MAF	2018-S	2018-W	Comb.
Height	chr01_38783628	1	38783628	0.01			5.1
	chr01_44466682	1	44466682	0.04		7.5	
	chr01_56298735	1	56298735	0.01		15.0	17.7
	chr01_60277909	1	60277909	0.21			6.4
	chr01_64419951	1	64419951	0.05			5.1
	chr02_8783653	2	8783653	0.12			9.2
	chr02_49406894	2	49406894	0.11		5.1	
	chr03_44142901	3	44142901	0.37		6.4	
	chr05_45290420	5	45290420	0.27		10.0	8.1
	chr05_60788679	5	60788679	0.44		5.3	
	chr05_63105625	5	63105625	0.39			5.7
	chr06_19193498	6	19193498	0.28		7.1	
Length	chr01_30483771	1	30483771	0.12	6.0		

Table 68 Continued

					LOD per environment		
Trait	Marker	Chr.	Position	MAF	2018-S	2018-W	Comb.
	chr01_39194536	1	39194536	0.48	6.2		
	chr01_51916615	1	51916615	0.02	5.5		
	chr01_57180307	1	57180307	0.14	7.0		
	chr02_7385541	2	7385541	0.01		5.6	
	chr02_23457329	2	23457329	0.26		6.2	
	chr02_55288059	2	55288059	0.23		5.2	
	chr02_70741591	2	70741591	0.35	7.7		
	chr03_37106873	3	37106873	0.01	15.8		
	chr05_14709625	5	14709625	0.47		6.5	
	chr07_13912695	7	13912695	0.03		5.2	
	chr07_34140989	7	34140989	0.07		11.2	
	chr07_44945546	7	44945546	0.31		7.8	
Width	chr01_12454497	1	12454497	0.01		20.8	
	chr01_55198318	1	55198318	0.50			5.1
	chr01_59594088	1	59594088	0.21		5.8	
	chr02_2229887	2	2229887	0.45			7.0
	chr02_3600427	2	3600427	0.02			9.8
	chr02_5849946	2	5849946	0.02	5.1		
	chr02_10514248	2	10514248	0.01	6.2		
	chr02_18593171	2	18593171	0.01		12.5	
	chr02_23654774	2	23654774	0.30			9.8
	chr02_36332369	2	36332369	0.46		8.6	
	chr02_50240388	2	50240388	0.01	5.1		
	chr02_55999271	2	55999271	0.03			6.5
	chr02_67646340	2	67646340	0.02			5.5
	chr02_72213994	2	72213994	0.16		5.6	
	chr02_72315287	2	72315287	0.07			6.3
	chr03_32413776	3	32413776	0.48	17.8		
	chr04_40678059	4	40678059	0.01	5.0		
	chr05_85463559	5	85463559	0.21	6.7		
	chr05_85600362	5	85600362	0.02			42.8
	chr06_20202626	6	20202626	0.11	5.1		
	chr06_51821545	6	51821545	0.29			6.8
	chr06_52890285	6	52890285	0.01	13.3		
	chr06_63334142	6	63334142	0.21		5.4	

Table 68 Continued

					LOD per environment		
Trait	Marker	Chr.	Position	MAF	2018-S	2018-W	Comb.
	chr07_35307487	7	35307487	0.23		5.7	
LDim	chr01_141729	1	141729	0.01		22.9	11.7
	chr01_8034796	1	8034796	0.42		6.9	
	chr01_39194536	1	39194536	0.48	5.6		
	chr01_51916615	1	51916615	0.02			7.6
	chr01_58014993	1	58014993	0.25	5.8		
	chr01_64419847	1	64419847	0.13	5.9		
	chr02_3956928	2	3956928	0.07		5.6	
	chr02_23457329	2	23457329	0.26		6.6	
	chr02_55999281	2	55999281	0.02		15.4	8.7
	chr02_70741591	2	70741591	0.35	8.8		
	chr02_72596610	2	72596610	0.41			5.2
	chr03_15865705	3	15865705	0.03			6.3
	chr03_37106873	3	37106873	0.01	14.1		
	chr04_54976573	4	54976573	0.40		7.8	6.5
	chr05_11053554	5	11053554	0.46			6.3
	chr05_12159559	5	12159559	0.42		8.6	
	chr05_16301829	5	16301829	0.03		5.1	
	chr05_19886465	5	19886465	0.03		5.3	
	chr07_8397806	7	8397806	0.09		5.1	
	chr07_49445354	7	49445354	0.06			7.1
Volume	chr01_8407450	1	8407450	0.07		9.4	
	chr01_51916615	1	51916615	0.02	6.2		
	chr01_55173851	1	55173851	0.05		10.1	
	chr01_62032017	1	62032017	0.27		6.3	
	chr02_16115116	2	16115116	0.27		9.5	6.6
	chr02_67026585	2	67026585	0.05			10.4
	chr03_44488168	3	44488168	0.01	17.9		
	chr04_9598694	4	9598694	0.01			5.1
	chr04_43034503	4	43034503	0.01		13.9	6.5
	chr04_53789486	4	53789486	0.01		5.1	
	chr04_58007989	4	58007989	0.01			5.9
	chr04_58007999	4	58007999	0.01		7.8	
	chr05_5327882	5	5327882	0.07	7.0		
	chr05_20440529	5	20440529	0.04			8.0
	chr05_24048805	5	24048805	0.07			8.3
	chr05_82463436	5	82463436	0.03			7.8

Table 68 Continued

					LOD per environment		
Trait	Marker	Chr.	Position	MAF	2018-S	2018-W	Comb.
	chr06_52890265	6	52890265	0.21	5.4		
	chr07_35307487	7	35307487	0.23		6.5	
	chr07_53029240	7	53029240	0.46	6.3		

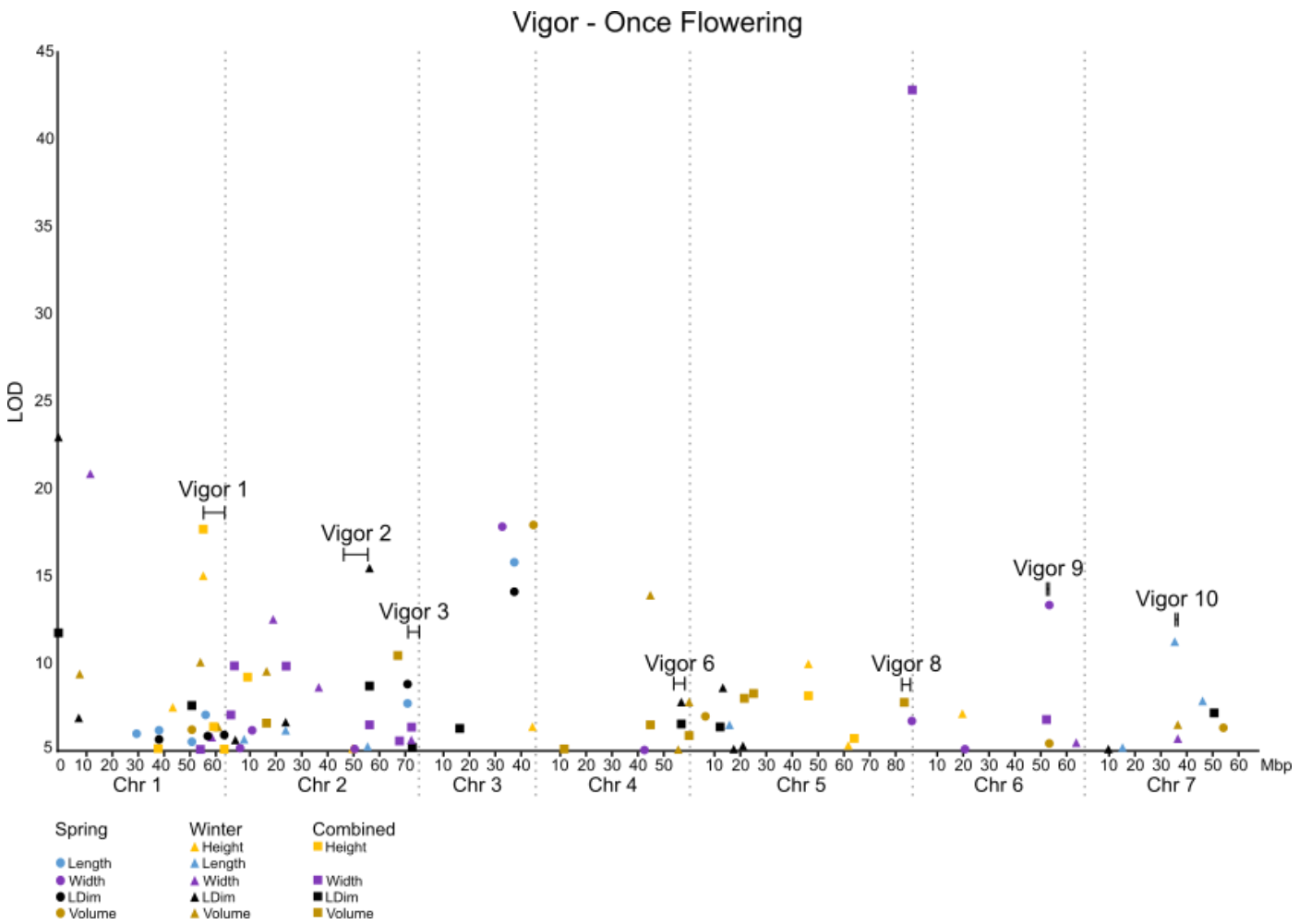

Figure 71 Overlaid Manhattan plots of significant marker-trait associations for plant vigor traits in once-flowering genotypes from diploid rose families in spring 2018 (2018-S), winter 2018 (2018-W), and combined seasons (Comb.). LDim indicates longest plant dimension. LOD = logarithm of the odds. Brackets indicate clusters of marker-trait associations. Vertical lines indicate ends of chromosomes. A LOD of 5 was used as the significance threshold.

In CF types, associations were observed on all chromosomes (Table 69, Fig. 72) and clusters similar to the OF types were observed (Table 65, Fig. 73). A cluster with associations for all vigor traits except length was observed in the 57-60 Mbp region of chromosome 1 and was considered the same as Vigor 1. This cluster included an association for volume with a LOD of 31.0 that explained 10% of the phenotypic variation in 2018-W and 25% in the combined-seasons analysis. A cluster for all vigor traits was present in the 46-55 Mbp region of chromosome 2 and was considered the same as Vigor 2. Unlike in the OF types, two clusters were observed on chromosome 3. Both involved all vigor traits except height. The first spanned from approximately 27 to 36 Mbp (Vigor 4); the second was in the 42-43 Mbp region (Vigor 5). In Vigor 4, the same marker, chr03_32497673, explained 40% of the variation in length (2018-S) and 40% of the variation in LDim (2018-W). No marker in Vigor 5 explained more than 10% of the phenotypic variation for a trait. Another cluster was observed from 0.18 to 8 Mbp on chromosome 5 (Vigor 7). One marker on chromosome 7, chr07_19164791, was significantly associated with length, width, LDim, and volume but was not considered a cluster. Associations were also present on chromosomes 4 and 6 but did not form a prominent cluster.

Significant marker-trait associations were also found for the remaining architecture traits (NPrimaries, ADI, and GHabit). In OF types, NPrimaries was associated with markers on all chromosomes (Table 70, Fig. 74). One of these, chr01_59942599, is located within the Vigor 1 cluster described above. Two markers on chromosome 4 within 3 Mbp of each other were also associated with NPrimaries. In CF

types, NPrimaries also had significant associations in Vigor 1 cluster (Table 71, Fig. 74). In OF types, ADI had significant associations on all chromosomes except chromosome 4, one of which (chr02_72315206) fell within the Vigor 3 cluster; no significant associations were seen in CF types. GHabit associations were scattered across the genome, but one in OF types fell within the Vigor 6 cluster.

Table 69 Significant marker-trait associations for plant vigor traits in continuous flowering genotypes from diploid rose families in winter 2018 (2018-W) and combined seasons (Comb.). No significant associations were found for spring 2018. LDim indicates longest plant dimension. Chr. = chromosome, MAF = minor allele frequency, LOD = logarithm of the odds. A LOD of 5 was used as the significance threshold.

					LOD per environment	
Trait	Marker	Chr.	Position	MAF	2018-W	Comb.
Height	chr01_31628545	1	31628545	0.12	6.1	
	chr01_57213102	1	57213102	0.46		6.7
	chr01_57245697	1	57245697	0.37	6.7	
	chr02_7573488	2	7573488	0.02		5.4
	chr02_52856512	2	52856512	0.09	5.8	
	chr02_67372940	2	67372940	0.29		6.2
	chr03_40096459	3	40096459	0.29	10.2	
	chr04_38183254	4	38183254	0.15		6.9
	chr05_7757177	5	7757177	0.02	7.5	6.6
	chr05_10843728	5	10843728	0.43	5.1	
	chr05_13293130	5	13293130	0.02	5.3	
	chr06_3120642	6	3120642	0.25		6.4
	chr06_19138618	6	19138618	0.09	6.4	
Length	chr02_46445953	2	46445953	0.10	7.8	
	chr02_53575455	2	53575455	0.15		5.2
	chr03_28196647	3	28196647	0.02		8.4
	chr03_32497673	3	32497673	0.02	35.8	
	chr03_36062671	3	36062671	0.26	6.5	
	chr03_42103736	3	42103736	0.16		5.2
	chr03_42933515	3	42933515	0.24	6.8	
	chr05_176358	5	176358	0.003		6.0
	chr05_2761965	5	2761965	0.39	9.2	

Table 69 Continued

					LOD per environment	
Trait	Marker	Chr.	Position	MAF	2018-W	Comb.
	chr06_13036085	6	13036085	0.09		7.9
	chr06_17064661	6	17064661	0.17	5.1	
	chr07_1196036	7	1196036	0.44		5.1
	chr07_1214054	7	1214054	0.003	11.0	
	chr07_19164791	7	19164791	0.03	6.6	
Width	chr01_57980644	1	57980644	0.20	7.1	
	chr01_59761205	1	59761205	0.003	5.6	
	chr02_6706670	2	6706670	0.10	5.5	
	chr02_16377349	2	16377349	0.08		12.1
	chr02_51140600	2	51140600	0.03		6.4
	chr03_12406348	3	12406348	0.06		5.3
	chr03_27333946	3	27333946	0.15		17.5
	chr03_36062671	3	36062671	0.26	9.3	
	chr03_39518359	3	39518359	0.20	7.3	
	chr03_42103736	3	42103736	0.16	5.9	
	chr04_31237960	4	31237960	0.03		6.1
	chr04_52526835	4	52526835	0.01	20.4	
	chr05_52444177	5	52444177	0.26		5.4
	chr05_85163758	5	85163758	0.15	6.8	
	chr06_13144313	6	13144313	0.09	7.6	
	chr07_19164791	7	19164791	0.03	6.2	
LDim	chr01_60174454	1	60174454	0.05		9.6
	chr01_64128920	1	64128920	0.24		7.4
	chr02_10514135	2	10514135	0.09		9.0
	chr02_46445953	2	46445953	0.10	7.7	
	chr03_25921330	3	25921330	0.16		13.4
	chr03_28181482	3	28181482	0.01		5.4
	chr03_32497673	3	32497673	0.02	36.6	
	chr03_36062671	3	36062671	0.26	7.1	
	chr03_42933515	3	42933515	0.24	9.7	
	chr04_50600714	4	50600714	0.02	6.0	
	chr05_2174967	5	2174967	0.38		7.3
	chr05_2761965	5	2761965	0.39	7.6	
	chr06_51911829	6	51911829	0.49		6.8
	chr07_1214054	7	1214054	0.003	11.1	

Table 69 Continued

					LOD per environment	
Trait	Marker	Chr.	Position	MAF	2018-W	Comb.
	chr07_19164791	7	19164791	0.03	6.0	
	chr07_20928497	7	20928497	0.04		8.5
Volume	chr01_497117	1	497117	0.003	48.2	
	chr01_59761205	1	59761205	0.003	31.0	6.9
	chr02_4459336	2	4459336	0.08	9.1	
	chr02_13970379	2	13970379	0.08		12.1
	chr02_54644667	2	54644667	0.41		5.3
	chr02_58714475	2	58714475	0.04		5.4
	chr03_31563795	3	31563795	0.02		11.0
	chr03_36062671	3	36062671	0.26	8.3	
	chr03_42103736	3	42103736	0.16	8.3	
	chr04_52526835	4	52526835	0.01	23.2	
	chr05_3858006	5	3858006	0.37	6.9	
	chr05_19109891	5	19109891	0.003		6.3
	chr05_76644398	5	76644398	0.47		6.5
	chr06_19057420	6	19057420	0.35		9.6
	chr07_19164791	7	19164791	0.03	10.1	

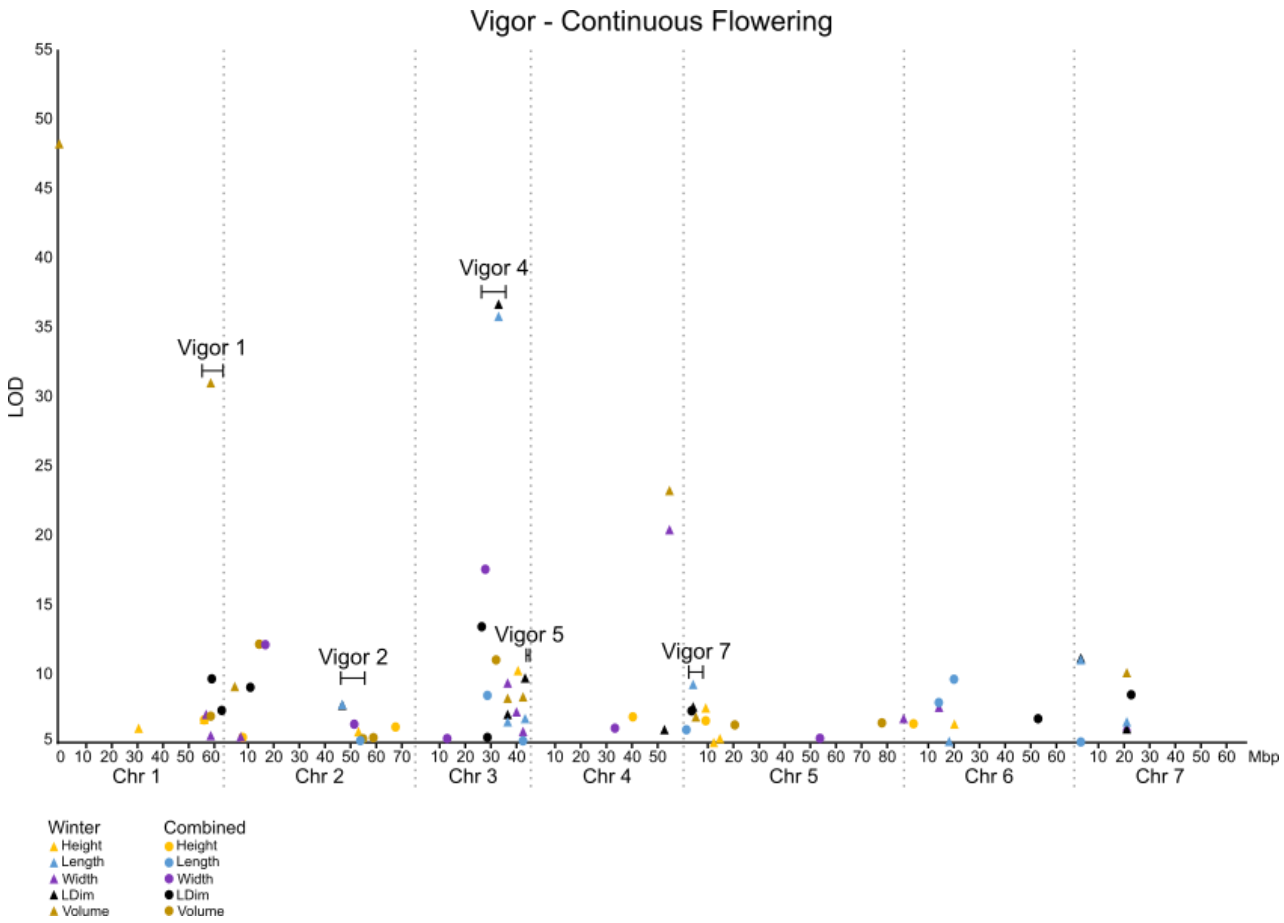

Figure 72 Overlaid Manhattan plots of significant marker-trait associations for plant vigor traits in continuous flowering genotypes from diploid rose families in winter 2018 (2018-W) and combined seasons (Comb.). No significant associations were found for spring 2018. LDim indicates longest plant dimension. LOD = logarithm of the odds. Brackets indicate clusters of marker-trait associations. Vertical lines indicate ends of chromosomes. A LOD of 5 was used as the significance threshold.

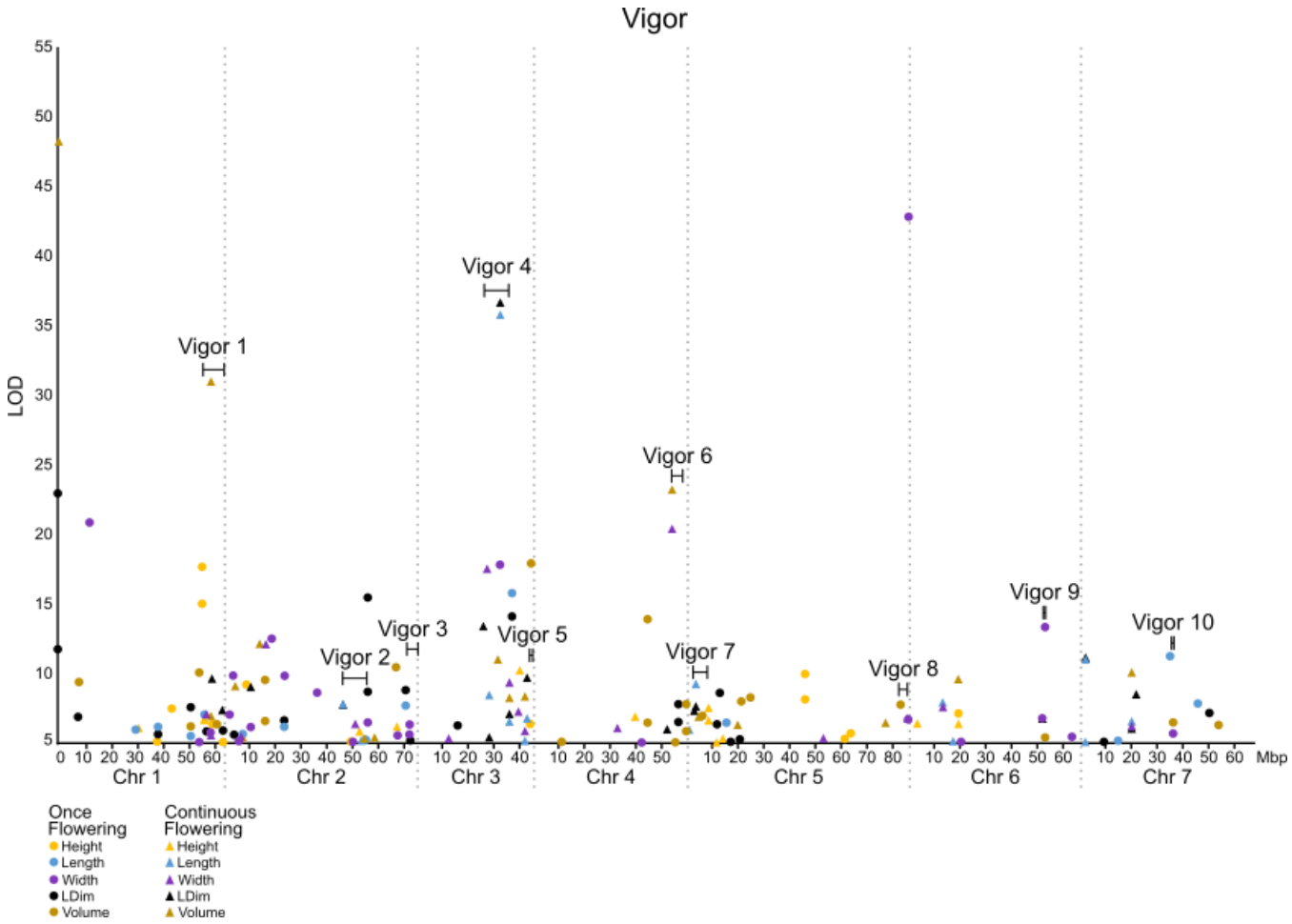

Figure 73 Overlaid Manhattan plots of significant marker-trait associations for plant vigor traits in continuous flowering and once-flowering genotypes from diploid rose families in spring 2018, winter 2018, and combined seasons. Analyses were run separately by flowering type and environment and significant results overlaid. LDim indicates longest plant dimension. LOD = logarithm of the odds. Brackets indicate clusters of marker-trait associations. Vertical lines indicate ends of chromosomes. A LOD of 5 was used as the significance threshold.

Table 70 Significant marker-trait associations for number of primary shoots (NPrimaries), apical dominance index (ADI), and growth habit (GHabit) in once-flowering genotypes from diploid rose families in winter 2018 (2018-W) and combined seasons (Comb.). No significant associations were found for spring 2018. Chr. = chromosome, MAF = minor allele frequency, LOD = logarithm of the odds. A LOD of 5 was used as the significance threshold.

					LOD per environment	
Trait	SNP	Chr.	Position	MAF	2018-W	Comb.
NPrimaries	chr01_36824890	1	36824890	0.02	9.5	5.3
	chr01_59942599	1	59942599	0.46	10.9	10.3
	chr02_1011029	2	1011029	0.07		5.6
	chr02_67662696	2	67662696	0.03	6.5	
	chr02_68236963	2	68236963	0.12		6.0
	chr02_74956637	2	74956637	0.48		5.1
	chr03_39751264	3	39751264	0.39	5.2	
	chr04_15498529	4	15498529	0.01	8.3	
	chr04_35721390	4	35721390	0.25		5.1
	chr04_38541135	4	38541135	0.19	6.5	
	chr04_49549904	4	49549904	0.07	5.2	
	chr05_3958587	5	3958587	0.04		5.7
	chr05_61450149	5	61450149	0.48	5.6	
	chr05_66867745	5	66867745	0.49		5.0
	chr06_58567111	6	58567111	0.04		6.7
	chr06_66995080	6	66995080	0.28	5.4	
	chr07_4319729	7	4319729	0.16	8.3	
	chr07_11150062	7	11150062	0.20		7.2
ADI	chr01_141729	1	141729	0.01	48.2	
	chr01_36861684	1	36861684	0.47	10.6	
	chr01_52171117	1	52171117	0.13	5.6	
	chr02_72315206	2	72315206	0.35	11.7	
	chr03_22756120	3	22756120	0.05	5.8	
	chr03_25461177	3	25461177	0.27	7.4	
	chr05_49499899	5	49499899	0.24	10.9	
	chr06_22019754	6	22019754	0.21	5.2	
	chr06_55875635	6	55875635	0.36	5.9	
	chr07_19165254	7	19165254	0.26	6.2	
GHabit	chr01_52709751	1	52709751	0.23	5.9	
	chr04_50853906	4	50853906	0.49	10.2	
	chr04_56408961	4	56408961	0.24	9.5	
	chr05_53211343	5	53211343	0.01	12.0	
	chr05_63683933	5	63683933	0.44	6.2	
	chr06_48630311	6	48630311	0.01	5.9	

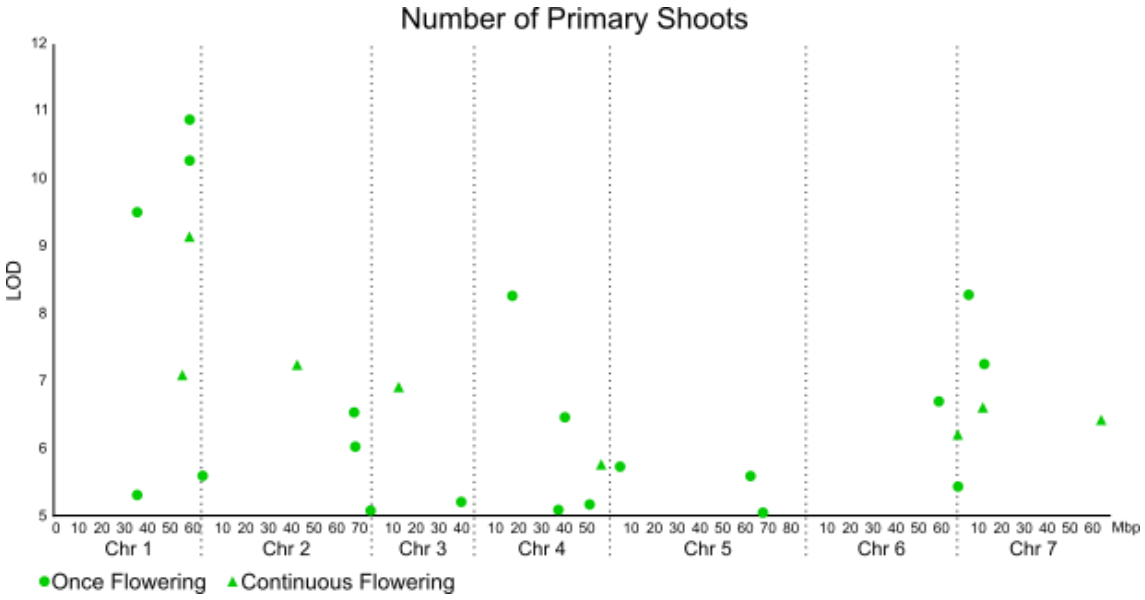

Figure 74 Overlaid Manhattan plots of significant marker-trait associations for number of primary shoots (NPrimaries) in continuous flowering and once-flowering genotypes from diploid rose families in winter 2018 and combined seasons. Analyses were run separately by flowering type and environment and significant results overlaid. LOD = logarithm of the odds. A LOD of 5 was used as the significance threshold.

Table 71 Significant marker-trait associations for number of primary shoots (NPrimaries) and growth habit (GHabit) in continuous flowering genotypes from diploid rose families in winter 2018 (2018-W). No significant associations were found for spring 2018 or combined seasons or for apical dominance index (ADI). Chr. = chromosome, MAF = minor allele frequency, LOD = logarithm of the odds. A LOD of 5 was used as the significance threshold.

Trait	Marker	Chr.	Position	MAF	LOD
NPrimaries	chr01_56746594	1	56746594	0.01	7.1
	chr01_59926096	1	59926096	0.07	9.1
	chr02_42606603	2	42606603	0.02	7.2
	chr03_12228585	3	12228585	0.07	6.9
	chr04_54550928	4	54550928	0.03	5.8
	chr06_66896388	6	66896388	0.003	6.2
	chr07_10493244	7	10493244	0.07	6.6
	chr07_62627000	7	62627000	0.33	6.4
GHabit	chr01_5404351	1	5404351	0.01	13.1
	chr02_42306480	2	42306480	0.18	10.5
	chr04_49239498	4	49239498	0.02	5.8
	chr05_58106809	5	58106809	0.17	5.8
	chr05_83035045	5	83035045	0.21	5.7
	chr06_51005415	6	51005415	0.32	5.1

V.4.3.3 Cultivar-family comparison

Only limited overlap between the families and cultivars for architecture marker-trait associations was observed. One marker associated with NPrimaries in the cultivars, chr07_12989436, was within approximately 1 Mbp of a marker associated with NPrimaries in OF types in the families. No such correspondence was observed for ADI between the two studies. The length and LDim associations in the cultivars fell within the Vigor 4 cluster in the families (Fig. 75). Two markers for volume in the cultivars, chr01_46639111 and chr04_55543431, fell within the Vigor 1 and Vigor 6 clusters in the families, respectively. The other markers for volume in the cultivars did not overlap with any of the major clusters in the families.

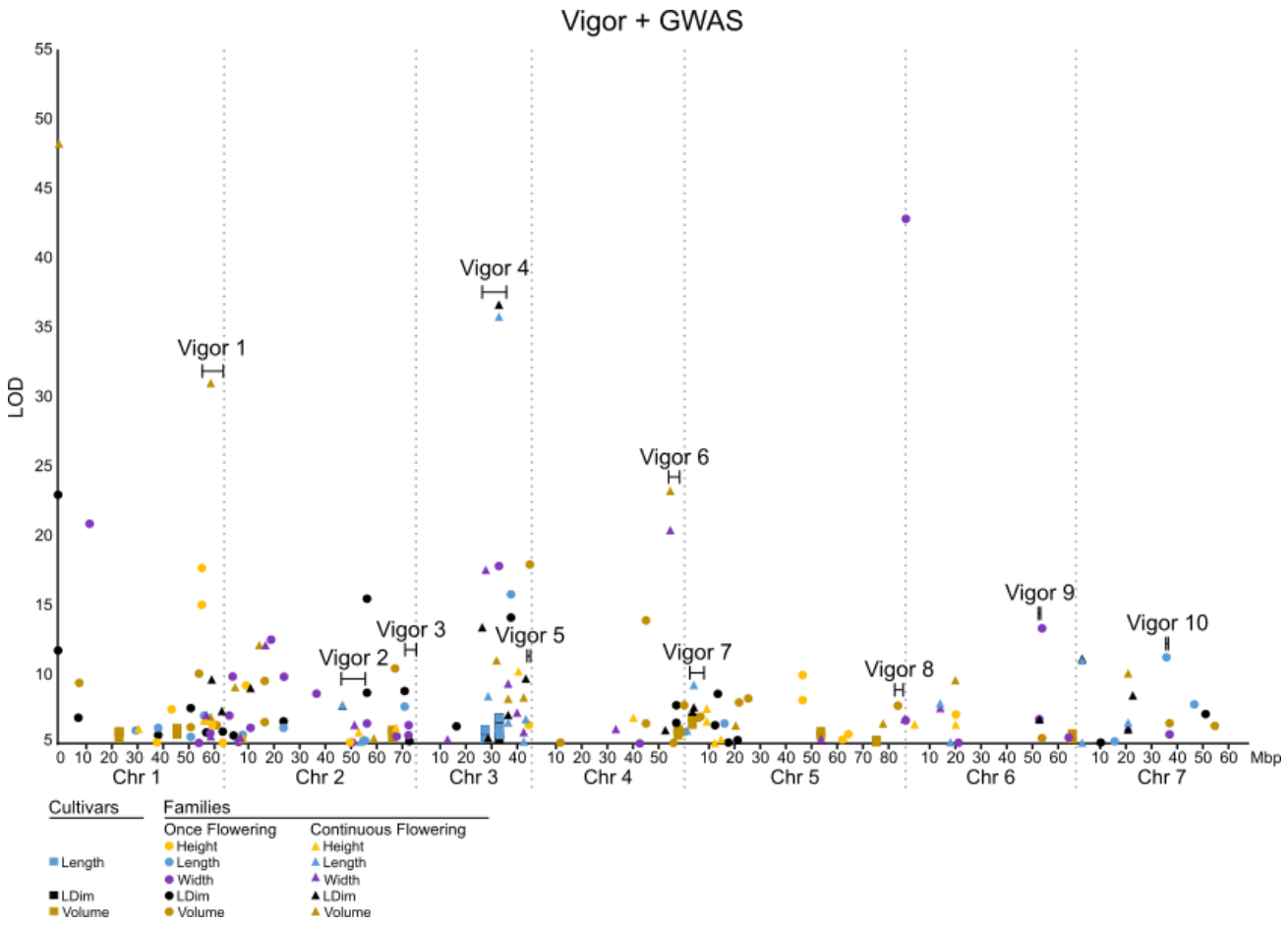

Figure 75 Overlaid Manhattan plots of significant marker-trait associations for plant vigor traits in 73 diploid rose cultivars and eight diploid rose families. Analyses were performed separately between cultivars and families. In the families, once-flowering and continuous flowering genotypes were analyzed separately. Environments were analyzed separately and their results overlaid. LDim indicates longest plant dimension. LOD = logarithm of the odds. Brackets indicate clusters of marker-trait associations. Vertical lines indicate ends of chromosomes. A LOD of 5 was used as the significance threshold.

V.5 Discussion

V.5.1 Population structure

The population structure findings, phylogeny, and kinship matrix of the cultivar panel generally agree with known or proposed pedigrees and classifications. Unlike Schulz et al. (2016), it was not found that population structure corresponded in part to growth type with groundcovers forming a subpopulation distinct from hybrid tea and floribunda roses. This is not necessarily surprising, however, given that the two sets of cultivars were of very different makeup. A cultivar set similar to the one used in this study was used by Soules (2009), who also found that the dendrogram corresponded well to American Rose Society classifications such as Tea, China, polyantha, etc. Similar to this study, Soules (2009) found that Tea-types clustered within China roses and that noisette types formed a unique group. Interestingly, Soules (2009) found that 'Mutabilis' was likely derived from both Tea and China roses, and this seems somewhat supported by this study: at K = 2, 'Mutabilis' grouped with the large Tea/China group; at K = 5, 'Mutabilis' grouped with a smaller, mostly China group; at K = 6, 'Mutabilis' grouped with the large, mostly Tea group, not with a smaller group of China roses. Contrary to Soules (2009), however, 'Rouletii' was not found to be a sport of 'Old Blush' but may instead be a child or other close relative. As Soules (2009) used a panel of 23 SSRs, it is not surprising that this study, which has greater genome coverage, clarified this relationship.

V.5.2 Association mapping

To identify markers for plant architecture, disease resistance, and flowering traits, a GWAS on 73 diploid rose cultivars and a single-marker analysis on eight diploid rose populations were performed. Genomic regions associated with disease severity, flowering, and plant architecture were identified. Based on the various findings of this study, some recommendations for future directions can be made.

V.5.2.1 Influence of *RoKSN*

Flowering type in rose is known to be controlled by the gene *RoKSN* (Iwata et al., 2012) in the region between approximately 27 and 34 Mbp on chromosome 3 (Hibrand Saint-Oyant et al., 2018). This region corresponds with the many significant associations for flowering and plant architecture traits prior to the division of the family data by flowering type, highlighting the need to control for flowering type in future genetic studies. Even when controlling for flowering type, however, the 27-34 Mbp region of chromosome 3 seems to impact a number of plant traits. The Vigor 4 cluster coincides with this region, as does the CLS 2 cluster and a marker associated with defoliation. Previously, Kawamura et al. (2015) found QTLs for growth habit and stem angle in the area of *RoKSN* which they attributed to linkage rather than to pleiotropic effects of *RoKSN*, noting that two gibberellic acid biosynthesis genes are in the same region and could well be affecting growth habit. Both this study and Kawamura et al. (2015) found significant correlations between growth habit and plant size (see Chapter III), and associations between the *RoKSN* area and growth habit, meaning the vigor associations in this area could be due to these genes. However, Iwata et al. (2012) did

determine that *RoKSN* can impact growth type, which could explain the significant association for growth type in the region. If that is the case, *RoKSN* could indirectly be responsible for some changes in plant size (length, LDim, etc.), as climbing roses tend to be larger. A third option is that all three genes are impacting plant architecture; however, more work is needed to determine to what extent each gene is contributing to the various architecture phenotypes.

V.5.2.2 Flower intensity clusters

When flowering type was controlled for in the families, clusters associated with flower productivity, not just flowering type, emerged. The most prominent of these are FLI 2 and FLI 3 on chromosomes 2 and 4, respectively, as FLI 2 contained a marker that explained 59% of the variation in AFLIC in 2019-OV and FLI 3 contained two markers that explained 85 and 78% of the variation in FLI_Max in 2018-CS. The FLI 2 marker is contained in a gene that codes for a protein of unknown function. Despite their high R^2 values, both FLI 3 markers are intergenic, though they are near a gene coding for a GATA transcription factor. Flower intensity needs to be examined in other populations both to confirm these results (including the surprisingly high R^2 values) and to identify other potentially associated regions. As flower productivity can be affected by many factors, many genes may be involved, and breeding efforts would benefit from identifying multiple of these genes.

V.5.2.3 Disease resistance clusters

Of the four major genes for black spot resistance, three have been previously mapped to chromosomes 1 and 5 with one having an unknown location (reviewed in

Debener (2019)). QTLs have also been identified on chromosomes 3 and 5 (Yan et al., 2019; Soufflet-Freslon et al., 2019). The clusters on chromosomes 2 and 6 in the families of this study, therefore, are unique and may represent novel resistance loci. All three BS clusters contain multiple putative disease resistance genes, mostly of the NBS-LRR type. It is surprising, though, that despite the evidence for a black spot resistance locus on chromosome 6, no associations for defoliation were found on chromosome 6.

Cercospora resistance is less well understood, and QTLs have been identified on chromosomes 1, 3, and 7 (Kang, 2020). The CLS 2 cluster on chromosome 3 in the families is in a similar position as the previously discovered QTL; however, the clusters on chromosomes 2 and 6 in this study are unique. All three CLS clusters contain multiple putative disease resistance genes of the NBS-LRR type. The potential new resistance loci for both cercospora and black spot merit further research, especially considering the importance of disease resistance to plant breeding.

V.5.2.4 Architecture traits

Only growth habit and height among the architecture traits in this study have been directly studied in previous genetic analyses. Kawamura et al. (2015) identified QTLs for height on chromosomes 2, 4, 5, 6, and 7. The QTL on chromosome 2, *Hgt-2*, is located near the SSR Rw29B1, which coincides with a position of 79.9 Mbp on chromosome 2. The vigor cluster in this study closest to *Hgt-2* is the Vigor 3 cluster in the 70-72 Mbp region of chromosome 2. Based on the sequences of nearby markers, *Hgt-5* is located in the 57-64 Mbp region of chromosome 4; thus, it overlaps with the Vigor 6 cluster in this study. *Hgt-3* is likely in the 21-25 Mbp region of chromosome 7

but may extend to 45 Mbp; thus, it may overlap with the small Vigor 10 cluster in this study.

QTLs have also been identified for shoot length, which is likely related to the vigor traits in this study, on chromosomes 1, 2, and 5 (Yan et al., 2007). The shoot length QTL on chromosome 2 is especially interesting, as it is in the vicinity of an auxin response gene, *RoAXR* (Spiller et al., 2011). The *Hgt-2* QTL of Kawamura et al. (2015) was also near this gene, and the two QTLs are likely the same. As the SSRs associated with the QTLs of Yan et al. (2007) do not map to only one location on the *R. chinensis* genome, it cannot be determined with certainty if the shoot length QTLs correspond to any of the vigor clusters in this study. Based on the general map position of the chromosome 1 shoot length QTL, however, it is possible that this QTL coincides with the Vigor 1 cluster in this study. Regardless, the high number of associations in the Vigor 1 cluster as well as the co-localization of vigor traits in the cultivars to that cluster indicate the presence of genetic control of plant size/vigor in the region.

NPrimaries has been assessed in roses previously (Wu et al., 2019b) but the genetic control has not been explored until now. An analogous trait, number of determined axes, has been studied in two biparental diploid rose families (Li-Marchetti et al., 2017) and QTLs identified on chromosomes 2, 5, and 6. None of these coincide with NPrimaries in the families, but the QTL on chromosome 5 may overlap with chr05_24876741, which was associated with NPrimaries in the cultivars. The wide distribution of significant associations for NPrimaries in both the cultivars and families

suggests that the trait may be fairly complex, assuming that the associations are not false positives; more study is warranted in either scenario.

While ADI has not been previously studied in roses, branching intensity (BIV), or the ratio of secondary shoots to the total number of buds on a primary shoot, has been studied in a biparental diploid rose family (Djennane et al., 2014). A QTL for BIV was identified on chromosome 2 and co-localized with *RwMAX2*, a homologue of the strigolactone signaling pathway gene *MAX2* in *Arabidopsis thaliana*. *RwMAX2* has been implicated in bud burst in roses (Djennane et al., 2014; Barbier et al., 2015). None of the associations with ADI in either the families or the cultivars were near *RwMAX2* or the three other *MAX* homologues identified in roses. A branching repressor gene, *RhBRC1*, has also been identified in roses (Barbier et al., 2015) and is located at approximately 5 Mbp on chromosome 7. The association for ADI closest to this gene was located at 7 Mbp on chromosome 7. Thus, most of the associations for ADI in this study are potentially new findings, indicating that branching is a complex trait that will necessitate further study.

V.5.3 Future directions

While the single-marker approach in the families proved informative, more work can still be done on these populations. The development of a consensus linkage map (Chapter IV) is a necessary precursor for a QTL analysis. A software such as FlexQTL™ (Bink et al., 2008) can be used to exploit the interrelatedness of these populations, increasing the power and enabling the tracing of critical alleles through the pedigree.

Based on the strong effects or potential effects of *RoKSN*, it would be advisable to control for flowering type in future studies. The cultivar panel proved to be too small to divide into continuous and once-flowering types for separate analysis as was done in the families. A larger cultivar panel in the future would enable better control for this major gene. The dearth of significant associations in the cultivar panel and the abundance of associations in the families further emphasizes the importance of having a large number of genotypes in an association mapping study. Incorporating the current datasets with those of other cultivars and progenies, including those of other ploidy levels, from the Texas A&M Rose Breeding and Genetics Program would greatly increase the power of the study. This would also have the side effect of producing results that would be more widely applicable: this study relies heavily on a mix of old garden roses (cultivars) and *R. wichurana* descendants (families) due to the constraint of ploidy level, but the Rose Breeding and Genetics Program as a whole draws from both old and modern roses and many different rose species. Validating and expanding these results are crucial steps for both understanding these traits and for enabling future marker-assisted selection.

CHAPTER VI

CONCLUSION

This study investigated the heritability of black spot and cercospora resistance, defoliation, flower intensity, and plant architecture traits in diploid rose cultivars and families; identified genomic regions associated with these traits; and developed a high-density integrated consensus linkage map for use in future studies.

Diploid rose families were developed using a combination of species, species hybrids, cultivars, and breeding lines (Chapter II) and phenotyped for disease resistance, defoliation, and flower intensity in College Station, TX in 2018 and Overton, TX in 2019. Broad-sense heritability was high for black spot, defoliation, and flower intensity, but low for cercospora. All four traits also had low narrow-sense heritability, indicating a high degree of non-additive effects. Black spot, cercospora, and defoliation also had high genotype by environment (month) interactions, while flower intensity did not. When the analysis was performed separately by flowering type, the non-additive effects for flower intensity declined further, though there was still moderate broad-sense heritability for flower intensity. Thus, while flower intensity is affected by flowering type, breeding for improved flower intensity within a single flowering type should still be a feasible breeding goal.

The families were also phenotyped for plant architecture (number of primary shoots, height, length, width, longest dimension, volume, apical dominance, and growth habit) in College Station, TX in 2018. Architecture traits generally had low to moderate

broad-sense heritability and low narrow-sense heritability, again indicating non-additive effects. Genotype by environment interactions were high, reflecting the growth of the plants over the course of the year. As architecture was found to vary with flowering type, heritability was also estimated when controlling for flowering type. Narrow-sense heritability estimates for length, width, longest dimension, and apical dominance were slightly higher in once-flowering genotypes than continuous flowering genotypes, suggesting that some germplasm likely has stronger additive effects for these traits; this germplasm should be identified and utilized for breeding.

Seventy-three diploid rose cultivars were phenotyped for the same traits in College Station, TX in 2018; architecture traits were assessed in an additional season (winter 2019). While repeatability estimates for black spot, cercospora, defoliation, and flower intensity were high based on the area and/or maximum scores, they were low based on the least squares means. As in the families, architecture traits had low to moderate repeatability. Genotype by environment interactions were lower in the cultivars than in the families. This may be due to germplasm differences or the relative maturity of the two sets of plants. When repeatabilities were estimated using winter data only (2018 and 2019), repeatabilities were higher and genotype by environment interactions were very low or zero. This indicates that these architecture traits may be stable over time.

To lay the groundwork for future marker-assisted selection for these traits of interest, association mapping was performed. Families and cultivars were both genotyped for single nucleotide polymorphisms (SNPs) via genotyping by sequencing.

After curation, 58,075 and 11,884 SNPs were retained for association mapping in the families and cultivars, respectively. This SNP dataset was also used to investigate the population structure of the cultivars. The cultivars formed two main subpopulations that could be further broken down into five to six subpopulations mostly consistent with their known pedigrees and a constructed phylogeny.

In the families, many associations were found for the traits of interest, some of which fell into small genomic regions (termed ‘clusters’). Three clusters of associations were identified for black spot and three for cercospora on chromosomes 2, 3, and 6; the chromosome 3 cluster overlapped between the two diseases and may coincide with previously identified quantitative trait loci (QTLs) for black spot and cercospora. The clusters on chromosomes 2 and 6 are novel and encompass several NBS-LRR genes. When flowering type was controlled for, five clusters associated with flower intensity were identified on chromosomes 2, 4, and 5, and ten clusters associated with plant vigor traits (height, length, width, longest dimension, and volume) were identified. Vigor clusters on chromosomes 1, 2, 4, and 7 may coincide with previously identified QTLs, but six other clusters appear to be novel. Presumably due to the small size of the cultivar panel, no marker-trait associations were found in the cultivars for disease, defoliation, or flowering; a few associations were found for architectural traits, some of which overlapped with the vigor clusters in the families. Thus, novel genomic regions associated with disease resistance and architecture were identified; further work is needed to narrow down the regions and validate them in different and/or larger datasets.

While the approach above yielded promising results, to improve the power of the analysis and to follow the inheritance of important alleles associated with desirable phenotypes, a QTL analysis is needed. Thus, linkage maps were constructed for three of the populations used above (J06-20-14-3 x 'Papa Hemeray', TAMU7-20 x 'Srdce Europy', and TAMU7-30 x 'Srdce Europy'). An integrated consensus map (ICM) constructed from these three maps contained 2,871 SNPs over 828.3 cM with an average density of 1.5 unique positions per cM. Moreover, the ICM was highly collinear with the rose genome. In marker number and density, the ICM was comparable to recent diploid rose maps and should facilitate the discovery of quantitative trait loci.

Thus, while several new traits and sources of germplasm were explored in this study, there is much room for future work. Future studies should continue to control for flowering type, as it can greatly impact flowering behavior and plant architecture. More years of architecture data are needed to confirm the stability of architecture over time, and location effects on architecture need to be explored. Furthermore, as the families were phenotyped shortly after planting, it is likely they were under less disease pressure due to lower levels of inoculum. More years and locations of data could provide better estimates of heritability. Finally, the association mapping results need to be refined and validated to enable future marker-assisted selection in roses.

REFERENCES

Alexander, D.H., J. Novembre, and K. Lange. 2009. Fast model-based estimation of ancestry in unrelated individuals. Genome Res. 19(9)**:** 1655-1664.

Amrine, J. 1996. *Phyllocoptes fructiphilus* and biological control of multiflora rose, 741-749. In: Lindquist, E. E., Sabelis, M. W. & Bruin, J. (eds.) Eriophyoid mites their biology, natural enemies and control. Oxford: Elsevier.

Amrine, J.W., D.F. Hindal, T.A. Stasny, R.L. Williams, and C.C. Coffman. 1988. Transmission of the rose rosette disease agent to *Rosa multiflora* by *Phyllocoptes fructiphilus* (Acari: Eriophyidae). Entomol. News. 99(5)**:** 239-252.

Anderson, N., and D.H. Byrne. 2007. Methods for *Rosa* germination. Acta Hort. 751**:** 503-507.

Appels, R., R. Morris, B.S. Gill, and C.E. May. 1998. Chromosome biology. Springer Science & Business Media, New York, NY.

Barbier, F., T. Péron, M. Lecerf, M.-D. Perez-Garcia, Q. Barrière, J. Rolčík, S. Boutet-Mercey, S. Citerne, R. Lemoine, B. Porcheron, H. Roman, N. Leduc, J. Le Gourrierec, J. Bertheloot, and S. Sakr. 2015. Sucrose is an early modulator of the key hormonal mechanisms controlling bud outgrowth in *Rosa hybrida*. J. of Experimental Bot. 66(9)**:** 2569-2582.

Bendahmane, M., A. Dubois, O. Raymond, and M.L. Bris. 2013. Genetics and genomics of flower initiation and development in roses. J. Experimental Bot. 64(4)**:** 847-857.

Benjamini, Y., and Y. Hochberg. 1995. Controlling the false discovery rate: a practical and powerful approach to multiple testing. J. Royal Stat. Soc. Ser. B (Methodological). 57(1)**:** 289-300.

Bentley, N., L. Grauke, and P. Klein. 2019. Genotyping by sequencing (GBS) and SNP marker analysis of diverse accessions of pecan (*Carya illinoinensis*). Tree Genet. Genomes. 15(1)**:** 8.

Bink, M., M. Boer, C. Ter Braak, J. Jansen, R. Voorrips, and E. van de Weg. 2008. Bayesian analysis of complex traits in pedigreed plant populations. Euphytica. 161(1-2)**:** 85-96.

Boumaza, R., S. Demotes-Mainard, L. Huché-Thélier, and V. Guerin. 2009. Visual characterization of the esthetic quality of the rosebush. J. Sensory Studies. 24(5)**:** 774-796.

Bourke, P.M., P. Arens, R.E. Voorrips, G.D. Esselink, C.F. Koning-Boucoiran, W.P. van't Westende, T. Santos Leonardo, P. Wissink, C. Zheng, and G. Geest. 2017. Partial preferential chromosome pairing is genotype dependent in tetraploid rose. Plant J. 90(2)**:** 330-343.

Bourke, P.M., G. van Geest, R.E. Voorrips, J. Jansen, T. Kranenburg, A. Shahin, R.G.F. Visser, P. Arens, M.J.M. Smulders, and C. Maliepaard. 2018. polymapR—linkage analysis and genetic map construction from F1 populations of outcrossing polyploids. Bioinformatics. 34(20)**:** 3496-3502.

Bruneau, A., J.R. Starr, and S. Joly. 2007. Phylogenetic relationships in the genus *Rosa*: new evidence from chloroplast DNA sequences and an appraisal of current knowledge. Systematic Bot. 32(2)**:** 366-378.

Byrne, D.H. 2015. Advances in rose breeding and genetics in North America. Acta Hort. 1064**:** 89-98.

Byrne, D.H., H.B. Pemberton, D.J. Holeman, T. Debener, T.M. Waliczek, and M.A. Palma. 2019. Survey of the rose community: desired rose traits and research issues. Acta Hort. 1232**:** 189-192.

Byrne, D.H., E. Roundey, P.E. Klein, and M. Yan. 2015. Combating rose rosette disease: are there resistant roses? Am. Rose. 43(5)**:** 78-83.

Cairns, T. 2000. Modern roses XI. Academic Press.

Cairns, T. 2003. Classification: horticultural classification schemes, 117-124. In: Roberts, A. V. (ed.) Encycl. of Rose Sci. Oxford: Elsevier.

Chavez, D.E., M.A. Palma, D.H. Byrne, C.R. Hall, and L.A. Ribera. 2019. Willingness to pay for rose attributes: helping provide consumer orientation to breeding programs. J. of Agr. and Appl. Economics. 52(1)**:** 1-15.

Choubane, D., A. Rabot, E. Mortreau, J. Legourrierec, T. Péron, F. Foucher, Y. Ahcène, S. Pelleschi-Travier, N. Leduc, L. Hamama, and S. Sakr. 2012. Photocontrol of bud burst involves gibberellin biosynthesis in *Rosa* sp. J. of Plant Physiol. 169(13)**:** 1271-1280.

Collard, B., M. Jahufer, J. Brouwer, and E. Pang. 2005. An introduction to markers, quantitative trait loci (QTL) mapping and marker-assisted selection for crop improvement: the basic concepts. Euphytica. 142(1-2)**:** 169-196.

Cooperman, C., and S. Jenkins. 1986. Conditions influencing growth and sporulation of *Cercospora asparagi* and Cercospora blight development in asparagus. Phytopathol. 76(6)**:** 617-622.

Crespel, L., M. Chirollet, C. Durel, D. Zhang, J. Meynet, and S. Gudin. 2002. Mapping of qualitative and quantitative phenotypic traits in Rosa using AFLP markers. Theor. Appl. Genet. 105(8)**:** 1207-1214.

Crespel, L., C. Le Bras, D. Relion, and P. Morel. 2014. Genotype×year interaction and broad-sense heritability of architectural characteristics in rose bush. Plant Breeding. 133(3)**:** 412-418.

Crespel, L., and J. Mouchotte. 2003. Breeding: methods of cross-breeding, 30-33. In: Roberts, A. V. (ed.) Encycl. of Rose Sci. Oxford: Elsevier.

Crespel, L., M. Sigogne, N. Donès, D. Relion, and P. Morel. 2013. Identification of relevant morphological, topological and geometrical variables to characterize the architecture of rose bushes in relation to plant shape. Euphytica. 191(1)**:** 129-140.

Davis, B.H. 1938. The Cercospora leaf spot of rose caused by *Mycosphaerella rosicola*. Mycologia. 30(3)**:** 282-298.

Debener, T. 2019. The beast and the beauty: what do we know about black spot in roses? Critical Rev. in Plant Sci. 38(4)**:** 313-326.

Debener, T., and D.H. Byrne. 2014. Disease resistance breeding in rose: current status and potential of biotechnological tools. Plant Sci. 228**:** 107-117.

Debener, T., and L. Mattiesch. 1999. Construction of a genetic linkage map for roses using RAPD and AFLP markers. Theor. Appl. Genet. 99(5)**:** 891-899.

Demotes-Mainard, S., G. Gueritaine, R. Boumaza, P. Favre, V. Guérin, L. Huché-Thélier, and B. Andrieu. 2009. Coordinated development of the architecture of the primary shoot in bush rose. Plant growth modeling and applications. 214-221.

Demotes-Mainard, S., L. Huché-Thélier, P. Morel, R. Boumaza, V. Guérin, and S. Sakr. 2013. Temporary water restriction or light intensity limitation promotes branching in rose bush. Scientia Hort. 150**:** 432-440.

Djennane, S., L. Hibrand-Saint Oyant, K. Kawamura, D. Lalanne, M. Laffaire, T. Thouroude, S. Chalain, S. Sakr, R. Boumaza, and F. Foucher. 2014. Impacts of light and temperature on shoot branching gradient and expression of strigolactone synthesis and signalling genes in rose. Plant, Cell & Environ. 37(3)**:** 742-757.

Dodds, K.G., J.C. McEwan, R. Brauning, R.M. Anderson, T.C. van Stijn, T. Kristjánsson, and S.M. Clarke. 2015. Construction of relatedness matrices using genotyping-by-sequencing data. BMC genomics. 16(1)**:** 1047.

Drewes-Alvarez, R. 2003. Disease: black spot, p. 148-153. In: Roberts, A. V. (ed.) Encyclopedia of Rose Science. Oxford: Elsevier.

Duangsong, U., K. Laosatit, P. Somta, and P. Srinives. 2018. Genetics of resistance to Cercospora leaf spot disease caused by *Cercospora canescens* and

Psuedocercospora cruenta in yardlong bean (*Vigna unguiculata* ssp. *sesquipedalis*) × grain cowpea (*V. unguiculata* ssp. *unguiculata*) populations. J. Genet. 97(5)**:** 1451-1456.

Dugo, M.d.l.L., Z. Satovic, T. Millan, J.I. Cubero, D. Rubiales, A. Cabrera, and A.M. Torres. 2005. Genetic mapping of QTLs controlling horticultural traits in diploid roses. Theor. Appl. Genet. 111(3)**:** 511-520.

Dunwell, W., S.K. Braman, J. Williams-Woodward, M. Paret, A. Windham, S. Frank, S.A. White, and A.V. LeBude. 2014. Shrub roses - *Rosa* spp., 63-94. In: White, S. A. & Klingeman, W. (eds.) IPM for shrubs in southeastern US nursery production. Clemson, SC: Southern Nursery IPM Working Group.

Earl, D.A., and B.M. vonHoldt. 2012. STRUCTURE HARVESTER: a website and program for visualizing STRUCTURE output and implementing the Evanno method. Conservation Genet. Resources. 4(2)**:** 359-361.

El Mokadem, H., J. Meynet, and L. Crespel. 2002. The occurrence of 2 n eggs in the dihaploids derived from *Rosa hybrida* L. Euphytica. 124(3)**:** 327-332.

Endelman, J.B., and C. Plomion. 2014. LPmerge: an R package for merging genetic maps by linear programming. Bioinformatics. 30(11)**:** 1623-1624.

Evanno, G., S. Regnaut, and J. Goudet. 2005. Detecting the number of clusters of individuals using the software STRUCTURE: a simulation study. Mol. Ecol. 14(8)**:** 2611-2620.

Fougère-Danezan, M., S. Joly, A. Bruneau, X.-F. Gao, and L.-B. Zhang. 2015. Phylogeny and biogeography of wild roses with specific attention to polyploids. Annals of Botany. 115(2)**:** 275-291.

Gachomo, E.W., and S.O. Kotchoni. 2007. Detailed description of developmental growth stages of *Diplocarpon rosae* in *Rosa*: a core building block for efficient disease management. Ann. Appl. Biol. 151(2)**:** 233-243.

Gar, O., D.J. Sargent, C.-J. Tsai, T. Pleban, G. Shalev, D.H. Byrne, and D. Zamir. 2011. An autotetraploid linkage map of rose (*Rosa hybrida*) validated using the strawberry (*Fragaria vesca*) genome sequence. PloS one. 6(5)**:** e20463-e20463.

Garbez, M., R. Symoneaux, É. Belin, Y. Caraglio, Y. Chéné, N. Dones, J.-B. Durand, G. Hunault, D. Relion, and M. Sigogne. 2018. Ornamental plants architectural characteristics in relation to visual sensory attributes: a new approach on the rose bush for objective evaluation of the visual quality. European J. Hort. Sci. 83(3)**:** 187-201.

Girault, T., V. Bergougnoux, D. Combes, J.D. Viemont, and N. Leduc. 2008. Light controls shoot meristem organogenic activity and leaf primordia growth during bud burst in *Rosa* sp. Plant, Cell & Environ. 31(11)**:** 1534-1544.

Gitonga, V.W., C.F. Koning-Boucoiran, K. Verlinden, O. Dolstra, R.G. Visser, C. Maliepaard, and F.A. Krens. 2014. Genetic variation, heritability and genotype by environment interaction of morphological traits in a tetraploid rose population. BMC Genet. 15(1)**:** 146.

Greyvenstein, O.F. 2013. Phenotyping of high temperature susceptibility in garden roses (*Rosa x hybrida*). Texas A&M University, College Station, TX. PhD Diss.

Gudin, S. 2003. Breeding: overview, p. 25-30. In: Roberts, A. V. (ed.) Encyclopedia of Rose Science. Oxford: Elsevier.

Guoliang, W. 2003. History of roses in cultivation: ancient Chinese roses, p. 387-395. In: Roberts, A. V. (ed.) Encyclopedia of Rose Science. Oxford: Elsevier.

Hagan, A., M. Rivas-Davila, J. Akridge, and J. Olive. 2005. Resistance of shrub and groundcover roses to black spot and Cercospora leaf spot, and impact of fungicide inputs on the severity of both diseases. J. Environ. Hort. 23(2)**:** 77-85.

Hattendorf, A., M. Linde, L. Mattiesch, T. Debener, and H. Kaufmann. 2003. Genetic analysis of rose resistance genes and their localisation in the rose genome. Acta Hort. 651**:** 123-130.

He, J., X. Zhao, A. Laroche, Z.-X. Lu, H. Liu, and Z. Li. 2014. Genotyping-by-sequencing (GBS), an ultimate marker-assisted selection (MAS) tool to accelerate plant breeding. Frontiers in Plant Sci. 5(484).

Heo, M.-S., K. Han, J.-K. Kwon, and B.-C. Kang. 2017. Development of SNP markers using genotyping-by-sequencing for cultivar identification in rose (*Rosa hybrida*). Hort., Environ., and Biotechnol. 58(3)**:** 292-302.

Hibrand Saint-Oyant, L., T. Ruttink, L. Hamama, I. Kirov, D. Lakhwani, N.N. Zhou, P.M. Bourke, N. Daccord, L. Leus, D. Schulz, H. Van de Geest, T. Hesselink, K. Van Laere, K. Debray, S. Balzergue, T. Thouroude, A. Chastellier, J. Jeauffre, L. Voisine, S. Gaillard, T.J.A. Borm, P. Arens, R.E. Voorrips, C. Maliepaard, E.

Neu, M. Linde, M.C. Le Paslier, A. Bérard, R. Bounon, J. Clotault, N. Choisne, H. Quesneville, K. Kawamura, S. Aubourg, S. Sakr, M.J.M. Smulders, E. Schijlen, E. Bucher, T. Debener, J. De Riek, and F. Foucher. 2018. A high-quality genome sequence of Rosa chinensis to elucidate ornamental traits. Nature Plants. 4(7)**:** 473-484.

Historical temperatures [Online]. 2020. Texas A&M AgriLife Research and Extension Center at Overton. Available: <http://etweather.tamu.edu/datatable/> [Accessed 12 May 2020].

Hodges, A.W., H. Khachatryan, M.A. Palma, and C.R. Hall. 2015. Production and marketing practices and trade flows in the United States green industry in 2013. J. Environ. Hort. 33(3)**:** 125-136.

Holland, J.B., W.E. Nyquist, and C.T. Cervantes-Martínez. 2003. Estimating and interpreting heritability for plant breeding: an update. Plant Breeding Rev. 22.

Holtz, Y., J.L. David, and V. Ranwez. 2017. The genetic map comparator: a user-friendly application to display and compare genetic maps. Bioinformatics. 33(9).

Horst, R.K., and R.A. Cloyd. 2007. Compendium of rose diseases and pests. American Phytopathological Society (APS Press), St. Paul, MN.

Huché-Thélier, L., R. Boumaza, S. Demotes-Mainard, A. Canet, R. Symoneaux, O. Douillet, and V. Guérin. 2011. Nitrogen deficiency increases basal branching and modifies visual quality of the rose bushes. Scientia Hort. 130(1)**:** 325-334.

Hutton, S. 2012. The future of the rose industry. Am. Rose. 41(12)**:** 36.

Iwata, H., A. Gaston, A. Remay, T. Thouroude, J. Jeauffre, K. Kawamura, L.H.S. Oyant, T. Araki, B. Denoyes, and F. Foucher. 2012. The TFL1 homologue KSN is a regulator of continuous flowering in rose and strawberry. Plant J. 69(1)**:** 116-125.

Jian, H., H. Zhang, K. Tang, S. Li, Q. Wang, T. Zhang, X. Qiu, and H. Yan. 2010. Decaploidy in *Rosa praelucens* Byhouwer (Rosaceae) endemic to Zhongdian Plateau, Yunnan, China. Caryologia. 63(2)**:** 162-167.

Joyaux, F. 2003. History of roses in cultivation: European (Pre-1800), p. 395-402. In: Roberts, A. V. (ed.) Encyclopedia of Rose Science. Oxford: Elsevier.

Kang, S. 2020. Resistance of garden roses to cercospora leaf spot. Texas A&M University, College Station, TX. Masters Thesis.

Kawamura, K., L. Hibrand-Saint Oyant, L. Crespel, T. Thouroude, D. Lalanne, and F. Foucher. 2011. Quantitative trait loci for flowering time and inflorescence architecture in rose. Theor. Appl. Genet. 122(4)**:** 661-675.

Kawamura, K., L. Hibrand-Saint Oyant, T. Thouroude, J. Jeauffre, and F. Foucher. 2015. Inheritance of garden rose architecture and its association with flowering behaviour. Tree Genet. & Genomes. 11(2)**:** 22.

Kevan, P.G., D. Eisikowitch, J.D. Ambrose, and J.R. Kemp. 1990. Cryptic dioecy and insect pollination in *Rosa setigera* Michx. (Rosaceae), a rare plant of Carolinian Canada. Biol. J. of the Linnean Soc. 40(3)**:** 229-243.

Khayat, E., and N. Zieslin. 1982. Environmental factors involved in the regulation of sprouting of basal buds in rose plants. J. Experimental Bot. 33(6)**:** 1286-1292.

Koning-Boucoiran, C.F., G.D. Esselink, M. Vukosavljev, W.P. Van't Westende, V.W. Gitonga, F.A. Krens, R.E. Voorrips, W.E. van de Weg, D. Schulz, and T. Debener. 2015. Using RNA-Seq to assemble a rose transcriptome with more than 13,000 full-length expressed genes and to develop the WagRhSNP 68k Axiom SNP array for rose (*Rosa* L.). Frontiers Plant Sci. 6.

Krüssman, G. 1981. The complete book of roses. Timber Press, Portland, Oregon.

Kumar, S., G. Stecher, M. Li, C. Knyaz, and K. Tamura. 2018. MEGA X: molecular evolutionary genetics analysis across computing platforms. Mol. Biol. Evolution. 35(6)**:** 1547-1549.

Laney, A.G., K.E. Keller, R.R. Martin, and I.E. Tzanetakis. 2011. A discovery 70 years in the making: characterization of the rose rosette virus. J. Gen. Virol. 92(7)**:** 1727-1732.

Lata, P. 1982. Cytological studies in the genus *Rosa*. Cytologia. 47(3-4)**:** 631-637.

Lewis, W.H. 2016. Nomenclatural novelties in *Rosa* (Rosaceae) subgenus Rosa recognized in North America. Novon: J. Botanical Nomenclature. 25(1)**:** 22-46.

Lewis, W.H., and R.E. Basye. 1961. Analysis of nine crosses between diploid *Rosa* species. Am. Soc. Hort. Sci. 78**:** 572-579.

Li-Marchetti, C., C. Le Bras, A. Chastellier, D. Relion, P. Morel, S. Sakr, L. Hibrand-Saint Oyant, and L. Crespel. 2017. 3D phenotyping and QTL analysis of a complex character: rose bush architecture. Tree Genet. & Genomes. 13(5)**:** 112.

Li, S., G. Yang, S. Yang, J. Just, H. Yan, N. Zhou, H. Jian, Q. Wang, M. Chen, and X. Qiu. 2019. The development of a high-density genetic map significantly

improves the quality of reference genome assemblies for rose. Scientific Rpt. 9(1)**:** 1-13.

Linde, M., A. Hattendorf, H. Kaufmann, and T. Debener. 2006. Powdery mildew resistance in roses: QTL mapping in different environments using selective genotyping. Theor. Appl. Genet. 113(6)**:** 1081-1092.

Lipka, A.E., F. Tian, Q. Wang, J. Peiffer, M. Li, P.J. Bradbury, M.A. Gore, E.S. Buckler, and Z. Zhang. 2012. GAPIT: genome association and prediction integrated tool. Bioinformatics. 28(18)**:** 2397-2399.

Liu, J., X. Fu, Y. Dong, J. Lu, M. Ren, N. Zhou, and C. Wang. 2018. MIKCC-type MADS-box genes in *Rosa chinensis*: the remarkable expansion of ABCDE model genes and their roles in floral organogenesis. Hort. Res. 5(1)**:** 25.

Liu, X., M. Huang, B. Fan, E.S. Buckler, and Z. Zhang. 2016. Iterative usage of fixed and random effect models for powerful and efficient genome-wide association studies. PLoS Genet. 12(2)**:** e1005767.

Lyon, L.J. 1968. Estimating Twig Production of Serviceberry from Crown Volumes. J. Wildlife Mgt. 32(1)**:** 115-119.

Madden, L.V., G. Hughes, and F. Van Den Bosch. 2007. The study of plant disease epidemics. Am. Phytopath. Soc., St. Paul, MN.

Mangandi, J., and N.A. Peres. 2009. Cercospora Leaf Spot of Rose. Gainesville, FL: University of Florida IFAS Extension.

Marriott, M. 2003. History of roses in cultivation: modern (post-1800), p. 402-409. In: Roberts, A. V. (ed.) Encyclopedia of Rose Science. Oxford: Elsevier.

Mian, M.A.R., A.M. Missaoui, D.R. Walker, D.V. Phillips, and H.R. Boerma. 2008. Frogeye leaf spot of soybean: a review and proposed race designations for isolates of *Cercospora sojina* Hara. Crop Sci. 48(1)**:** 14-24.

Moghaddam, H.H., L. Leus, J. De Riek, J. Van Huylenbroeck, and E. Van Bockstaele. 2012. Construction of a genetic linkage map with SSR, AFLP and morphological markers to locate QTLs controlling pathotype-specific powdery mildew resistance in diploid roses. Euphytica. 184(3)**:** 413-427.

Morel, P., L. Crespel, G. Galopin, and B. Moulia. 2012. Effect of mechanical stimulation on the growth and branching of garden rose. Scientia Hort. 135**:** 59-64.

Morel, P., G. Galopin, and N. Donès. 2009. Using architectural analysis to compare the shape of two hybrid tea rose genotypes. Scientia Hort. 120(3)**:** 391-398.

Morishige, D.T., P.E. Klein, J.L. Hilley, S.M.E. Sahraeian, A. Sharma, and J.E. Mullet. 2013. Digital genotyping of sorghum–a diverse plant species with a large repeat-rich genome. BMC genomics. 14(1)**:** 448.

Münnekhoff, A.K., M. Linde, and T. Debener. 2017. The gene diversity pattern of *Diplocarpon rosae* populations is shaped by the age, diversity and fungicide treatment of their host populations. Plant Pathol. 66(8)**:** 1288-1298.

Myles, S., J. Peiffer, P.J. Brown, E.S. Ersoz, Z. Zhang, D.E. Costich, and E.S. Buckler. 2009. Association mapping: critical considerations shift from genotyping to experimental design. Plant Cell. 21(8)**:** 2194-2202.

Nakamura, N., H. Hirakawa, S. Sato, S. Otagaki, S. Matsumoto, S. Tabata, and Y. Tanaka. 2018. Genome structure of *Rosa multiflora*, a wild ancestor of cultivated roses. DNA Res. 25(2)**:** 113-121.

Nguyen, T.H.N., D. Schulz, T. Winkelmann, and T. Debener. 2017. Genetic dissection of adventitious shoot regeneration in roses by employing genome-wide association studies. Plant Cell Rpt. 36(9)**:** 1493-1505.

Nguyen, T.H.N., S. Tänzer, J. Rudeck, T. Winkelmann, and T. Debener. 2020. Genetic analysis of adventitious root formation in vivo and in vitro in a diversity panel of roses. Scientia Hort. 266**:** 109277.

NRCS. 2019. Web Soil Survey - Burleson County [Online]. United States Department of Agriculture. Available: <http://websoilsurvey.sc.egov.usda.gov/App/WebSoilSurvey.aspx> [Accessed 12 May 2020].

NWS. 2019. College Station extremes, normals, and annual summaries [Online]. National Weather Service. Available: https://www.weather.gov/hgx/climate_cll_normals_summary#2018 [Accessed 24 April 2020].

Oraguzie, N.C., S.E. Gardiner, E.H. Rikkerink, and H.N. Silva. 2007. Association mapping in plants. Springer, New York, NY.

Ouellette, L.A., R.W. Reid, S.G. Blanchard, and C.R. Brouwer. 2018. LinkageMapView—rendering high-resolution linkage and QTL maps. Bioinformatics. 34(2)**:** 306-307.

Peek, J.M. 1970. Relation of canopy area and volume to production of three woody species. Ecology. 51(6)**:** 1098-1101.

Perez-Harguindeguy, N., S. Diaz, E. Garnier, S. Lavorel, H. Poorter, P. Jaureguiberry, M. Bret-Harte, W. Cornwell, J. Craine, and D. Gurvich. 2016. New handbook for standardised measurement of plant functional traits worldwide. Aust. J. Bot. 64**:** 715-716.

Pham, A.-T., D.K. Harris, J. Buck, A. Hoskins, J. Serrano, H. Abdel-Haleem, P. Cregan, Q. Song, H.R. Boerma, and Z. Li. 2015. Fine mapping and characterization of candidate genes that control resistance to *Cercospora sojina* K. Hara in two soybean germplasm accessions. PloS one. 10(5).

Preedy, K., and C. Hackett. 2016. A rapid marker ordering approach for high-density genetic linkage maps in experimental autotetraploid populations using multidimensional scaling. Theor. Appl. Genet. 129(11)**:** 2117-2132.

Pritchard, J.K., M. Stephens, and P. Donnelly. 2000. Inference of population structure using multilocus genotype data. Genetics. 155(2)**:** 945-959.

Purcell, S., and C. Chang. 2015. PLINK 1.9. https://www.cog-genomics.org/plink2.

Purcell, S., B. Neale, K. Todd-Brown, L. Thomas, M.A. Ferreira, D. Bender, J. Maller, P. Sklar, P.I. De Bakker, and M.J. Daly. 2007. PLINK: a tool set for whole-genome association and population-based linkage analyses. Am. J. Human Genet. 81(3)**:** 559-575.

Rajapakse, S., D. Byrne, L. Zhang, N. Anderson, K. Arumuganathan, and R. Ballard. 2001. Two genetic linkage maps of tetraploid roses. Theor. Appl. Genet. 103(4)**:** 575-583.

Rastas, P., F.C. Calboli, B. Guo, T. Shikano, and J. Merilä. 2016. Construction of ultradense linkage maps with Lep-MAP2: stickleback F 2 recombinant crosses as an example. Genome Biol. and evolution. 8(1)**:** 78-93.

Raymond, O., J. Gouzy, J. Just, H. Badouin, M. Verdenaud, A. Lemainque, P. Vergne, S. Moja, N. Choisne, and C. Pont. 2018. The *Rosa* genome provides new insights into the domestication of modern roses. Nature Genet. 50(6)**:** 772-777.

Rehder, A., and T.R. Dudley. 1940. Manual of cultivated trees and shrubs hardy in North America: exclusive of the subtropical and warmer temperate regions. Macmillan New York.

Rieksta, D., G. Jakobsone, and A. Rihtere. 2003. Classical breeding of *Rosa rugosa* roses and in vitro cultivation of immature embryos as an expanded resource for selection. Acta Hort. 612**:** 35-38.

Rife, T., and J.A. Poland. 2014. Field Book: an open-source application for field data collection on Android. Crop Sci. 54(4)**:** 1624-1627.

Ritz, C.M., and V. Wissemann. 2005. The genus *Rosa* (Rosoideae, Rosaceae) revisited: molecular analysis of nrITS-1 and atpB-rbcL intergenic spacer (IGS) versus conventional taxonomy. Botanical J. Linnean Soc. 147(3)**:** 275-290.

Roberts, A.V., T. Gladis, and H. Brumme. 2009. DNA amounts of roses (*Rosa* L.) and their use in attributing ploidy levels. Plant Cell Rpt. 28(1)**:** 61-71.

Ronin, Y.I., D.I. Mester, D.G. Minkov, E. Akhunov, and A.B. Korol. 2017. Building ultra-high-density linkage maps based on efficient filtering of trustable markers. Genetics. 206(3)**:** 1285-1295.

Schulz, D., M. Linde, O. Blechert, and T. Debener. 2009. Evaluation of genus *Rosa* germplasm for resistance to black spot, downy mildew and powdery mildew. European J. Hort. Sci. 74(1)**:** 1.

Schulz, D.F., R.T. Schott, R.E. Voorrips, M.J. Smulders, M. Linde, and T. Debener. 2016. Genome-wide association analysis of the anthocyanin and carotenoid contents of rose petals. Frontiers in Plant Sci. 7.

Smulders, M.J., P. Arens, P.M. Bourke, T. Debener, M. Linde, J. De Riek, L. Leus, T. Ruttink, S. Baudino, and L.H. Saint-Oyant. 2019. In the name of the rose: a roadmap for rose research in the genome era. Hort. Res. 6(1)**:** 1-17.

Smulders, M.J.M., P. Arens, C.F.S. Koning-Boucoiran, V.W. Gitonga, F.A. Krens, A. Atanassov, I. Atanassov, K.E. Rusanov, M. Bendahmane, A. Dubois, O. Raymond, J.C. Caissard, S. Baudino, L. Crespel, S. Gudin, S.C. Ricci, N. Kovatcheva, J. Van Huylenbroeck, L. Leus, V. Wissemann, H. Zimmermann, I. Hensen, G. Werlemark, and H. Nybom. 2011. Rosa, 243-275. In: Kole, C. (ed.) Wild Crop Relatives: Genomic and Breeding Resources: Plantation and Ornamental Crops. Berlin, Heidelberg: Springer.

Soufflet-Freslon, V., B. Marolleau, T. Thouroude, A. Chastellier, S. Pierre, M. Bellanger, B. Le Cam, C. Bonneau, L. Porcher, and A. Leclere. 2019.

Development of tools to study rose resistance to black spot. Acta Hort. 1232**:** 213-220.

Soules, V.A. 2009. Analysis of genetic diversity and relationships in the China rose group. Texas A&M University, College Station, TX. Masters Thesis.

Spethmann, W., and B. Feuerhahn. 2003. Genetics: species crosses, p. 299-312. In: Roberts, A. V. (ed.) Encyclopedia of Rose Science. Oxford: Elsevier.

Spiller, M., M. Linde, L. Hibrand-Saint Oyant, C.-J. Tsai, D.H. Byrne, M.J. Smulders, F. Foucher, and T. Debener. 2011. Towards a unified genetic map for diploid roses. Theor. Appl. Genet. 122(3)**:** 489-500.

Thorne, M.S., Q.D. Skinner, M.A. Smith, J.D. Rodgers, W.A. Laycock, and S.A. Cerekci. 2002. Evaluation of a technique for measuring canopy volume of shrubs. Rangeland Ecol. & Mgt. 55(3)**:** 235-241.

Ueckert, J.A. 2014. Understanding and manipulating polyploidy in garden roses. Texas A&M University, College Station, TX. Masters Thesis.

Ueda, Y., and S. Akimoto. 2001. Cross-and self-compatibility in various species of the genus *Rosa*. J. Hort. Sci. Biotechnol. 76(4)**:** 392-395.

UPOV. 2010. Rose: guidelines for the conduct of tests for distinctness, uniformity and stability. Geneva: International Union for the Protection of New Varieties of Plants.

U.S. Dept. Agr. 2015. Census of horticultural specialties (2014). Washington, D.C., Natl. Agr. Stat. Serv.

van Muijen, D., R. Basnet, N. Dek, C. Maliepaard, and E. Gutteling. 2017. Mapfuser: an integrative toolbox for consensus map construction and Marey maps. bioRxiv. 200311.

VanRaden, P.M. 2008. Efficient methods to compute genomic predictions. J. Dairy Sci. 91(11)**:** 4414-4423.

Videira, S., J. Groenewald, C. Nakashima, U. Braun, R.W. Barreto, P.J. de Wit, and P. Crous. 2017. Mycosphaerellaceae–chaos or clarity? Studies in Mycol. 87**:** 257-421.

Von Malek, B., W. Weber, and T. Debener. 2000. Identification of molecular markers linked to *Rdr1*, a gene conferring resistance to blackspot in roses. Theor. Appl. Genet. 101(5-6)**:** 977-983.

Voorrips, R.E. 2002. MapChart: software for the graphical presentation of linkage maps and QTLs. J. Heredity. 93(1)**:** 77-78.

Vukosavljev, M., P. Arens, R.E. Voorrips, W.P. van‘t Westende, G. Esselink, P.M. Bourke, P. Cox, E. van de Weg, R.G. Visser, and C. Maliepaard. 2016. High-density SNP-based genetic maps for the parents of an outcrossed and a selfed tetraploid garden rose cross, inferred from admixed progeny using the 68k rose SNP array. Hort. Res. 3(1)**:** 1-8.

Waliczek, T.M., D. Byrne, and D. Holeman. 2018. Opinions of landscape roses available for purchase and preferences for the future market. HortTechnol. 28(6)**:** 807-814.

Weiland, J., and G. Koch. 2004. Sugarbeet leaf spot disease (*Cercospora beticola* Sacc.). Mol. Plant Pathol. 5(3)**:** 157-166.

Whitaker, V.M., J.M. Bradeen, T. Debener, A. Biber, and S.C. Hokanson. 2010. *Rdr3*, a novel locus conferring black spot disease resistance in tetraploid rose: genetic analysis, LRR profiling, and SCAR marker development. Theor. Appl. Genet. 120(3)**:** 573-585.

Wickham, H. 2009. ggplot2: elegant graphics for data analysis. New York: Springer-Verlag.

Windham, M., A. Windham, F. Hale, and J. Amrine Jr. 2014. Observations on rose rosette disease. Am. Rose. 42(9)**:** 56-62.

Wissemann, V. 2003. Classification: conventional taxonomy (wild roses), p. 111-117. In: Roberts, A. V. (ed.) Encyclopedia of Rose Science. Oxford: Elsevier.

Wolf, F.A. 1912. The perfect stage of *Actinonema rosae*. Botanical Gaz. 54(3)**:** 218-234.

Wu, X., S. Liang, and D.H. Byrne. 2019a. Architectural components of compact growth habits in diploid roses. HortTechnol. 29(5)**:** 1-5.

Wu, X., S. Liang, and D.H. Byrne. 2019b. Heritability of plant architecture in diploid roses (*Rosa* spp.). HortSci. 54(2)**:** 236-239.

Würschum, T. 2012. Mapping QTL for agronomic traits in breeding populations. Theor. Appl. Genet. 125(2)**:** 201-210.

Yan, M., D. Byrne, P. Klein, W. van de Weg, J. Yang, and L. Cai. 2019. Black spot partial resistance in diploid roses: QTL discovery and linkage map creation. Acta Hort. 1232**:** 135-141.

Yan, M., D.H. Byrne, P.E. Klein, J. Yang, Q. Dong, and N. Anderson. 2018. Genotyping-by-sequencing application on diploid rose and a resulting high-density SNP-based consensus map. Hort. Res. 5(1)**:** 17.

Yan, Z., C. Denneboom, A. Hattendorf, O. Dolstra, T. Debener, P. Stam, and P. Visser. 2005a. Construction of an integrated map of rose with AFLP, SSR, PK, RGA, RFLP, SCAR and morphological markers. Theor. Appl. Genet. 110(4)**:** 766-777.

Yan, Z., O. Dolstra, T. Hendriks, T. Prins, P. Stam, and P. Visser. 2005b. Vigour evaluation for genetics and breeding in rose. Euphytica. 145(3)**:** 339-347.

Yan, Z., P. Visser, T. Hendriks, T. Prins, P. Stam, and O. Dolstra. 2007. QTL analysis of variation for vigour in rose. Euphytica. 154(1-2)**:** 53.

Yokoya, K., A. Roberts, J. Mottley, R. Lewis, and P. Brandham. 2000. Nuclear DNA amounts in roses. Ann. Bot. 85(4)**:** 557-561.

Yu, C., L. Luo, H. Pan, X. Guo, H. Wan, and Q. Zhang. 2015. Filling gaps with construction of a genetic linkage map in tetraploid roses. Frontiers in plant science. 5**:** 796.

Yu, J., G. Pressoir, W.H. Briggs, I.V. Bi, M. Yamasaki, J.F. Doebley, M.D. McMullen, B.S. Gaut, D.M. Nielsen, and J.B. Holland. 2006. A unified mixed-model method for association mapping that accounts for multiple levels of relatedness. Nature Genet. 38(2)**:** 203-208.

Zlesak, D. 2004. The hanging drop pollen germination assay-a tool to assess fertility. Rose Hybridizers Assoc. Nwsl. 35(3)**:** 10-12.

Zlesak, D.C. 1998. Rugosas, a breeding challenge. Rose Hybridizers Assoc. Nwsl. 29(2).

Zlesak, D.C. 2009. Pollen diameter and guard cell length as predictors of ploidy in diverse rose cultivars, species, and breeding lines. Flor. and Orn. Biotechnol. 3(1)**:** 53-70.

Zurn, J.D., D.C. Zlesak, M. Holen, J.M. Bradeen, S.C. Hokanson, and N.V. Bassil. 2018. Mapping a novel black spot resistance locus in the climbing rose Brite Eyes™(‘RADbrite’). Frontiers Plant Sci. 9**:** 1730.

APPENDIX A

RESULTS OF DIPLOID ROSE POLLINATIONS MADE FROM 2015 TO 2017 BY THE TEXAS A&M ROSE BREEDING AND GENETICS PROGRAM AND WEEKS ROSES.

Female	Male	Year	Num. pollinations	Num. hips	Num. seeds	Num. seedlings
Baltimore Belle	M4-4	2016	60	0	0	0
Baltimore Belle	Papa Hemeray	2016	65	0	0	0
Basye's Purple	J06-20-14-3	2015	20	3	9	4
Basye's Purple	J06-20-14-3	2016	68	30	40	3
Basye's Purple	Old Blush	2016	44	7	9	2
Basye's Purple	*R. palustris* f. *plena* EB-ARE	2015	16	2	8	0
Basye's Purple	*R. palustris* f. *plena* OB-ARE	2015	6	0	0	6
Basye's Purple	Srdce Europy	2016	1	0	0	0
Champney's Pink Cluster	Old Blush	2016	10	0	0	0
Champney's Pink Cluster	*R. palustris* f. *plena* EB-ARE	2016	32	0	0	0
Champney's Pink Cluster	*R. palustris* EB-MM	2016	16	1	3	0
J06-20-14-3	Basye's Purple	2016	353	40	14	0
J06-20-14-3	Papa Hemeray	2015		44	270	87
J06-20-14-3	Papa Hemeray	2016	194	111	385	104
J06-20-14-3	*R. palustris* f. *plena* EB-ARE	2015	34	1	1	0
J06-20-14-3	*R. palustris* f. *plena* EB-ARE	2016		56	138	21
J06-20-14-3	*R. palustris* EB-MM	2016		91	783	119
J06-20-14-3	*R. palustris* f. *plena* OB-ARE	2015	127	6		0
J06-20-14-3	*R. palustris* f. *plena* OB-ARE	2016		23	19	5
J06-20-14-3	*R. palustris* OB-PrM	2017	22	5	21	0
J06-20-14-3	Srdce Europy	2016	48	18	0	0
Lena (Baiena)	*R. palustris* f. *plena* EB-ARE	2016	35	12	26	5
Lena (Baiena)	*R. palustris* f. *plena* EB-ARE	2017	335	3	4	0
Lena (Baiena)	*R. palustris* EB-MM	2017	417	15	18	2

Female	Male	Year	Num. pollinations	Num. hips	Num. seeds	Num. seedlings
Lena (Baiena)	*R. palustris* f. *plena* OB-ARE	2016	32	8	20	14
Lena (Baiena)	*R. palustris* f. *plena* OB-ARE	2017	111	2	2	0
Lena (Baiena)	*R. palustris* OB-PrM	2017	32	10	41	0
Lena (Baiena)	Snow Pavement	2017		65	184	4
Lena (Baiena)	Sweet Vigorosa	2017	74	2	2	0
Lena (Baiena)	Topaz Jewel (MORyelrug)	2017		34	51	
M4-4	Basye's Purple	2015	42	8	17	4
M4-4	Basye's Purple	2016	141	28	12	3
M4-4	*R. palustris* f. *plena* EB-ARE	2015	52	26	50	1
M4-4	*R. palustris* f. *plena* EB-ARE	2016	252	59	87	12
M4-4	*R. palustris* f. *plena* EB-ARE	2017	22	17	25	0
M4-4	*R. palustris* EB-MM	2016	95	45	365	12
M4-4	*R. palustris* EB-MM	2017	241	213	1211	76
M4-4	*R. palustris* f. *plena* OB-ARE	2015	12	4	6	2
M4-4	*R. palustris* f. *plena* OB-ARE	2016	211	75	26	3
M4-4	*R. palustris* f. *plena* OB-ARE	2017	98	72	59	3
M4-4	*R. palustris* OB-PrM	2017	26	18	25	1
M4-4	Srdce Europy	2016	62	50	78	34
M4-4	Sweet Vigorosa	2017	91	57	23	7
Moser House Shed Rose	M4-4	2017	79	1	2	1
Old Blush	Basye's Purple	2015	19	2	1	0
Old Blush	*R. palustris* f. *plena* EB-ARE	2015	29	4	6	1
Old Blush	*R. palustris* f. *plena* EB-ARE	2016	84	10	19	2
Old Blush	*R. palustris* f. *plena* EB-ARE	2017	207	17	28	2
Old Blush	*R. palustris* EB-MM	2016	88	22	45	9
Old Blush	*R. palustris* EB-MM	2017	114	33	150	2
Old Blush	*R. palustris* f. *plena* OB-ARE	2015	6	3	5	2
Old Blush	*R. palustris* f. *plena* OB-ARE	2016	156	36	12	1
Old Blush	*R. palustris* f. *plena* OB-ARE	2017	119	25	61	
Old Blush	Srdce Europy	2016	20	10	30	2

Female	Male	Year	Num. pollinations	Num. hips	Num. seeds	Num. seedlings
Ole (Baiole)	*R. palustris* f. *plena* EB-ARE	2016	60	25	75	27
Ole (Baiole)	*R. palustris* f. *plena* EB-ARE	2017	146	12	30	0
Ole (Baiole)	*R. palustris* EB-MM	2017	373	58	408	17
Ole (Baiole)	*R. palustris* f. *plena* OB-ARE	2016	67	12	39	16
Ole (Baiole)	Snow Pavement	2017		33	137	28
Ole (Baiole)	Topaz Jewel (MORyelrug)	2017		52	105	10
Oso Happy Smoothie (ZLEcharlie)	J06-20-14-3	2015	2	0	0	0
Oso Happy Smoothie (ZLEcharlie)	M4-4	2015	17	11	44	13
Oso Happy Smoothie (ZLEcharlie)	Papa Hemeray	2015	16	5	9	3
Oso Happy Smoothie (ZLEcharlie)	*R. palustris* f. *plena* EB-ARE	2016	312	63	87	5
Oso Happy Smoothie (ZLEcharlie)	*R. palustris* EB-MM	2016	43	3	9	0
Oso Happy Smoothie (ZLEcharlie)	*R. palustris* f. *plena* OB-ARE	2016	379	34	48	8
Oso Happy Smoothie (ZLEcharlie)	Srdce Europy	2016	75	10	38	11
Papa Hemeray	Basye's Purple	2015	14	0	0	0
Papa Hemeray	*R. palustris* f. *plena* EB-ARE	2015	18	2	3	0
Papa Hemeray	*R. palustris* f. *plena* EB-ARE	2016	253	116	263	31
Papa Hemeray	*R. palustris* f. *plena* EB-ARE	2017	83	5	5	0
Papa Hemeray	*R. palustris* EB-MM	2016	90	50	229	7
Papa Hemeray	*R. palustris* EB-MM	2017	214	93	445	4
Papa Hemeray	*R. palustris* f. *plena* OB-ARE	2015	38	24	128	11
Papa Hemeray	*R. palustris* f. *plena* OB-ARE	2016	271	51	128	12
Papa Hemeray	*R. palustris* f. *plena* OB-ARE	2017	23	1	2	0
Purple Pavement	M4-4	2017	56	12	396	25
R. palustris f. *plena* EB-ARE	J06-20-14-3	2015	65	18	27	4

Female	Male	Year	Num. pollinations	Num. hips	Num. seeds	Num. seedlings
R. palustris f. *plena* EB-ARE	M4-4	2015	41	6	8	1
R. palustris f. *plena* EB-ARE	Papa Hemeray	2015	61	16	24	0
R. palustris f. *plena* OB-ARE	J06-20-14-3	2015	23	6	10	2
R. palustris f. *plena* OB-ARE	M4-4	2015	14	1	1	0
R. rugosa f. *alba*-ARE	M4-4	2017	14	1	13	10
R. rugosa f. *alba*-ARE	*R. palustris* EB-MM	2017	8	7	280	70
R. setigera-ARE	Lena (Baiena)	2016	27	26	225	90
R. setigera-ARE	Ole (Baiole)	2016	34	31	236	122
R. setigera-CH-33-17-50	M4-4	2016	158	0	0	0
R. setigera-CH-33-17-50	Papa Hemeray	2016	43	0	0	0
R. setigera-CH-33-18-42	M4-4	2016	42	0	0	0
R. setigera-CH-33-18-52	Papa Hemeray	2016	205	0	0	0
R. setigera-CH-HRG	M4-4	2016	3	0	0	0
R. setigera-CH-NBW	M4-4	2016	14	0	0	0
R. setigera-CH-NL	M4-4	2016	83	0	0	0
R. setigera-CH-U1	Old Blush	2016	23	0	0	0
R. setigera-CH-U2	Papa Hemeray	2016	14	0	0	0
R. setigera-CH-U2	Srdce Europy	2016	4	0	0	0
R. setigera-CH-U3	M4-4	2016	19	0	0	0
R. setigera-CH-U3	Oso Happy Smoothie (ZLEcharlie)	2016	8	0	0	0
R. setigera-CH-U4	Oso Happy Smoothie (ZLEcharlie)	2016	1	0	0	0
Red Drift (Meigalpio)	*R. palustris* f. *plena* EB-ARE	2015	66	1	1	0
Sarah van Fleet	J06-20-14-3	2017	12	2	11	
Snow Pavement	Lena (Baiena)	2017		50	1821	346
Snow Pavement	Ole (Baiole)	2017		21	509	103
Snow Pavement	*R. palustris* f. *plena* OB-ARE	2017		20	257	85
TAMU7-20	Oso Happy Smoothie (ZLEcharlie)	2016	226	85	415	76

Female	Male	Year	Num. pollinations	Num. hips	Num. seeds	Num. seedlings
TAMU7-20	Oso Happy Smoothie (ZLEcharlie)	2017	169	119	713	120
TAMU7-20	*R. palustris* f. *plena* EB-ARE	2016	53	4	11	1
TAMU7-20	*R. palustris* EB-MM	2016	51	25	95	1
TAMU7-20	*R. palustris* f. *plena* OB-ARE	2016	78	5	3	0
TAMU7-20	Srdce Europy	2016	135	64	388	80
TAMU7-30	Oso Happy Smoothie (ZLEcharlie)	2016		110	255	74
TAMU7-30	Oso Happy Smoothie (ZLEcharlie)	2017	198	141	1010	245
TAMU7-30	*R. palustris* f. *plena* EB-ARE	2016	96	7	13	0
TAMU7-30	*R. palustris* EB-MM	2016	56	0	0	0
TAMU7-30	*R. palustris* f. *plena* OB-ARE	2016	226	8	8	2
TAMU7-30	Srdce Europy	2016	81	38	302	117
Topaz Jewel (MORyelrug)	Lena (Baiena)	2017		1	2	
Topaz Jewel (MORyelrug)	Ole (Baiole)	2017		5	6	0
Topaz Jewel (MORyelrug)	*R. palustris* f. *plena* EB-ARE	2016	5	0	0	0
Topaz Jewel (MORyelrug)	*R. palustris* f. *plena* OB-ARE	2016	13	0	0	0

APPENDIX B

INTEGRATED CONSENSUS MAP FOR DIPLOID ROSE

Map begins on next page.

LG1 [1]

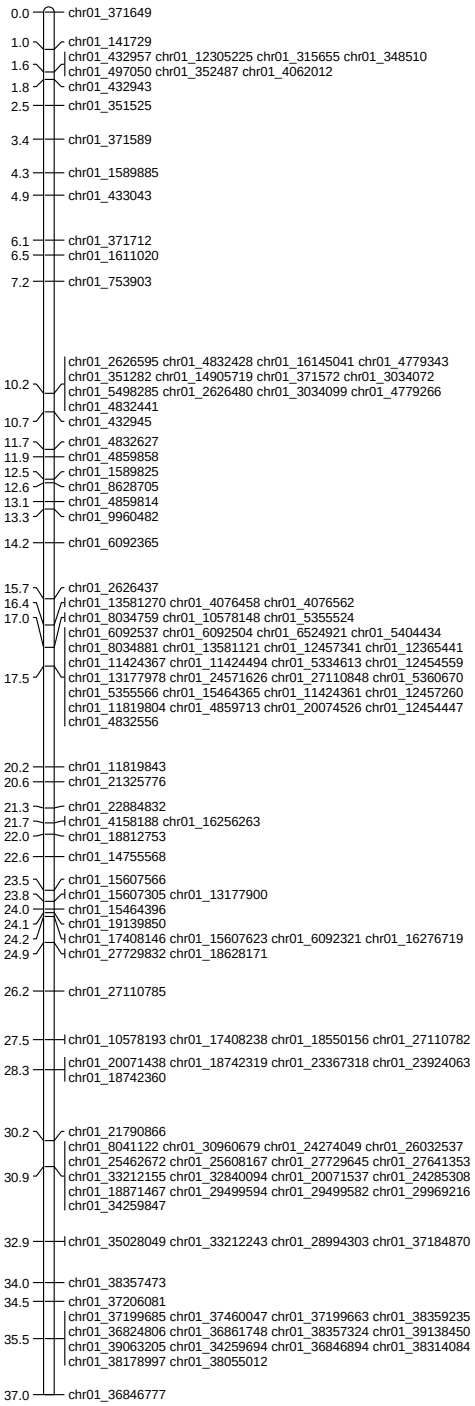
0.0 chr01_371649
1.0 chr01_141729
1.6 chr01_432957 chr01_12305225 chr01_315655 chr01_348510
chr01_497050 chr01_352487 chr01_4062012
1.8 chr01_432943
2.5 chr01_351525
3.4 chr01_371589
4.3 chr01_1589885
4.9 chr01_433043
6.1 chr01_371712
6.5 chr01_1611020
7.2 chr01_753903
chr01_2626595 chr01_4832428 chr01_16145041 chr01_4779343
chr01_351282 chr01_14905719 chr01_371572 chr01_3034072
10.2 chr01_5498285 chr01_2626480 chr01_3034099 chr01_4779266
chr01_4832441
10.7 chr01_432945
11.7 chr01_4832627
11.9 chr01_4859858
12.5 chr01_1589825
12.6 chr01_8628705
13.1 chr01_4859814
13.3 chr01_9960482
14.2 chr01_6092365
15.7 chr01_2626437
16.4 chr01_13581270 chr01_4076458 chr01_4076562
17.0 chr01_8034759 chr01_10578148 chr01_5355524
chr01_6092537 chr01_6092504 chr01_6524921 chr01_5404434
chr01_8034881 chr01_13581121 chr01_12457341 chr01_12365441
chr01_11424367 chr01_11424494 chr01_5334613 chr01_12454559
17.5 chr01_13177978 chr01_24571626 chr01_27110848 chr01_5360670
chr01_5355566 chr01_15464365 chr01_11424361 chr01_12457260
chr01_11819804 chr01_4859713 chr01_20074526 chr01_12454447
chr01_4832556
20.2 chr01_11819843
20.6 chr01_21325776
21.3 chr01_22884832
21.7 chr01_4158188 chr01_16256263
22.0 chr01_18812753
22.6 chr01_14755568
23.5 chr01_15607566
23.8 chr01_15607305 chr01_13177900
24.0 chr01_15464396
24.1 chr01_19139850
24.2 chr01_17408146 chr01_15607623 chr01_6092321 chr01_16276719
24.9 chr01_27729832 chr01_18628171
26.2 chr01_27110785
27.5 chr01_10578193 chr01_17408238 chr01_18550156 chr01_27110782
28.3 chr01_20071438 chr01_18742319 chr01_23367318 chr01_23924063
chr01_18742360
30.2 chr01_21790866
chr01_8041122 chr01_30960679 chr01_24274049 chr01_26032537
chr01_25462672 chr01_25608167 chr01_27729645 chr01_27641353
30.9 chr01_33212155 chr01_32840094 chr01_20071537 chr01_24285308
chr01_18871467 chr01_29499594 chr01_29499582 chr01_29969216
chr01_34259847
32.9 chr01_35028049 chr01_33212243 chr01_28994303 chr01_37184870
34.0 chr01_38357473
34.5 chr01_37206081
chr01_37199685 chr01_37460047 chr01_37199663 chr01_38359235
35.5 chr01_36824806 chr01_36861748 chr01_38357324 chr01_39138450
chr01_39063205 chr01_34259694 chr01_36846894 chr01_38314084
chr01_38178997 chr01_38055012
37.0 chr01_36846777

LG1 [2]

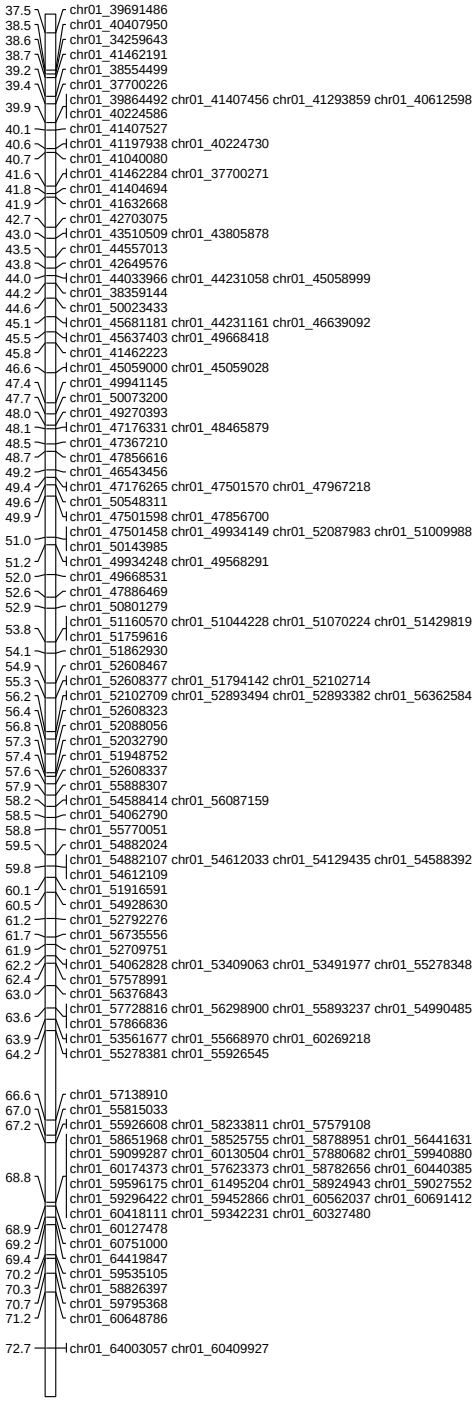
37.5 chr01_39691486
38.5 chr01_40407950
38.6 chr01_34259643
38.7 chr01_41462191
39.2 chr01_38554499
39.4 chr01_37700226
chr01_39864492 chr01_41407456 chr01_41293859 chr01_40612598
39.9 chr01_40224586
40.1 chr01_41407527
40.6 chr01_41197938 chr01_40224730
40.7 chr01_41040080
41.6 chr01_41462284 chr01_37700271
41.8 chr01_41404694
41.9 chr01_41632668
42.7 chr01_42703075
43.0 chr01_43510509 chr01_43805878
43.5 chr01_44557013
43.8 chr01_42649576
44.0 chr01_44033966 chr01_44231058 chr01_45058999
44.2 chr01_38359144
44.6 chr01_50023433
45.1 chr01_45681181 chr01_44231161 chr01_46639092
45.5 chr01_45637403 chr01_49668418
45.8 chr01_41462223
46.6 chr01_45059000 chr01_45059028
47.4 chr01_49941145
47.7 chr01_50073200
48.0 chr01_49270393
48.1 chr01_47176331 chr01_48465879
48.5 chr01_47367210
48.7 chr01_47856616
49.2 chr01_46543456
49.4 chr01_47176265 chr01_47501570 chr01_47967218
49.6 chr01_50548311
49.9 chr01_47501598 chr01_47856700
chr01_47501458 chr01_49934149 chr01_52087983 chr01_51009988
51.0 chr01_50143985
51.2 chr01_49934248 chr01_49568291
52.0 chr01_49668531
52.6 chr01_47886469
52.9 chr01_50801279
chr01_51160570 chr01_51044228 chr01_51070224 chr01_51429819
53.8 chr01_51759616
54.1 chr01_51862930
54.9 chr01_52608467
55.3 chr01_52608377 chr01_51794142 chr01_52102714
56.2 chr01_52102709 chr01_52893494 chr01_52893382 chr01_56362584
56.4 chr01_52608323
56.8 chr01_52088056
57.3 chr01_52032790
57.4 chr01_51948752
57.6 chr01_52608337
57.9 chr01_55888307
58.2 chr01_54588414 chr01_56087159
58.5 chr01_54062790
58.8 chr01_55770051
59.5 chr01_54882024
chr01_54882107 chr01_54612033 chr01_54129435 chr01_54588392
59.8 chr01_54612109
60.1 chr01_51916591
60.5 chr01_54928630
61.2 chr01_52792276
61.7 chr01_56735556
61.9 chr01_52709751
62.2 chr01_54062828 chr01_53409063 chr01_53491977 chr01_55278348
62.4 chr01_57578991
63.0 chr01_56376843
chr01_57728816 chr01_56298900 chr01_55893237 chr01_54990485
63.6 chr01_57866836
63.9 chr01_53561677 chr01_55668970 chr01_60269218
64.2 chr01_55278381 chr01_55926545
66.6 chr01_57138910
67.0 chr01_55815033
67.2 chr01_55926608 chr01_58233811 chr01_57579108
chr01_58651968 chr01_58525755 chr01_58788951 chr01_56441631
chr01_59099287 chr01_60130504 chr01_57880682 chr01_59940880
chr01_60174373 chr01_57623373 chr01_58782656 chr01_60440385
68.8 chr01_59596175 chr01_61495204 chr01_58924943 chr01_59027552
chr01_59296422 chr01_59452866 chr01_60562037 chr01_60691412
chr01_60418111 chr01_59342231 chr01_60327480
68.9 chr01_60127478
69.2 chr01_60751000
69.4 chr01_64419847
70.2 chr01_59535105
70.3 chr01_58826397
70.7 chr01_59795368
71.2 chr01_60648786
72.7 chr01_64003057 chr01_60409927

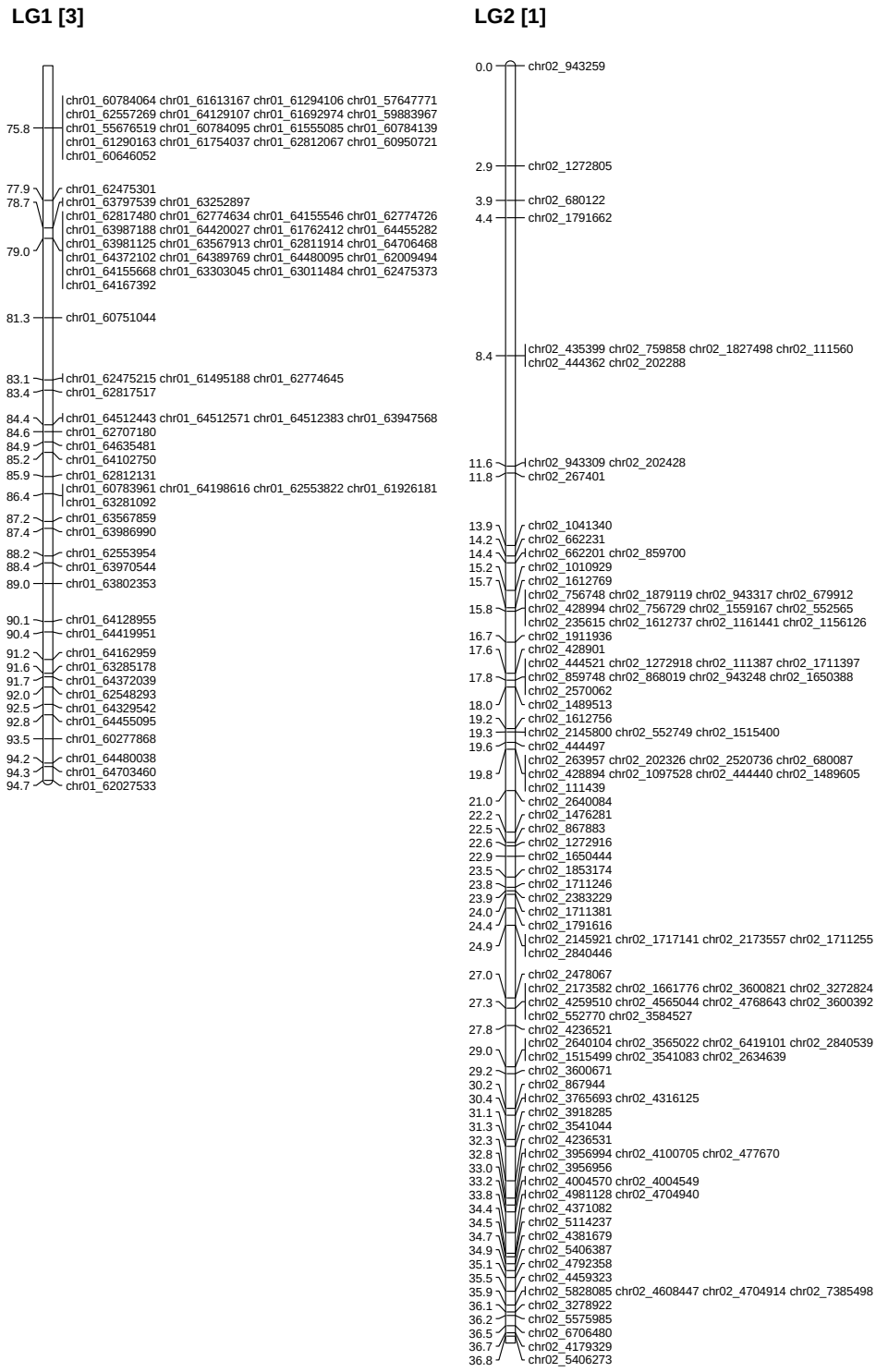
LG1 [3]
75.8 chr01_60784064 chr01_61613167 chr01_61294106 chr01_57647771 chr01_62557269 chr01_64129107 chr01_61692974 chr01_59883967 chr01_55676519 chr01_60784095 chr01_61555085 chr01_60784139 chr01_61290163 chr01_61754037 chr01_62812067 chr01_60950721 chr01_60646052
77.9 chr01_62475301
78.7 chr01_63797539 chr01_63252897 chr01_62817480 chr01_62774634 chr01_64155546 chr01_62774726 chr01_63987188 chr01_64420027 chr01_61762412 chr01_64455282
79.0 chr01_63981125 chr01_63567913 chr01_62811914 chr01_64706468 chr01_64372102 chr01_64389769 chr01_64480095 chr01_62009494 chr01_64155668 chr01_63303045 chr01_63011484 chr01_62475373 chr01_64167392
81.3 chr01_60751044
83.1 chr01_62475215 chr01_61495188 chr01_62774645
83.4 chr01_62817517
84.4 chr01_64512443 chr01_64512571 chr01_64512383 chr01_63947568
84.6 chr01_62707180
84.9 chr01_64635481
85.2 chr01_64102750
85.9 chr01_62812131
86.4 chr01_60783961 chr01_64198616 chr01_62553822 chr01_61926181 chr01_63281092
87.2 chr01_63567859
87.4 chr01_63986990
88.2 chr01_62553954
88.4 chr01_63970544
89.0 chr01_63802353
90.1 chr01_64128955
90.4 chr01_64419951
91.2 chr01_64162959
91.6 chr01_63285178
91.7 chr01_64372039
92.0 chr01_62548293
92.5 chr01_64329542
92.8 chr01_64455095
93.5 chr01_60277868
94.2 chr01_64480038
94.3 chr01_64703460
94.7 chr01_62027533
LG2 [1]
0.0 chr02_943259
2.9 chr02_1272805
3.9 chr02_680122
4.4 chr02_1791662
8.4 chr02_435399 chr02_759858 chr02_1827498 chr02_111560 chr02_444362 chr02_202288
11.6 chr02_943309 chr02_202428
11.8 chr02_267401
13.9 chr02_1041340
14.2 chr02_662231
14.4 chr02_662201 chr02_859700
15.2 chr02_1010929
15.7 chr02_1612769 chr02_756748 chr02_1879119 chr02_943317 chr02_679912
15.8 chr02_428994 chr02_756729 chr02_1559167 chr02_552565 chr02_235615 chr02_1612737 chr02_1161441 chr02_1156126
16.7 chr02_1911936
17.6 chr02_428901 chr02_444521 chr02_1272918 chr02_111387 chr02_1711397
17.8 chr02_859748 chr02_868019 chr02_943248 chr02_1650388 chr02_2570062
18.0 chr02_1489513
19.2 chr02_1612756
19.3 chr02_2145800 chr02_552749 chr02_1515400
19.6 chr02_444497
19.8 chr02_263957 chr02_202326 chr02_2520736 chr02_680087 chr02_428894 chr02_1097528 chr02_444440 chr02_1489605 chr02_111439
21.0 chr02_2640084
22.2 chr02_1476281
22.5 chr02_867883
22.6 chr02_1272916
22.9 chr02_1650444
23.5 chr02_1853174
23.8 chr02_1711246
23.9 chr02_2383229
24.0 chr02_1711381
24.4 chr02_1791616
24.9 chr02_2145921 chr02_1717141 chr02_2173557 chr02_1711255 chr02_2840446
27.0 chr02_2478067
27.3 chr02_2173582 chr02_1661776 chr02_3600821 chr02_3272824 chr02_4259510 chr02_4565044 chr02_4768643 chr02_3600392 chr02_552770 chr02_3584527
27.8 chr02_4236521
29.0 chr02_2640104 chr02_3565022 chr02_6419101 chr02_2840539 chr02_1515499 chr02_3541083 chr02_2634639
29.2 chr02_3600671
30.2 chr02_867944
30.4 chr02_3765693 chr02_4316125
31.1 chr02_3918285
31.3 chr02_3541044
32.3 chr02_4236531
32.8 chr02_3956994 chr02_4100705 chr02_477670
33.0 chr02_3956956
33.2 chr02_4004570 chr02_4004549
33.8 chr02_4981128 chr02_4704940
34.4 chr02_4371082
34.5 chr02_5114237
34.7 chr02_4381679
34.9 chr02_5406387
35.1 chr02_4792358
35.5 chr02_4459323
35.9 chr02_5828085 chr02_4608447 chr02_4704914 chr02_7385498
36.1 chr02_3278922
36.2 chr02_5575985
36.5 chr02_6706480
36.7 chr02_4179329
36.8 chr02_5406273

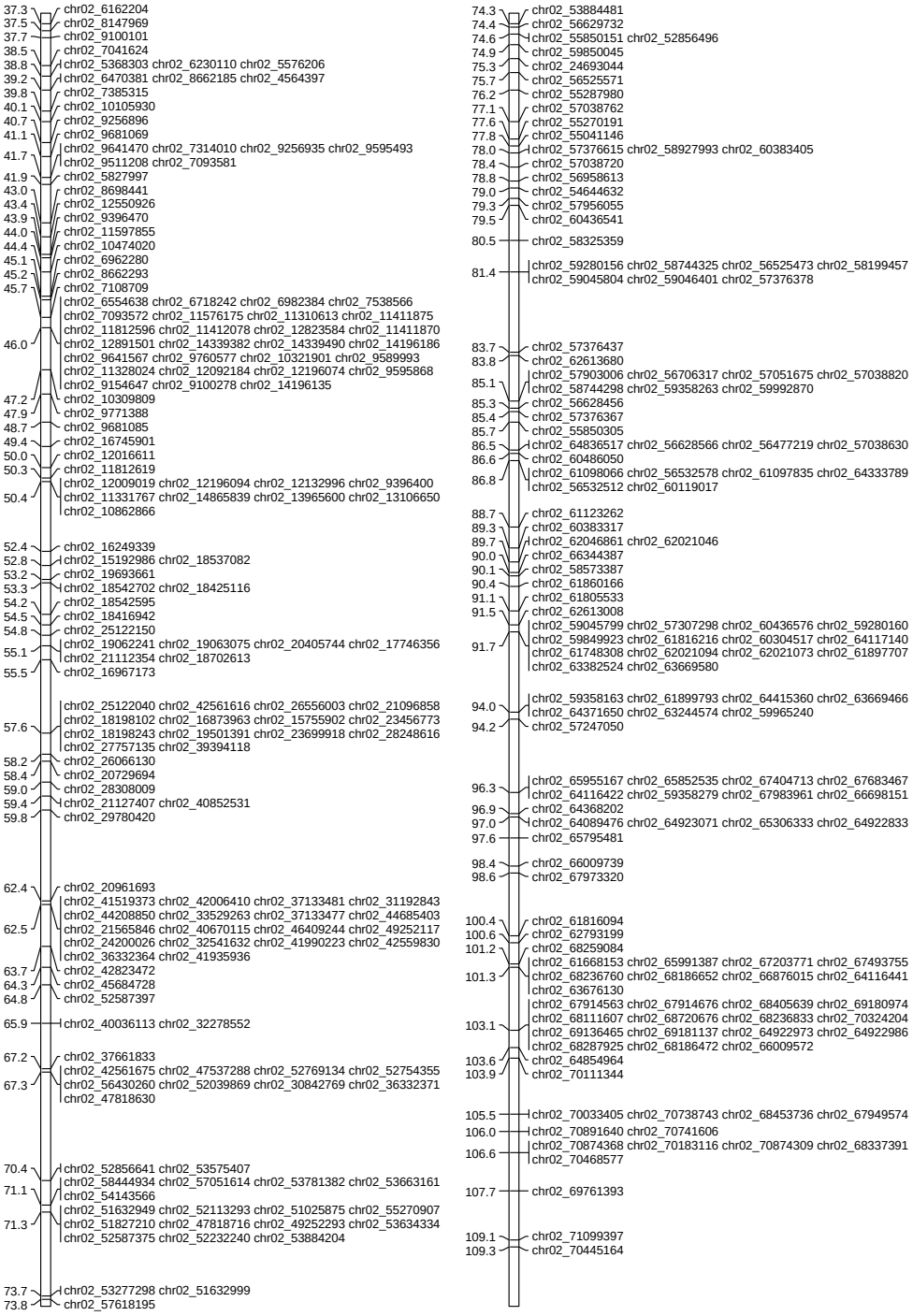
LG2 [2]
37.3 chr02_6162204
37.5 chr02_8147969
37.7 chr02_9100101
38.5 chr02_7041624
38.8 chr02_5368303 chr02_6230110 chr02_5576206
39.2 chr02_6470381 chr02_8662185 chr02_4564397
39.8 chr02_7385315
40.1 chr02_10105930
40.7 chr02_9256896
41.1 chr02_9681069
41.7 chr02_9641470 chr02_7314010 chr02_9256935 chr02_9595493
chr02_9511208 chr02_7093581
41.9 chr02_5827997
43.0 chr02_8698441
43.4 chr02_12550926
43.9 chr02_9396470
44.0 chr02_11597855
44.4 chr02_10474020
45.1 chr02_6962280
45.2 chr02_8662293
45.7 chr02_7108709
chr02_6554638 chr02_6718242 chr02_6982384 chr02_7538566
chr02_7093572 chr02_11576175 chr02_11310613 chr02_11411875
chr02_11812596 chr02_11412078 chr02_12823584 chr02_11411870
46.0 chr02_12891501 chr02_14339382 chr02_14339490 chr02_14196186
chr02_9641567 chr02_9760577 chr02_10321901 chr02_9589993
chr02_11328024 chr02_12092184 chr02_12196074 chr02_9595868
chr02_9154647 chr02_9100278 chr02_14196135
47.2 chr02_10309809
47.9 chr02_9771388
48.7 chr02_9681085
49.4 chr02_16745901
50.0 chr02_12016611
50.3 chr02_11812619
chr02_12009019 chr02_12196094 chr02_12132996 chr02_9396400
50.4 chr02_11331767 chr02_14865839 chr02_13965600 chr02_13106650
chr02_10862866
52.4 chr02_16249339
52.8 chr02_15192986 chr02_18537082
53.2 chr02_19693661
53.3 chr02_18542702 chr02_18425116
54.2 chr02_18542595
54.5 chr02_18416942
54.8 chr02_25122150
55.1 chr02_19062241 chr02_19063075 chr02_20405744 chr02_17746356
chr02_21112354 chr02_18702613
55.5 chr02_16967173
chr02_25122040 chr02_42561616 chr02_26556003 chr02_21096858
chr02_18198102 chr02_16873963 chr02_15755902 chr02_23456773
57.6 chr02_18198243 chr02_19501391 chr02_23699918 chr02_28248616
chr02_27757135 chr02_39394118
58.2 chr02_26066130
58.4 chr02_20729694
59.0 chr02_28308009
59.4 chr02_21127407 chr02_40852531
59.8 chr02_29780420
62.4 chr02_20961693
chr02_41519373 chr02_42006410 chr02_37133481 chr02_31192843
chr02_44208850 chr02_33529263 chr02_37133477 chr02_44685403
62.5 chr02_21565846 chr02_40670115 chr02_46409244 chr02_49252117
chr02_24200026 chr02_32541632 chr02_41990223 chr02_42559830
chr02_36332364 chr02_41935936
63.7 chr02_42823472
64.3 chr02_45684728
64.8 chr02_52587397
65.9 chr02_40036113 chr02_32278552
67.2 chr02_37661833
chr02_42561675 chr02_47537288 chr02_52769134 chr02_52754355
67.3 chr02_56430260 chr02_52039869 chr02_30842769 chr02_36332371
chr02_47818630
70.4 chr02_52856641 chr02_53575407
71.1 chr02_58444934 chr02_57051614 chr02_53781382 chr02_53663161
chr02_54143566
chr02_51632949 chr02_52113293 chr02_51025875 chr02_55270907
71.3 chr02_51827210 chr02_47818716 chr02_49252293 chr02_53634334
chr02_52587375 chr02_52232240 chr02_53884204
73.7 chr02_53277298 chr02_51632999
73.8 chr02_57618195
LG2 [3]
74.3 chr02_53884481
74.4 chr02_56629732
74.6 chr02_55850151 chr02_52856496
74.9 chr02_59850045
75.3 chr02_24693044
75.7 chr02_56525571
76.2 chr02_55287980
77.1 chr02_57038762
77.6 chr02_55270191
77.8 chr02_55041146
78.0 chr02_57376615 chr02_58927993 chr02_60383405
78.4 chr02_57038720
78.8 chr02_56958613
79.0 chr02_54644632
79.3 chr02_57956055
79.5 chr02_60436541
80.5 chr02_58325359
81.4 chr02_59280156 chr02_58744325 chr02_56525473 chr02_58199457
chr02_59045804 chr02_59046401 chr02_57376378
83.7 chr02_57376437
83.8 chr02_62613680
chr02_57903006 chr02_56706317 chr02_57051675 chr02_57038820
85.1 chr02_58744298 chr02_59358263 chr02_59992870
85.3 chr02_56628456
85.4 chr02_57376367
85.7 chr02_55850305
86.5 chr02_64836517 chr02_56628566 chr02_56477219 chr02_57038630
86.6 chr02_60486050
chr02_61098066 chr02_56532578 chr02_61097835 chr02_64333789
86.8 chr02_56532512 chr02_60119017
88.7 chr02_61123262
89.3 chr02_60383317
89.7 chr02_62046861 chr02_62021046
90.0 chr02_66344387
90.1 chr02_58573387
90.4 chr02_61860166
91.1 chr02_61805533
91.5 chr02_62613008
chr02_59045799 chr02_57307298 chr02_60436576 chr02_59280160
chr02_59849923 chr02_61816216 chr02_60304517 chr02_64117140
91.7 chr02_61748308 chr02_62021094 chr02_62021073 chr02_61897707
chr02_63382524 chr02_63669580
chr02_59358163 chr02_61899793 chr02_64415360 chr02_63669466
94.0 chr02_64371650 chr02_63244574 chr02_59965240
94.2 chr02_57247050
chr02_65955167 chr02_65852535 chr02_67404713 chr02_67683467
96.3 chr02_64116422 chr02_59358279 chr02_67983961 chr02_66698151
96.9 chr02_64368202
97.0 chr02_64089476 chr02_64923071 chr02_65306333 chr02_64922833
97.6 chr02_65795481
98.4 chr02_66009739
98.6 chr02_67973320
100.4 chr02_61816094
100.6 chr02_62793199
101.2 chr02_68259084
chr02_61668153 chr02_65991387 chr02_67203771 chr02_67493755
101.3 chr02_68236760 chr02_68186652 chr02_66876015 chr02_64116441
chr02_63676130
chr02_67914563 chr02_67914676 chr02_68405639 chr02_69180974
chr02_68111607 chr02_68720676 chr02_68236833 chr02_70324204
103.1 chr02_69136465 chr02_69181137 chr02_64922973 chr02_64922986
chr02_68287925 chr02_68186472 chr02_66009572
103.6 chr02_64854964
103.9 chr02_70111344
105.5 chr02_70033405 chr02_70738743 chr02_68453736 chr02_67949574
106.0 chr02_70891640 chr02_70741606
chr02_70874368 chr02_70183116 chr02_70874309 chr02_68337391
106.6 chr02_70468577
107.7 chr02_69761393
109.1 chr02_71099397
109.3 chr02_70445164

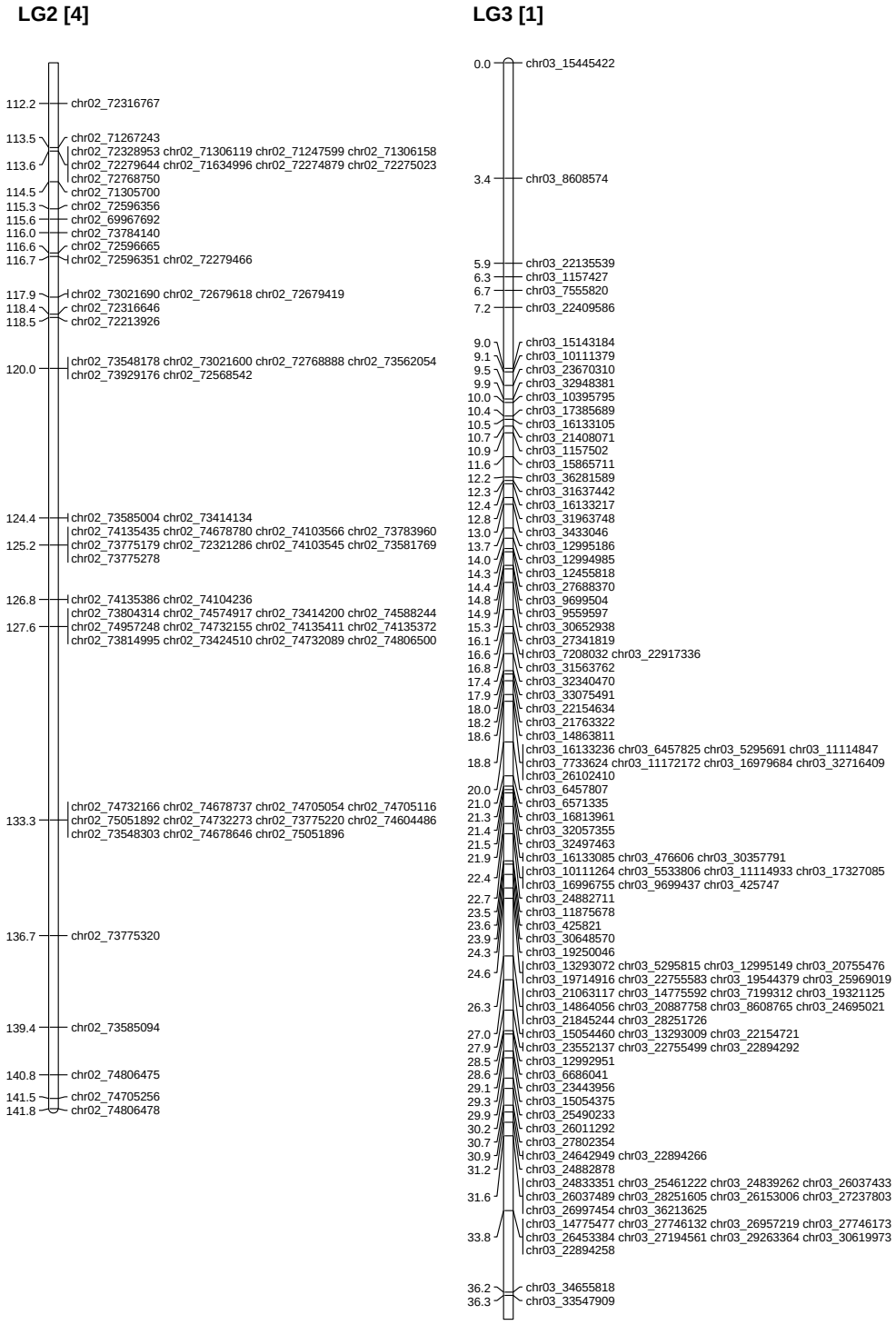
LG2 [4]
112.2 chr02_72316767
113.5 chr02_71267243
chr02_72328953 chr02_71306119 chr02_71247599 chr02_71306158
113.6 chr02_72279644 chr02_71634996 chr02_72274879 chr02_72275023
chr02_72768750
114.5 chr02_71305700
115.3 chr02_72596356
115.6 chr02_69967692
116.0 chr02_73784140
116.6 chr02_72596665
116.7 chr02_72596351 chr02_72279466
117.9 chr02_73021690 chr02_72679618 chr02_72679419
118.4 chr02_72316646
118.5 chr02_72213926
120.0 chr02_73548178 chr02_73021600 chr02_72768888 chr02_73562054
chr02_73929176 chr02_72568542
124.4 chr02_73585004 chr02_73414134
chr02_74135435 chr02_74678780 chr02_74103566 chr02_73783960
125.2 chr02_73775179 chr02_72321286 chr02_74103545 chr02_73581769
chr02_73775278
126.8 chr02_74135386 chr02_74104236
chr02_73804314 chr02_74574917 chr02_73414200 chr02_74588244
127.6 chr02_74957248 chr02_74732155 chr02_74135411 chr02_74135372
chr02_73814995 chr02_73424510 chr02_74732089 chr02_74806500
chr02_74732166 chr02_74678737 chr02_74705054 chr02_74705116
133.3 chr02_75051892 chr02_74732273 chr02_73775220 chr02_74604486
chr02_73548303 chr02_74678646 chr02_75051896
136.7 chr02_73775320
139.4 chr02_73585094
140.8 chr02_74806475
141.5 chr02_74705256
141.8 chr02_74806478
LG3 [1]
0.0 chr03_15445422
3.4 chr03_8608574
5.9 chr03_22135539
6.3 chr03_1157427
6.7 chr03_7555820
7.2 chr03_22409586
9.0 chr03_15143184
9.1 chr03_10111379
9.5 chr03_23670310
9.9 chr03_32948381
10.0 chr03_10395795
10.4 chr03_17385689
10.5 chr03_16133105
10.7 chr03_21408071
10.9 chr03_1157502
11.6 chr03_15865711
12.2 chr03_36281589
12.3 chr03_31637442
12.4 chr03_16133217
12.8 chr03_31963748
13.0 chr03_3433046
13.7 chr03_12995186
14.0 chr03_12994985
14.3 chr03_12455818
14.4 chr03_27688370
14.8 chr03_9699504
14.9 chr03_9559597
15.3 chr03_30652938
16.1 chr03_27341819
16.6 chr03_7208032 chr03_22917336
16.8 chr03_31563762
17.4 chr03_32340470
17.9 chr03_33075491
18.0 chr03_22154634
18.2 chr03_21763322
18.6 chr03_14863811
chr03_16133236 chr03_6457825 chr03_5295691 chr03_11114847
18.8 chr03_7733624 chr03_11172172 chr03_16979684 chr03_32716409
chr03_26102410
20.0 chr03_6457807
21.0 chr03_6571335
21.3 chr03_16813961
21.4 chr03_32057355
21.5 chr03_32497463
21.9 chr03_16133085 chr03_476606 chr03_30357791
22.4 chr03_10111264 chr03_5533806 chr03_11114933 chr03_17327085
chr03_16996755 chr03_9699437 chr03_425747
22.7 chr03_24882711
23.5 chr03_11875678
23.6 chr03_425821
23.9 chr03_30648570
24.3 chr03_19250046
24.6 chr03_13293072 chr03_5295815 chr03_12995149 chr03_20755476
chr03_19714916 chr03_22755583 chr03_19544379 chr03_25969019
chr03_21063117 chr03_14775592 chr03_7199312 chr03_19321125
26.3 chr03_14864056 chr03_20887758 chr03_8608765 chr03_24695021
chr03_21845244 chr03_28251726
27.0 chr03_15054460 chr03_13293009 chr03_22154721
27.9 chr03_23552137 chr03_22755499 chr03_22894292
28.5 chr03_12992951
28.6 chr03_6686041
29.1 chr03_23443956
29.3 chr03_15054375
29.9 chr03_25490233
30.2 chr03_26011292
30.7 chr03_27802354
30.9 chr03_24642949 chr03_22894266
31.2 chr03_24882878
chr03_24833351 chr03_25461222 chr03_24839262 chr03_26037433
31.6 chr03_26037489 chr03_28251605 chr03_26153006 chr03_27237803
chr03_26997454 chr03_36213625
chr03_14775477 chr03_27746132 chr03_26957219 chr03_27746173
33.8 chr03_26453384 chr03_27194561 chr03_29263364 chr03_30619973
chr03_22894258
36.2 chr03_34655818
36.3 chr03_33547909

LG3 [2]

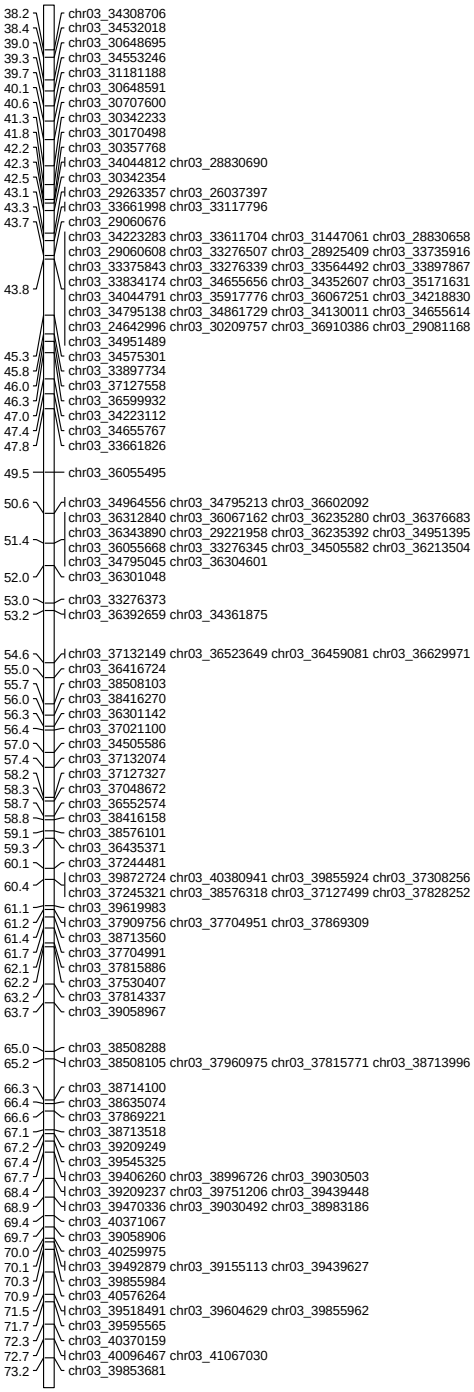
38.2 chr03_34308706
38.4 chr03_34532018
39.0 chr03_30648695
39.3 chr03_34553246
39.7 chr03_31181188
40.1 chr03_30648591
40.6 chr03_30707600
41.3 chr03_30342233
41.8 chr03_30170498
42.2 chr03_30357768
42.3 chr03_34044812 chr03_28830690
42.5 chr03_30342354
43.1 chr03_29263357 chr03_26037397
43.3 chr03_33661998 chr03_33117796
43.7 chr03_29060676
chr03_34223283 chr03_33611704 chr03_31447061 chr03_28830658
chr03_29060608 chr03_33276507 chr03_28925409 chr03_33735916
chr03_33375843 chr03_33276339 chr03_33564492 chr03_33897867
43.8 chr03_33834174 chr03_34655656 chr03_34352607 chr03_35171631
chr03_34044791 chr03_35917776 chr03_36067251 chr03_34218830
chr03_34795138 chr03_34861729 chr03_34130011 chr03_34655614
chr03_24642996 chr03_30209757 chr03_36910386 chr03_29081168
chr03_34951489
45.3 chr03_34575301
45.8 chr03_33897734
46.0 chr03_37127558
46.3 chr03_36599932
47.0 chr03_34223112
47.4 chr03_34655767
47.8 chr03_33661826
49.5 chr03_36055495
50.6 chr03_34964556 chr03_34795213 chr03_36602092
chr03_36312840 chr03_36067162 chr03_36235280 chr03_36376683
chr03_36343890 chr03_29221958 chr03_36235392 chr03_34951395
51.4 chr03_36055668 chr03_33276345 chr03_34505582 chr03_36213504
chr03_34795045 chr03_36304601
52.0 chr03_36301048
53.0 chr03_33276373
53.2 chr03_36392659 chr03_34361875
54.6 chr03_37132149 chr03_36523649 chr03_36459081 chr03_36629971
55.0 chr03_36416724
55.7 chr03_38508103
56.0 chr03_38416270
56.3 chr03_36301142
56.4 chr03_37021100
57.0 chr03_34505586
57.4 chr03_37132074
58.2 chr03_37127327
58.3 chr03_37048672
58.7 chr03_36552574
58.8 chr03_38416158
59.1 chr03_38576101
59.3 chr03_36435371
60.1 chr03_37244481
chr03_39872724 chr03_40380941 chr03_39855924 chr03_37308256
60.4 chr03_37245321 chr03_38576318 chr03_37127499 chr03_37828252
61.1 chr03_39619983
61.2 chr03_37909756 chr03_37704951 chr03_37869309
61.4 chr03_38713560
61.7 chr03_37704991
62.1 chr03_37815886
62.2 chr03_37530407
63.2 chr03_37814337
63.7 chr03_39058967
65.0 chr03_38508288
65.2 chr03_38508105 chr03_37960975 chr03_37815771 chr03_38713996
66.3 chr03_38714100
66.4 chr03_38635074
66.6 chr03_37869221
67.1 chr03_38713518
67.2 chr03_39209249
67.4 chr03_39545325
67.7 chr03_39406260 chr03_38996726 chr03_39030503
68.4 chr03_39209237 chr03_39751206 chr03_39439448
68.9 chr03_39470336 chr03_39030492 chr03_38983186
69.4 chr03_40371067
69.7 chr03_39058906
70.0 chr03_40259975
70.1 chr03_39492879 chr03_39155113 chr03_39439627
70.3 chr03_39855984
70.9 chr03_40576264
71.5 chr03_39518491 chr03_39604629 chr03_39855962
71.7 chr03_39595565
72.3 chr03_40370159
72.7 chr03_40096467 chr03_41067030
73.2 chr03_39853681

LG3 [3]

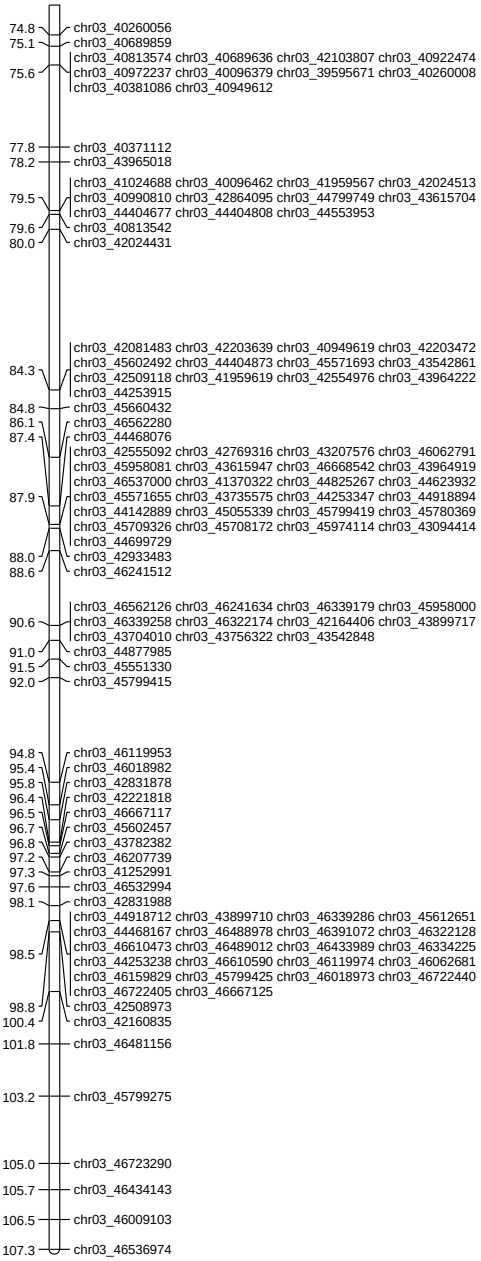
74.8 chr03_40260056
75.1 chr03_40689859
chr03_40813574 chr03_40689636 chr03_42103807 chr03_40922474
75.6 chr03_40972237 chr03_40096379 chr03_39595671 chr03_40260008
chr03_40381086 chr03_40949612
77.8 chr03_40371112
78.2 chr03_43965018
chr03_41024688 chr03_40096462 chr03_41959567 chr03_42024513
79.5 chr03_40990810 chr03_42864095 chr03_44799749 chr03_43615704
chr03_44404677 chr03_44404808 chr03_44553953
79.6 chr03_40813542
80.0 chr03_42024431
chr03_42081483 chr03_42203639 chr03_40949619 chr03_42203472
chr03_45602492 chr03_44404873 chr03_45571693 chr03_43542861
84.3 chr03_42509118 chr03_41959619 chr03_42554976 chr03_43964222
chr03_44253915
84.8 chr03_45660432
86.1 chr03_46562280
87.4 chr03_44468076
chr03_42555092 chr03_42769316 chr03_43207576 chr03_46062791
chr03_45958081 chr03_43615947 chr03_46668542 chr03_43964919
chr03_46537000 chr03_41370322 chr03_44825267 chr03_44623932
87.9 chr03_45571655 chr03_43735575 chr03_44253347 chr03_44918894
chr03_44142889 chr03_45055339 chr03_45799419 chr03_45780369
chr03_45709326 chr03_45708172 chr03_45974114 chr03_43094414
chr03_44699729
88.0 chr03_42933483
88.6 chr03_46241512
chr03_46562126 chr03_46241634 chr03_46339179 chr03_45958000
90.6 chr03_46339258 chr03_46322174 chr03_42164406 chr03_43899717
chr03_43704010 chr03_43756322 chr03_43542848
91.0 chr03_44877985
91.5 chr03_45551330
92.0 chr03_45799415
94.8 chr03_46119953
95.4 chr03_46018982
95.8 chr03_42831878
96.4 chr03_42221818
96.5 chr03_46667117
96.7 chr03_45602457
96.8 chr03_43782382
97.2 chr03_46207739
97.3 chr03_41252991
97.6 chr03_46532994
98.1 chr03_42831988
chr03_44918712 chr03_43899710 chr03_46339286 chr03_45612651
chr03_44468167 chr03_46488978 chr03_46391072 chr03_46322128
98.5 chr03_46610473 chr03_46489012 chr03_46433989 chr03_46334225
chr03_44253238 chr03_46610590 chr03_46119974 chr03_46062681
chr03_46159829 chr03_45799425 chr03_46018973 chr03_46722440
chr03_46722405 chr03_46667125
98.8 chr03_42508973
100.4 chr03_42160835
101.8 chr03_46481156
103.2 chr03_45799275
105.0 chr03_46723290
105.7 chr03_46434143
106.5 chr03_46009103
107.3 chr03_46536974

LG4 [1]

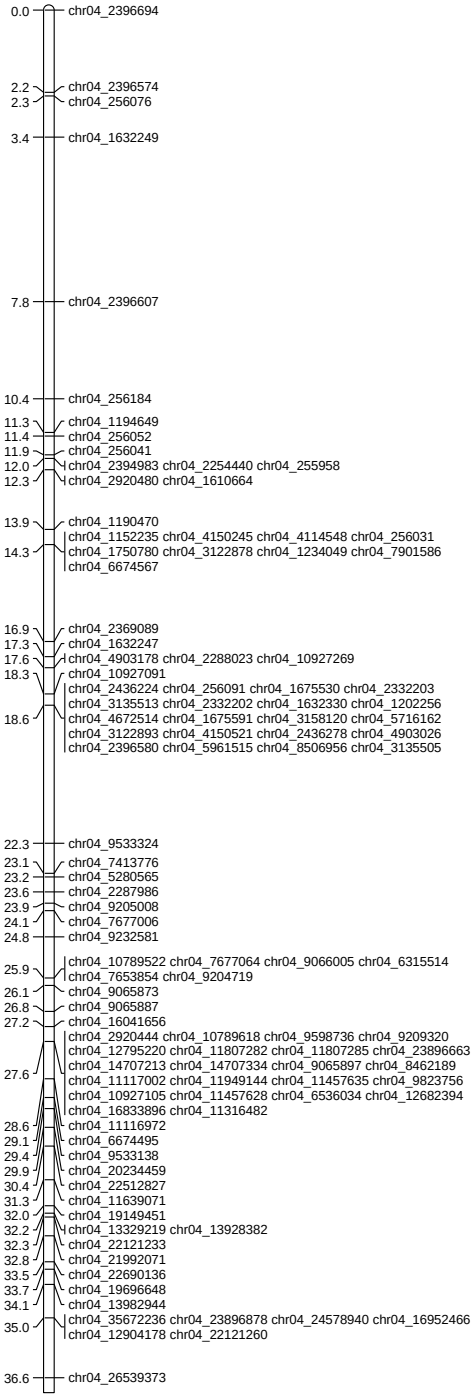
0.0 chr04_2396694
2.2 chr04_2396574
2.3 chr04_256076
3.4 chr04_1632249
7.8 chr04_2396607
10.4 chr04_256184
11.3 chr04_1194649
11.4 chr04_256052
11.9 chr04_256041
12.0 chr04_2394983 chr04_2254440 chr04_255958
12.3 chr04_2920480 chr04_1610664
13.9 chr04_1190470
chr04_1152235 chr04_4150245 chr04_4114548 chr04_256031
14.3 chr04_1750780 chr04_3122878 chr04_1234049 chr04_7901586
chr04_6674567
16.9 chr04_2369089
17.3 chr04_1632247
17.6 chr04_4903178 chr04_2288023 chr04_10927269
18.3 chr04_10927091
chr04_2436224 chr04_256091 chr04_1675530 chr04_2332203
chr04_3135513 chr04_2332202 chr04_1632330 chr04_1202256
18.6 chr04_4672514 chr04_1675591 chr04_3158120 chr04_5716162
chr04_3122893 chr04_4150521 chr04_2436278 chr04_4903026
chr04_2396580 chr04_5961515 chr04_8506956 chr04_3135505
22.3 chr04_9533324
23.1 chr04_7413776
23.2 chr04_5280565
23.6 chr04_2287986
23.9 chr04_9205008
24.1 chr04_7677006
24.8 chr04_9232581
25.9 chr04_10789522 chr04_7677064 chr04_9066005 chr04_6315514
chr04_7653854 chr04_9204719
26.1 chr04_9065873
26.8 chr04_9065887
27.2 chr04_16041656
chr04_2920444 chr04_10789618 chr04_9598736 chr04_9209320
chr04_12795220 chr04_11807282 chr04_11807285 chr04_23896663
27.6 chr04_14707213 chr04_14707334 chr04_9065897 chr04_8462189
chr04_11117002 chr04_11949144 chr04_11457635 chr04_9823756
chr04_10927105 chr04_11457628 chr04_6536034 chr04_12682394
chr04_16833896 chr04_11316482
28.6 chr04_11116972
29.1 chr04_6674495
29.4 chr04_9533138
29.9 chr04_20234459
30.4 chr04_22512827
31.3 chr04_11639071
32.0 chr04_19149451
32.2 chr04_13329219 chr04_13928382
32.3 chr04_22121233
32.8 chr04_21992071
33.5 chr04_22690136
33.7 chr04_19696648
34.1 chr04_13982944
35.0 chr04_35672236 chr04_23896878 chr04_24578940 chr04_16952466
chr04_12904178 chr04_22121260
36.6 chr04_26539373

LG4 [2]

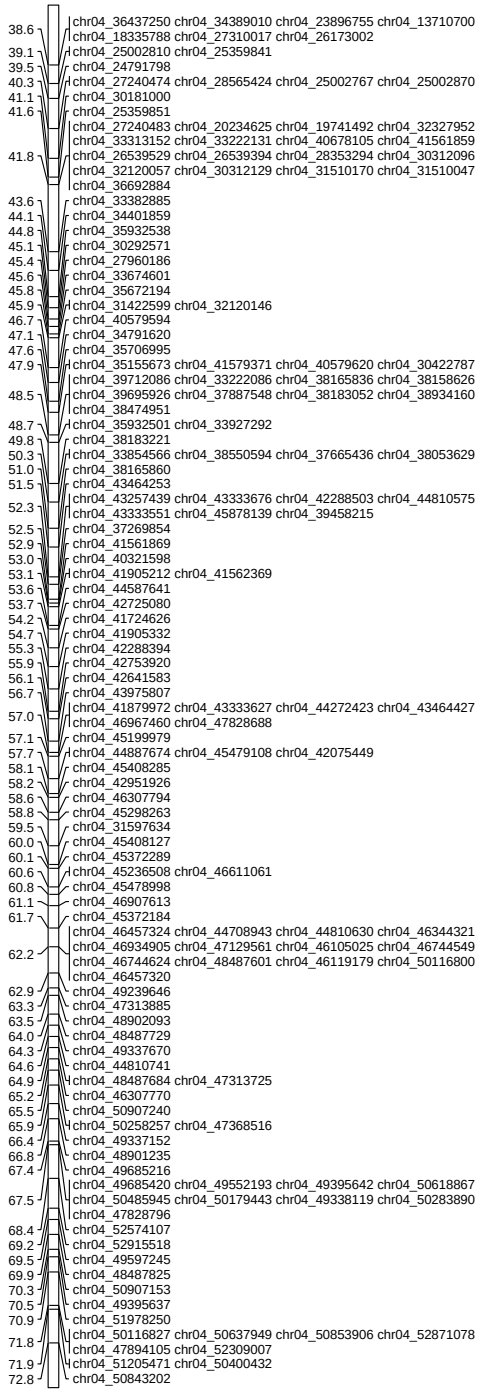
38.6 chr04_36437250 chr04_34389010 chr04_23896755 chr04_13710700
chr04_18335788 chr04_27310017 chr04_26173002
39.1 chr04_25002810 chr04_25359841
39.5 chr04_24791798
40.3 chr04_27240474 chr04_28565424 chr04_25002767 chr04_25002870
41.1 chr04_30181000
41.6 chr04_25359851
chr04_27240483 chr04_20234625 chr04_19741492 chr04_32327952
chr04_33313152 chr04_33222131 chr04_40678105 chr04_41561859
41.8 chr04_26539529 chr04_26539394 chr04_28353294 chr04_30312096
chr04_32120057 chr04_30312129 chr04_31510170 chr04_31510047
chr04_36692884
43.6 chr04_33382885
44.1 chr04_34401859
44.8 chr04_35932538
45.1 chr04_30292571
45.4 chr04_27960186
45.6 chr04_33674601
45.8 chr04_35672194
45.9 chr04_31422599 chr04_32120146
46.7 chr04_40579594
47.1 chr04_34791620
47.6 chr04_35706995
47.9 chr04_35155673 chr04_41579371 chr04_40579620 chr04_30422787
chr04_39712086 chr04_33222086 chr04_38165836 chr04_38158626
48.5 chr04_39695926 chr04_37887548 chr04_38183052 chr04_38934160
chr04_38474951
48.7 chr04_35932501 chr04_33927292
49.8 chr04_38183221
50.3 chr04_33854566 chr04_38550594 chr04_37665436 chr04_38053629
51.0 chr04_38165860
51.5 chr04_43464253
chr04_43257439 chr04_43333676 chr04_42288503 chr04_44810575
52.3 chr04_43333551 chr04_45878139 chr04_39458215
52.5 chr04_37269854
52.9 chr04_41561869
53.0 chr04_40321598
53.1 chr04_41905212 chr04_41562369
53.6 chr04_44587641
53.7 chr04_42725080
54.2 chr04_41724626
54.7 chr04_41905332
55.3 chr04_42288394
55.9 chr04_42753920
56.1 chr04_42641583
56.7 chr04_43975807
chr04_41879972 chr04_43333627 chr04_44272423 chr04_43464427
57.0 chr04_46967460 chr04_47828688
57.1 chr04_45199979
57.7 chr04_44887674 chr04_45479108 chr04_42075449
58.1 chr04_45408285
58.2 chr04_42951926
58.6 chr04_46307794
58.8 chr04_45298263
59.5 chr04_31597634
60.0 chr04_45408127
60.1 chr04_45372289
60.6 chr04_45236508 chr04_46611061
60.8 chr04_45478998
61.1 chr04_46907613
61.7 chr04_45372184
chr04_46457324 chr04_44708943 chr04_44810630 chr04_46344321
chr04_46934905 chr04_47129561 chr04_46105025 chr04_46744549
62.2 chr04_46744624 chr04_48487601 chr04_46119179 chr04_50116800
chr04_46457320
62.9 chr04_49239646
63.3 chr04_47313885
63.5 chr04_48902093
64.0 chr04_48487729
64.3 chr04_49337670
64.6 chr04_44810741
64.9 chr04_48487684 chr04_47313725
65.2 chr04_46307770
65.5 chr04_50907240
65.9 chr04_50258257 chr04_47368516
66.4 chr04_49337152
66.8 chr04_48901235
67.4 chr04_49685216
chr04_49685420 chr04_49552193 chr04_49395642 chr04_50618867
67.5 chr04_50485945 chr04_50179443 chr04_49338119 chr04_50283890
chr04_47828796
68.4 chr04_52574107
69.2 chr04_52915518
69.5 chr04_49597245
69.9 chr04_48487825
70.3 chr04_50907153
70.5 chr04_49395637
70.9 chr04_51978250
71.8 chr04_50116827 chr04_50637949 chr04_50853906 chr04_52871078
chr04_47894105 chr04_52309007
71.9 chr04_51205471 chr04_50400432
72.8 chr04_50843202

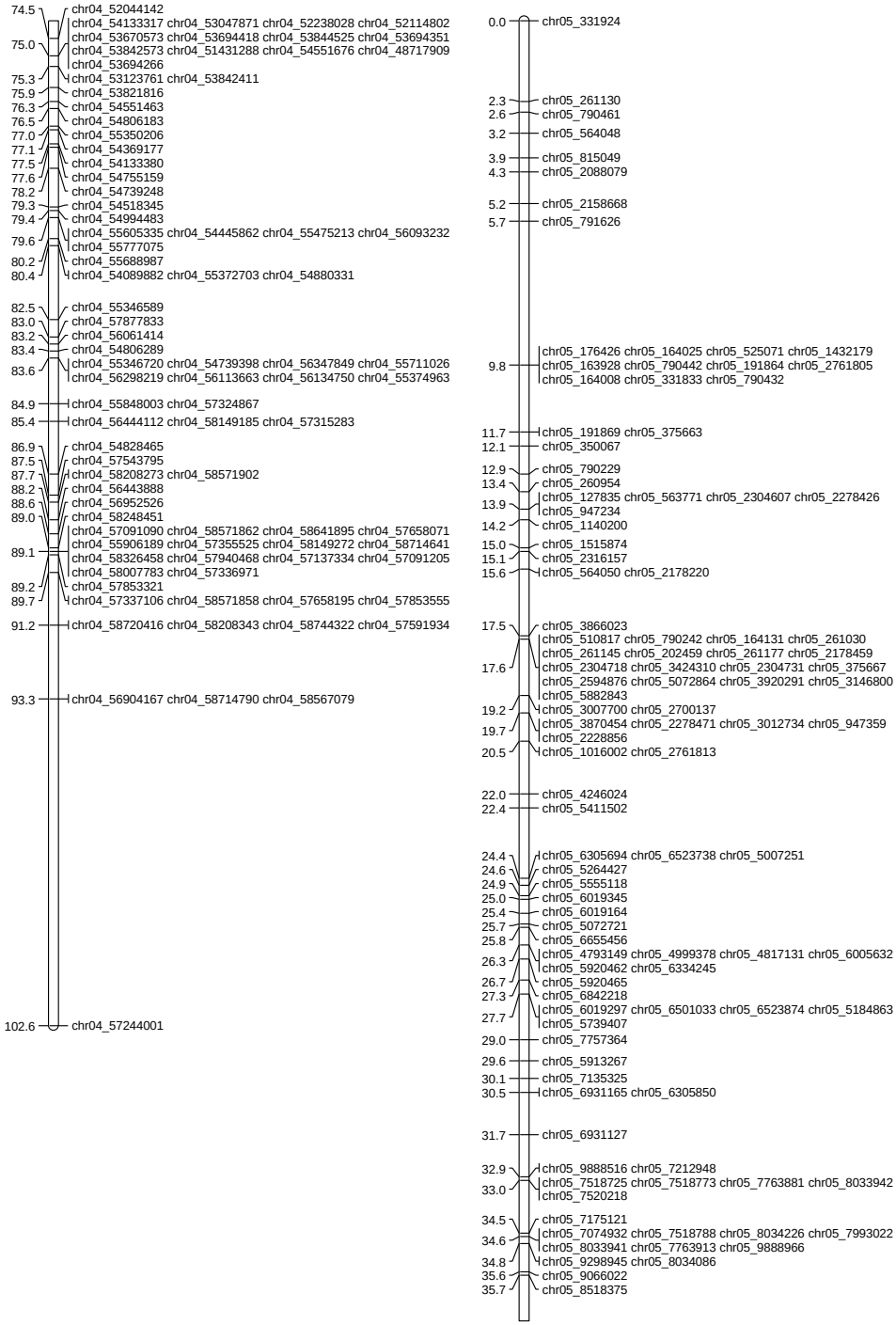
LG4 [3]
74.5 chr04_52044142
chr04_54133317 chr04_53047871 chr04_52238028 chr04_52114802
75.0 chr04_53670573 chr04_53694418 chr04_53844525 chr04_53694351
chr04_53842573 chr04_51431288 chr04_54551676 chr04_48717909
chr04_53694266
75.3 chr04_53123761 chr04_53842411
75.9 chr04_53821816
76.3 chr04_54551463
76.5 chr04_54806183
77.0 chr04_55350206
77.1 chr04_54369177
77.5 chr04_54133380
77.6 chr04_54755159
78.2 chr04_54739248
79.3 chr04_54518345
79.4 chr04_54994483
chr04_55605335 chr04_54445862 chr04_55475213 chr04_56093232
79.6 chr04_55777075
80.2 chr04_55688987
80.4 chr04_54089882 chr04_55372703 chr04_54880331
82.5 chr04_55346589
83.0 chr04_57877833
83.2 chr04_56061414
83.4 chr04_54806289
chr04_55346720 chr04_54739398 chr04_56347849 chr04_55711026
83.6 chr04_56298219 chr04_56113663 chr04_56134750 chr04_55374963
84.9 chr04_55848003 chr04_57324867
85.4 chr04_56444112 chr04_58149185 chr04_57315283
86.9 chr04_54828465
87.5 chr04_57543795
87.7 chr04_58208273 chr04_58571902
88.2 chr04_56443888
88.6 chr04_56952526
89.0 chr04_58248451
chr04_57091090 chr04_58571862 chr04_58641895 chr04_57658071
chr04_55906189 chr04_57355525 chr04_58149272 chr04_58714641
89.1 chr04_58326458 chr04_57940468 chr04_57137334 chr04_57091205
chr04_58007783 chr04_57336971
89.2 chr04_57853321
89.7 chr04_57337106 chr04_58571858 chr04_57658195 chr04_57853555
91.2 chr04_58720416 chr04_58208343 chr04_58744322 chr04_57591934
93.3 chr04_56904167 chr04_58714790 chr04_58567079
102.6 chr04_57244001
LG5 [1]
0.0 chr05_331924
2.3 chr05_261130
2.6 chr05_790461
3.2 chr05_564048
3.9 chr05_815049
4.3 chr05_2088079
5.2 chr05_2158668
5.7 chr05_791626
chr05_176426 chr05_164025 chr05_525071 chr05_1432179
9.8 chr05_163928 chr05_790442 chr05_191864 chr05_2761805
chr05_164008 chr05_331833 chr05_790432
11.7 chr05_191869 chr05_375663
12.1 chr05_350067
12.9 chr05_790229
13.4 chr05_260954
chr05_127835 chr05_563771 chr05_2304607 chr05_2278426
13.9 chr05_947234
14.2 chr05_1140200
15.0 chr05_1515874
15.1 chr05_2316157
15.6 chr05_564050 chr05_2178220
17.5 chr05_3866023
chr05_510817 chr05_790242 chr05_164131 chr05_261030
chr05_261145 chr05_202459 chr05_261177 chr05_2178459
17.6 chr05_2304718 chr05_3424310 chr05_2304731 chr05_375667
chr05_2594876 chr05_5072864 chr05_3920291 chr05_3146800
chr05_5882843
19.2 chr05_3007700 chr05_2700137
chr05_3870454 chr05_2278471 chr05_3012734 chr05_947359
19.7 chr05_2228856
20.5 chr05_1016002 chr05_2761813
22.0 chr05_4246024
22.4 chr05_5411502
24.4 chr05_6305694 chr05_6523738 chr05_5007251
24.6 chr05_5264427
24.9 chr05_5555118
25.0 chr05_6019345
25.4 chr05_6019164
25.7 chr05_5072721
25.8 chr05_6655456
chr05_4793149 chr05_4999378 chr05_4817131 chr05_6005632
26.3 chr05_5920462 chr05_6334245
26.7 chr05_5920465
27.3 chr05_6842218
chr05_6019297 chr05_6501033 chr05_6523874 chr05_5184863
27.7 chr05_5739407
29.0 chr05_7757364
29.6 chr05_5913267
30.1 chr05_7135325
30.5 chr05_6931165 chr05_6305850
31.7 chr05_6931127
32.9 chr05_9888516 chr05_7212948
chr05_7518725 chr05_7518773 chr05_7763881 chr05_8033942
33.0 chr05_7520218
34.5 chr05_7175121
chr05_7074932 chr05_7518788 chr05_8034226 chr05_7993022
34.6 chr05_8033941 chr05_7763913 chr05_9888966
34.8 chr05_9298945 chr05_8034086
35.6 chr05_9066022
35.7 chr05_8518375

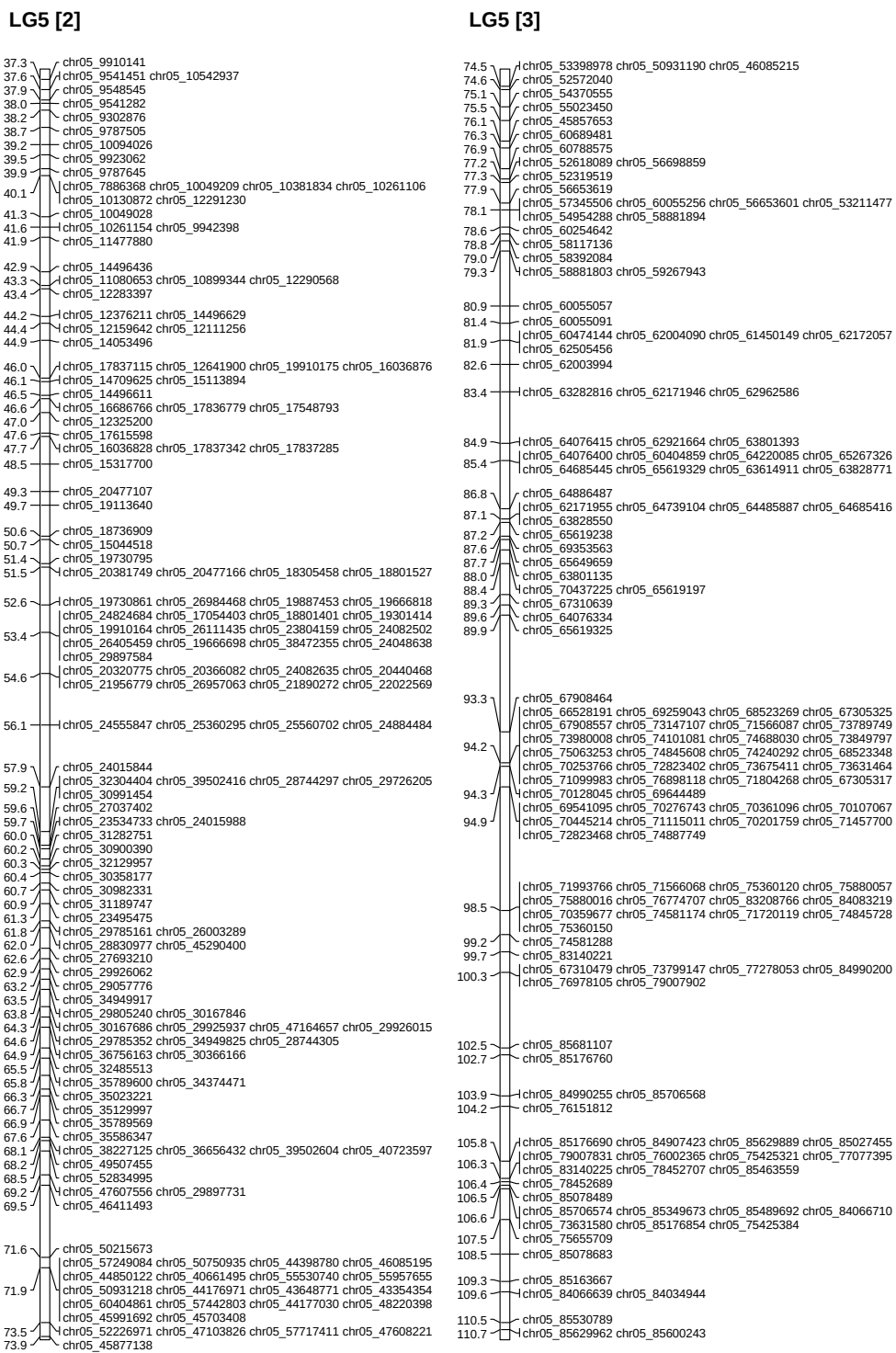
LG5 [2]
LG5 [3]
37.3 chr05_9910141
37.6 chr05_9541451 chr05_10542937
37.9 chr05_9548545
38.0 chr05_9541282
38.2 chr05_9302876
38.7 chr05_9787505
39.2 chr05_10094026
39.5 chr05_9923062
39.9 chr05_9787645
40.1 chr05_7886368 chr05_10049209 chr05_10381834 chr05_10261106 chr05_10130872 chr05_12291230
41.3 chr05_10049028
41.6 chr05_10261154 chr05_9942398
41.9 chr05_11477880
42.9 chr05_14496436
43.3 chr05_11080653 chr05_10899344 chr05_12290568
43.4 chr05_12283397
44.2 chr05_12376211 chr05_14496629
44.4 chr05_12159642 chr05_12111256
44.9 chr05_14053496
46.0 chr05_17837115 chr05_12641900 chr05_19910175 chr05_16036876
46.1 chr05_14709625 chr05_15113894
46.5 chr05_14496611
46.6 chr05_16686766 chr05_17836779 chr05_17548793
47.0 chr05_12325200
47.6 chr05_17615598
47.7 chr05_16036828 chr05_17837342 chr05_17837285
48.5 chr05_15317700
49.3 chr05_20477107
49.7 chr05_19113640
50.6 chr05_18736909
50.7 chr05_15044518
51.4 chr05_19730795
51.5 chr05_20381749 chr05_20477166 chr05_18305458 chr05_18801527
52.6 chr05_19730861 chr05_26984468 chr05_19887453 chr05_19666818
53.4 chr05_24824684 chr05_17054403 chr05_18801401 chr05_19301414 chr05_19910164 chr05_26111435 chr05_23804159 chr05_24082502 chr05_26405459 chr05_19666698 chr05_38472355 chr05_24048638 chr05_29897584
54.6 chr05_20320775 chr05_20366082 chr05_24082635 chr05_20440468 chr05_21956779 chr05_26957063 chr05_21890272 chr05_22022569
56.1 chr05_24555847 chr05_25360295 chr05_25560702 chr05_24884484
57.9 chr05_24015844
59.2 chr05_32304404 chr05_39502416 chr05_28744297 chr05_29726205 chr05_30991454
59.6 chr05_27037402
59.7 chr05_23534733 chr05_24015988
60.0 chr05_31282751
60.2 chr05_30900390
60.3 chr05_32129957
60.4 chr05_30358177
60.7 chr05_30982331
60.9 chr05_31189747
61.3 chr05_23495475
61.8 chr05_29785161 chr05_26003289
62.0 chr05_28830977 chr05_45290400
62.6 chr05_27693210
62.9 chr05_29926062
63.2 chr05_29057776
63.5 chr05_34949917
63.8 chr05_29805240 chr05_30167846
64.3 chr05_30167686 chr05_29925937 chr05_47164657 chr05_29926015
64.6 chr05_29785352 chr05_34949825 chr05_28744305
64.9 chr05_36756163 chr05_30366166
65.5 chr05_32485513
65.8 chr05_35789600 chr05_34374471
66.3 chr05_35023221
66.7 chr05_35129997
66.9 chr05_35789569
67.6 chr05_35586347
68.1 chr05_38227125 chr05_36656432 chr05_39502604 chr05_40723597
68.2 chr05_49507455
68.5 chr05_52834995
69.2 chr05_47607556 chr05_29897731
69.5 chr05_46411493
71.6 chr05_50215673
71.9 chr05_57249084 chr05_50750935 chr05_44398780 chr05_46085195 chr05_44850122 chr05_40661495 chr05_55530740 chr05_55957655 chr05_50931218 chr05_44176971 chr05_43648771 chr05_43354354 chr05_60404861 chr05_57442803 chr05_44177030 chr05_48220398 chr05_45991692 chr05_45703408
73.5 chr05_52226971 chr05_47103826 chr05_57717411 chr05_47608221
73.9 chr05_45877138
74.5 chr05_53398978 chr05_50931190 chr05_46085215
74.6 chr05_52572040
75.1 chr05_54370555
75.5 chr05_55023450
76.1 chr05_45857653
76.3 chr05_60689481
76.9 chr05_60788575
77.2 chr05_52618089 chr05_56698859
77.3 chr05_52319519
77.9 chr05_56653619
78.1 chr05_57345506 chr05_60055256 chr05_56653601 chr05_53211477 chr05_54954288 chr05_58881894
78.6 chr05_60254642
78.8 chr05_58117136
79.0 chr05_58392084
79.3 chr05_58881803 chr05_59267943
80.9 chr05_60055057
81.4 chr05_60055091
81.9 chr05_60474144 chr05_62004090 chr05_61450149 chr05_62172057 chr05_62505456
82.6 chr05_62003994
83.4 chr05_63282816 chr05_62171946 chr05_62962586
84.9 chr05_64076415 chr05_62921664 chr05_63801393
85.4 chr05_64076400 chr05_60404859 chr05_64220085 chr05_65267326 chr05_64685445 chr05_65619329 chr05_63614911 chr05_63828771
86.8 chr05_64886487
87.1 chr05_62171955 chr05_64739104 chr05_64485887 chr05_64685416 chr05_63828550
87.2 chr05_65619238
87.6 chr05_69353563
87.7 chr05_65649659
88.0 chr05_63801135
88.4 chr05_70437225 chr05_65619197
89.3 chr05_67310639
89.6 chr05_64076334
89.9 chr05_65619325
93.3 chr05_67908464
94.2 chr05_66528191 chr05_69259043 chr05_68523269 chr05_67305325 chr05_67908557 chr05_73147107 chr05_71566087 chr05_73789749 chr05_73980008 chr05_74101081 chr05_74688030 chr05_73849797 chr05_75063253 chr05_74845608 chr05_74240292 chr05_68523348 chr05_70253766 chr05_72823402 chr05_73675411 chr05_73631464 chr05_71099983 chr05_76898118 chr05_71804268 chr05_67305317
94.3 chr05_70128045 chr05_69644489
94.9 chr05_69541095 chr05_70276743 chr05_70361096 chr05_70107067 chr05_70445214 chr05_71115011 chr05_70201759 chr05_71457700 chr05_72823468 chr05_74887749
98.5 chr05_71993766 chr05_71566068 chr05_75360120 chr05_75880057 chr05_75880016 chr05_76774707 chr05_83208766 chr05_84083219 chr05_70359677 chr05_74581174 chr05_71720119 chr05_74845728 chr05_75360150
99.2 chr05_74581288
99.7 chr05_83140221
100.3 chr05_67310479 chr05_73799147 chr05_77278053 chr05_84990200 chr05_76978105 chr05_79007902
102.5 chr05_85681107
102.7 chr05_85176760
103.9 chr05_84990255 chr05_85706568
104.2 chr05_76151812
105.8 chr05_85176690 chr05_84907423 chr05_85629889 chr05_85027455
106.3 chr05_79007831 chr05_76002365 chr05_75425321 chr05_77077395 chr05_83140225 chr05_78452707 chr05_85463559
106.4 chr05_78452689
106.5 chr05_85078489
106.6 chr05_85706574 chr05_85349673 chr05_85489692 chr05_84066710 chr05_73631580 chr05_85176854 chr05_75425384
107.5 chr05_75655709
108.5 chr05_85078683
109.3 chr05_85163667
109.6 chr05_84066639 chr05_84034944
110.5 chr05_85530789
110.7 chr05_85629962 chr05_85600243

LG5 [4]

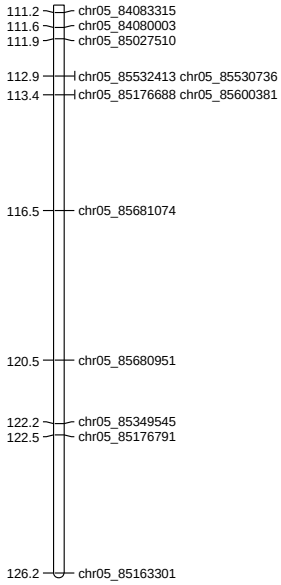
111.2 chr05_84083315
111.6 chr05_84080003
111.9 chr05_85027510
112.9 chr05_85532413 chr05_85530736
113.4 chr05_85176688 chr05_85600381
116.5 chr05_85681074
120.5 chr05_85680951
122.2 chr05_85349545
122.5 chr05_85176791
126.2 chr05_85163301

LG6 [1]

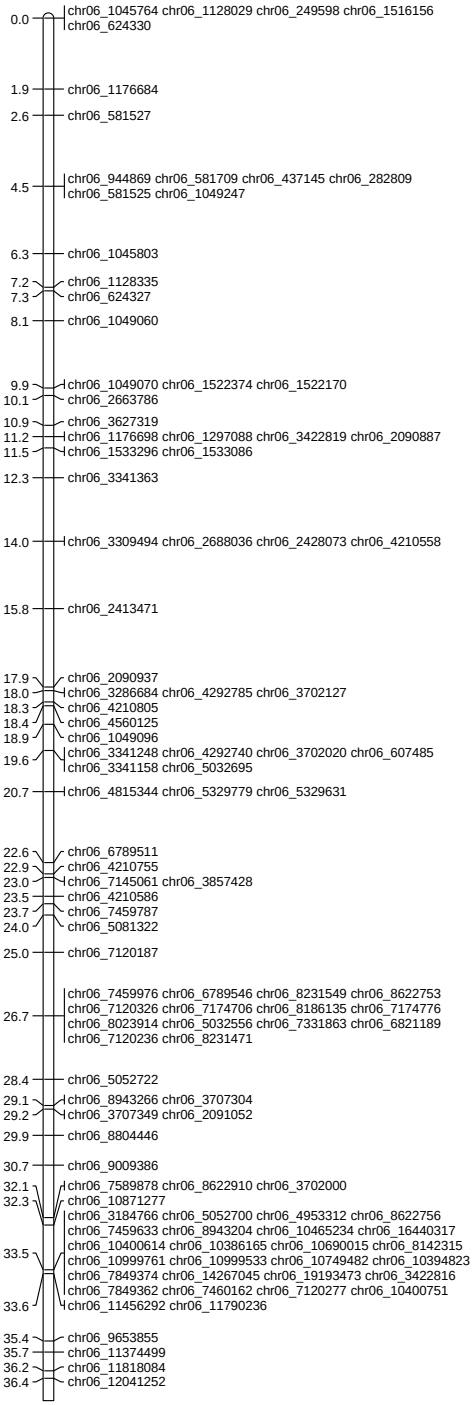
0.0 chr06_1045764 chr06_1128029 chr06_249598 chr06_1516156
chr06_624330
1.9 chr06_1176684
2.6 chr06_581527
4.5 chr06_944869 chr06_581709 chr06_437145 chr06_282809
chr06_581525 chr06_1049247
6.3 chr06_1045803
7.2 chr06_1128335
7.3 chr06_624327
8.1 chr06_1049060
9.9 chr06_1049070 chr06_1522374 chr06_1522170
10.1 chr06_2663786
10.9 chr06_3627319
11.2 chr06_1176698 chr06_1297088 chr06_3422819 chr06_2090887
11.5 chr06_1533296 chr06_1533086
12.3 chr06_3341363
14.0 chr06_3309494 chr06_2688036 chr06_2428073 chr06_4210558
15.8 chr06_2413471
17.9 chr06_2090937
18.0 chr06_3286684 chr06_4292785 chr06_3702127
18.3 chr06_4210805
18.4 chr06_4560125
18.9 chr06_1049096
19.6 chr06_3341248 chr06_4292740 chr06_3702020 chr06_607485
chr06_3341158 chr06_5032695
20.7 chr06_4815344 chr06_5329779 chr06_5329631
22.6 chr06_6789511
22.9 chr06_4210755
23.0 chr06_7145061 chr06_3857428
23.5 chr06_4210586
23.7 chr06_7459787
24.0 chr06_5081322
25.0 chr06_7120187
26.7 chr06_7459976 chr06_6789546 chr06_8231549 chr06_8622753
chr06_7120326 chr06_7174706 chr06_8186135 chr06_7174776
chr06_8023914 chr06_5032556 chr06_7331863 chr06_6821189
chr06_7120236 chr06_8231471
28.4 chr06_5052722
29.1 chr06_8943266 chr06_3707304
29.2 chr06_3707349 chr06_2091052
29.9 chr06_8804446
30.7 chr06_9009386
32.1 chr06_7589878 chr06_8622910 chr06_3702000
32.3 chr06_10871277
chr06_3184766 chr06_5052700 chr06_4953312 chr06_8622756
chr06_7459633 chr06_8943204 chr06_10465234 chr06_16440317
33.5 chr06_10400614 chr06_10386165 chr06_10690015 chr06_8142315
chr06_10999761 chr06_10999533 chr06_10749482 chr06_10394823
chr06_7849374 chr06_14267045 chr06_19193473 chr06_3422816
chr06_7849362 chr06_7460162 chr06_7120277 chr06_10400751
33.6 chr06_11456292 chr06_11790236
35.4 chr06_9653855
35.7 chr06_11374499
36.2 chr06_11818084
36.4 chr06_12041252

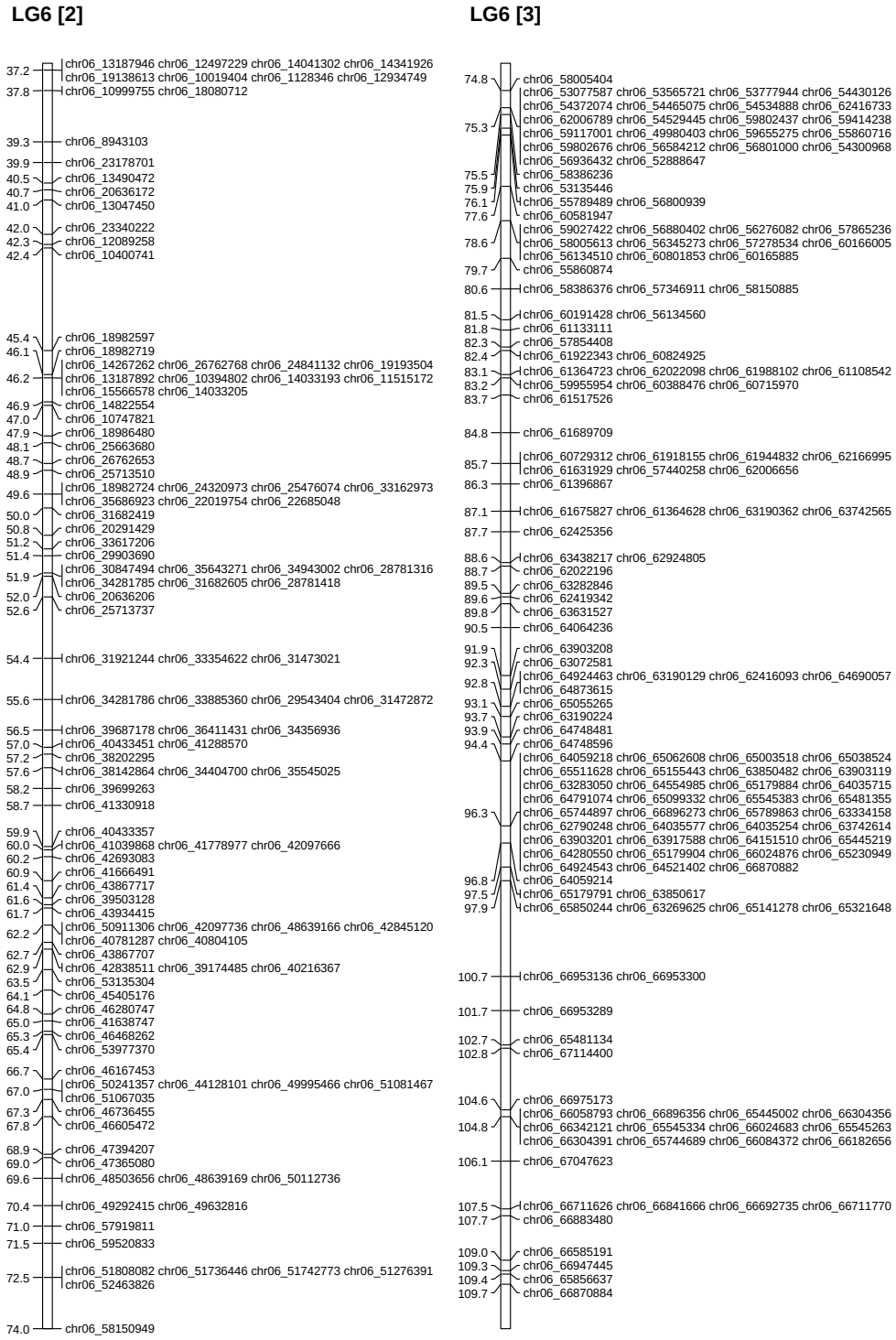
LG6 [2]
37.2 chr06_13187946 chr06_12497229 chr06_14041302 chr06_14341926
chr06_19138613 chr06_10019404 chr06_1128346 chr06_12934749
37.8 chr06_10999755 chr06_18080712
39.3 chr06_8943103
39.9 chr06_23178701
40.5 chr06_13490472
40.7 chr06_20636172
41.0 chr06_13047450
42.0 chr06_23340222
42.3 chr06_12089258
42.4 chr06_10400741
45.4 chr06_18982597
46.1 chr06_18982719
chr06_14267262 chr06_26762768 chr06_24841132 chr06_19193504
46.2 chr06_13187892 chr06_10394802 chr06_14033193 chr06_11515172
chr06_15566578 chr06_14033205
46.9 chr06_14822554
47.0 chr06_10747821
47.9 chr06_18986480
48.1 chr06_25663680
48.7 chr06_26762653
48.9 chr06_25713510
49.6 chr06_18982724 chr06_24320973 chr06_25476074 chr06_33162973
chr06_35686923 chr06_22019754 chr06_22685048
50.0 chr06_31682419
50.8 chr06_20291429
51.2 chr06_33617206
51.4 chr06_29903690
51.9 chr06_30847494 chr06_35643271 chr06_34943002 chr06_28781316
chr06_34281785 chr06_31682605 chr06_28781418
52.0 chr06_20636206
52.6 chr06_25713737
54.4 chr06_31921244 chr06_33354622 chr06_31473021
55.6 chr06_34281786 chr06_33885360 chr06_29543404 chr06_31472872
56.5 chr06_39687178 chr06_36411431 chr06_34356936
57.0 chr06_40433451 chr06_41288570
57.2 chr06_38202295
57.6 chr06_38142864 chr06_34404700 chr06_35545025
58.2 chr06_39699263
58.7 chr06_41330918
59.9 chr06_40433357
60.0 chr06_41039868 chr06_41778977 chr06_42097666
60.2 chr06_42693083
60.9 chr06_41666491
61.4 chr06_43867717
61.6 chr06_39503128
61.7 chr06_43934415
62.2 chr06_50911306 chr06_42097736 chr06_48639166 chr06_42845120
chr06_40781287 chr06_40804105
62.7 chr06_43867707
62.9 chr06_42838511 chr06_39174485 chr06_40216367
63.5 chr06_53135304
64.1 chr06_45405176
64.8 chr06_46280747
65.0 chr06_41638747
65.3 chr06_46468262
65.4 chr06_53977370
66.7 chr06_46167453
67.0 chr06_50241357 chr06_44128101 chr06_49995466 chr06_51081467
chr06_51067035
67.3 chr06_46736455
67.8 chr06_46605472
68.9 chr06_47394207
69.0 chr06_47365080
69.6 chr06_48503656 chr06_48639169 chr06_50112736
70.4 chr06_49292415 chr06_49632816
71.0 chr06_57919811
71.5 chr06_59520833
72.5 chr06_51808082 chr06_51736446 chr06_51742773 chr06_51276391
chr06_52463826
74.0 chr06_58150949
LG6 [3]
74.8 chr06_58005404
chr06_53077587 chr06_53565721 chr06_53777944 chr06_54430126
chr06_54372074 chr06_54465075 chr06_54534888 chr06_62416733
75.3 chr06_62006789 chr06_54529445 chr06_59802437 chr06_59414238
chr06_59117001 chr06_49980403 chr06_59655275 chr06_55860716
chr06_59802676 chr06_56584212 chr06_56801000 chr06_54300968
chr06_56936432 chr06_52888647
75.5 chr06_58386236
75.9 chr06_53135446
76.1 chr06_55789489 chr06_56800939
77.6 chr06_60581947
chr06_59027422 chr06_56880402 chr06_56276082 chr06_57865236
78.6 chr06_58005613 chr06_56345273 chr06_57278534 chr06_60166005
chr06_56134510 chr06_60801853 chr06_60165885
79.7 chr06_55860874
80.6 chr06_58386376 chr06_57346911 chr06_58150885
81.5 chr06_60191428 chr06_56134560
81.8 chr06_61133111
82.3 chr06_57854408
82.4 chr06_61922343 chr06_60824925
83.1 chr06_61364723 chr06_62022098 chr06_61988102 chr06_61108542
83.2 chr06_59955954 chr06_60388476 chr06_60715970
83.7 chr06_61517526
84.8 chr06_61689709
chr06_60729312 chr06_61918155 chr06_61944832 chr06_62166995
85.7 chr06_61631929 chr06_57440258 chr06_62006656
86.3 chr06_61396867
87.1 chr06_61675827 chr06_61364628 chr06_63190362 chr06_63742565
87.7 chr06_62425356
88.6 chr06_63438217 chr06_62924805
88.7 chr06_62022196
89.5 chr06_63282846
89.6 chr06_62419342
89.8 chr06_63631527
90.5 chr06_64064236
91.9 chr06_63903208
92.3 chr06_63072581
chr06_64924463 chr06_63190129 chr06_62416093 chr06_64690057
92.8 chr06_64873615
93.1 chr06_65055265
93.7 chr06_63190224
93.9 chr06_64748481
94.4 chr06_64748596
chr06_64059218 chr06_65062608 chr06_65003518 chr06_65038524
chr06_65511628 chr06_65155443 chr06_63850482 chr06_63903119
chr06_63283050 chr06_64554985 chr06_65179884 chr06_64035715
chr06_64791074 chr06_65099332 chr06_65545383 chr06_65481355
96.3 chr06_65744897 chr06_66896273 chr06_65789863 chr06_63334158
chr06_62790248 chr06_64035577 chr06_64035254 chr06_63742614
chr06_63903201 chr06_63917588 chr06_64151510 chr06_65445219
chr06_64280550 chr06_65179904 chr06_66024876 chr06_65230949
chr06_64924543 chr06_64521402 chr06_66870882
96.8 chr06_64059214
97.5 chr06_65179791 chr06_63850617
97.9 chr06_65850244 chr06_63269625 chr06_65141278 chr06_65321648
100.7 chr06_66953136 chr06_66953300
101.7 chr06_66953289
102.7 chr06_65481134
102.8 chr06_67114400
104.6 chr06_66975173
chr06_66058793 chr06_66896356 chr06_65445002 chr06_66304356
104.8 chr06_66342121 chr06_65545334 chr06_66024683 chr06_65545263
chr06_66304391 chr06_65744689 chr06_66084372 chr06_66182656
106.1 chr06_67047623
107.5 chr06_66711626 chr06_66841666 chr06_66692735 chr06_66711770
107.7 chr06_66883480
109.0 chr06_66585191
109.3 chr06_66947445
109.4 chr06_65856637
109.7 chr06_66870884

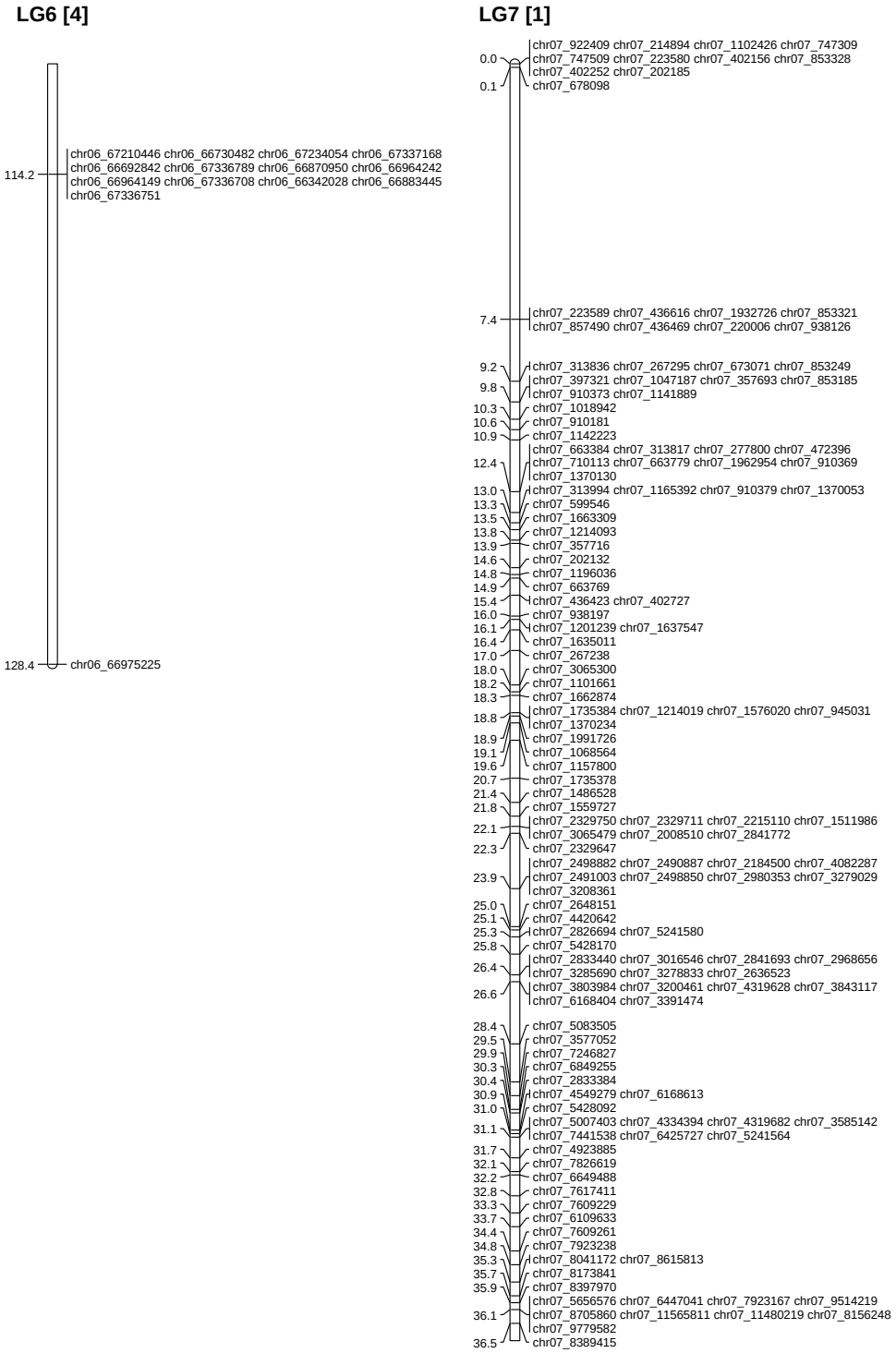
LG6 [4]
114.2
chr06_67210446 chr06_66730482 chr06_67234054 chr06_67337168
chr06_66692842 chr06_67336789 chr06_66870950 chr06_66964242
chr06_66964149 chr06_67336708 chr06_66342028 chr06_66883445
chr06_67336751
128.4
chr06_66975225
LG7 [1]
0.0
chr07_922409 chr07_214894 chr07_1102426 chr07_747309
chr07_747509 chr07_223580 chr07_402156 chr07_853328
chr07_402252 chr07_202185
0.1
chr07_678098
7.4
chr07_223589 chr07_436616 chr07_1932726 chr07_853321
chr07_857490 chr07_436469 chr07_220006 chr07_938126
9.2
chr07_313836 chr07_267295 chr07_673071 chr07_853249
9.8
chr07_397321 chr07_1047187 chr07_357693 chr07_853185
chr07_910373 chr07_1141889
10.3
chr07_1018942
10.6
chr07_910181
10.9
chr07_1142223
12.4
chr07_663384 chr07_313817 chr07_277800 chr07_472396
chr07_710113 chr07_663779 chr07_1962954 chr07_910369
chr07_1370130
13.0
chr07_313994 chr07_1165392 chr07_910379 chr07_1370053
13.3
chr07_599546
13.5
chr07_1663309
13.8
chr07_1214093
13.9
chr07_357716
14.6
chr07_202132
14.8
chr07_1196036
14.9
chr07_663769
15.4
chr07_436423 chr07_402727
16.0
chr07_938197
16.1
chr07_1201239 chr07_1637547
16.4
chr07_1635011
17.0
chr07_267238
18.0
chr07_3065300
18.2
chr07_1101661
18.3
chr07_1662874
18.8
chr07_1735384 chr07_1214019 chr07_1576020 chr07_945031
chr07_1370234
18.9
chr07_1991726
19.1
chr07_1068564
19.6
chr07_1157800
20.7
chr07_1735378
21.4
chr07_1486528
21.8
chr07_1559727
22.1
chr07_2329750 chr07_2329711 chr07_2215110 chr07_1511986
chr07_3065479 chr07_2008510 chr07_2841772
22.3
chr07_2329647
23.9
chr07_2498882 chr07_2490887 chr07_2184500 chr07_4082287
chr07_2491003 chr07_2498850 chr07_2980353 chr07_3279029
chr07_3208361
25.0
chr07_2648151
25.1
chr07_4420642
25.3
chr07_2826694 chr07_5241580
25.8
chr07_5428170
26.4
chr07_2833440 chr07_3016546 chr07_2841693 chr07_2968656
chr07_3285690 chr07_3278833 chr07_2636523
26.6
chr07_3803984 chr07_3200461 chr07_4319628 chr07_3843117
chr07_6168404 chr07_3391474
28.4
chr07_5083505
29.5
chr07_3577052
29.9
chr07_7246827
30.3
chr07_6849255
30.4
chr07_2833384
30.9
chr07_4549279 chr07_6168613
31.0
chr07_5428092
31.1
chr07_5007403 chr07_4334394 chr07_4319682 chr07_3585142
chr07_7441538 chr07_6425727 chr07_5241564
31.7
chr07_4923885
32.1
chr07_7826619
32.2
chr07_6649488
32.8
chr07_7617411
33.3
chr07_7609229
33.7
chr07_6109633
34.4
chr07_7609261
34.8
chr07_7923238
35.3
chr07_8041172 chr07_8615813
35.7
chr07_8173841
35.9
chr07_8397970
36.1
chr07_5656576 chr07_6447041 chr07_7923167 chr07_9514219
chr07_8705860 chr07_11565811 chr07_11480219 chr07_8156248
chr07_9779582
36.5
chr07_8389415

LG7 [2]

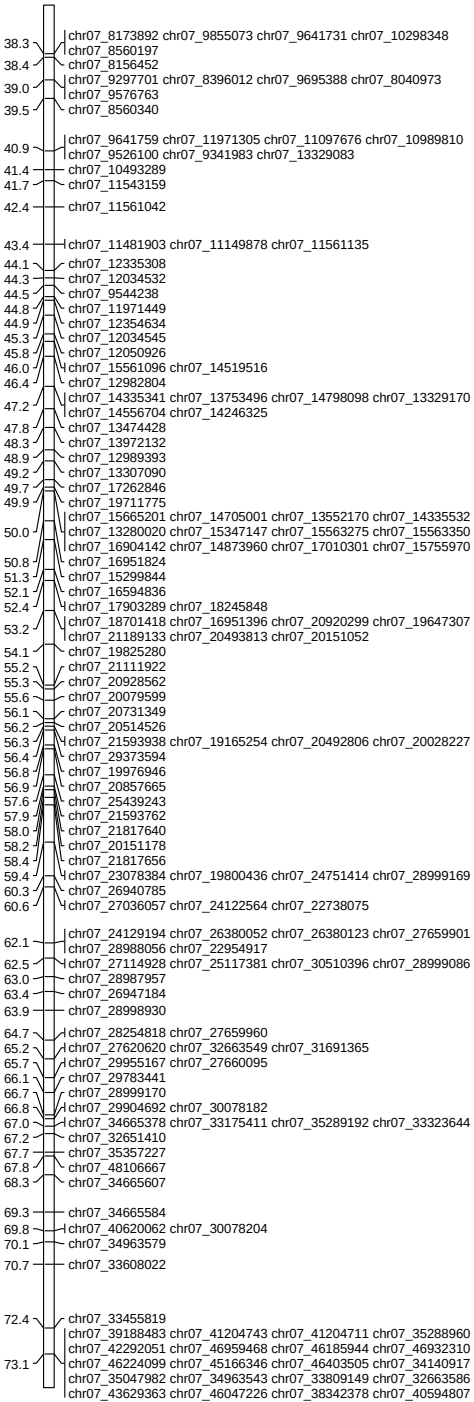
38.3 chr07_8173892 chr07_9855073 chr07_9641731 chr07_10298348
38.4 chr07_8560197
39.0 chr07_8156452
39.5 chr07_9297701 chr07_8396012 chr07_9695388 chr07_8040973
chr07_9576763
40.9 chr07_8560340
41.4 chr07_9641759 chr07_11971305 chr07_11097676 chr07_10989810
41.7 chr07_9526100 chr07_9341983 chr07_13329083
42.4 chr07_10493289
43.4 chr07_11543159
44.1 chr07_11561042
44.3 chr07_11481903 chr07_11149878 chr07_11561135
44.5 chr07_12335308
44.8 chr07_12034532
44.9 chr07_9544238
45.3 chr07_11971449
45.8 chr07_12354634
46.0 chr07_12034545
46.4 chr07_12050926
47.2 chr07_15561096 chr07_14519516
47.8 chr07_12982804
48.3 chr07_14335341 chr07_13753496 chr07_14798098 chr07_13329170
48.9 chr07_14556704 chr07_14246325
49.2 chr07_13474428
49.7 chr07_13972132
49.9 chr07_12989393
50.0 chr07_13307090
50.8 chr07_17262846
51.3 chr07_19711775
52.1 chr07_15665201 chr07_14705001 chr07_13552170 chr07_14335532
52.4 chr07_13280020 chr07_15347147 chr07_15563275 chr07_15563350
53.2 chr07_16904142 chr07_14873960 chr07_17010301 chr07_15755970
54.1 chr07_16951824
55.2 chr07_15299844
55.3 chr07_16594836
55.6 chr07_17903289 chr07_18245848
56.1 chr07_18701418 chr07_16951396 chr07_20920299 chr07_19647307
56.2 chr07_21189133 chr07_20493813 chr07_20151052
56.3 chr07_19825280
56.4 chr07_21111922
56.8 chr07_20928562
56.9 chr07_20079599
57.6 chr07_20731349
57.9 chr07_20514526
58.0 chr07_21593938 chr07_19165254 chr07_20492806 chr07_20028227
58.2 chr07_29373594
58.4 chr07_19976946
59.4 chr07_20857665
60.3 chr07_25439243
60.6 chr07_21593762
62.1 chr07_21817640
62.5 chr07_20151178
63.0 chr07_21817656
63.4 chr07_23078384 chr07_19800436 chr07_24751414 chr07_28999169
63.9 chr07_26940785
64.7 chr07_27036057 chr07_24122564 chr07_22738075
65.2 chr07_24129194 chr07_26380052 chr07_26380123 chr07_27659901
65.7 chr07_28988056 chr07_22954917
66.1 chr07_27114928 chr07_25117381 chr07_30510396 chr07_28999086
66.7 chr07_28987957
66.8 chr07_26947184
67.0 chr07_28998930
67.2 chr07_28254818 chr07_27659960
67.7 chr07_27620620 chr07_32663549 chr07_31691365
67.8 chr07_29955167 chr07_27660095
68.3 chr07_29783441
69.3 chr07_28999170
69.8 chr07_29904692 chr07_30078182
70.1 chr07_34665378 chr07_33175411 chr07_35289192 chr07_33323644
70.7 chr07_32651410
72.4 chr07_35357227
73.1 chr07_48106667
chr07_34665607
chr07_34665584
chr07_40620062 chr07_30078204
chr07_34963579
chr07_33608022
chr07_33455819
chr07_39188483 chr07_41204743 chr07_41204711 chr07_35288960
chr07_42292051 chr07_46959468 chr07_46185944 chr07_46932310
chr07_46224099 chr07_45166346 chr07_46403505 chr07_34140917
chr07_35047982 chr07_34963543 chr07_33809149 chr07_32663586
chr07_43629363 chr07_46047226 chr07_38342378 chr07_40594807

LG7 [3]

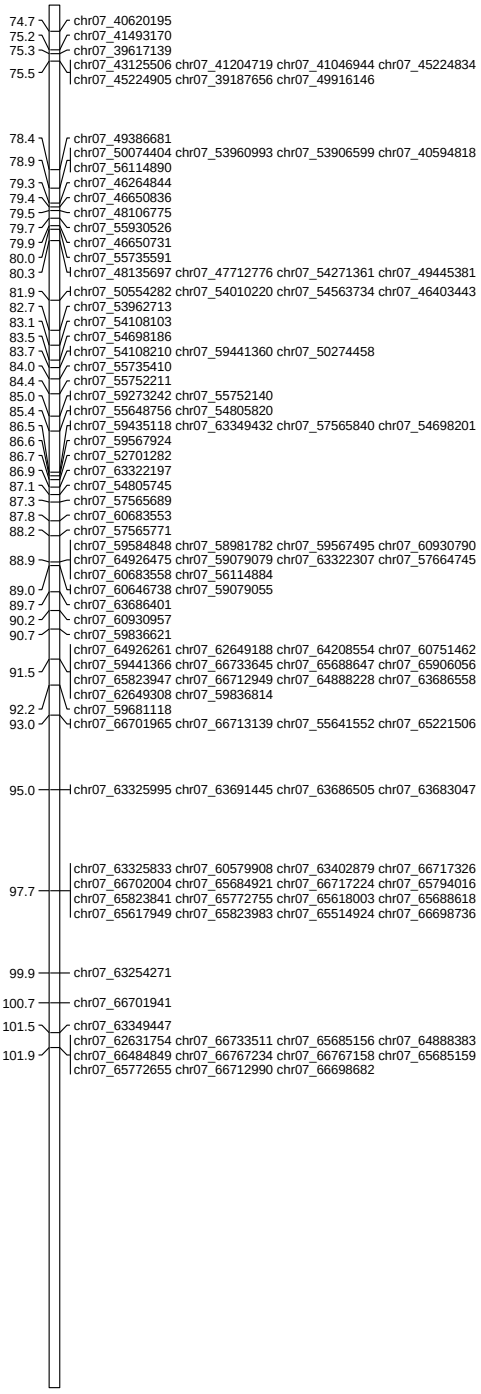
74.7 chr07_40620195
75.2 chr07_41493170
75.3 chr07_39617139
75.5 chr07_43125506 chr07_41204719 chr07_41046944 chr07_45224834
chr07_45224905 chr07_39187656 chr07_49916146
78.4 chr07_49386681
78.9 chr07_50074404 chr07_53960993 chr07_53906599 chr07_40594818
chr07_56114890
79.3 chr07_46264844
79.4 chr07_46650836
79.5 chr07_48106775
79.7 chr07_55930526
79.9 chr07_46650731
80.0 chr07_55735591
80.3 chr07_48135697 chr07_47712776 chr07_54271361 chr07_49445381
81.9 chr07_50554282 chr07_54010220 chr07_54563734 chr07_46403443
82.7 chr07_53962713
83.1 chr07_54108103
83.5 chr07_54698186
83.7 chr07_54108210 chr07_59441360 chr07_50274458
84.0 chr07_55735410
84.4 chr07_55752211
85.0 chr07_59273242 chr07_55752140
85.4 chr07_55648756 chr07_54805820
86.5 chr07_59435118 chr07_63349432 chr07_57565840 chr07_54698201
86.6 chr07_59567924
86.7 chr07_52701282
86.9 chr07_63322197
87.1 chr07_54805745
87.3 chr07_57565689
87.8 chr07_60683553
88.2 chr07_57565771
88.9 chr07_59584848 chr07_58981782 chr07_59567495 chr07_60930790
chr07_64926475 chr07_59079079 chr07_63322307 chr07_57664745
chr07_60683558 chr07_56114884
89.0 chr07_60646738 chr07_59079055
89.7 chr07_63686401
90.2 chr07_60930957
90.7 chr07_59836621
91.5 chr07_64926261 chr07_62649188 chr07_64208554 chr07_60751462
chr07_59441366 chr07_66733645 chr07_65688647 chr07_65906056
chr07_65823947 chr07_66712949 chr07_64888228 chr07_63686558
chr07_62649308 chr07_59836814
92.2 chr07_59681118
93.0 chr07_66701965 chr07_66713139 chr07_55641552 chr07_65221506
95.0 chr07_63325995 chr07_63691445 chr07_63686505 chr07_63683047
97.7 chr07_63325833 chr07_60579908 chr07_63402879 chr07_66717326
chr07_66702004 chr07_65684921 chr07_66717224 chr07_65794016
chr07_65823841 chr07_65772755 chr07_65618003 chr07_65688618
chr07_65617949 chr07_65823983 chr07_65514924 chr07_66698736
99.9 chr07_63254271
100.7 chr07_66701941
101.5 chr07_63349447
101.9 chr07_62631754 chr07_66733511 chr07_65685156 chr07_64888383
chr07_66484849 chr07_66767234 chr07_66767158 chr07_65685159
chr07_65772655 chr07_66712990 chr07_66698682

LG7 [4]

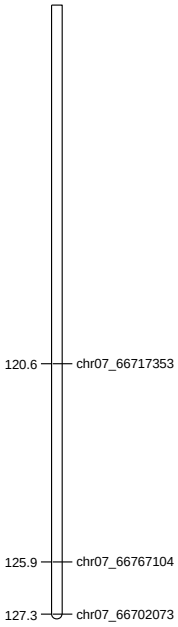
120.6
chr07_66717353
125.9
chr07_66767104
127.3
chr07_66702073